SH
11
A2F53
FISH

U.S. Department
of Commerce

Volume 118
Number 3
July 2020

Fishery Bulletin

U.S. Department of Commerce

Wilbur L. Ross Jr.
Secretary

National Oceanic and Atmospheric Administration

Neil A. Jacobs
Acting Administrator

National Marine Fisheries Service

Chris Oliver
Assistant Administrator
for Fisheries

Fishery Bulletin (ISSN 0090-0656) is published quarterly by the Scientific Publications Office, National Marine Fisheries Service, NOAA, 7600 Sand Point Way NE, Seattle, WA 98115-0070.

Although the contents of this publication have not been copyrighted and may be reprinted entirely, reference to source is appreciated.

The Secretary of Commerce has determined that the publication of this periodical is necessary according to law for the transaction of public business of this Department. Use of funds for printing of this periodical has been approved by the Director of the Office of Management and Budget.

For Sale by the Superintendent of Documents, U.S. Government Publishing Office, Washington, DC 20401. Subscription price per year: $32.00 domestic and $44.80 foreign. Cost per single issue: $19.00 domestic and $26.60 foreign. **See back for order form.**

Fishery Bulletin

Scientific Editor
José I. Castro
National Marine Fisheries Service, NOAA
263 13th Avenue South
Saint Petersburg, Florida 33701

Managing Editor
Kathryn Dennis
Scientific Publications Office
National Marine Fisheries Service, NOAA
1845 Wasp Boulevard, Building 176
Honolulu, Hawaii 96818

Associate Editor
Cara Mayo
Scientific Publications Office
National Marine Fisheries Service, NOAA
7600 Sand Point Way NE
Seattle, Washington 98115-0070

Editorial Board

Henry L. Bart Jr.	Tulane University, New Orleans, Louisiana
Matthew D. Campbell	National Marine Fisheries Service, Pascagoula, Mississippi
Shannon L. Cass-Calay	National Marine Fisheries Service, Miami, Florida
William B. Driggers III	National Marine Fisheries Service, Pascagoula, Mississippi
Gretchen L. Grammer	South Australian Research and Development Institute, Adelaide, Australia
Richard Langton	National Marine Fisheries Service, Walpole, Maine (retired)
Richard S. McBride	National Marine Fisheries Service, Woods Hole, Massachusetts
Richard L. Merrick	National Marine Fisheries Service, Falmouth, Massachusetts (retired)
Richard D. Methot	National Marine Fisheries Service, Seattle, Washington
Lisa J. Natanson	National Marine Fisheries Service, Narragansett, Rhode Island
Joseph M. Quattro	University of South Carolina, Columbia, South Carolina
Mark S. Peterson	University of Southern Mississippi, Ocean Springs, Mississippi
John F. Walter III	National Marine Fisheries Service, Miami, Florida
Bruce Wright	Aleutian Pribilof Island Association, Anchorage, Alaska

***Fishery Bulletin* website: https://spo.nmfs.noaa.gov/fb.htm**

Fishery Bulletin carries original research reports on investigations in fishery science, engineering, and economics. It began as the Bulletin of the United States Fish Commission in 1881; it became the Bulletin of the Bureau of Fisheries in 1904 and the *Fishery Bulletin* of the U.S. Fish and Wildlife Service in 1941. Separates were issued as documents through volume 46; the last document was no. 1103. Beginning with volume 47 in 1931 and continuing through volume 62 in 1963, each separate appeared as a numbered bulletin. A new system began in 1963, with volume 63, in which papers are bound together in a single issue. Beginning with volume 70, number 1, January 1972, *Fishery Bulletin* became a periodical, issued quarterly. In this form, it is available by subscription from the Superintendent of Documents, U.S. Government Publishing Office, Washington, DC 20401. It is also available free in limited numbers to libraries, research institutions, and state and federal agencies and in exchange for other scientific publications.

U.S. Department of Commerce
Seattle, Washington

Volume 118
Number 3
July 2020

Fishery Bulletin

Contents

Articles

209–224 **Stephen R. Scherrer and Kevin C. Weng**

Evaluating movements of opakapaka (*Pristipomoides filamentosus*) relative to a restricted fishing area by using acoustic telemetry and a depth-constrained estimator of linear home ranges

225–239 **Meghan Owings, Christopher Chabot, and Winsor Watson III**

Effects of the biomedical bleeding process on the behavior and hemocyanin levels of the American horseshoe crab (*Limulus polyphemus*)

240–249 **Jorge A. Trujillo-Córdova, Emanuel Mimila-Herrera, Natalí Cárdenas-Palomo, and Jorge A. Herrera-Silveira**

Use of aerial surveys for assessing abundance of the whale shark (*Rhincodon typus*) and the giant manta (*Mobula birostris*) in the northern Caribbean Sea off Mexico

250–267 **James Kennedy and Halldór G. Ólafsson**

Intra- and interannual variation in fecundity and egg size of lumpfish (*Cyclopterus lumpus*) in Iceland

268–274 **Melissa Cook, Jaymie L. Reneker, Redwood W. Nero, Brian A. Stacy, and David S. Hanisko**

Effects of freezing on decomposition of sea turtle carcasses used for research studies

275–283 **Renee Mercaldo-Allen, Paul Clark, Dylan Redman, Yuan Liu, Shannon Meseck, Lisa Milke, Julie M. Rose, and Ronald Goldberg**

Temperature-related changes in species composition of juvenile finfish on a rock reef in Long Island Sound

SMITHSONIAN
NOV 08 2022
LIBRARIES

The National Marine Fisheries Service (NMFS) does not approve, recommend, or endorse any proprietary product or proprietary material mentioned in this publication. No reference shall be made to NMFS, or to this publication furnished by NMFS, in any advertising or sales promotion that would indicate or imply that NMFS approves, recommends, or endorses any proprietary product or proprietary material mentioned herein or that has as its purpose an intent to cause directly or indirectly the advertised product to be used or purchased because of this NMFS publication.

The NMFS Scientific Publications Office is not responsible for the contents of the articles.

284–296 **Greg Ardini, Chad Demarest, and Katherine McArdle**

Costs of at-sea monitoring under government and private contracts in the groundfish fishery of the northeastern United States

297–314 **D. Nick Weber, Bryan S. Frazier, Nicholas M. Whitney, James Gelsleichter, and Gorka Sancho**

Stress response and postrelease mortality of blacktip sharks (*Carcharhinus limbatus*) captured in shore-based and charter-boat-based recreational fisheries

315–318 **Guidelines for authors**

National Marine
Fisheries Service
NOAA

Fishery Bulletin
established in 1881

Spencer F. Baird
First U.S. Commissioner
of Fisheries and founder
of *Fishery Bulletin*

Evaluating movements of opakapaka (*Pristipomoides filamentosus*) relative to a restricted fishing area by using acoustic telemetry and a depth-constrained estimator of linear home ranges

Stephen R. Scherrer (contact author)[1]
Kevin C. Weng[2]

Email address for contact author: scherrer@hawaii.edu

[1] Department of Oceanography
School of Ocean and Earth Science and Technology
University of Hawaii at Manoa
1000 Pope Road
Marine Science Building 609
Honolulu, Hawaii 96822

[2] Virginia Institute of Marine Science
College of William and Mary
P.O. Box 1346
Gloucester Point, Virginia 23062-1346

Abstract—Networks of no-take fishery reserves have emerged as a tool for managing deepwater fish species. In Hawaii and elsewhere, such areas are used to manage deepwater snapper species. However, little is known regarding the movements of these species relative to protected areas. We used passive acoustic telemetry to track crimson jobfish (*Pristipomoides filamentosus*), also known as opakapaka, in one of Hawaii's bottomfish restricted fishing areas to understand the size required for a reserve to protect this species. From January 2017 through January 2018, 179 fish were tagged. Only 10 fish were classified as alive on the basis of movements indicated by detections in tracking data (tracks). For these fish, the median time between the first and last detection of an individual on an acoustic receiver array was 414.5 d with a mean number of detections per individual of 28,321. Linear estimates of home range averaged 3.7 and 6.0 km in conservative and optimistic scenarios, smaller than the median linear habitat dimension of Hawaii's reserves. Fish were detected within the reserve on 97% or more of the days they were tracked. These results indicate that current reserves in Hawaii are likely sufficient in scale to confer positive biological benefits to opakapaka that reside within their borders.

Deepwater demersal fish species are typically characterized by slow growth and late maturity, making them vulnerable to overexploitation (Cailliet et al., 2001; Newman et al., 2016). Restricted fishing areas in deep water have emerged as a tool for rebuilding and maintaining the stocks of these species (Williams et al., 2009; Friedlander et al., 2014; Huvenne et al., 2016; Uehara et al., 2019). Key to understanding the benefits of these reserves is quantifying their ability to retain and protect fish species during critical life stages to confer positive, beneficial effects (Roberts et al., 2003). However, biological considerations are often unknown or neglected when reserve areas are designed, and those omissions can lead to uncertain outcomes (Halpern, 2003). Understanding the ecology and movements of these fish species in proposed or implemented areas is critical to planning and evaluation processes (Palumbi, 2004). Passive acoustic telemetry is a popular and versatile tool for tracking and quantifying fish movements in marine reserves (Crossin et al., 2017). However, deepwater fish species are more susceptible to postrelease mortality than shallow-water species because of barotrauma and other stressors (Edwards et al., 2019).

Deepwater demersal fish are a valuable resource throughout the Indo-Pacific (Kami, 1972; Williams et al., 2012; Newman et al., 2015, 2016; Wakefield et al., 2017; Hill et al., 2018). Multispecies complexes of such fish are both economically and culturally important, supporting commercial, recreational, and subsistence fishing (Craig et al., 1993; Pooley, 1993). In the Hawaiian Archipelago, these fish species are referred to as bottomfish, and management of the stock of these fish is focused on 6 species of eteline snappers and 1 endemic species of grouper. These species, known locally as the *Deep-7*, inhabit island slopes and banks at depths between 100 and 400 m (Kelley and Ikehara, 2006; Oyafuso et al., 2017).

Manuscript submitted 21 September 2019.
Manuscript accepted 26 June 2020.
Fish. Bull. 118:209–224 (2020).
Online publication date: 29 July 2020.
doi: 10.7755/FB.118.3.1

The views and opinions expressed or implied in this article are those of the author (or authors) and do not necessarily reflect the position of the National Marine Fisheries Service, NOAA.

The crimson jobfish (*Pristipomoides filamentosus*), called opakapaka in Hawaii, accounts for the largest fraction of commercial and recreational catch of bottomfish among the Deep-7 species. During the 2017–2018 fishing year, opakapaka accounted for over half of this fishery's $1.6 million ex-vessel value (Harding[1]).

An annual catch limit and a network of restricted fishing reserves were introduced to this fishery as a management strategy in 1998 in response to stock assessments indicating declines in the spawning potential ratio for onaga (*Etelis coruscans*) and ehu (*E. carbunculus*), the second- and third-most abundant species caught by this fishery, respectively, and 2 other species of the Deep-7 (Friedlander et al., 2014; Langseth et al., 2018). The state of Hawaii implemented bottomfish restricted fishing areas (BRFAs) to recover stocks with the goal of protecting 20% of bottomfish habitat in the main Hawaiian Islands (Friedlander et al., 2014). By using improved knowledge of preferred bottomfish habitat, in 2007 the BRFAs were restructured with a goal of further reducing fishing pressure and the number of reserve areas was reduced from 19 to 12 (Parke, 2007; Friedlander et al., 2014). Several studies conducted since have further documented the habitat associations of bottomfish species in the Hawaiian Islands (Misa et al., 2013; Moore et al., 2016; Oyafuso et al., 2017). In August 2019, 4 more reserves were reopened, leaving 8 closed areas.

The BRFAs are controversial among fishery stakeholders (Hospital and Beavers[2]). Studies have shown that fish size and abundance have increased within several of the BRFAs (Sackett et al., 2014), and there is some evidence that spillover to neighboring fished areas has occurred (Sackett et al., 2017). Despite these conservation benefits, some bottomfish fishermen in recent years have lobbied managers to do away with some or all of the protected areas (WPRFMC[3]). They argue that management measures do not adequately balance the economic effects experienced by fishermen with conservation benefits to the fish stocks (Oyafuso et al., 2019). The National Marine Fisheries Service, Hawaii Department of Land and Natural Resources, and Western Pacific Regional Fishery Management Council, who together oversee bottomfish resources in Hawaii, need data on the size of the home range and movement of bottomfish species to determine their future management strategies (WPRFMC[4]).

Prior to our study, there had been little empirical data to assess how the spatial scale of protection offered by the BRFAs compares to the routine movements of opakapaka and other bottomfish species (WPRFMC[4]). Coarse estimates of movements of opakapaka in the Hawaiian Archipelago were obtained through a mark-release-recapture tagging study (O'Malley[5]). As reported by O'Malley, researchers and fishermen partners tagged 4571 opakapaka. Only 113 of these individuals were later recaptured (2.5%). Individuals were recaptured up to 61 km from their tagging location; however, most individuals appeared to move shorter distances, with 86% of recaptured fish recovered less than 10 km from their tagging site (median time at liberty: 325 d).

In a handful of studies, passive acoustic telemetry has been used to track bottomfish in Hawaii. An active tracking study followed 2 juvenile opakapaka over 5-d and 6-d periods in Kaneohe Bay and described patterns of crepuscular movement between day and night habitats occurring within areas of 0.4 km^2 (Moffitt and Parrish, 1996). The habitat occupied by juveniles, however, differed significantly from that described for adults (Moffitt and Parrish, 1996). In another study, the movements of captive-bred and wild-caught juvenile fish (number of samples [*n*]=46) were tracked with an array of 6 receivers until their emigration from nursery grounds days to weeks after release (median time at liberty: 9 d). However, it was unclear if these individuals transitioned directly to adult habitat (Parrish et al., 2015). Adult opakapaka were tracked in 2004 (*n*=12; median time at liberty: 6 d; 5-receiver array), 2006 (*n*=5; median time at liberty: 0 d; 3-receiver array), and 2007 (*n*=10; median time at liberty: 1 d; 7-receiver array) as they moved over the boundary demarking the Kahoolawe Island Reserve, an area restricted to fishing but not a part of the BRFA system (Ziemann and Kelley[6,7,8]). Fish were again observed undertaking crepuscular movements, leaving the area at night and returning in the morning; however, the size and position of the acoustic array were insufficient to determine the extent of movements.

---

[1] Harding, K. 2018. Personal commun. Div. Aquat. Resour., Hawaii Dep. Land Nat. Resour., 1151 Punchbowl St., Rm. 330, Honolulu, HI 96813.

[2] Hospital, J., and C. Beavers. 2011. Management of the main Hawaiian Islands bottomfish fishery: fishers' attitudes, perceptions, and comments. NOAA, Natl. Mar. Fish. Serv., Pac. Isl. Fish. Sci. Cent. Admin. Rep. H-11-06, 46 p. [Available from website.]

[3] WPRFMC (Western Pacific Regional Fishery Management Council). 2013. Minutes of the 158th meeting of the Western Pacific Regional Fishery Management Council; 16–18 October, Honolulu, HI, 89 p. WPRFMC, Honolulu, HI. [Available from website.]

[4] WPRFMC (Western Pacific Regional Fishery Management Council). 2015. WPRFMC five-year research priorities under the MSRA 2014–2019, 12 p. WPRFMC, Honolulu, HI. [Available from website.]

[5] O'Malley, J. 2015. A review of the cooperative Hawaiian bottomfish tagging program of the Pacific Islands Fisheries Science Center and the Pacific Islands Fisheries Group. NOAA, Natl. Mar. Fish. Serv., Pac. Isl. Fish. Sci. Cent. Admin. Rep. H-15-05, 36 p. [Available from website.]

[6] Ziemann, D. A., and C. Kelley. 2004. Detection and documentation of bottomfish spillover from the Kahoolawe Island Reserve, 15 p. Final report. Oceanic Institute, Waimanalo, HI. [Available from Oceanic Institute, 41-202 Kalanianaole Hwy., Waimanalo, HI 96795.]

[7] Ziemann, D. A., and C. Kelley. 2007. Detection and documentation of bottomfish spillover from the Kahoolawe Island Reserve, 20 p. Final report. Oceanic Institute, Waimanalo, HI. [Available from Oceanic Institute, 41-202 Kalanianaole Hwy., Waimanalo, HI 96795.]

[8] Ziemann, D. A., and C. Kelley. 2008. Detection and documentation of bottomfish spillover from the Kahoolawe Island Reserve, Phase III final report, 25 p. Oceanic Institute, Waimanalo, HI. [Available from Oceanic Institute, 41-202 Kalanianaole Hwy., Waimanalo, HI 96795.]

Only one tagging study has described bottomfish movements in relation to the BRFAs. Weng (2013) passively tracked onaga (n=12; median time at liberty: 41 d; 8-receiver array) and ehu (n=6; median time at liberty: 28 d; 8-receiver array) in BRFA B, off Niihau, Hawaii (Fig. 1). The majority of tagged fish spent most of their time within the BRFA, indicating that the protected area was a reasonable size for bottomfish species.

Previous studies of bottomfish movement in Hawaii have used small tracking arrays, tagged small numbers of fish, tracked fish over short durations, or were limited to observations made only during marking and recapture. Therefore, the effectiveness of the BRFA network for retaining Deep-7 fish is unclear. The goal of this study was to use passive acoustic telemetry to determine if the movements of individual opakapaka were confined to one of these reserves or if they extended beyond the boundaries of the BRFA. The linear home ranges of tagged fish were then compared with the scale of protection provided by the current BRFA network. Finally, we looked at how individual fish spent time in and moved between protected and non-protected waters.

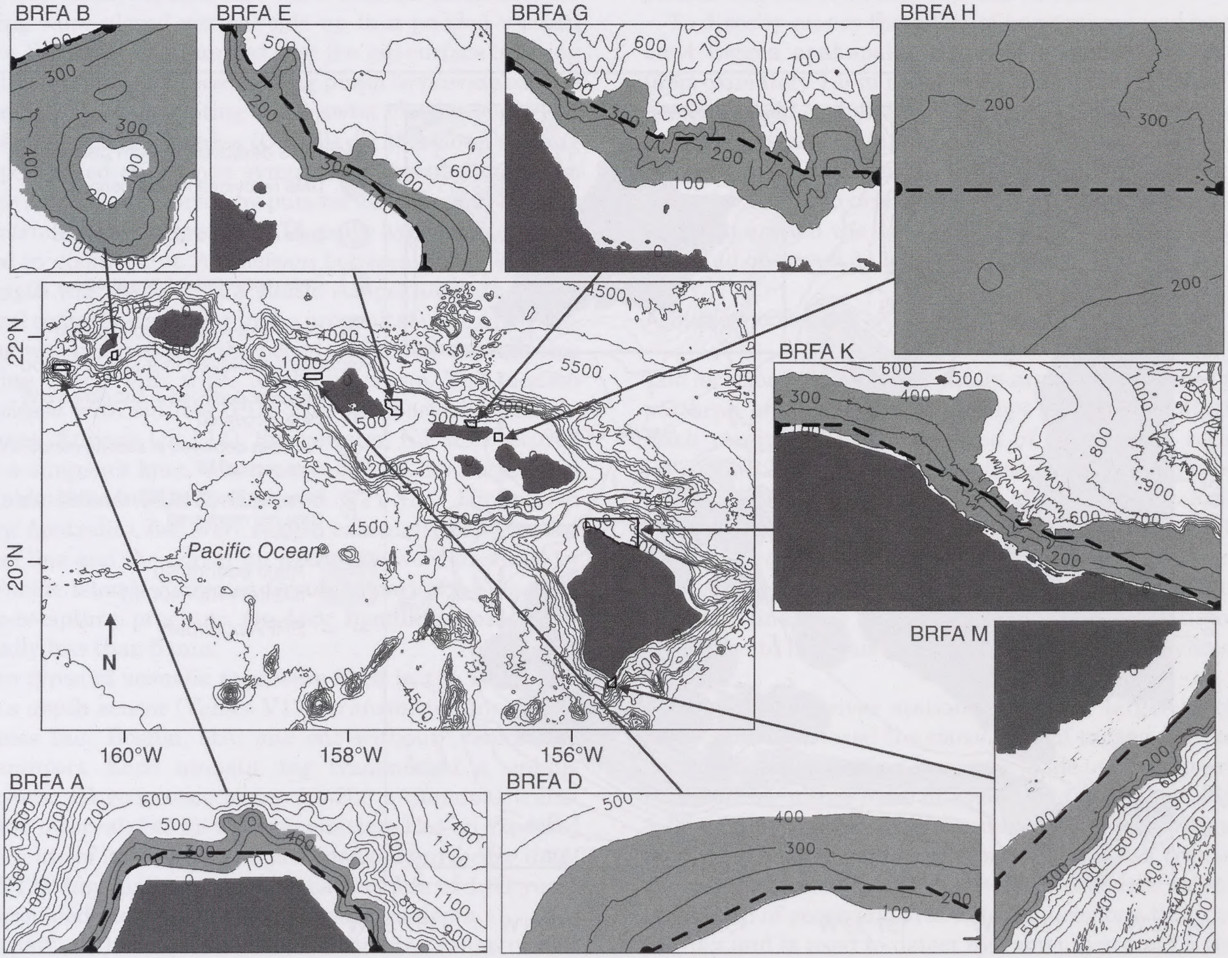

Figure 1

Map of the main Hawaiian Islands surrounded by plots of the 8 bottomfish restricted fishing areas (BRFAs) in which opakapaka (*Pristipomoides filamentosus*), as well as 5 other deepwater snapper species and 1 grouper species, are protected. The boundaries of each outer map correspond to BRFA boundaries except where nonlinear boundaries occur and none of the nonlinear BRFA boundaries intersect bottomfish habitat. A linear habitat dimension, or the distance across a habitat, was estimated for each BRFA by using a least-cost (shortest) path algorithm for comparison with the observed linear home ranges of individual opakapaka tagged in the Makapuu region off southeastern Oahu between 2017 and 2019. The start and end points for each path, indicated by black semicircles on the plot margins, are at a depth of 120 m, the preferred depth of opakapaka. The thick dashed line indicates the least-cost path through the BRFA in each plot. Paths are constrained by the depth range of 100–400 m, indicated by the light gray area in each plot. Solid black lines indicate depth contours in meters.

Materials and methods

Study area

The Makapuu region (21°33′30″N, 157°52′30″W) was selected as the study area because it contains both protected and non-protected habitat with sufficient area to capture the scale of bottomfish movements observed during a previous multi-island pilot study (Fig. 2). The area is important to the commercial fishery and in close proximity to the population center of Honolulu.

The region is located off Oahu's windward side and extends outward from Makapuu Point, the southeastern tip of the island of Oahu, north to the Lanikai Peninsula. A flat, broad shelf protrudes east from the island's southern edge before terminating in a deep slope that forms the western edge of the Kaiwi Channel. The shelf narrows to the north, joining with a series of deeper shelves, and forms submarine canyons. The BRFA in this region (BRFA E) extends from 2.4 km offshore westward across the shelf in line with Koko Head crater to the south and Kailua to the north (Fig. 2). Within BRFA E, habitat between the 100- and 400-m depth contours encompasses an area of approximately 49 km^2.

Fish capture and tagging

Fish in this study were captured with the assistance of local fishermen by using vertical deep-drop hook-and-line gear and hydraulic or electric line pullers commonly

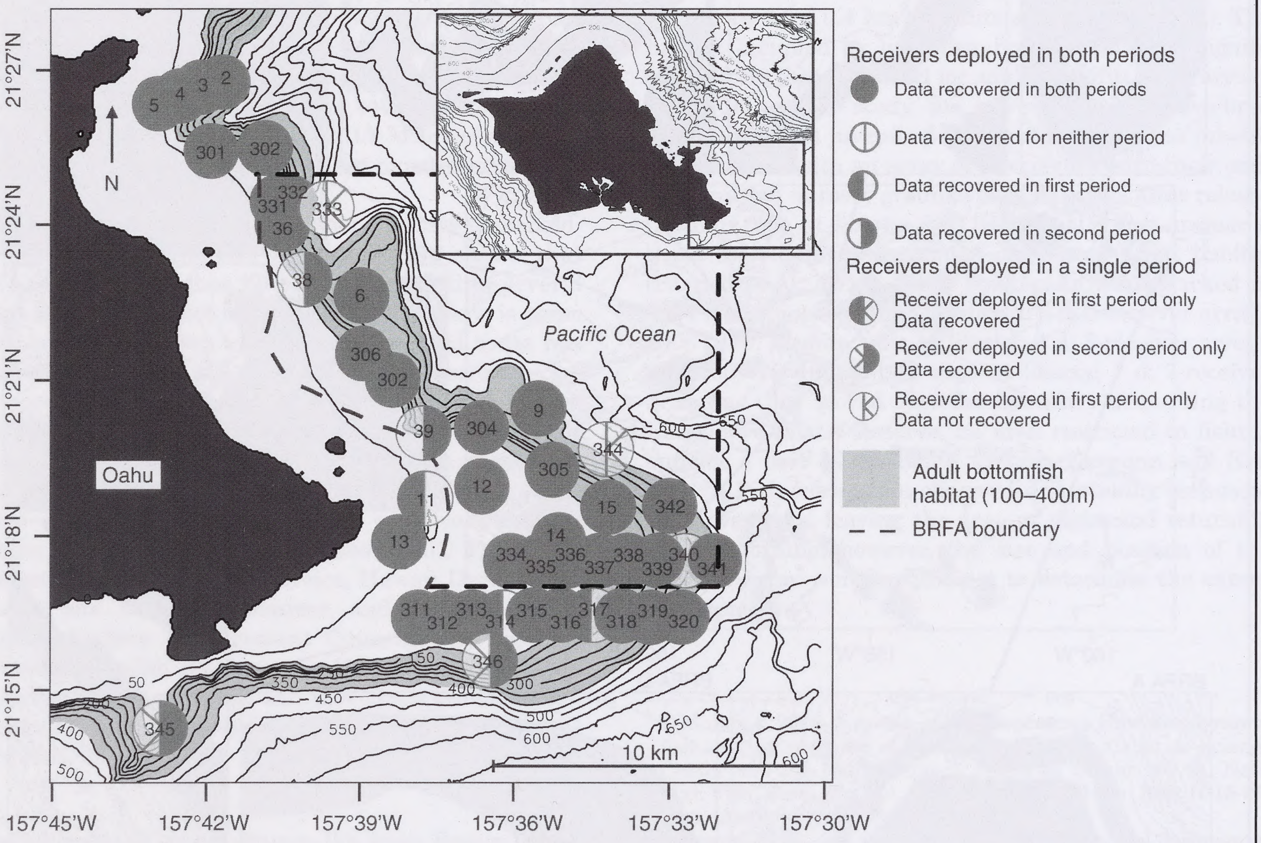
21°27'N
21°24'N
21°21'N
21°18'N
21°15'N
157°45'W
157°42'W
157°39'W
157°36'W
157°33'W
157°30'W
N
Oahu
Pacific Ocean
10 km
5
4
3
2
301
302
332
331
333
36
38
6
306
302
39
304
9
344
11
12
305
15
342
13
14
334
335
336
337
338
339
340
341
311
312
313
314
315
316
317
318
319
320
346
345
50
350
450
550
400
300
500
600
650
Receivers deployed in both periods
Data recovered in both periods
Data recovered for neither period
Data recovered in first period
Data recovered in second period
Receivers deployed in a single period
Receiver deployed in first period only Data recovered
Receiver deployed in second period only Data recovered
Receiver deployed in first period only Data not recovered
Adult bottomfish habitat (100–400m)
BRFA boundary

Figure 2

Map showing the acoustic receiver array deployed in the first analysis period (June 2017–April 2018) and second analysis period (May 2018–January 2019) during which the movements of tagged opakapaka (*Pristipomoides filamentosus*) were tracked in the Makapuu region off the southeastern coast of Oahu, Hawaii (inset). The black dashed line indicates the boundaries of the bottomfish restricted fishing area (BRFA) in this region. Solid gray circles roughly correspond to the detection footprints of individual receivers that were deployed and recovered and from which data were successfully downloaded. Open gray circles indicate stations that could not be recovered or have data downloaded from them (because of the station's loss or failure to log data). Half-shaded circles represent stations from which data were collected for only one period. Half circles containing one side of an *X* represent a period in which the receiver was not deployed. The light gray area represents adult bottomfish habitat (at depths of 100–400 m), and dark gray areas represent land. Black lines indicate depth contours in meters.

used to catch bottomfish in Hawaii (Glazier[9]). Hooks were baited with squid, anchovies, sardines, or saury for bait. Hook-and-line gear were configured with no more than 6 baited hooks at a time. Chum, or *palu* in the Hawaiian language, is used to attract bottomfish while fishing and consists of finely chopped bait (and sometimes a filler material, such wheat chaff, rice, or oats). Palu was released when the rig was at depth to attract and aggregate bottomfish. To reduce barotrauma, when possible after a fish was hooked, the rate at which the mainline was pulled was slowed, to allow some compensative off-gassing of the swim bladder to occur, but was still fast enough to limit predation during ascent.

Fish were brought aboard the vessel for surgical tagging and then immediately released into the water. Once the hook was removed, fish that were deemed acceptable for tagging were placed ventral side up in a padded v-board cradle. Seawater was pumped over the gill surface by using a saltwater hose or a recirculating pump to provide oxygen to the fish. Routine venting of the swim bladder is not recommended for this species (O'Malley[5]); therefore, venting was performed only when symptoms of barotrauma were severe and was conducted by puncturing the swim bladder or protruding stomach with an 18-gauge hypodermic needle stored in disinfectant. An incision between 1.5 and 2.5 cm in length was made with a sterile scalpel along the fish's ventral centerline anterior to the urogenital pore. An acoustic tag was inserted into the peritoneal cavity through this opening, along with triple antibiotic cream. The incision was closed with sutures (PDS Plus Antibacterial[10] monofilament, Ethicon US LLC, Bridgewater, NJ) and secured with a surgeon's knot. When conventional dart tags were available (10-cm PDS-2, Hallprint PTY Inc., Hindmarsh Valley, Australia), fish were tagged externally between the lateral line and the dorsal fin. Dart tags were provided by the Pacific Islands Fisheries Group as part of a long-term mark-recapture program. On-deck handling times were typically less than 5 min.

Two types of acoustic tags were used in the study, one with a depth sensor (Vemco V13P transmitter, Innovasea Systems Inc., Boston, MA) and one without (Vemco V13 transmitter). Each acoustic tag transmitted a unique ultrasonic ID code once every 90–200 s (nominal transmission interval: 145 s). V13 transmitters had an expected battery life of 2.25 years and provided only presence data, and V13P tags had an expected battery life of 1.63 years and provided records of both presence and depth.

As part of the determination of the size range of fish suitable for tagging, V13 and V13P tags were weighed. The minimum size of opakapaka eligible for tagging with each type of tag was calculated by using a conservative threshold of 2% of bodyweight and a species-specific allometric relationship between fork length (FL) and weight (Uchiyama and Kazama[11]). The minimum FL suitable for tagging was 31 cm for fish with V13 tags and 33 cm for fish with V13P tags.

Four main strategies for release were used in an attempt to balance rapid recompression and predator avoidance: 1) release at the seafloor by using a drop-shot device (Blacktip Catch and Release Recompression Tool, West Marine, Watsonville, CA; *n*=74), 2) midwater release (30–60 m) by using a drop-shot device (SeaQualizer Descending Device, SeaQualizer, Davie, FL; *n*=70), 3) surface or near-surface release (*n*=18), and 4) release, either at the surface (*n*=8) or by using a drop-shot device (*n*=2), after driving the vessel rapidly away from the fishing location. The method of release was not recorded for 3 individuals.

To directly assess the effect of barotrauma and surgery on 4 tagged opakapaka, we built a mid-water net pen (approximately 1.5 m high, with a diameter of 2.5 m) and used it to hold each individual at a depth of 20 m following capture and surgery. After 30–60 min, we descended to the net pen by scuba diving to observe the fish, noting condition and ability to orient and maintain neutral buoyancy. We then opened the net pen, allowing each fish to swim free, and observed its swimming ability.

Acoustic monitoring

The locations of fish in the study area were inferred from patterns of presence and absence at receiver stations. Each receiver station consisted of an acoustic receiver (Vemco VR2W or VR2AR, Innovasea Systems Inc.) and an acoustic release (Vemco VR2AR or Lightweight Release Transponder, Sonardyne International Ltd., Hampshire, UK) buoyed by 3 or 4 trawl floats and anchored to the seafloor with approximately 80 kg of concrete. Each mooring line was sheathed within a 38-mm-diameter PVC tube to minimize the potential for entanglement or fraying.

Individual receiver stations formed a larger tracking array that monitored the movement of tagged fish in the study area. The tracking array was made up of 5 sub-arrays representing either *fence* or *sparse* configurations (Fig. 2). A fence sub-array is a line of receivers deployed with overlapping detection regions so that a tagged fish transiting the line of receivers will be detected. A sparse sub-array is a group of receivers with detection regions that do not overlap and is used to detect movements around a region with much of the region unmonitored.

The fence sub-arrays, or fences, were designed to detect individuals crossing BRFA borders. Because a fence placed on the border would detect fish located inside or outside the BRFA, it was necessary to have 2 fences—one outside the BRFA at a distance from the border greater than the receiver's detection range and another located inside the BRFA's border by a similar distance. Four fences were deployed where the boundaries of the BRFA intersected with bottomfish habitat. One pair of fences was used to monitor the northern border, and the other pair was used to monitor the southern border. The placement of each fence was optimized by using an algorithm with respect to the following factors: the probability of detecting a tag transmission at a receiver across a range of depths, the bathymetry along the fence's transect, the height of the receiver from the seafloor, the desired height of the water column to be monitored, the swimming speed of individual opakapaka, and a probability of at least 25% for detecting any given transmission from a tag.

---

[9] Glazier, E. 2007. Hawaiʻi pelagic handline fisheries: history, trends, and current status, 73 p. Final background document prepared for the Western Pacific Fisheries Management Council. Pac. Isl. Off., Impact Assessment Inc., Honolulu, HI. [Available from website.]

[10] Mention of trade names or commercial companies is for identification purposes only and does not imply endorsement by the National Marine Fisheries Service, NOAA.

[11] Uchiyama, J. H., and T. K. Kazama. 2003. Updated weight-on-length relationships for pelagic fishes caught in the central North Pacific Ocean and bottomfishes from the Northwestern Hawaiian Islands. NOAA, Natl. Mar. Fish. Serv., Pac. Isl. Fish. Sci. Cent. Admin. Rep. H-03-01, 34 p. [Available from website.]

The probabilities of a receiver detecting transmissions from tags across a range of distances were determined through range testing experiments. Results of range experiments indicate that 5% of tag transmissions could be received at a distance of 847 m from the receiver. One quarter of tag transmissions were detectable at a distance of 545 m, and 12.5% of tag transmissions were detectable at a distance of 765 m (Scherrer et al., 2018). Therefore, to achieve a minimum detection rate of 25%, spacing between adjacent receivers in a fence configuration could not exceed 1530 m. To be conservative, the fence algorithm was initialized with a 12.5% detection range of 600 m and a 25% detection range of 500 m. Each receiver station was deployed from the vessel over its target location and was allowed to sink freely to the seafloor. By using the position of the vessel at the time of deployment as the station's position, the largest distance between 2 receivers in any of the fence configurations was 1232 m.

A single sparse sub-array was used to monitor individual movements between areas within the BRFA. The positions of individual receivers within the sparse sub-array were determined in iterative stages by using a telemetry optimization algorithm (Pedersen et al., 2014) and bathymetry of the Hawaiian Archipelago at resolutions of 50 m and 1 km (Johnson[12]). The locations of their deployment were selected within the bounds of BRFA E after constraining depth between 75 and 475 m. Aggregations of up to 100 opakapaka have been observed from manned submersibles 2–10 m above the seafloor in the Penguin Banks region, located just west of the island of Molokai (Haight, 1989; Haight et al., 1993; Kelley and Moriwake[13]). Therefore, a preferred depth of 6 m above the seafloor was selected. A maximum receiver detection range of 847 m was determined by using results from deepwater range tests we have previously reported (Scherrer et al., 2018).

Receivers in deep water are particularly susceptible to close-proximity detection interference (CPDI), a phenomenon in which a receiver may fail to detect transmissions from tags at close distances (Kessel et al., 2015; Scherrer et al., 2018). Results from predictive modeling indicate that CPDI occurs for receivers in depths exceeding 200 m. However, CPDI is not believed to have affected the detection of fish transiting through fence sub-arrays because multiple transmissions would be sent by a tagged fish while it was within the detection range of the receiver before and after encountering the region affected by CPDI.

Data analysis

Categorizing fish status Data collected from acoustic receivers were downloaded and stored in the database application VUE, vers. 2.4 (Innovasea Systems Inc.). Potentially false detections were flagged by this software and subsequently removed from the data set. Data of the movements, or *tracks*, of fish were then exported to a comma-separated values file for further analysis in R, vers. 3.5.0 (R Core Team, 2018). A 30-s filter window was then used to flag any tags that were detected on multiple receivers to ensure that any movements detected represented real changes in position and not just periods particularly favorable to detection of acoustic signals.

High postrelease mortality and moderate to high rates of residency at a single station made determining fish status important. Simply, it is difficult to distinguish a fish with a small home range near a single receiver from a tag laying on the bottom near a receiver. A decision tree was developed to assist in classifying fish detected on the receiver on the basis of features of their tracks (Fig. 3). Tracks were assigned to 1 of 3 categories: *expired tracks* of fish that were believed to be dead, *valid tracks* of fish believed to be alive, and *uncertain tracks* of fish for which status could not be determined. Following this initial classification, we reviewed records of each tag and made adjustments to status when appropriate.

It is similarly difficult to distinguish the tracks of a rapidly moving tagged fish from the movements of a shark that has eaten a tagged fish; therefore, we tagged individuals of several predator species to assist in determining parameters for track classification. We tagged 8 sandbar sharks (*Carcharhinus plumbeus*), 1 silky shark (*C. falciformis*), and 1 Galapagos shark (*C. galapagensis*). All tagged sharks were detected on the receiver array during the analysis period. Their behavior patterns were characterized by frequent movement between stations (mean movements per day: 8.9 [standard deviation (SD) 10.7]), detection at multiple stations in a single day (mean number of stations detected per day: 3.5 [SD 1.6]), and movement over large distances (mean linear home range: 18.1 km [SD 5.7]). Because a tagged fish eaten by a predator is likely to be digested and its tag regurgitated within about 1 week (Medved, 1985), we doubled this time period to be

---

[12] Johnson, P. 2011. Main Hawaiian Islands multibeam bathymetry synthesis: 50-meter bathymetry and topography. Hawaii Mapping Res. Group, Sch. Ocean Earth Sci. Tech., Univ. Hawaii Manoa, Honolulu, HI. [Data available from website, accessed May 2011.]

[13] Kelley, C. D., and V. N. Moriwake. 2012. Appendix 3. Essential fish habitat descriptions, part 1: Hawaiian bottomfish. *In* Final fishery management plan for coral reef ecosystems of the western Pacific region, vol. 3. Essential fish habitat for management unit species, p. A3-02–A3-111. [Available from West. Pac. Reg. Fish. Manage. Counc., 1164 Bishop St., Ste. 1400, Honolulu, HI 96813.]

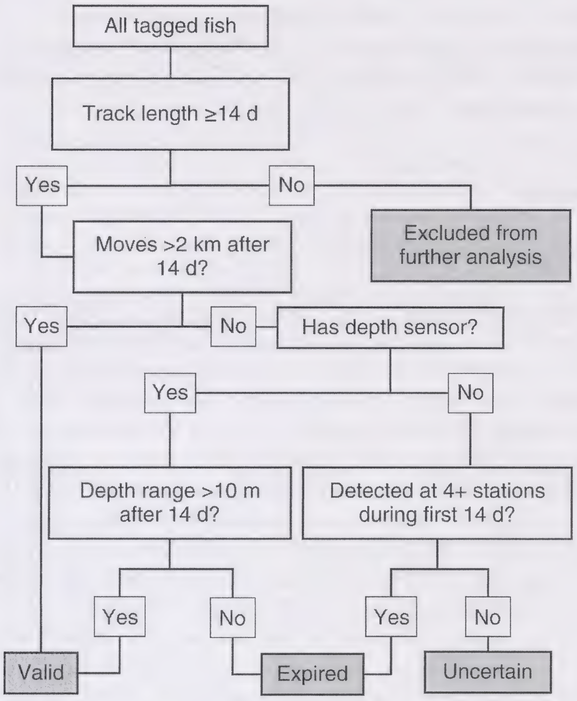

Figure 3

The decision tree used to classify the survival, or status, of each tagged opakapaka (*Pristipomoides filamentosus*) on the basis of the records of their movements, or tracks, collected between June 2017 and January 2019 from acoustic receivers deployed in the Makapuu region off southeastern Oahu, Hawaii.

conservative and defined *shark-like* movement as detection at 4 or more stations during the first 14 d of the track. A predation event was identified when tag data indicated movements with shark-like qualities followed by cessation of movement. Tracks shorter than 14 d were discarded (because these movements might be those of opakapaka that were inside shark stomachs).

Further classification was based on movement. Results of range testing indicate that, under optimal conditions, receivers could detect tag transmissions at distances up to 1.0 km. Therefore, detections on 2 receivers less than 2 km apart could be detections of a stationary tag laying between them. Consequently, tracks of fish that moved between 2 stations separated by more than 2.2 km 14 d after tagging were considered valid. However, if no horizontal movements were observed for a given individual, its status could still be classified if its tags were capable of reporting changes in depth greater than those that could be attributed to tidal fluctuations. Following the 14th day after tagging, a valid classification was assigned to tracks from individuals with depth-sensing tags if vertical movement ranges exceeded 10 m. This threshold was selected because it is greater than the maximum fluctuation in depth that could be explained by tidal changes alone.

Tracks from tags lacking depth sensors that did not indicate movement after 14 d were classified as expired if they had a strong shark-like movement pattern at the beginning of the track. The track of a fish detected at fewer than 4 stations during the first 2 weeks was classified as uncertain. Visual inspection of the tracks of such fish were indistinguishable from tracks of stationary tags attached to fish that were known to be dead but also resembled highly resident fish that were known to be alive from depth records.

Analysis scenarios Two scenarios were developed by using the classification of each fish's track, to select which tracking data would be included in further analyses. The first scenario included only valid tracks and represents a conservative outlook on the data. The second scenario included both valid and uncertain tracks. The group of tracks with an uncertain classification likely includes a mixture of both valid tracks from highly resident fish that were detected consistently at a single receiver and detections of stationary tags belonging to fish that died after they were tagged. For this reason, the second scenario should be considered an optimistic outlook.

Testing for size-selective survivorship bias Correlation between body size and survivorship outcome for tagged opakapaka was tested by comparing the distribution of FLs from fish with valid tracks to that of the total population of tagged fish. A subset of lengths equal in number to the fish with valid tracks was selected at random without replacement from the measured FLs of all sampled fish. The mean and SD of this subset of lengths were recorded, and the process was repeated 10,000 times. These summary statistics were used to calculate 95% confidence intervals (CIs) for comparing the size of surviving opakapaka with the size of all of the opakapaka that were tagged.

Analysis periods The receiver array was deployed and recovered twice during the study (Fig. 2). Five stations were lost midway through the study and were replaced; therefore, the data for these replacement stations exist only for the later period after the second deployment. Three receiver stations were lost later in the study, such that data for these sites exist only for the earlier period. Because the stations lost during these periods differed, the data were split into 2 periods for analysis corresponding with each realized array configuration. The first analysis period began on 26 May 2017 and ended on 15 April 2018. The second analysis period was from 6 May 2018 through 6 January 2019.

Calculating individual home range A number of methods for quantifying home range have been proposed with application varying depending on the study environment and the technology and method used (Stickel, 1954; Stumpf and Mohr, 1962; Schadt et al., 2002; Börger et al., 2006; Dwyer et al., 2015). Because adult opakapaka are associated with a narrow depth band, their habitat can be thought of as a river winding along island slopes and flanked by areas where individuals are unlikely to occur. In river systems, a constrained linear home range estimator provides a more robust estimate of space use when compared with estimates from the use of a minimum convex polygon, kernel utilization, and other common methods used to quantify home range; therefore, we used a constrained linear home range estimator to calculate the size of the home range for each individual on the basis of its known locations from detection records (Dwyer et al., 2015).

The home range distance for each individual was calculated as the least-cost path between receivers that detected that fish's tag. Least-cost paths were constrained to depths between 100 and 400 m by using the marmap package, vers. 1.0.3, in R (Pante and Simon-Bouhet, 2013). In effect, if the linear path between 2 stations crossed a depth falling outside this range, the path would shift to the nearest point with a depth inside the acceptable range, resulting in a longer path consistent with present knowledge of habitat use of bottomfish. Home range distances calculated for the 2 analysis periods were compared by using nonparametric sign-rank tests.

Comparing home range distance to size of reserves Least-cost estimates of home range for opakapaka were compared with the size of the BRFAs by using a metric of the linear habitat available within each of the 8 reserves. Because BRFAs include both preferred and non-preferred habitat, we quantified a linear habitat dimension for each BRFA by using the same depth-constrained least-cost path approach that was used to calculate individual fish home ranges. For the 7 BRFAs located along slopes, a path was calculated between the 2 sides of the BRFA's boundary intersecting bottomfish habitat by using bathymetry with a 50-m resolution. The start and end points for each path were at a depth of 120 m, the preferred depth of opakapaka. The east–west distance across the rectangular area was used to define the linear habitat dimension of the BRFA containing depths exclusively within those defined as bottomfish habitat.

Quantifying movement frequency and site fidelity Detections of fish on receiver fences were used to determine the proportion of time individuals spent within protected areas of the study area and the frequency of movements across the reserve's boundaries. When a fish moved into the reserve, a tag was first detected at a receiver outside of the reserve, followed by detection at a receiver inside the reserve. Similarly, when a fish moved out of the reserve, it was detected first at a receiver inside the reserve, followed by detection at a receiver located outside the reserve. The fraction of time an individual spent within the reserve was standardized by the total time that individual was tracked to calculate its proportional time of protection. The number of movements across reserve boundaries was then standardized by the track duration, defined as the number of days elapsed between the first and final detections of a tag on the array during each analysis period, to estimate the frequency at which they moved between protected and non-protected areas. The correlation between the proximity of a fish's tagging location to the boundary of the reserve and the frequency with which that fish crossed the boundary was also quantified, by using Pearson's correlation coefficient (*r*).

Results

Fish capture and tagging

Between 9 January 2017 and 11 January 2018, 179 opakapaka were tagged and released within the Makapuu region. Of those fish, 125 were also tagged with conventional dart tags. All fish tagged were larger than the minimum size requirement of 31 cm FL, ranging in size from 34 to 76 cm FL (median: 45.5 cm FL; interquartile range [IQR]: 41–53 cm FL). Tags attached to 168 fish were detected at least once on the receiver array between 26 June 2017 and 6 January 2019. Of those detected tags, 68 tags included a depth sensor and transmitted pressure data in addition to their unique ID codes.

None of the fish held in the net pen had symptoms of severe barotrauma, with all 4 individuals maintaining neutral buoyancy and proper orientation. Each fish swam away once the net pen was opened. However, 2–5 sharks were observed in near proximity within 10 min of each deployment of the pen.

Categorizing fish status

The classifications of tracks were used to determine the status of the 168 tagged opakapaka detected on the array between 26 June 2017 and 6 January 2019: 10 tracks were classified as valid, 35 tracks were classified as uncertain, and 83 tracks were classified as expired. Tracks of 40 individuals with durations less than 14 d were excluded from analysis, and no tracks were available for 11 fish with tags that were not detected on the array during either analysis period (Table 1). Using the decision tree, we initially assigned a valid classification to 30 tracks; however, 20 of these tracks were later reclassified. These tracks were reclassified because of faulty depth sensors, detection patterns that could be otherwise explained by a tag on the seafloor detected only under optimal acoustic conditions, or daily depth patterns that closely resembled those of the bluntnose sixgill shark (*Hexanchus griseus*) (Comfort and Weng, 2015). Twelve of the tracks initially considered to be valid were reclassified as uncertain, and 8 tracks were reclassified as expired.

With the assumption that only the fish with valid tracks survived after tagging, the estimated survivorship rate was 5.6%. Including uncertain tracks raises this estimate to 25.1%. Because some fish were tagged prior to the start of the study, track duration was used to compare and standardize results between individuals. In contrast, time at liberty, which encompasses the period from an individual's tagging to the last detection of its tag, would be inappropriate for standardizing analysis

Table 1

The number of tracks, algorithmically determined and after reclassification, for 179 tagged opakapaka (*Pristipomoides filamentosus*) detected on an acoustic receiver array between 26 June 2017 and 6 January 2019 in the Makapuu region off Oahu, Hawaii. The survival or status of detected fish was determined by using an algorithm to classify their tracks into 3 categories: *valid tracks* of fish believed to be alive, *uncertain tracks* of fish for which status could not be determined, and *expired tracks* of fish that were believed to be dead. Tracks of 40 fish with durations less than 14 d were excluded from analysis, and no tracks were available for 11 fish that were not detected on the array.

	No. of tracks	
Status	Algorithmically determined	After reclassification
Valid	30	10
Uncertain	24	35
Expired	74	83
Excluded from analysis	40	40
Undetected	11	11
Total	179	179

results because it includes days before the analysis period began. The durations of tracks for fish believed to be alive ranged between 161 and 560 d (median: 414.5 d; IQR: 297–496 d), and the durations of uncertain tracks were between 66 and 560 d (median: 357 d; IQR: 219–491 d) (Table 2).

Analysis scenarios

The status of each fish was used to construct conservative and optimistic analysis scenarios. The conservative scenario included only 10 tracks, those of fish determined to be alive. The optimistic scenario used tracks of 45 fish, including 35 tracks classified as uncertain in addition to the 10 tracks used in the conservative scenario.

Testing for size-selective survivorship bias

The mean length of opakapaka considered under both conservative and optimistic scenarios fell within the 95% CIs obtained from simulation data sampled without replacement: the mean length from the conservative scenario, for example, was 42.6 cm FL (95% CI: 42.1–54.5). However, the SD of mean lengths for fish included under both scenarios was smaller than the 95% CI obtained from simulation data sampled without replacement: the SD from the conservative scenario was 2.8 cm FL (95% CI: 4.9–14.4), and the SD from the optimistic scenario was 7.2 cm FL (95% CI: 8.15–11.8). These results indicate that the mean size of fish included in each scenario did not significantly differ from that of the tagged sample; however, the smallest and largest tagged fish were underrepresented in the data (Fig. 4).

Analysis periods

Receivers were recovered and downloaded twice, once mid-study and once at the end of the study, separating the analysis into 2 periods. Under the conservative scenario, all 10 fish with valid tracks were detected on the receiver array during the first period and 8 fish were detected on the array during the second period. Under the optimistic scenario, 45 fish were detected on the receiver array in total, with 44 fish detected during the first period and 37 fish detected during the second period.

Equipment losses affected the array's overall performance. During the first analysis period (26 June 2017–15 April 2018), 2 receiver stations from the fence sub-arrays were lost, station 333 (depth: 325 m) and station 340 (depth: 324 m) (Fig. 2). Losing station 333 truncated the northern fence so that the 25% minimum detection threshold extended to an estimated depth of 370 m rather than 400 m as planned. Losing station 340 left a gap in the southern boundary fence inside the BRFA. The possibility that individuals could move into the BRFA through this gap undetected cannot be ruled out. During the second analysis period (6 May 2018–6 January 2019), 3 stations from the fence sub-arrays were lost (Fig. 2). Stations 314 (depth: 78 m) and 317 (depth: 150 m) were part of the southern fence outside the BRFA. The receiver at station 340 (depth: 331 m), part of the southern fence inside the BRFA, once again broke free of its mooring and was later recovered. The logs from this receiver indicate that it broke free of its mooring within 3 weeks of deployment. The gaps caused by receiver losses in the second period mean that it was possible for tagged individuals to move into and out of the BRFA undetected during this time.

Calculating individual home range distance

Estimates of linear home range varied between 3.2 and 9.4 km under the conservative scenario and between 0.0 and 19.7 km under the optimistic scenario during the first analysis period. The median observed home range distance during this time was 5.8 km (IQR: 3.2–8.1 km) for the conservative scenario and 3.2 km (IQR: 1.6–6.1 km) under the optimistic scenario. Home ranges observed during the second period were between 1.7 and 8.1 km with a median distance of 3.7 km (IQR: 2.4–6.0 km) under the conservative scenario and between 0.0 and 8.1 km with a median distance of 2.4 km (IQR: 1.7–3.7 km) under the optimistic scenario.

Observed home ranges were mostly consistent between both periods. Results of nonparametric sign-rank tests indicate that home range did not significantly differ across these 2 periods for either scenario ($P>0.05$). Regardless of period, the median home range calculated for any fish during the study was 6.0 km (IQR: 5.5–8.1 km) under the conservative scenario and 3.7 km (IQR: 1.7–7.2 km) under the optimistic scenario.

Table 2

Summary information for movement data, or tracks, of tagged opakapaka (*Pristipomoides filamentosus*) that were monitored with an acoustic receiver array during the first analysis period (P1), June 2017–April 2018, and the second analysis period (P2), May 2018–January 2019, within and near the bottomfish restricted fishing area (BRFA) in the Makapuu region off Oahu, Hawaii. Information includes the number of days during which detections were made and the number of movements across BRFA boundaries that were detected. Tracks of fish believed to be alive were classified as valid, tracks of fish for which status could not be determined were considered uncertain.

Tag ID code	Status	Fork length (cm)	Tagging date	Time at liberty (d)	Track duration (d)	No. of transmissions detected	No. of days with detections	Home range (km)		Total no. of boundary movements detected	Time in BRFA (%)	
								P1	P2		P1	P2
2122	Uncertain	47.0	2018-01-09	216	95	483	16	5.5	4.7	4	93	100
2127	Uncertain	49.5	2018-01-09	96	95	950	68	5.1	0.0	14	96	0
2133	Valid	43.0	2018-01-09	190	35	457	28	5.5	1.7	6	99	100
2136	Valid	42.0	2018-01-09	452	335	21,062	301	6.0	2.4	0	100	100
2139	Uncertain	50.0	2018-01-09	456	338	470	127	3.8	5.1	0	100	100
2140	Uncertain	39.5	2018-01-09	234	49	68	13	3.4	4.7	0	100	100
2157	Uncertain	52.5	2018-01-10	66	66	515	35	5.5	0.0	18	56	0
28171	Uncertain	52.0	2018-01-11	446	331	2351	212	2.4	2.4	0	100	100
28175	Uncertain	48.0	2018-01-11	391	276	920	125	11.8	3.7	0	100	100
28177	Uncertain	42.5	2018-01-11	437	144	679	41	13.2	3.8	4	100	16
28178	Uncertain	50.0	2018-01-11	352	158	19	11	3.4	5.1	0	100	100
28179	Valid	45.0	2018-01-11	454	339	60,130	339	5.5	3.8	69	98	98
28181	Uncertain	53.0	2018-01-11	446	331	9716	170	1.7	0.0	0	100	100
28185	Uncertain	34.0	2018-01-11	453	338	549	163	3.2	1.6	0	0	0
30683	Uncertain	41.5	2017-08-28	714	463	18,651	397	1.6	0.0	0	0	0
30684	Uncertain	43.0	2017-08-28	726	475	77,111	475	3.7	2.4	28	0	0
30690	Uncertain	42.0	2017-08-28	725	474	44,580	467	6.0	0.0	0	100	100
30694	Uncertain	36.0	2017-08-28	725	474	44,364	457	6.1	0.0	2	100	100
30695	Valid	36.5	2017-08-28	716	453	3605	297	7.1	2.4	2	100	100
30703	Uncertain	54.0	2017-08-28	681	429	577	94	2.4	2.4	0	100	100
30705	Valid	40.5	2017-08-29	724	474	17,055	462	6.1	8.1	86	99	97
30707	Uncertain	53.0	2017-08-29	724	474	33,067	456	0.0	1.7	0	100	100
30714	Uncertain	47.0	2017-06-24	764	410	12,364	152	0.0	1.7	0	100	100
30715	Uncertain	38.0	2017-06-24	856	538	57,792	535	0.0	1.7	0	100	100
30717	Uncertain	36.5	2017-06-24	73	71	277	7	0.0	0.0	0	100	0
30721	Valid	45.0	2017-06-24	856	538	64,477	538	3.2	6.0	0	100	100
30722	Uncertain	45.0	2017-06-24	856	538	99,377	522	0.0	1.7	0	100	100
30729	Uncertain	49.5	2017-06-25	187	186	1175	60	8.4	0.0	0	100	0
30734	Uncertain	55.5	2017-06-25	772	435	570	75	1.6	2.4	0	100	100
30739	Uncertain	40.0	2017-06-26	121	121	77	24	1.6	0.0	0	100	0
30742	Uncertain	47.0	2017-06-26	505	116	199	25	1.6	2.4	0	100	100
30743	Uncertain	43.0	2017-08-28	726	475	63,462	465	1.6	2.4	0	100	100
30747	Uncertain	44.0	2017-08-28	176	176	22,474	172	3.2	0.0	0	100	0
30749	Uncertain	61.0	2018-01-11	201	78	111	42	2.4	2.4	0	100	100
30751	Uncertain	70.0	2018-01-11	364	249	11,103	221	1.6	4.7	0	100	100
36810	Unknown	44.0	2017-06-24	637	319	1558	61	0.0	1.7	0	100	100
51581	Unknown	61.5	2017-01-13	1012	370	22,062	276	0.0	0.0	0	100	100
51582	Alive	41.0	2017-03-18	380	280	8109	222	3.8	0.0	0	100	0
51584	Unknown	51.0	2017-03-18	813	299	5446	234	1.7	0.0	0	100	100
51585	Unknown	44.0	2017-03-18	820	234	152	50	1.6	1.6	0	100	100
51586	Alive	46.0	2017-03-18	961	447	39,084	447	3.2	3.7	0	100	100
51587	Unknown	48.0	2017-03-18	982	397	629	139	1.6	1.6	0	100	100
51588	Alive	44.0	2017-03-18	286	186	16,105	186	7.1	0.0	6	80	0
51596	Alive	42.5	2017-08-28	726	475	44,371	475	3.2	6.0	0	100	100
51598	Unknown	44.5	2017-08-29	514	256	114	59	1.7	0.0	0	100	100

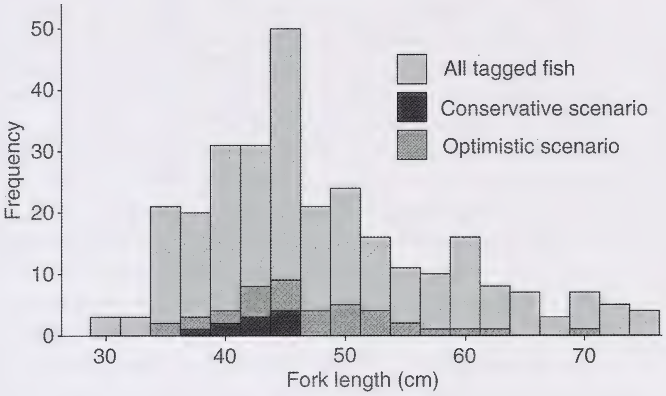

Figure 4

Frequency distributions of fork lengths for all opakapaka (*Pristipomoides filamentosus*) tagged and measured in the Makapuu region off the coast of Oahu, Hawaii, between January 2017 and January 2018 (number of samples [n]=179, light gray bars) and those for fish used in 2 survivorship scenarios. The conservative scenario includes only valid tracks, from tags on fish determined to be alive (n=10, black bars). The optimistic scenario includes uncertain tracks, from tags on fish for which survival could not be determined, as well as valid tracks (n=45, dark gray bars).

Comparing home range distance to size of reserves

The median linear habitat dimension of the BRFA network was 11.40 km (IQR: 8.32–16.02 km) (Fig. 1). Under the conservative survivorship scenario, with the exception of BRFA B, home ranges observed for opakapaka were less than the linear habitat dimension of the BRFAs (Fig. 5). Three individuals (6.7% of 45) included in the optimistic scenario had home range estimates greater than the median linear habitat dimension of the BRFAs.

Quantifying movement frequency and site fidelity

Tracked fish generally stayed within the boundaries of the protected reserve. Under the conservative scenario, 5 of the 10 fish with valid tracks were detected crossing BRFA boundaries a combined 39 times during the first analysis period. This group had a high degree of site fidelity; on average, these fish spent 97.7% (SD 6.2) of their time within the BRFA during this period. Under the optimistic scenario, 11 of the 45 fish with valid or uncertain tracks were detected crossing BRFA boundaries a combined 94 times. Site fidelity was similarly high for these fish; on average, fish detected in this period spent 91.6% (SD 25.8) of their time within the BRFA.

Fish were rarely observed crossing reserve boundaries. Under the conservative scenario, the median number of total movements across BRFA boundaries for fish detected moving between protected and unprotected areas was 6 crossings/fish (IQR: 6–12 crossings/fish) over a track duration of 280 d (IQR: 230–293 d). Standardized by track duration, the median number of movements into or out of the BRFA for the 5 fish that crossed boundaries was 0.043 crossings·d^{-1}·fish^{-1} (IQR: 0.021–0.057 crossings·d^{-1}·fish^{-1}), a rate equivalent to 1 crossing every 23.3 d. However, rates for individuals were as high as 0.064 crossings/d, equivalent to 1 crossing every 15.7 d. Under the optimistic scenario, the median number of total movements across BRFA boundaries was 6 crossings/fish (IQR: 3.5–13.5 crossings/fish) over a median track duration of 95 d (IQR: 76.5–224.5 d). Standardized by track duration, the median number of movements into or out of the BRFA for the 11 fish that crossed boundaries was 0.061 crossings·d^{-1}·fish^{-1} (IQR: 0.028–0.168 crossings·d^{-1}·fish^{-1}), equivalent to 1 crossing every 16.4 d. However, rates for individuals were as high as 0.273 crossings/d, equivalent to 1 crossing every 3.6 d.

Under the conservative scenario, 2 of 8 fish considered to be alive and detected during the second analysis period crossed BRFA boundaries a combined total of 130 times (74 times and 56 times) over a track duration of 245 d. On average, the 8 fish spent the majority of their time (mean: 99.3% [SD 6.2]) within the BRFA. Standardized by their track lengths, these 2 fish moved into or out of the BRFA with 0.229 and 0.302 crossings/d, equivalent to 1 crossing every 4.4 and 3.3 d, respectively. Under the optimistic scenario, 5 of the 37 fish detected during the second period crossed the BRFA boundaries 145 times total. Similar to that of fish in the conservative scenario, site fidelity was high; on average, fish detected in this period spent 89.8% (SD 28.9) of their time within the BRFA. The median fish in this group crossed the BRFA boundaries at an average rate of 0.028 crossings/d (IQR: 0.003–0.149 crossings/d) over a mean track duration of 245 d (IQR: 245–245 d). Standardized by track duration, this rate was equivalent to 1 movement over reserve boundaries every 35.4 d. However, rates of individuals were as high as 0.156 crossings/d, equivalent to 1 crossing every 6.4 d.

Irrespective of analysis period or array shape, the 10 fish with tracks used in the conservative scenario were detected within the BRFA on 97.6% (SD 6.2) of days they were tracked, compared with 91.6% (SD 25.7) of tracked days for the 45 fish in the optimistic scenario. Under the conservative scenario, 226 total detected movements between protected and non-protected areas were made by 5 fish over a median track duration of 339 d (IQR: 186–453 d). These fish moved across boundaries at a rate of 0.17 crossings·d^{-1}·fish^{-1} (IQR: 0.03–0.18 crossings·d^{-1}·fish^{-1}) or 1 crossing every 5.8 d. Eleven of the 45 fish for which tracks were considered under the optimistic scenario were detected crossing the reserve boundaries a combined 301 times. The median fish spent 100% (1st quartile: 100; 3rd quartile: 100) of their time within the BRFA. The median fish detected moving across boundaries crossed BRFA boundaries 6 times (IQR: 3.5–24) over a median track duration of 350 d (IQR: 173.5–495.5 d), corresponding to 0.04 crossings/d

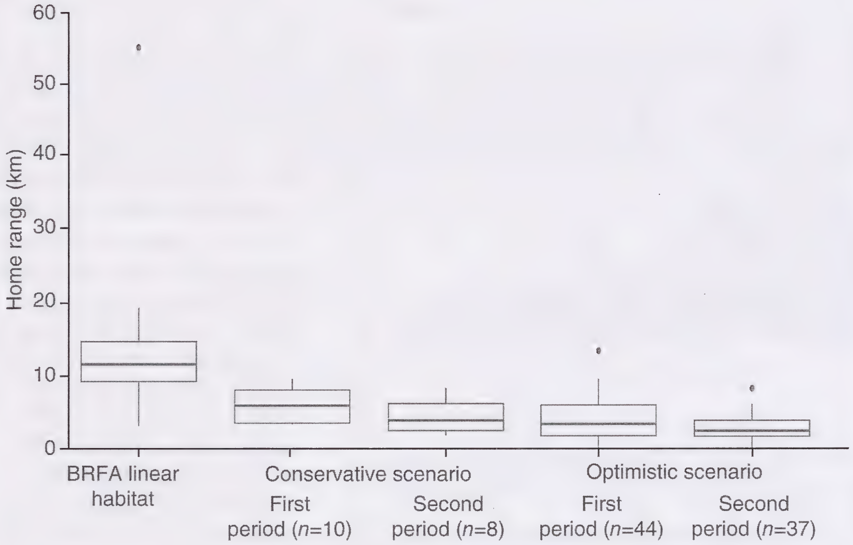

Figure 5

Box plot comparing the linear habitat dimensions of the 8 bottomfish restricted fishing areas (BRFAs) in the main Hawaiian Islands to the linear home ranges calculated for tagged opakapaka (*Pristipomoides filamentosus*) under 2 survivorship scenarios and for 2 analysis periods. The movements of tagged fish were tracked with an acoustic receiver array in the Makapuu region off Oahu and were analyzed during 26 June 2017–15 April 2018 (first analysis period) and 6 May 2018–6 January 2019 (second period). The conservative scenario includes only tracks of fish determined to be alive. The optimistic scenario includes tracks of fish for which survival could not be determined as well those of fish determined to be alive. The thick line within the box indicates the median, the upper and lower parts of the box represent the first and third quartiles (the 25th and 75th percentiles), the whiskers extending above and below the box correspond to 1.5 times the interquartile range, and dots represent values outside this range. *n*=number of samples.

(IQR: 0.015–0.21 crossings/d) and equivalent to 1 movement over reserve boundaries every 27 d. Rates of individuals were as high as 0.27 crossings/d, equivalent to 1 crossing every 3.7 d. Under both conservative and optimistic scenarios, there was a moderate correlation between the distance an individual's tagging location was from the reserve boundary and the probability that an individual was detected leaving the reserve (conservative: r=–0.43; optimistic: r=–0.36). Across both scenarios, only 1 fish (tag ID code: 28179) was detected leaving the reserve and did not return.

Discussion

In this study, opakapaka were monitored by using acoustic telemetry to compare home ranges of individual fish to estimates of the scale of protection under Hawaii's BRFA system. All of the linear home ranges calculated for fish under a conservative survivorship scenario were similar to each other in magnitude and smaller than the linear habitat dimension of BRFA E, where the fish were tracked. Only 2 fish included in the optimistic survivorship scenario had linear home ranges that exceeded the linear habitat dimension of BRFA E; however, it is possible that these fish had been eaten by predators. We were unable to detect any long-range movements of opakapaka because it was not possible to detect acoustic tags beyond the range of the receiver array. However, our findings are supported by the results of conventional tagging experiments for this species in which the majority of fish (>85%) were recaptured within 10 km of their tagging location (O'Malley[5]; Uehara et al., 2019). Despite minor differences, tracks of fish were similar under both conservative and optimistic survivorship scenarios. The median home range was relatively small (6.0 km for the conservative scenario and 3.6 km for the optimistic scenario). This result is not surprising because significant movement was a key requirement to qualify for the conservative scenario.

When broadening our comparison to include the 7 additional BRFAs, we found that the typical home range for tagged opakapaka under both scenarios was smaller than the minimum linear habitat dimension for all but 1 BRFA. It should be noted that the small linear habitat estimated for this reserve, BRFA B off the island of Niihau, is not representative of the total habitat within the area because the method used to quantify linear habitat uses the shortest path across the reserve and does not account for the large offshore pinnacle within this reserve (Fig. 1). When a similar least-cost path approach is applied around the pinnacle, the linear habitat of this BRFA increases from 3.0 km to 9.2 km. Our results are broadly consistent with those of studies that used baited underwater camera stations, indicating that the BRFAs do provide protection for bottomfish (Sackett et al., 2017). Our findings are also in agreement with those of aforementioned conventional tagging work done in the region in which the majority of fish were recaptured in close proximity to their tagging location (Kobayashi, 2008; O'Malley[5]).

Movements of opakapaka with valid tracks in this study are within the range of those reported for other snappers of the family Lutjanidae, species that have high site fidelity and limited home ranges with rare long-distance movements. Tinhan et al. (2014) reported that amarillo snapper (*Lutjanus argentiventris*) were detected in the Gulf of California within a 0.61-km^2 marine reserve on 49% (SD 30) of the days after they were tagged, and red snapper (*L. campechanus*) in the Gulf of Mexico have been associated within 26.3 m (SD 35.4) of artificial reefs (Piraino and Szedlmayer, 2014). In Hawaii, no discernable movement was observed for over 83.5% of tagged common bluestripe snapper (*L. kasmira*), and 95% of those fish were recaptured within 150 m of the location of their initial release (Friedlander et al., 2002). In another study, individual ehu and onaga tracked relative to BRFA B off the island of Niihau spent almost all of their time within the reserve and were detected moving distances up to 8.9 km (Weng, 2013). Even larger ranges have been described for green jobfish (*Aprion virescens*), a bottomfish species not included in the Deep-7 management unit, with individuals observed moving up to 18 km (Meyer et al., 2007). Movements of opakapaka deemed to be alive in this study fall between these reported ranges. However, we used range testing experiments to determine that 2.2 km would be used as the movement criteria to categorize fish status. Therefore, any tracks from surviving individuals with movements that were exclusively of shorter distances were classified as uncertain and included only in the optimistic scenario.

Estimates of postrelease survivorship of fish tagged in this study are low, between 5.6% and 25.1% depending on the inclusion of tracks classified as uncertain. These low survivorship rates mirror those of conventional mark-recapture work in which observed recapture rates for this species were 2.5% (O'Malley[5]), 12.0% (Kobayashi, 2008), and 8.7% (Uehara et al., 2019). Survivorship rates as high as 66.7% have been reported for opakapaka tagged with acoustic transmitters in the Kahoolawe Island Reserve (Ziemann and Kelley[8]); however, assumption of an individual's survival in that study was based on detection of a tag on at least one receiver, and no further steps to ascertain survivorship were performed. In our study, we applied a rigorous approach to determining the status of our fish and included in our analysis only tracks with durations of at least 14 d. If our approach to classifying tagged fish were applied to fish in the study conducted in the Kahoolawe Island Reserve, only 30.8% of tagged opakapaka would have been included. When we discussed approaches with authors of this other study, one of them told us that tagged fish were evaluated at the surface upon release and that those in poor condition were recaptured and their tag was removed (Kelley[14]).

Mortality following tagging is a major challenge to study of the movements of deepwater fish species (Edwards et al., 2019). The 2 major causes of mortality in our study are believed to be barotrauma and predation. Deep-7 species are physoclystic, that is, the gas bladder is not open to the gastrointestinal tract, making them particularly susceptible to barotrauma injuries from expansion of the swim bladder during rapid ascent following hooking (DeMartini et al., 1996; Edwards et al., 2019). Severe injury may result in organ damage and death (Rogers et al., 2011). Results from studies of methods that can mitigate barotrauma in deepwater rockfish species (*Sebastes* spp.) indicate that slow ascent rates, limited on-deck handling times, and rapid recompression improve survivorship outcomes (Rogers et al., 2011). External symptoms of barotrauma observed during this project included esophageal eversion and exophthalmia due to swim bladder expansion. Rapid release of air and deflation of the body cavity while the peritoneal incision was made was not uncommon and was likely caused by a rupture in the swim bladder. Barotrauma can also lead to physical and behavioral impairment that can result in subsequent predation (Rankin et al., 2017).

Sharks, marine mammals, and other potential predators were also a significant source of mortality. During our sampling, a number of opakapaka were consumed partially or totally by predators during ascent following hooking. Detection records for 65 tagged fish indicate a series of rapid movements between receivers immediately after tagging followed by no further detections or persistent detections at a single receiver. This type of tracking record is consistent with a tagged fish being inside the stomach of a predator with movement cessation occurring with expulsion of the tag. We suspect that the pulu used to aggregate bottomfish for capture in our study also attracted predators and exacerbated this issue. For future studies, it would be wise to first consider how variation in tagging methods may offset the mortality associated with tagging this and other deepwater fish species. Given the high rates of postrelease mortality observed in our study, protocols that reliably improve survivorship for this species should be explored.

Acoustic telemetry is an established tool for evaluating animal movements relative to marine reserves. Its application in this study at depths greater than 200 m is relatively novel and presented a number of challenges that studies in shallower environments do not have to address (Arnold and Dewar, 2001; Heupel et al., 2006; Pedersen et al., 2014; Edwards et al., 2019). A considerable amount of hardware associated with each receiver station was deployed over the duration of this study at operational depths that exceeded those accessible by scuba diving. Deployment at these depths necessitated servicing of receiver stations from a suitably sized vessel and introduced additional points of failure for each station and uncertainty to the data retrieved from them.

---

[14] Kelley, C. 2019. Personal commun. Dep. Oceanogr., Sch. Ocean Earth Sci. Tech., Univ. Hawaii Manoa, 1000 Pope Rd., Honolulu, HI 96822.

Close-proximity detection interference is a factor that must be accounted for when deploying acoustic tracking arrays at depths exceeding 200 m (Scherrer et al., 2018). Using a conservative model for predicting CPDI and a detection range of 847 m, we estimated that at 20 m above the seafloor, CPDI effects could extend between 70 and 451 m from the receiver depending on the receiver's depth. This model assumes that no energy is lost at the seafloor and sea surface and should be considered a worst-case scenario. Given the nominal transmission rate of the tags used and assuming an average swimming speed of 1 body length/s, we do not believe CPDI affected our ability to detect the passage of tagged fish transiting through fence receiver subarrays. However, if tagged individuals spent extensive time in the vicinity of deeper receivers, CPDI may have led to an underestimation of residency rates.

The loss of several stations reduced the capacity of the acoustic receiver array to monitor fish within and transiting into or out of the BRFA. Theoretical detection rates were calculated by using a telemetry optimization algorithm and the locations of receivers recovered during each analysis period (Pedersen et al., 2014). We estimated that receiver losses reduced the proportion of monitored habitat (100–400 m) within BRFA E from the planned 27.0% to 23.2% during the first analysis period. During the first period, the loss of receiver stations 333 and 340 from fence sub-arrays within the BRFA introduced the potential for undetected passage of individuals that transited into the BRFA, and such missed detections would result in an underestimation of site fidelity within the BRFA. Because observed site fidelity within the BRFA was quite high, it is unlikely that undetected movements significantly altered the conclusions of this analysis. During the second analysis period, loss of stations 314 and 317 from the outer southern fence sub-array and station 340 from the interior southern fence sub-array created a path where fish could theoretically swim undetected between protected and non-protected waters. The loss of these stations means that detected movements between protected and non-protected regions may underestimate true movement frequency and site fidelity within the reserve during this period.

Although genetic panmixia has been reported for opakapaka across the Hawaiian Archipelago, there is growing evidence to support spatially structured approaches to management (Gaither et al., 2011). Panmixia can occur even through a limited exchange of larvae and adult individuals, but large-scale exchanges are required to support spatially distinct populations (Wright, 1931; Botsford et al., 2003). Long-range movements greater than 300 km have been reported for tagged opakapaka, but the high degree of site fidelity observed in our study and reported from conventional mark-recapture studies indicates that such movements are rare for this species (Kobayashi, 2008; O'Malley[5]). These observations are consistent with those of baited-camera studies that indicate disproportionate measures of abundance and population structure between opakapaka inside and outside of reserve boundaries (Sackett et al., 2017). Furthermore, results from the use of simulation models of larval dispersal across the archipelago indicate that larvae are primarily retained in 4 self-sustained zones with only limited advection (Vaz, 2012). These observations support the use of spatially structured approaches to assessment and management of this species.

Acknowledgments

We thank the following individuals for their contributions to the project described here: M. Abe, L. Yamada, T. Swenarton, J. Harden, K. Pollock, C. Yamada, G. Shirakata, A. Lawyer, D. Lau, A. Shor, and R. Barnes. We are grateful to E. Franklin, J. Drazen, A. Neuheimer, E. Nosal, and 3 anonymous reviewers for their feedback on this manuscript. This work was funded by the Division of Aquatic Resources, Hawaii Department of Land and Natural Resources, through the Sport Fish Restoration (Dingell-Johnson) Program. This paper is University of Hawaii at Manoa School of Ocean and Earth Science and Technology contribution no. 10895.

Literature cited

Arnold, G., and H. Dewar.
2001. Electronic tags in marine fisheries research: a 30-year perspective. *In* Electronic tagging and tracking in marine fisheries (J. R. Sibert and J. L. Nielsen, eds.), p. 7–64. Kluwer Academic Publishers, Dordrecht, Netherlands.

Börger, L., N. Franconi, G. De Michele, A. Gantz, F. Meschi, A. Manica, S. Lovari, and T. Coulson.
2006. Effects of sampling regime on the mean and variance of home range size estimates. J. Anim. Ecol. 75:1393–1405.

Botsford, L. W., F. Micheli, and A. Hastings.
2003. Principles for the design of marine reserves. Ecol. Appl. 13:25–31.

Cailliet, G. M., A. H. Andrews, E. J. Burton, D. L. Watters, D. E. Kline, and L. A. Ferry-Graham.
2001. Age determination and validation studies of marine fishes: do deep-dwellers live longer? Exp. Gerontol. 36:739–764.

Comfort, C. M., and K. C. Weng.
2015. Vertical habitat and behaviour of the bluntnose sixgill shark in Hawaii. Deep-Sea Res., II 115:116–126.

Craig, P., B. Ponwith, F. Aitaoto, and D. Hamm.
1993. The commercial, subsistence, and recreational fisheries of American Samoa. Mar. Fish. Rev. 55(2):109–116.

Crossin, G. T., M. R. Heupel, C. M. Holbrook, N. E. Hussey, S. K. Lowerre-Barbieri, V. M. Nguyen, G. D. Raby, and S. J. Cooke.
2017. Acoustic telemetry and fisheries management. Ecol. Appl. 27:1031–1049.

DeMartini, E. E., F. A. Parrish, and D. M. Ellis.
1996. Barotrauma-associated regurgitation of food: implications for diet studies of Hawaiian pink snapper, *Pristipomoides filamentosus* (family Lutjanidae). Fish. Bull. 94:250–256.

Dwyer, R. G., H. A. Campbell, T. R. Irwin, and C. E. Franklin.
2015. Does the telemetry technology matter? Comparing estimates of aquatic animal space-use generated from

GPS-based and passive acoustic tracking. Mar. Freshw. Res. 66:654–664.

Edwards, J. E., J. Pratt, N. Tress, and N. E. Hussey.
2019. Thinking deeper: uncovering the mysteries of animal movement in the deep sea. Deep-Sea Res. Oceanogr., I 146:24–43.

Friedlander, M., J. D. Parrish, and R. C. DeFelice.
2002. Ecology of the introduced snapper *Lutjanus kasmira* (Forsskal) in the reef fish assemblage of a Hawaiian bay. J. Fish Biol. 60:28–48.

Friedlander, A. M., K. A. Stamoulis, J. N. Kittinger, J. C. Drazen, and B. N. Tissot.
2014. Chapter five—understanding the scale of marine protection in Hawai'i: from community-based management to the remote Northwestern Hawaiian Islands. Adv. Mar. Biol. 69:153–203.

Gaither, M. R., S. A. Jones, C. Kelley, S. J. Newman, L. Sorenson, and B. W. Bowen.
2011. High connectivity in the deepwater snapper *Pristipomoides filamentosus* (Lutjanidae) across the Indo-Pacific with isolation of the Hawaiian Archipelago. PLoS ONE 6(12):e28913.

Haight, W. R.
1989. Trophic relationships, density and habitat associations of deepwater snappers (Lutjanidae) from Penguin Bank, Hawaii. M.S. thesis, 89 p. Univ. Hawaii Manoa, Honolulu, HI.

Haight, W. R., D. R. Kobayashi, and K. E. Kawamoto.
1993. Biology and management of deepwater snappers of the Hawaiian Archipelago. Mar. Fish. Rev. 55(2):20–27.

Halpern, B. S.
2003. The impact of marine reserves: do reserves work and does reserve size matter? Ecol. Appl. 13(sp1):117–137.

Heupel, M. R., J. M. Semmens, and A. J. Hobday.
2006. Automated acoustic tracking of aquatic animals: scales, design and deployment of listening station arrays. Mar. Freshw. Res. 57:1–13.

Hill, N. J., T. Peatman, C. B. Wakefield, S. J. Newman, T. Halafihi, J. Kinch, C. T. T. Edwards, S. J. Nicol, and A. J. Williams.
2018. Improving guidelines for implementing harvest strategies in capacity-limited fisheries—lessons from Tonga's deepwater line fishery. Mar. Policy 98:85–91.

Huvenne, V. A. I., B. J. Bett, D. G. Masson, T. P. Le Bas, and A. J. Wheeler.
2016. Effectiveness of a deep-sea cold-water coral marine protected area, following eight years of fisheries closure. Biol. Conserv. 200:60–69.

Kami, H. T.
1972. The *Pristipomoides* (Pisces: Lutjanidae) of Guam with notes on their biology and fisheries aspects. M.S. thesis, 140 p. Univ. Guam, Mangilao, Guam.

Kelley, C. D., and W. Ikehara.
2006. The impacts of bottomfishing on Raita and West St. Rogatien Banks in the Northwestern Hawaiian Islands. Atoll Res. Bull. 543:305–318.

Kessel, S. T., N. E. Hussey, D. M. Webber, S. H. Gruber, J. M. Young, M. J. Smale, and A. T. Fisk.
2015. Close proximity detection interference with acoustic telemetry: the importance of considering tag power output in low ambient noise environments. Anim. Biotelem. 3:5.

Kobayashi, D. R.
2008. Spatial connectivity of Pacific insular species: insights from modeling and tagging. Ph.D. thesis, 215 p. Univ. Technol. Sydney, Sydney, Australia. [Available from website.]

Langseth, B., J. Syslo, A. Yau, M. Kapur, and J. Brodziak.
2018. Stock assessment for the main Hawaiian Islands Deep 7 bottomfish complex in 2018, with catch projections through 2022. NOAA Tech. Memo. NMFS-PIFSC-69, 217 p.

Medved, R. J.
1985. Gastric evacuation in the sandbar shark, *Carcharhinus plumbeus*. J. Fish Biol. 26:239–253.

Meyer, C. G., Y. P. Papastamatiou, and K. N. Holland.
2007. Seasonal, diel, and tidal movements of green jobfish (*Aprion virescens*, Lutjanidae) at remote Hawaiian atolls: implications for marine protected area design. Mar. Biol. 151:2133–2143.

Misa, W. F. X. E., J. C. Drazen, C. D. Kelley, and V. N. Moriwake.
2013. Establishing species-habitat associations for 4 eteline snappers with the use of a baited stereo-video camera system. Fish. Bull. 111:293–308.

Moffitt, R. B., and F. A. Parrish.
1996. Habitat and life history of juvenile Hawaiian pink snapper, *Pristipomoides filamentosus*. Pac. Sci. 50:371–381.

Moore, C., J. C. Drazen, B. T. Radford, C. Kelley, and S. J. Newman.
2016. Improving essential fish habitat designation to support sustainable ecosystem-based fisheries management. Mar. Policy 69:32–41.

Newman, S. J., C. B. Wakefield, A. J. Williams, J. M. O'Malley, S. J. Nicol, E. E. DeMartini, T. Halafihi, J. Kaltavara, R. L. Humphreys, B. M. Taylor, et al.
2015. International workshop on methodological evolution to improve estimates of life history parameters and fisheries management of data-poor deep-water snappers and groupers. Mar. Policy 60:182–185.

Newman, S. J., A. J. Williams, C. B. Wakefield, S. J. Nicol, B. M. Taylor, and J. M. O'Malley.
2016. Review of the life history characteristics, ecology and fisheries for deep-water tropical demersal fish in the Indo-Pacific region. Rev. Fish Biol. Fish. 26:537–562.

Oyafuso, Z. S., J. C. Drazen, C. H. Moore, and E. C. Franklin.
2017. Habitat-based species distribution modelling of the Hawaiian deepwater snapper-grouper complex. Fish. Res. 195:19–27.

Oyafuso, Z. S., P. S. Leung, and E. C. Franklin.
2019. Evaluating bioeconomic tradeoffs of fishing reserves via spatial optimization. Mar. Policy 100:163–172.

Palumbi, S. R.
2004. Marine reserves and ocean neighborhoods: the spatial scale of marine populations and their management. Annu. Rev. Environ. Resour. 29:31–68.

Pante, E., and B. Simon-Bouhet.
2013. marmap: a package for importing, plotting and analyzing bathymetric and topographic data in R. PLoS ONE 8(9):e73051.

Parke, M.
2007. Linking Hawaii fisherman reported commercial bottomfish catch data to potential bottomfish habitat and proposed restricted fishing areas using GIS and spatial analysis. NOAA Tech. Memo. NMFS-PIFSC-11, 37 p.

Parrish, F. A., N. T. Hayman, C. Kelley, and R. C. Boland.
2015. Acoustic tagging and monitoring of cultured and wild juvenile crimson jobfish (*Pristipomoides filamentosus*) in a nursery habitat. Fish. Bull. 113:231–241.

Pedersen, M. W., G. Burgess, and K. C. Weng.
2014. A quantitative approach to static sensor network design. Methods Ecol. Evol. 5:1043–1051.

Piraino, M. N., and S. T. Szedlmayer.
2014. Fine-scale movements and home ranges of red snapper around artificial reefs in the northern Gulf of Mexico. Trans. Am. Fish. Soc. 143:988–998.

Pooley, S. G.
1993. Economics and Hawaii's marine fisheries. Mar. Fish. Rev. 55(2):93–101.

R Core Team.
2018. R: a language and environment for statistical computing. R Foundation for Statistical Computing, Vienna, Austria. [Available from website, accessed June 2018.]

Rankin, P. S., R. W. Hannah, M. T. O. Blume, T. J. Miller-Morgan, and J. R. Heidel.
2017. Delayed effects of capture-induced barotrauma on physical condition and behavioral competency of recompressed yelloweye rockfish, *Sebastes ruberrimus*. Fish. Res. 186:258–268.

Roberts, C. M., G. Branch, R. H. Bustamante, J. C. Castilla, J. Dugan, B. S. Halpern, K. D. Lafferty, H. Leslie, J. Lubchenco, D. McArdle, et al.
2003. Application of ecological criteria in selecting marine reserves and developing reserve networks. Ecol. Appl. 13(sp1):215–228.

Rogers, B. L., C. G. Lowe, and E. Fernández-Juricic.
2011. Recovery of visual performance in rosy rockfish (*Sebastes rosaceus*) following exophthalmia resulting from barotrauma. Fish. Res. 112:1–7.

Sackett, D. K., J. C. Drazen, V. N. Moriwake, C. D. Kelley, B. D. Schumacher, and W. F. X. E. Misa.
2014. Marine protected areas for deepwater fish populations: an evaluation of their effects in Hawai'i. Mar. Biol. 161:411–425.

Sackett, D. K., C. D. Kelley, and J. C. Drazen.
2017. Spilling over deepwater boundaries: evidence of spillover from two deepwater restricted fishing areas in Hawaii. Mar. Ecol. Prog. Ser. 568:175–190.

Schadt, S., F. Knauer, P. Kaczensky, E. Revilla, T. Wiegand, and L. Trepl.
2002. Rule-based assessment of suitable habitat and patch connectivity for the Eurasian lynx. Ecol. Appl. 12:1469–1483.

Scherrer, S. R., B. P. Rideout, G. Giorli, E.-M. Nosal, and K. C. Weng.
2018. Depth- and range-dependent variation in the performance of aquatic telemetry systems: understanding and predicting the susceptibility of acoustic tag–receiver pairs to close proximity detection interference. PeerJ 6:e4249.

Stickel, L. F.
1954. A comparison of certain methods of measuring ranges of small mammals. J. Mammal. 35:1–15.

Stumpf, W. A., and C. O. Mohr.
1962. Linearity of home ranges of California mice and other animals. J. Wildl. Manage. 26:149–154.

Tinhan, T., B. Erisman, O. Aburto-Oropeza, A. Weaver, D. Vázquez-Arce, and C. G. Lowe.
2014. Residency and seasonal movements in *Lutjanus argentiventris* and *Mycteroperca rosacea* at Los Islotes Reserve, Gulf of California. Mar. Ecol. Prog. Ser. 501:191–206.

Uehara, M., A. Ebisawa, I. Ohta, and Y. Aomuma.
2019. Effectiveness of deepwater marine protected areas: implication for Okinawan demersal fisheries management. Fish. Res. 215:123–130.

Vaz, A. C.
2012. Here today, gone tomorrow: flow variability, larval dispersal and fisheries management in Hawai'i. Ph.D. diss., 122 p. Univ. Hawaii Manoa, Honolulu, HI. [Available from website.]

Wakefield, C. B., J. M. O'Malley, A. J. Williams, B. M. Taylor, R. S. Nichols, T. Halafihi, R. L. Humphreys, J. Kaltavara, S. J. Nicol, and S. J. Newman.
2017. Ageing bias and precision for deep-water snappers: evaluating nascent otolith preparation methods using novel multivariate comparisons among readers and growth parameter estimates. ICES J. Mar. Sci. 74:193–203.

Weng, K. C.
2013. A pilot study of deepwater fish movement with respect to marine reserves. Anim. Biotelem. 1:17.

Williams, A., N. J. Bax, R. J. Kloser, F. Althaus, B. Barker, and G. Keith.
2009. Australia's deep-water reserve network: implications of false homogeneity for classifying abiotic surrogates of biodiversity. ICES J. Mar. Sci. 66:214–224.

Williams, A. J., S. J. Nicol, N. Bentley, P. J. Starr, S. J. Newman, M. A. McCoy, J. Kinch, P. G. Williams, F. Magron, G. M. Pilling, et al.
2012. International workshop on developing strategies for monitoring data-limited deepwater demersal line fisheries in the Pacific Ocean. Rev. Fish Biol. Fish. 22:527–531.

Wright, S.
1931. Evolution in Mendelian populations. Genetics 16:97–159.

National Marine
Fisheries Service
NOAA

Fishery Bulletin
established in 1881

Spencer F. Baird
First U.S. Commissioner
of Fisheries and founder
of *Fishery Bulletin*

Effects of the biomedical bleeding process on the behavior and hemocyanin levels of the American horseshoe crab (*Limulus polyphemus*)

Meghan Owings (contact author)[1]
Christopher Chabot[2]
Winsor Watson III[1]

Email address for contact author: mwowings1@gmail.com

[1] Department of Biological Sciences
School of Marine Sciences and Ocean Engineering
University of New Hampshire
46 College Road
Durham, New Hampshire 03824

[2] Department of Biological Sciences
Plymouth State University
17 High Street
Plymouth, New Hampshire 03264

Abstract—When the blood of American horseshoe crabs (*Limulus polyphemus*) is extracted to create *Limulus* amebocyte lysate, the crabs are often subjected to warm temperatures and time out of water, in addition to blood loss. The goal of this study was to determine the effects of these 3 stressors on the locomotor activity and hemocyanin (HCY) levels of American horseshoe crabs. We found that a full bleeding treatment involving all 3 stressors had the biggest impact on mortality and HCY levels, followed by bleeding along with at least 1 other stressor. All of the treatments resulted in similar small changes in their overall activity and in the types of biological rhythms expressed. There was greater overall activity in animals that had higher HCY levels ($P<0.0001$). We also found that HCY levels were lowest in the spring and early summer and highest in the late summer and fall. In each month, males had higher HCY levels than females. These results indicate that low HCY concentrations can negatively affect the health of horseshoe crabs. If biomedical facilities take sex differences and seasonal fluctuations in HCY levels into account, they might be able to reduce some of the deleterious effects of the bleeding process.

Manuscript submitted 23 January 2020.
Manuscript accepted 20 July 2020.
Fish. Bull. 118:225–239 (2020).
Online publication date: 13 August 2020.
doi: 10.7755/FB.118.3.2

The views and opinions expressed or implied in this article are those of the author (or authors) and do not necessarily reflect the position of the National Marine Fisheries Service, NOAA.

Limulus amebocyte lysate, a substance that can be extracted from the blood of the American horseshoe crab (*Limulus polyphemus*), is widely used to test the sterility of pharmaceuticals and medical implants. In order to provide sufficient *Limulus* amebocyte lysate, approximately 600,000 American horseshoe crabs are bled each year (ASMFC, 2019). It is not clear if this level of harvest can be sustained because of the lethal and sublethal effects of the bleeding procedure. Findings from several studies indicate that blood extraction results in varying levels of mortality (reviewed in Krisfalusi-Gannon et al., 2018). Although the entire biomedical bleeding process involves several stressors, the blood removal itself results in increased rates of mortality compared with those of control animals (Rudloe, 1983; Kurz and James-Pirri, 2002), and the amount of blood removed has an impact on how many die from the procedure. When animals had 10–30% of their blood volume removed, only 8% of the animals died, but when 40% of their volume was removed, the mortality rate was 29% (Hurton and Berkson, 2006). Mortality rates associated with the full bleeding treatment, which includes some additional stressors described later, have ranged from 5% to 30% (Thompson, 1998; Walls and Berkson, 2000, 2003; Hurton and Berkson, 2006; Leschen and Correia, 2010; Anderson et al., 2013), with differential mortality rates between the sexes (15% for males and up to 29% for females; Leschen and Correia, 2010; James-Pirri et al., 2012).

When American horseshoe crabs are harvested and transported back and forth to the bleeding facilities, they are subjected to a variety of stressors, including exposure to air and warm temperatures. For example, they spend a significant amount of time out of water when they are left on the decks of boats, and on docks, or are in the trucks that transport them to and from bleeding facilities (ASMFC[1]). In addition, because they are often in direct sunlight on vessels and docks or are transported in trucks with poor temperature control (ASMFC[1]), they are exposed to temperatures that are much warmer than the water from which they are captured. Finally, because up to 30% of their blood is removed, many of the important functions of hemolymph will be compromised (Novitsky, 1984; James-Pirri et al., 2012). The 6 major biomedical companies in the United States have slightly different collection, handling, and bleeding procedures; nonetheless, American horseshoe crabs must endure varying amounts of 3 stressors: air exposure, elevated temperatures, and blood loss.

---

[1] ASMFC (Atlantic States Marine Fisheries Commission). 2012. 2012 review of the fishery management plan in 2011 for horseshoe crab (*Limulus polyphemus*), 15 p. Prepared by the ASMFC Horseshoe Crab Plan Review Team. ASMFC, Arlington, VA. [Available from website.]

Although mortality often occurs as a result of the biomedical bleeding process, it is not clear what parts of the process have the greatest impacts on the probability that animals will die during, or after, the procedure. Hurton and Berkson (2006) found that mortalities of American horseshoe crabs significantly increased when they exposed them to a combination of stressors, and studies of techniques in the capture of other marine species also have revealed that mortality is affected by the synergistic combination of multiple stressors (Schisler et al., 2000; Schulz and Dabrowski, 2001; Hatch and Blaustein, 2003). Therefore, Hurton and Berkson (2006) highlighted the need for studying the cumulative effect of the multiple stressors that American horseshoe crabs experience during the bleeding process. One of the major goals of this study was to identify which of these stressors contributes to the behavioral and physiological deficits (described later) that have been observed in some American horseshoe crabs subjected to the entire process.

American horseshoe crabs that survive the biomedical bleeding process may take some time to fully recover. For example, Novitsky (1984) found that it takes 3–7 d for a bled American horseshoe crab to regain its total blood volume and up to 4 months for amebocytes to return to baseline levels. James-Pirri et al. (2012) reported that bled American horseshoe crabs released back into their natural environment had a random direction of movement compared with the movement patterns of control animals, and Anderson et al. (2013) found that the bleeding process led to decreases in activity levels, expression of circatidal rhythms, linear and angular movement velocities, and hemocyanin (HCY) levels. Finally, we recently found that, although bled animals released back into their natural habitat had seasonal movement patterns and overall activity levels that were similar to control animals, bled females spawned less during the 2-week period after they were released (Owings et al., 2019). This result motivated us to examine the effect of bleeding in a more controlled environment, one in which we could more continuously monitor behavior and HCY levels of animals.

Because of the variety of important functions of HCY, reductions in HCY levels due to bleeding could lead to decreases in fitness of the American horseshoe crab. Hemocyanin is important for transporting oxygen (Redmond, 1955; Mangum, 1980), eliciting the primary immune response (Coates et al., 2011), contributing to wound repair and cuticle hardening (Adachi et al., 2005a), molting (Adachi et al., 2005a, 2005b; Kuballa and Elizur, 2008; Kuballa et al., 2011; Glazer et al., 2013), and osmoregulation (Paul and Pirow, 1998). Furthermore, environmental conditions, such as increased temperatures and air exposure, can affect HCY concentrations (Mangum, 1980; Burnett, 1988; Coates et al., 2012). In fact, the combination of warm temperatures, which elevate the metabolic rate of animals and reduce the amount of oxygen in the water, air exposure, which makes it harder for gills to obtain oxygen, and blood loss, which makes oxygen transportation more difficult, can compromise the ability of the American horseshoe crab to provide sufficient oxygen to cells in need. Therefore, the combination of stressors associated with the bleeding process could have much more severe consequences than blood loss alone.

In this study, our main objective was to determine which of the 3 stressors or combination of these stressors (Table 1) had the largest impact on the behavior and physiology of the American horseshoe crab. Animals were collected from the Great Bay Estuary in Durham, New Hampshire, baseline levels of HCY and locomotor activity were obtained, and subsets of the animals were exposed to each stressor combination (e.g., bled and exposed to air, unbled and exposed to air, and bled and elevated temperatures). Then we monitored their behavior and HCY levels for 2 weeks posttreatment in the laboratory.

Materials and methods

Animal collection and experimental setup

In 2016, 48 male American horseshoe crabs were collected by scuba divers at Fox Point in the Great Bay Estuary during June–October. In 2017, 63 female American horseshoe crabs were collected by scuba divers at Fox Point in June and July. All captured crabs were brought back to the University of New Hampshire Jackson Estuarine Laboratory (JEL), where an initial blood sample was collected and animals were fitted with HOBO[2] accelerometers (HOBO Pendant G Data Loggers, Onset Computer Corp., Bourne, MA). The HOBO accelerometers were used to record triaxial orthogonal measurements of the acceleration (in meters per second) of individual American horseshoe crabs, and they were programmed to record a reading every minute. The accelerometers were attached to the dorsal carapace of each individual by first creating a harness, with 2 cable ties attached to the center of the prosoma with duct tape and cyanoacrylate, and then placing the accelerometer faceup in the harness and fastening cable ties over it. This arrangement made it relatively easy to weekly remove the accelerometers, download the data, and then replace them again with minimal disturbance of the animals.

---

[2] Mention of trade names or commercial companies is for identification purposes only and does not imply endorsement by the National Marine Fisheries Service, NOAA.

Table 1

The combinations of stressors and the time periods for treatments to which groups of American horseshoe crabs (*Limulus polyphemus*), collected in the Great Bay Estuary in New Hampshire, were exposed during laboratory experiments in 2016 and 2017. Treatments included 1 or more of the following 3 stressors: exposure to air, exposure to heat, or bleeding. These 3 stressors were chosen to simulate what American horseshoe crabs experience during the biomedical bleeding process, as well as during capture and transport. Several of the treatments were repeated in 2016 and 2017. In 2017, for some of the groups exposed to air, animals were covered with moist burlap. The average water temperature for each month is also provided.

	Time period				
	2016			2017	
Treatment group	June	August	October	June	July
Temperature	18.4°C	22.3°C	14.0°C	17.7°C	20.7°C
Control	×			×	×
Bled	×			×	×
Air		×			
Air (burlap)				×	×
Air and bled		×			
Air and bled (burlap)				×	×
Air and heat			×		
Air and heat (burlap)				×	×
Air, heat, and bled			×	×	×
Air, heat, and bled (burlap)				×	×

Animals were then placed into individual circular mesh enclosures (1-m diameter) within larger flow-through 850-L tanks (183 × 92 × 50 cm) filled with estuarine water and located outside of JEL. There were 2 enclosures per tank, and they were exposed to natural light and a dark cycle (enclosures were not covered). HOBO temperature data loggers (Onset Computer Corp.) were placed in the tanks to monitor the water temperature for the duration of each of the experiments. Behavioral data were collected for 1 week prior to exposure of animals to a given treatment, and then blood samples were taken and data were downloaded from the accelerometers.

Once the accelerometers were reattached, individuals underwent their designated treatment (described later) and then were returned to their tanks. Animals were kept in these tanks for 2 weeks after undergoing treatment, and their activity was monitored continuously, as described previously. Additional hemolymph samples were taken from each animal 7 and 14 d after their treatments.

Treatment groups

Animals were assigned to different treatment groups on the basis of which of the following 3 stressors, or combination of these stressors, to which they were exposed: bleeding, air exposure, and heat (Table 1). All experiments were carried out during June–October of 2016 and June–July of 2017. In 2016, 3 trials were completed, with 2 treatment groups of 8 animals each, per trial. In 2017, 2 trials were carried out, 1 trial in June and 1 trial in July, and each trial involved all of the treatment groups. There were 5 animals per treatment group in June and 4 animals per group in July.

Biomedical bleeding procedure

After all animals were monitored for baseline activity for 1 week, another 1-mL hemolymph sample was taken, and they were exposed to their randomly designated stressors (Table 2). The full bleeding treatment took 52 h, a time that was chosen to mimic the procedure used in several previously published studies (Hurton and Berkson, 2006; Leschen and Correia, 2010; Anderson et al., 2013; Owings et al., 2019) and to be similar to what animals may experience when bled by companies in the biomedical industry. First, American horseshoe crabs were placed in 189-L plastic barrels, and HOBO temperature data loggers were placed in each of the barrels. Then, the barrels were placed outside of JEL for 4 h, or next to a space heater in the JEL greenhouse, depending upon the temperature and ambient sunlight during the selected day; mean temperature during this time, for all trials, was 31.5°C (standard deviation [SD] 1.9). This step was designed to replicate the duration of time spent on the deck of a boat or on a dock in the summer prior to transport to a biomedical bleeding facility.

After the first 4 h, the barrels were placed in the back of a car and driven around for an additional 4 h to simulate time spent in a truck traveling to a bleeding facility

Table 2

Summary of the schedule of treatment activities for each experiment conducted in 2016 and 2017 on American horseshoe crabs (*Limulus polyphemus*) collected in the Great Bay Estuary in New Hampshire. Animals were assigned to different treatment groups and exposed to stressors to determine their effects on locomotor activity and hemocyanin levels.

Day	Treatment activity
1	1-mL hemolymph sample taken. Placed in individual tanks for 1 week for collection of baseline behavioral data.
8	1-mL hemolymph sample taken. First day of treatment.
9	Second day of treatment. Hemolymph extracted if bled.
10	Third and last day of treatment. Returned to tanks.
17	1-mL hemolymph sample taken. Data downloaded from accelerometers.
24	1-mL hemolymph sample taken. Experiment ended.

(23.3°C [SD 2.4]). Then, the barrels were placed indoors for 16 h at JEL to simulate time spent overnight at a bleeding facility (20.0°C [SD 2.1]). Finally, 30% of their hemolymph was extracted (Hurton et al., 2005), and they were returned to their barrels where they remained for another 24 h to replicate a second night at a bleeding facility (19.4°C [SD 1.9]). The barrels were then placed back into a car for 4 h (22.3°C [SD 2.2]) to simulate transportation back to the dock, where they would be loaded on vessels and returned to their capture location. Lastly, all animals were returned to their respective flow-through estuarine-water tanks, and their activity and HCY levels were monitored for another 2 weeks.

Control animals remained in their tanks throughout the duration of the experiment, except when blood samples were collected or data were downloaded from accelerometers. Animals that were in the control group also remained in the outdoor tanks, except for when 30% of their hemolymph was extracted on day 10 and for the brief periods of time when blood samples were collected approximately every 7–10 d. The animals that were exposed to one or more of the stressors were treated as outlined as follows, and each stressor was provided in the same manner as described previously for the full treatment:

- Bled: animals were subjected to hemolymph extraction on the second day of treatment.
- Air: on the first day of treatment, animals were placed inside the barrels inside JEL for the first 4 h. They were not left outside in direct sunlight or next to a space heater.
- Heat: animals were exposed to direct sunlight or next to a space heater for the first 4 h.
- Burlap: animals were treated like those in the group exposed to air but were covered with moist burlap when they were in the barrels.
- Two stressors: animals were treated just like those exposed to the full treatment, except at least one of the stressors was omitted. For example, animals exposed to air and bled were treated the same as those subjected to the full treatment, but they were not exposed to heat while they were in the barrels.
- All 3 stressors (full treatment): described previously.

Hemolymph extraction

Hemolymph was extracted following the procedures of Armstrong and Conrad (2008) and Anderson et al. (2013). First, the membrane between the prosoma and opisthosoma was exposed and cleaned with 70% ethanol. Then an 18-gauge needle was inserted through the membrane and into the underlying heart, and hemolymph was withdrawn and placed in pre-chilled 50-mL conical tubes. An estimated 30% of the total hemolymph volume was extracted, if possible. The tubes containing the extracted blood were then placed on ice until further examination. Total hemolymph volume for each individual was calculated by using the following equation from Hurton et al. (2005):

$$H = 25.7e^{0.1928(IO)};$$

where H = hemolymph volume (in milliliters); and
IO = interocular width (in centimeters).

Concentrations of HCY (in milligrams per milliliters) were measured by using a modified procedure from Coates et al. (2012) and Anderson et al. (2013). Briefly, hemolymph samples were centrifuged for 10 min at 3000 g and 4°C. Then, an aliquot of hemolymph was diluted (1:100) in 0.1 M Tris-HCl buffer (pH 7.5) in a quartz cuvette with a path length of 1 cm. The absorbance was measured at 280 nm on an Ultrospec 3100 pro UV/Visible spectrophotometer (Biochrom Ltd., Cambridge, UK). Values were standardized by using a predetermined absorption coefficient of 1.39 mg/mL HCY solution (Coates et al., 2012). This value was verified by using a Pierce Modified Lowry Protein Assay Kit (ThermoFisher Scientific Inc., Waltham, MA).

Data analyses

Because of variations in the baseline data for all the animals exposed to treatments, data were converted and are shown as percentages of baseline for HCY levels and overall activity. This conversion or normalization approach also allowed us to pool treatment groups together (Table 3), except for the air, heat, and bled groups between 2016 and 2017 because there were significant differences in baseline HCY and activity levels between these groups in the these years as well as a large difference in water temperatures (2016: 14.0°C [SD 1.9]; 2017: 19.2°C [SD 1.7]).

Multivariate analyses of variance (MANOVA) were used to test for effects of time and treatment groups on HCY

Table 3

Treatment groups for which data were pooled in analyses of the effects of stressors on American horseshoe crabs (*Limulus polyphemus*) in laboratory experiments conducted in 2016 and 2017. Treatments included 1 or more of the following 3 stressors: exposure to air, exposure to heat, or bleeding. For every treatment that was repeated more than one time, data for baseline levels of hemocyanin and activity, and for water temperatures, were pooled, except for data from applications of the full bleeding treatment (all 3 stressors) in 2016, because of differences in baseline data and water temperatures between 2016 and 2017. Data from the only 2 experiments involving the full treatment in 2017 were grouped because of similarities in baseline hemocyanin and activity levels, as well as in water temperatures. In 2017, for some of the groups exposed to air or heat, animals were covered with moist burlap. The time periods of treatments and the average water temperature for each month are also provided. Animals used in experiments were collected in the Great Bay Estuary in New Hampshire.

	Time period					
	2016			2017		
Treatment group	June	August	October	June	July	Pooled
Temperature	18.4°C	22.3°C	14.0°C	17.7°C	20.7°C	
Control	×			×	×	Yes
Bled	×			×	×	Yes
Air		×				No
Air (burlap)				×	×	Yes
Air and bled		×				No
Air and bled (burlap)				×	×	Yes
Air and heat			×			No
Heat (burlap)				×	×	Yes
Air, heat, and bled			×	×	×	2016: No; 2017: Yes
Air, heat, and bled (burlap)				×	×	Yes

levels and on overall activity. Two-way analyses of variance were also used to test for effects of different months and years, as well as of different months and sexes, on HCY levels. Tukey's honestly significant difference (HSD) post hoc test was used to examine significant differences between means of treatment groups for HCY and overall activity levels across different months, years, and sexes, with a threshold significance level (α) of 0.05. Unpaired Student's *t*-tests were used to compare baseline HCY levels in animals that died with those in animals that survived. Correlation and linear regression analyses were used to determine relationships between HCY concentrations and overall activity levels.

An acceleration threshold of 0.1 m/s^2 (Watson et al., 2016) was used to classify an animal as being either active or inactive. Then these data were examined in 5-min bins, and if an animal exceeded the 0.1 m/s^2 threshold during any of the minutes in that 5-min bin, it was considered to have been active for that 5-min period. These values were used to create actograms by using ActogramJ and were analyzed to determine the types of rhythms expressed by animals (Schmid et al., 2011). Specifically, the Lomb–Scargle method was used to determine when animals had significant circatidal (~12.4 h) or daily (~24 h) rhythms, with peaks exceeding an α of 0.001 (tidal range: 10–14 h; daily range: 22–26 h). Animals were considered arrhythmic if no significant peaks were observed in either range).

Results

Mortality

Combined mortality rates varied across the different experimental groups, and with the exception of the control group, there was at least one mortality resulting from each of the 3 different individual stressors (air exposure, heat, and bleeding) (Table 4). The overall mortality rate from all of the treatment groups, not including control animals, was 17%. All mortalities (number of samples [*n*]=15) occurred 1–2 d posttreatment, except for the death of one animal in the group exposed to all stressors that died 12 d posttreatment.

In 2016, when we used all males, there were only 2 mortalities throughout all of the treatment groups (Table 4). One mortality was in the bled group (*n*=7), and the second was in the group bled and exposed to air (*n*=7). In 2017, we used all females, and there were 13 mortalities. In June 2017, there were 4 mortalities, all in American horseshoe crabs that received the full bleeding treatment. In July 2017, there were 9 mortalities, including 6 of the 8 animals in the full bleeding treatment groups (with and without burlap). It should be noted that the water temperatures were warmer in July than in June (average: 17.7°C [SD 2.1] in June and 20.7°C [SD 1.2] in July), and this difference in temperatures might have been one reason why there were more mortalities in July.

Table 4

Number of mortalities and mortality rates of American horseshoe crabs (*Limulus polyphemus*) in each of the different treatment groups of experiments that exposed animals to air, heat, or bleeding. Several of the treatments were repeated in 2016 and 2017. In 2017, for some of the groups exposed to air, animals were covered with moist burlap. The time periods of treatments and the average water temperature are provided for each month. Mortalities are given as the number of animals that died per the number of animals in a treatment, and mortality rates are given as percentages. Animals used in experiments were collected in the Great Bay Estuary in New Hampshire.

	Time period					
	2016			2017		
Treatment group	June	August	October	June	July	Combined mortality rate
Temperature	18.4°C	22.3°C	14.0°C	17.7°C	20.7°C	
Control	0/8			0/4	0/4	0%
Bled	1/7; 14%			0/5	0/4	6%
Air		0/8				0%
Air (burlap)				0/5	2/4; 50%	22%
Air and bled		1/7; 14%				14%
Air and bled (burlap)				0/4	1/4; 25%	13%
Air and heat			0/7			0%
Air and heat (burlap)				0/4	0/4	0%
Air, heat, and bled			0/8	2/4; 50%	4/4; 100%	2016: 0%; 2017: 75%
Air, heat, and bled (burlap)				2/5; 40%	2/4; 50%	44%

Hemocyanin levels

Effects of different treatments The average baseline HCY level for all animals was 40 mg/mL (SD 20), with a maximum value of 96 mg/mL and a minimum value of 2 mg/mL. Because of this variability in the initial HCY levels, data are expressed as percent changes from the baseline levels. Every treatment group had a decrease over time in HCY levels from the baseline concentration, including the control group (MANOVA: $F_{(9,240)}$=6.09, $P<0.0001$) and all groups combined (MANOVA: $F_{(2,240)}$=44.5, $P<0.0001$), but changes were more pronounced in certain groups (Fig. 1). There was a significant interaction between treatment and time on HCY levels (MANOVA: $F_{(18,240)}$=2.112, P=0.006). Post hoc analyses revealed that the HCY concentrations in the control group and the groups exposed to air (with burlap), and heat (with burlap) treatments (data not shown) were significantly higher than those of the group that received the full bleeding treatment (air, heat, and bled) over time (Tukey's HSD test: $P<0.05$).

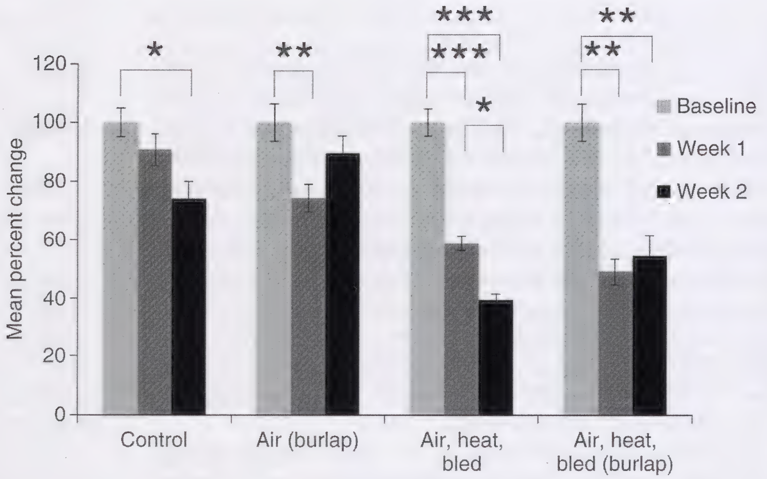

Figure 1

Mean percent change in hemocyanin concentrations of American horseshoe crabs (*Limulus polyphemus*) from baseline levels before treatments to levels 1 and 2 weeks after exposure to stressors in laboratory experiments conducted in 2016 and 2017. The treatment groups included a control group (number of animals [n]=16), a group of animals exposed to air only and covered with moist burlap (n=7), and groups of animals exposed to air, heat, and bleeding without (n=8) and with (n=5) a burlap cover. Significant differences between baseline levels and levels 1 and 2 weeks after treatment are denoted with asterisks: $P<0.05$ (*), $P<0.01$ (**), and $P<0.001$ (***). Error bars indicate standard errors of the mean. Animals used in experiments were collected in the Great Bay Estuary in New Hampshire.

Seasonal differences Male American horseshoe crabs were collected from

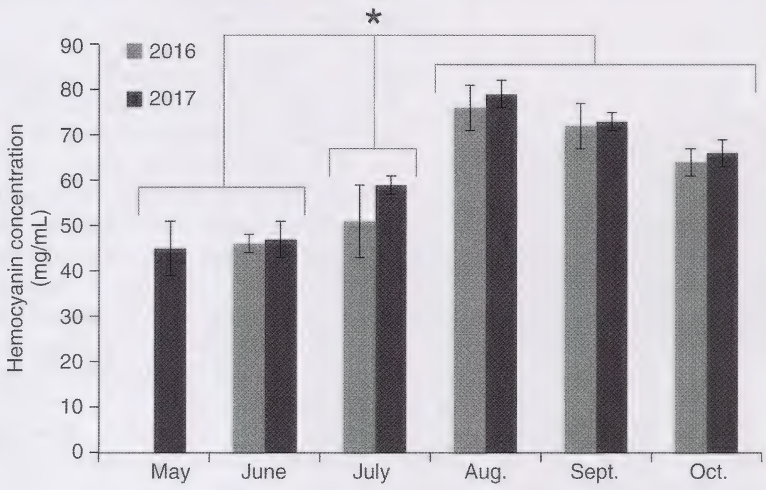

Figure 2

Monthly mean hemocyanin concentrations of male American horseshoe crabs (*Limulus polyphemus*) collected during 2016 and 2017 in the Great Bay Estuary in New Hampshire. The numbers of animals for which hemocyanin concentrations were measured in 2016 and 2017 are respectively 0 and 12 in May, 16 and 10 in June, 3 and 31 in July, 16 and 38 in August, 16 and 15 in September, and 16 and 8 in October. Significant differences between months ($P<0.001$) are denoted with an asterisk (*). Error bars indicate the standard errors of the mean.

June through October in both 2016 and 2017. Males obtained in the fall had significantly higher HCY levels than those collected in the spring in both years (MANOVA: $F_{(5,240)}=30.31, P<0.0001$), and overall HCY levels were significantly higher in 2017 than in 2016 (MANOVA: $F_{(1,240)}=76.36$, $P<0.0001$) (Fig. 2). Results of post hoc analyses indicate that animals collected in May and June had similar HCY levels, animals collected in July had HCY concentrations that were significantly higher than the levels of animals captured in May and June, and animals collected in August–October had similar HCY concentrations, the highest average HCY levels of around 70 mg/mL (Tukey's HSD test: $P<0.05$). Animals collected in August had the highest peak in HCY levels among animals captured in any month, and animals collected in May had the lowest levels.

In 2017, hemolymph samples were collected from both males and females, and the HCY concentrations followed the same seasonal variations discussed previously, with both males and females having the lowest levels in the spring. In addition, we found some differences in monthly HCY levels (MANOVA: $F_{(5,222)}=26.63$, $P<0.0001$) between the sexes (MANOVA: $F_{(1,222)}=23.27$, $P<0.0001$) (Fig. 3), with males having significantly higher HCY levels in all months than females, except in July and October.

Relationship between hemocyanin levels and mortality Because of the higher number of mortalities in 2017 (13) than in 2016 (2), only data from 2017 were used for this analysis. The average HCY concentration for the animals in the groups that did not have mortalities was 23 mg/mL (SD 14). In contrast, the baseline HCY level in animals that died ($n=14$) was 13 mg/mL (SD 9), which is significantly lower than that in animals that survived ($n=21$; 30 mg/mL [SD 14]; unpaired Student's t-test: $P=0.008$). In general, animals that had low baseline levels at the start of treatment, which included a combination of stressors, were at a greater risk of dying from the procedure.

Combined effects of stressors and hemocyanin levels on mortality Using all of the data previously presented here, we were able to determine a HCY threshold of mortality risk for animals that are collected for the bleeding process (Fig. 4). For the animals that were collected between 2016 and 2017, the maximum baseline HCY level was 120 mg/mL, and the average starting baseline level was 24 mg/mL. Animals that died as a

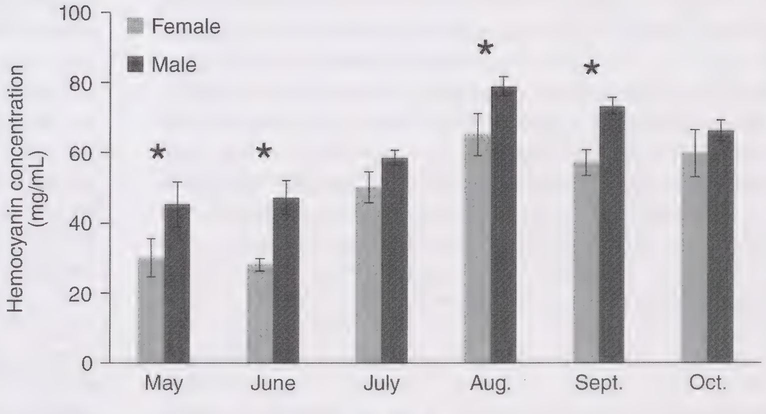

Figure 3

Comparison of monthly mean hemocyanin concentrations in male and female American horseshoe crabs (*Limulus polyphemus*) collected from the Great Bay Estuary in New Hampshire in 2017. The numbers of males and females for which hemocyanin concentrations were measured are respectively 11 and 12 in May, 74 and 10 in June, 6 and 31 in July, 13 and 38 in August, 12 and 15 in September, and 4 and 8 in October. Months with a significant difference in levels between sexes ($P<0.05$) are denoted with an asterisk (*). Error bars indicate the standard errors of the mean.

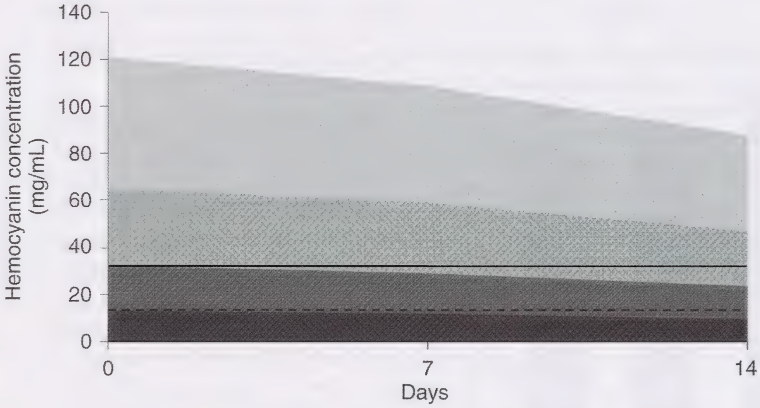

Figure 4

Hemocyanin (HCY) levels of American horseshoe crabs (*Limulus polyphemus*), collected from the Great Bay Estuary in New Hampshire, in relation to their mortality risk during the 14 d after exposure to stressors in laboratory experiments conducted in 2016 and 2017. The solid black line indicates the mortality risk threshold of 32 mg/mL. Animals with initial HCY levels above this value rarely died during the bleeding process. The dashed black line represents the most critical threshold of 13 mg/mL, a baseline concentration at which animals were most likely to die as a result of the bleeding process. Shades of gray indicate the health status of animals based on HCY levels before the bleeding process, with darker shades indicating low health: animals were not as affected by bleeding if they had HCY concentrations of 32–65 mg/mL and especially if their levels were 65–120 mg/mL.

result of being exposed to one of the treatments tended to have lower levels (average: 13 mg/mL; range: 2–32 mg/mL) than those that survived (average: 46 mg/mL [SD 19]). Therefore, there appears to be a healthy threshold level of HCY (13 mg/mL), and if animals that have HCY levels below this threshold are bled, they have a much greater probability of not surviving the procedure (Fig. 4). In addition, HCY levels tend to decrease in American horseshoe crabs held in captivity; hence, they might fall below this healthy threshold value of HCY over time (Fig. 4). For example, in control animals, we saw an average 10% decrease in HCY levels over a 1-week period (7 d) and a 27% decrease over a 2-week period (14 d) from baseline levels (day 0) (Fig. 2). Therefore, animals that start with low levels of HCY, and that are held in captivity before they are bled, are least likely to survive.

Effects of bleeding and associated stressors on crab behavior

Overall activity levels Overall, there were no consistent changes in the overall activity levels of American horseshoe crabs exposed to any of the treatments (Fig. 5). In comparison with their activity during the 1-week control period, only the groups exposed to air, or air and heat, expressed a significant change in activity either 1 or 2 weeks after their respective treatments (Table 1). The activity levels of animals in the group exposed to air were significantly lower in week 2 than in the control week, and the activity of the group exposed to air and heat increased significantly in week 1 and then went back down in week 2.

Biological rhythms Across treatment groups, and over time, American horseshoe crabs expressed a variety of daily and tidal rhythms, and some animals were arrhythmic. Initially, 37% of the animals exhibited tidal rhythms, 38% had daily rhythms, and 25% expressed no statistically significant rhythms. Although the majority of control animals (14 of 16 crabs) maintained their baseline rhythms throughout the duration of the study (Fig. 6), a number of the animals in the other treatment groups shifted from one type of rhythm to another at some point after the control week. It did not appear as if burlap made much difference; therefore, for this analysis, we grouped similar treatments that did or did not involve the use of burlap. We found that only 2–3 animals in each treatment group, including those that were exposed to the full treatment (2 of 12 crabs), switched their rhythms in the week following the treatment, except the air and heat treatment group. In this group, almost half (7 of 15) of the American horseshoe crabs switched rhythms immediately after their treatments, and then they tended to continue expressing that pattern for the rest of the study.

Relationship between activity and hemocyanin levels Taken together, the data reported here indicate that a reduction in HCY levels reduces the overall activity of American horseshoe crabs and increases the likelihood that animals could die if exposed to other stressors, such as bleeding. Therefore, we examined the relationship between overall activity levels and HCY levels in 87 animals in both 2016 and 2017, and we found that animals that were the most active also tended to have higher HCY levels (n=87; $F_{(1,86)}$=17.01, P<0.0001, coefficient of multiple determination [R^2]=0.16) (Fig. 7).

Discussion

The main objective of this study was to determine which of the stressors, or combination of stressors, associated with the biomedical bleeding process has the greatest impact on the physiology and behavior of the American horseshoe crab. Overall, we found that 1) the full bleeding treatment (exposed to air and heat and bled) had the largest effect on mortality and HCY concentrations, 2) animals with a baseline HCY level <13 mg/mL were most likely to die or be impaired by the bleeding process, and 3) lower HCY levels were correlated with lower activity levels. In

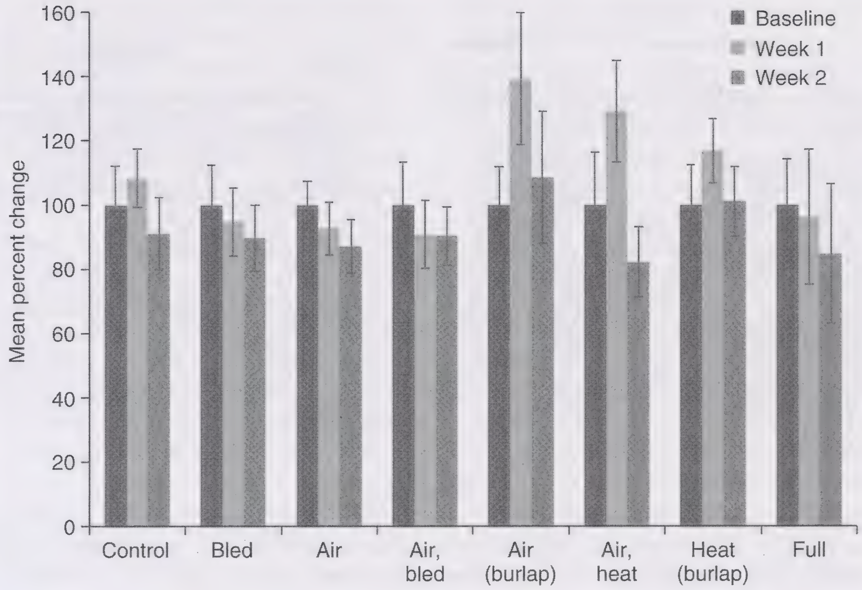

Figure 5

The effect of various treatments on activity of American horseshoe crabs (*Limulus polyphemus*). Activity data obtained 1 and 2 weeks after treatments, both in 2016 and 2017, are expressed as the percentage of their baseline activity levels before treatments (100%). The treatment groups included a control group (number of animals [*n*]=16), a group that was only bled (*n*=14), groups exposed only to air without (*n*=8) and with (*n*=8) a moist burlap cover, a group exposed to air and bled (*n*=6), a group exposed to air and heat (*n*=7), a group exposed only to heat with a burlap cover (*n*=8), and a group that received the full treatment of exposure to air, heat, and bleeding (*n*=5). Error bars indicate the standard errors of the mean. Animals used in experiments were collected in the Great Bay Estuary in New Hampshire.

addition, results indicate that there was a seasonal trend in baseline HCY levels, and females had lower starting HCY levels than males during all months sampled.

Mortality

Throughout all of the trials in this study, mortality rates differed between treatment groups, with an overall mortality rate of 17% (excluding control animals). Although this overall mortality rate is similar to the estimated range of mortality rates of 5–30% reported in previous studies (Thompson, 1998; Walls and Berkson, 2000, 2003; Hurton and Berkson, 2006; Leschen and Correia, 2010; Anderson et al., 2013), the upper end of our mortality range (75% in 2017) is high in comparison to that of many previous studies. The sample size, however, was quite low for the full treatment group in 2017. As a result, we are hesitant to draw any firm conclusions about this finding. We should also point out that the number of mortalities was highest in July, and that was also the case in a recent study that was conducted in a similar manner at JEL (Thomas[3]). Therefore, the combination of seasonally low HCY levels and high water temperatures might make animals more susceptible to the bleeding process at certain times of the year.

We did not see any mortalities in the control group or in the groups exposed to air, air and heat, or air and heat (with burlap), but the group exposed to air (with burlap) had 2 mortalities. This finding indicates that these stressors on their own are not lethal and that blood loss is the greatest risk factor. This result supports previous findings of a 10–20% increase in mortality rates in animals that were subjected to only hemolymph extraction compared with the mortality rate of control animals (Rudloe, 1983; Kurz and James-Pirri, 2002).

We had more mortalities in 2017 (27%) than in 2016 (4%). This difference could be explained by the fact that we used only males in 2016 and both males and females in 2017. This conclusion is supported by previously reported sex differences in mortality rates (Leschen and Correia, 2010; James-Pirri et al., 2012): 15% of males and up to 29% of females. We have ruled out temperature differences between the years because average water temperatures reached 22.3°C in 2016 and peaked around 20.7°C in 2017. Finally, the only difference in treatment groups between the 2 years was the addition of burlap to

---

[3] Thomas, T. 2019. Unpubl. data. Plymouth State Univ., 17 High St., Plymouth, NH 03264.

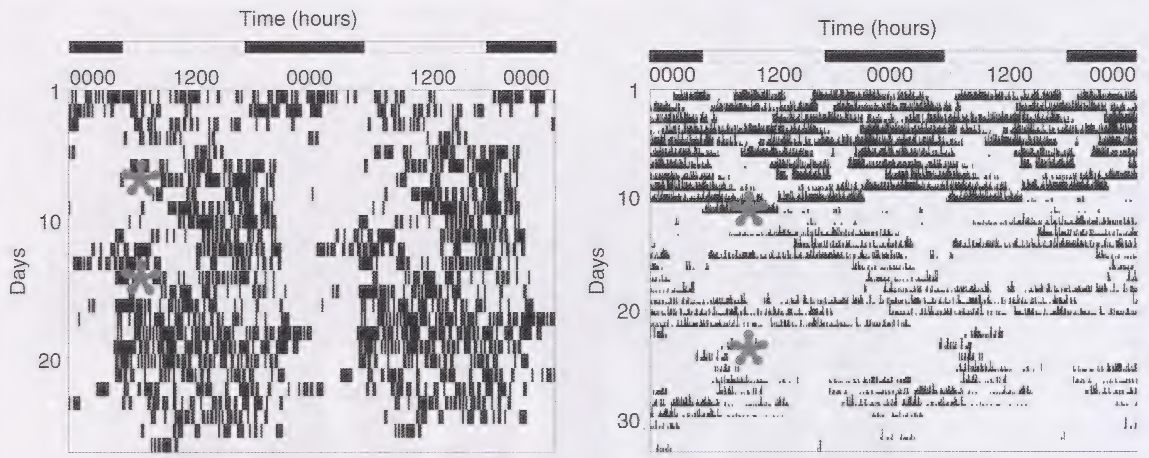

Figure 6

Actograms showing activity over time for American horseshoe crabs (*Limulus polyphemus*) collected in the Great Bay Estuary in New Hampshire and exposed to stressors in laboratory experiments conducted in 2016. Data are presented for one animal from the control group (left) and one animal from the group that received the full treatment of exposure to air, heat, and bleeding (right). The x-axis is double-plotted, with a span of 48 h, to make rhythms more evident. The white and black horizontal bars at the top of each actogram represent the light and dark periods of the day. Values on the y-axis represent ~4 weeks of treatment for each animal in October 2016. Large gray asterisks indicate the time of the treatment (top star) and the time 2 weeks posttreatment when data were downloaded from the accelerometer attached to each animal (bottom star). The animal on the right had a tidal rhythm (dominant period: 12.6 h) during its treatment.

keep the animals moist in some groups in 2017, and this change was intended to mitigate any lethal or sublethal effects.

When mortalities did occur, the vast majority (14 of 15 mortalities) took place within 1–2 d of the treatment of animals. One possible way to reduce mortalities might be to try to return American horseshoe crabs to their natural environment as soon as possible, an approach that is consistent with the U.S. Food and Drug Administration mandate that American horseshoe crabs be returned within 24–72 h after time of collection (ASMFC[4]).

Hemocyanin levels

Changes over time We observed several different trends in HCY concentrations, both over time and within treatment groups. First, we saw a decrease in HCY levels over time, especially within the first week, in all groups, including the control group. This decrease is likely due to the animals being kept in captivity and is consistent with results of a previous study in the same location (Anderson et al., 2013). According to Coates et al. (2012), the immune competence of American horseshoe crabs is negatively affected

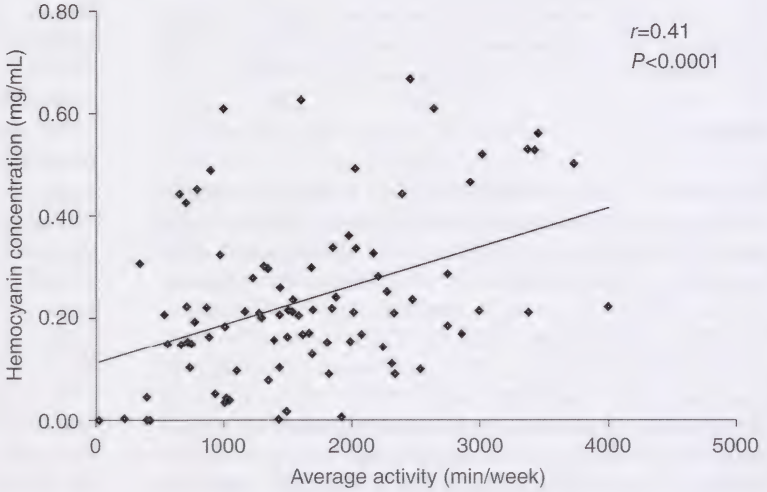

Figure 7

Relationship between hemocyanin and average activity levels of American horseshoe crabs (*Limulus polyphemus*) collected in the Great Bay Estuary in New Hampshire and used in laboratory experiments in 2016 and 2017 (number of animals=87, coefficient of correlation [r]=0.41, $P<0.0001$). The diagonal line indicates the trend for the data.

---

[4] ASMFC (Atlantic States Marine Fisheries Commission). 1998. Interstate fishery management plan for horseshoe crab. ASMFC Fish. Manage. Rep. 32, 40 p. ASMFC, Arlington, VA. [Available from website.]

by the stress associated with holding animals in captivity. The specific effects of low blood protein and HCY levels on American horseshoe crab physiology and behavior has not been well studied to date, except for the observation made over 100 years ago that lower protein levels are associated with starvation and mortality (Alsberg, 1914). More recently, high mortality rates of American horseshoe crabs have been documented in animals kept in captivity. This high mortality appears to be caused by hepatic insufficiency, protein-losing enteropathy, nutritional imbalance or deficiency, and protein-losing nephropathy (Novitsky, 2009; Carmichael and Brush, 2012). These findings support a proposal that would require biomedical facilities to use high-quality water and frequent feeding to maintain the health of American horseshoe crabs that are being held before and after bleeding (Armstrong and Conrad, 2008).

Effects of different treatments We also saw changes in HCY levels due to different treatments, indicating that captivity was not the only factor contributing to decreases in HCY levels over time. In particular, HCY levels were significantly lower in the animals exposed to the full bleeding treatment (air, heat, and bled) than in those exposed to other treatments. The stressor that caused the greatest decrease in HCY levels was heat, a finding that is consistent with previous reports that HCY concentrations decreased as temperatures increased (from 8°C to 23°C) (Chen et al., 1995; Hennig and Andreatta, 1998). Coates et al. (2012). To make matters worse, the oxygen affinity of HCY, like other respiratory pigments, decreases as temperature increases (Redfield, 1934; Burnett et al., 1988). Therefore, not only do American horseshoe crabs that experience the biomedical bleeding procedure have less HCY but also the HCY they do have cannot hold as much oxygen. Furthermore, because warmer seawater holds less oxygen than cooler water and animals have a higher metabolism and lower HCY levels at higher temperatures, the combination of stressors could cause long-term hypoxia. Therefore, we suggest that hypoxia could be one major cause of both the mortalities and reduced activity that we, and others, have documented.

Changes in HCY levels might also lead to mortalities or alterations in behavior because of the role that HCY plays in the function of the immune system. Hemocyanin is converted into a phenoloxidase-like enzyme by hemocyte components (Adachi et al., 2003), and the enzymatic oxidation is important in the cuticle formation and immune reaction in arthropods (Ashida and Brey, 1997; Söderhäll and Cerenius, 1998). Therefore, the effects of different factors on hemocyte levels can also have an indirect impact on HCY function, specifically in regards to temperature. For example, in the Atlantic sand fiddler (*Uca pugilator*), temperature affected clotting times, levels of plasma protein, and total hemocyte numbers (Clare and Lumb, 1994). Seasonal changes in hemocyte antibacterial activity as temperatures change has been observed for another crab species, the green crab (*Carcinus maenas*) (Chisholm and Smith, 1994). All of these effects of temperature on hemocyte levels indicate that HCY levels could also be affected by high temperatures, especially in the American horseshoe crab.

Air exposure can have negative effects both on its own and in combination with heat and blood loss. As blood flows through the book gills of an American horseshoe crab, gas exchange occurs and HCY becomes saturated with oxygen. During air exposure, the book gills can become desiccated, ventilation ceases, and the heart rate drops considerably. Therefore, little gas exchange takes place and hemolymph circulation throughout the body decreases significantly (Watson and Wyse, 1978; Watson, 1980). As stated previously, heat increases crab metabolism, resulting in a need for more oxygen, and when HCY levels are low, HCY cannot carry as much oxygen. Therefore, the combination of warm temperatures, air exposure, and blood loss could lead to severe hypoxia. Also, amebocytes, the granular cell that plays a crucial role in defending American horseshoe crabs against pathogens, are created through cell differentiation that is sourced from the gill flaps (Gibson and Hilly, 1992). Presumably, then, any harm to the gills could cause amebocyte growth to be hampered and could reduce immune function. However, although exposure to air can have negative impacts on the physiology of American horseshoe crabs, it does not appear to be as detrimental as exposure to heat, perhaps, because the placement of gills on the ventral surface of animals generally produces a microclimate that increases humidity and decreases desiccation. Still, when both stressors are combined, they likely have a synergistic effect.

Hemocyanin composes 90% of total hemolymph protein in the American horseshoe crab (Ding et al., 2005), and an estimated 30% of the hemolymph volume is extracted from American horseshoe crabs during the bleeding process. Although they can rapidly regain most of their blood volume, it takes much longer for them to replace the lost HCY. Therefore, HCY concentrations decrease, and this decline in levels can lead to some of the health issues described previously. In this study, we measured HCY levels for only 2 weeks posttreatment, but findings from previous studies indicate that it takes many weeks for HCY levels to recover following bleeding. For example, Anderson et al. (2013) reported that HCY levels were still low after 6 weeks, and James-Pirri et al. (2012) found significantly reduced levels of total hemolymph protein in bled animals compared with levels in control animals 17 d after bleeding, with bled animals having 20% less hemolymph protein than control animals.

In summary, the combination of blood loss, exposure to air (which reduces and slows the heart rate; Watson and Wyse, 1978; Watson, 1980), and exposure to heat (which increases metabolism) appears to have the most dramatic impacts on both mortalities and behavior of the American horseshoe crab. Although these same stressors can also have a negative effect on the immune system, in our study the most dramatic effects occurred during the first week after animals were bled; hence, the impacts from various treatments likely occurred too early to have been caused by immunodeficiency or infection. Our view is that the impairments caused by the bleeding process are likely a result of the fact that all the stressors involved influence the ability of American horseshoe crabs to obtain sufficient oxygen and to circulate it to all their tissues.

Seasonal and sex differences Another interesting finding from this study was that there were significant effects of season and sex on HCY levels. Concentrations of HCY were the lowest in May and June and the highest in August and September. The spawning season in the Great Bay Estuary in 2016 was 9 May–10 June, and in 2017 it was 16 May–16 June; these seasons correspond to the period during which HCY levels were the lowest. Furthermore, during all months sampled (May–October), females had lower HCY levels than males, especially in May and June. Females have greater variability in their estimated hemolymph volume, likely because females carry eggs that displace space in body cavities that could be filled with hemolymph (Hurton et al., 2005). Although the impact of eggs might explain the lower HCY levels in females in May and June, it does not necessarily account for the consistently lower HCY levels in females, compared with those in males, later in the year or for the low levels of HCY in males during the spawning season.

Egg production is an energetically expensive process (Bryant and Hartnoll, 1995; Nicol et al., 1995; Guillou and Lumingas, 1999; Chaparro and Flores, 2002; Jørgensen et al., 2006), as is making several trips to spawning beaches within the same season, often with males attached to their carapace. These energetic costs, combined with low HCY levels, might explain, in part, why females are likely to be more heavily affected and physiologically stressed from the bleeding process. This idea is certainly consistent with findings from one of our recent studies indicating that females were less likely than males to have normal activity levels when bled and released into their natural habitat, especially during the spawning season (Owings et al., 2019).

In the past, females have been harvested more than males for bleeding because of their size and larger hemolymph volume. For example, in Pleasant Bay, Massachusetts, 66% of the American horseshoe crabs collected up until 2001 were female (Rutecki et al., 2004). Captured females also tend to be larger than the average females of the populations in Pleasant Bay because harvesters select for larger females (Rutecki et al., 2004). In this area, over 50% of the harvest and bleeding occurs during, or shortly after, the spawning season. Because larger females are being selected and these animals are also more fecund (Leschen et al., 2006), this selection practice risks reducing the number of eggs being produced and fertilized over time and may alter population dynamics. Given that females have lower HCY levels throughout the year, have added metabolic costs during spawning, have their lowest HCY levels in the spring during the spawning season, and have higher mortality rates than males when they are bled, it is reasonable to suggest that more attention should be focused on regulating when females can be harvested and making the bleeding process less detrimental to them.

Relationship between hemocyanin levels and mortality

In this study, we found that animals with lower baseline HCY levels suffered greater sublethal and lethal effects when exposed to multiple stressors from the bleeding process. The baseline HCY levels in animals that died in different treatment groups were significantly lower than in animals that survived in those same treatment groups. The treatment groups that had mortalities included the groups of animals that were exposed to air and heat and were bled (with and without burlap), animals that were exposed to air and were bled (with burlap), and animals exposed to air (with burlap). Therefore, air and bleeding were the most significant stressors because animals in poor initial health that were exposed to these factors were more likely to die.

In order to use this information to reduce mortalities, biomedical facilities might take a hemolymph sample before bleeding animals and proceed to bleed only animals with HCY levels that fall above a certain estimated healthy threshold (we suggest a level later in this paragraph). Facilities already are required to prescreen for injured American horseshoe crabs before bleeding them. If biomedical companies could take this precaution one step further and take an initial blood sample, or develop a faster and easier way to determine the health status of an American horseshoe crab, they could significantly reduce mortality rates. For example, on the basis of data from our study, American horseshoe crabs with a HCY level of 32 mg/mL or below should not be bled.

The absolute critical level from this study was 13 mg/mL: any individual that had this baseline HCY level, and was exposed to at least 2 of the different stressors, died. How close animals are to this threshold changes across sexes (with females having lower baseline HCY levels), over a season (with higher HCY levels in late summer and fall), and during the length of time an animal is held in captivity (HCY levels decrease as the amount of time in captivity increases, declines that are probably related to nutrition). The latter point is important to keep in mind because the longer an animal is kept in captivity, or in the holding ponds at the facilities, the more their HCY levels will decrease and eventually they may fall below the critical threshold. In short, mortalities could be reduced if there was a simple way to check HCY levels right before bleeding an American horseshoe crab.

Effects of bleeding and associated stressors on crab behavior

The stressors associated with the biomedical bleeding process had only a small impact on the overall activity of some of the American horseshoe crabs in this study. However, this effect was greatest and most obvious in animals that started the process with low HCY levels (Fig. 7). In contrast, in some treatment groups, we observed an increase in activity during the first week posttreatment.

This post-handling hyperactivity is not uncommon in American horseshoe crabs and some crustaceans. Anderson et al. (2013) suggested that this increase in initial activity could have been due to 1) an effort to escape after handling (Rudloe and Hernnkind, 1976); 2) a need to search for food in order to replenish lost energy reserves, as has been reported for the edible crab (*Cancer pagurus*) (Patterson et al., 2009); or 3) disorientation from the bleeding process (Kurz and James-Pirri, 2002). However, if these explanations were valid, we should have observed increased locomotion by the animals in many of the other treatment groups as well.

Some animals in all the treatment groups changed the types of biological rhythms they expressed during the course of the experiment, with the most clear-cut changes observed in the group of animals exposed to air and heat (with and without burlap). However, it should be noted that the group of animals that were subjected to air, heat, and bleeding in 2017 had a large number of mortalities; therefore, it was difficult to discern the impacts of the full bleeding process on the types of rhythms exhibited by the animals in this group. These findings are similar to those reported by Anderson et al. (2013), but in contrast to our results, they observed a decrease in the expression of tidal rhythms.

Handling might also cause animals to change their behavior and the types of rhythms they express. For every treatment group, we picked animals out of the water either to treat them according to the different stressors they were assigned or to take a blood sample (during the treatment period and 1 week posttreatment). Therefore, when we observed changes in the expression of rhythms 2 weeks posttreatment, it may not have been a delayed effect from the bleeding process but a response to being handled. For example, even 2 of the 16 control animals switched from a tidal rhythm to a daily rhythm after they were handled, and in cases where treated animals changed rhythms after about 2 weeks, the shifts almost always occurred right after they were handled. This switch in behavior after handling is not uncommon, and it took place in a number of cases in a previous study of feeding and handling (senior author, unpubl. data).

Nevertheless, despite the occasional animal that changed activity immediately following handling late in a trial, it should be noted that no control animals changed rhythms after they were handled and sampled following the 1-week control period. In contrast, there were many other animals that were clearly impacted by the treatments: these animals changed the rhythms they expressed after their treatments and kept the new activity rhythm throughout the remainder of the experiment, even after the handling associated with the blood sampling done over the 2-week period after treatment. Therefore, as indicated by results from a number of previous studies, the biomedical bleeding process has both lethal and sublethal effects. Moreover, given the data obtained during this study, exposure to warm temperatures and losing a significant amount of blood appear to have the greatest impacts on the behavior and physiology of the American horseshoe crab.

Acknowledgments

This research project could not have been completed without the help of D. Shay and the staff of the University of New Hampshire JEL. We would also like to thank all the graduate and undergraduate students at the University of New Hampshire and Plymouth State University who helped us with many aspects of this work. This study was supported by a Leslie S. Hubbard Marine Program Endowment grant and Marine Biology Graduate Program grant to the senior author and by funding from New Hampshire Sea Grant (R/HCE-4) to C. Chabot and W. Watson.

Literature cited

Adachi, K., T. Hirata, T. Nishioka, and M. Sakaguchi.
2003. Hemocyte components in crustaceans convert hemocyanin into a phenoloxidase-like enzyme. Comp. Biochem. Physiol. B 134:135–141.

Adachi, K., H. Endo, T. Watanabe, T. Nishioka, and T. Hirata.
2005a. Hemocyanin in the exoskeleton of crustaceans; enzymatic properties and immunolocalization. Pigment Cell Res. 18:136–143.

Adachi, K., K. Wakamatsu, S. Ito, N. Miyamoto, T. Kokubo, T. Nishioka, and T. Hirata.
2005b. An oxygen transporter hemocyanin can act on the late pathway of melanin synthesis. Pigment Cell Res. 18:214–219.

Alsberg, C. L.
1914. Note on the proteins of the blood of *Limulus Polyphemus* L. J. Biol. Chem. 19:77–82.

Anderson, R. L., W. H. Watson III, and C. C. Chabot.
2013. Sublethal behavioral and physiological effects of the biomedical bleeding process on the American horseshoe crab, *Limulus Polyphemus*. Biol. Bull. 225:137–151.

Armstrong, P., and M. Conrad.
2008. Blood collection from the American horseshoe crab, *Limulus polyphemus*. J. Vis. Exp. 20:e958.

Ashida, M., and P. Y. Brey.
1997. Recent advances in prophenoloxidase research. *In* Molecular mechanisms of the insect immune response (P. T. Brey and D. Hultmark, eds.), p. 135–172. Chapman and Hall, London.

ASMFC (Atlantic States Marine Fisheries Commission).
2019. 2019 horseshoe crab benchmark stock assessment and peer review report, 237 p. ASMFC, Arlington, VA. [Available from website.]

Bryant, A. D., and R. G. Hartnoll.
1995. Reproductive investment in two spider crabs with different breeding strategies. J. Exp. Mar. Biol. Ecol. 188:261–275.

Burnett, L. E.
1988. Physiological responses to air exposure: acid-base balance and the role of branchial water stores. Am. Zool. 28:125–135.

Burnett, L. E., D. A. Scholnick, and C. P. Mangum.
1988. Temperature sensitivity of molluscan and arthropod hemocyanins. Biol. Bull. 174:153–162.

Carmichael, R. H., and E. Brush.
2012. Three decades of horseshoe crab rearing: a review of conditions for captive growth and survival. Rev. Aquac. 4:32–43.

Chaparro, O. R., and M. L. Flores.
2002. Reproductive output of *Crepidula fecunda* females: distribution of energy in the production of gametes and capsular walls. N.Z. J. Mar. Freshw. Res. 36:661–673.

Chen, J.-C., M.-N. Lin, Y.-Y. Ting, and J.-N. Lin.
1995. Survival, haemolymph osmolality and tissue water of *Panaeus chinensis* juveniles acclimated to different salinity and temperature levels. Comp. Biochem. Physiol. A 110:253–258.

Chisholm, J. R. S., and V. J. Smith.
1994. Variation of antibacterial activity in the haemocytes of the shore crab, *Carcinus maenas*, with temperature. J. Mar. Biol. Assoc. U.K. 74:979–982.

Clare, A. S., and G. Lumb.
1994. Identification of haemocytes and their role in clotting in the blue crab, *Callinectes sapidus*. Mar. Biol. 118: 601–610.

Coates, C. J., S. M. Kelly, and J. Nairn.
2011. Possible role of phosphatidylserine–hemocyanin interaction in the innate immune response of *Limulus polyphemus*. Dev. Comp. Immunol. 35:155–163.

Coates, C. J., E. L. Bradford, C. A. Krome, and J. Nairn.
2012. Effect of temperature on biochemical and cellular properties of captive *Limulus polyphemus*. Aquaculture 334–337:30–38.

Ding, J. L., K. C. Tan, S. Thangamani, N. Kusuma, W. K. Seow, T. H. H. Bui, J. Wang, and B. Ho.
2005. Spatial and temporal coordination of expression of immune genes during *Pseudomonas* infection of the horseshoe crab, *Carcinoscorpius rotundicauda*. Genes Immun. 6:557–574.

Gibson, D. G., III, and J. B. Hilly.
1992. Production of horseshoe crab amebocytes in vitro. U.S. Patent 5,082,782, filed 27 December 1988 and issued 21 January 1992.

Glazer, L., M. Tom, S. Weil, Z. Roth, I. Khalaila, B. Mittelman, and A. Sagi.
2013. Hemocyanin with phenoloxidase activity in the chitin matrix of the crayfish gastrolith. J. Exp. Biol. 216:1898–1904.

Guillou, M., and L. J. L. Lumingas.
1999. Variation in the reproductive strategy of the sea urchin *Spaerechinus granularis* (Echinodermate: Echinoidea) related to food availability. J. Mar. Biol. Assoc. U.K. 79:131–136.

Hatch, A. C., and A. R. Blaustein.
2003. Combined effects of UV-B radiation and nitrate fertilizer on larval amphibians. Ecol. Appl. 13: 1083–1093.

Hennig, O. L., and E. R. Andreatta.
1998. Effect of temperature in an intensive nursery system for *Penaeus paulensis* (Pérez Farfante, 1967). Aquaculture 164:167–172.

Hurton, L., and J. Berkson.
2006. Potential causes of mortality for horseshoe crabs (*Limulus polyphemus*) during the biomedical bleeding process. Fish. Bull. 104:293–298.

Hurton, L., J. Berkson, and S. Smith.
2005. Estimation of total hemolymph volume in the horseshoe crab *Limulus polyphemus*. Mar. Freshw. Behav. Physiol. 38:139–147.

James-Pirri, M.-J., P. A. Veillette, and A. S. Leschen.
2012. Selected hemolymph constituents of captive, biomedically bled, and wild caught adult female American horseshoe crabs (*Limulus polyphemus*). Mar. Freshw. Behav. Physiol. 45:281–289.

Jørgensen, C., B. Ernande, Ø. Fiksen, and U. Dieckmann.
2006. The logic of skipped spawning in fish. Can. J. Fish. Aquat. Sci. 63:200–211.

Krisfalusi-Gannon, J., W. Ali, K. Dellinger, L. Robertson, T. E. Brady, M. K. M. Goddard, R. Tinker-Kulberg, C. L. Lepley, and A. L. Dellinger.
2018. The role of horseshoe crabs in the biomedical industry and recent trends impacting species sustainability. Front. Mar. Sci. 5:185.

Kuballa, A. V., and A. Elizur.
2008. Differential expression profiling of components associated with exoskeletal hardening in crustaceans. BMC Genomics 9:575.

Kuballa, A. V., T. A. Holton, B. Peterson, and A. Elizur.
2011. Moult cycle specific differential gene expression profiling of the crab *Portunus pelagicus*. BMC Genomics 12:147.

Kurz, W., and M. J. James-Pirri.
2002. The impact of biomedical bleeding on horseshoe crab, *Limulus polyphemus*, movement patterns on Cape Cod, Massachusetts. Mar. Freshw. Behav. Physiol. 35:261–268.

Leschen, A. S., and S. J. Correia.
2010. Mortality in female horseshoe crabs (*Limulus polyphemus*) from biomedical bleeding and handling: implications for fisheries management. Mar. Freshw. Behav. Physiol. 43:135–147.

Leschen, A. S., S. P. Grady, and I. Valiela.
2006. Fecundity and spawning of the Atlantic horseshoe crab, *Limulus polyphemus*, in Pleasant Bay, Cape Cod, Massachusetts, USA. Mar. Ecol. 27:54–65.

Mangum, C. P.
1980. Respiratory function of hemocyanins. Am. Zool. 20:19–38.

Nicol, S., W. De La Mare, and M. Stolp.
1995. The energetic cost of egg production in Antarctic krill (*Euphausia superba*). Antarct. Sci. 7:25–30.

Novitsky, T. J.
1984. Discovery to commercialization: the blood of the horseshoe crab. Oceanus 27:13–18.
2009. Biomedical applications of *Limulus* amebocyte lysate. *In* Biology and conservation of horseshoe crabs (J. T. Tanacredi, M. L. Botton, and D. R. Smith, eds.), p. 315–329. Springer, Boston, MA.

Owings, M., C. Chabot, and W. Watson III.
2019. Effects of the biomedical bleeding process on the behavior of the American horseshoe crab, *Limulus polyphemus*, in its natural habitat. Biol. Bull. 236:207–223.

Patterson, L., J. T. A. Dick, and R. W. Elwood.
2009. Claw removal and feeding ability in the edible crab, *Cancer pagurus*: implications for fishery practice. Appl. Anim. Behav. Sci. 116:302–305.

Paul, R. J., and R. Pirow.
1998. The physiological significance of respiratory proteins in invertebrates. Zoology 100:298–306.

Redfield, A. C.
1934. The haemocyanins. Biol. Rev. 9:175–212.

Redmond, J. R.
1955. The respiratory function of hemocyanin in crustacea. J. Cell. Comp. Physiol. 46:209–247.

Rudloe, A.
1983. The effect of heavy bleeding on mortality of the horseshoe crab, *Limulus polyphemus*, in the natural environment. J. Invertebr. Pathol. 42:167–176.

Rudloe, A., and W. F. Herrnkind.
1976. Orientation of *Limulus polyphemus* in the vicinity of breeding beaches. Mar. Behav. Physiol. 4:75–89.

Rutecki, D., R. H. Carmichael, and I. Valiela.
2004. Magnitude of harvest of Atlantic horseshoe crabs, *Limulus polyphemus*, in Pleasant Bay, Massachusetts. Estuaries 27:179–187.

Schisler, G. J., E. P. Bergersen, and P. G. Walker.
2000. Effects of multiple stressors on morbidity and mortality of fingerling rainbow trout infected with *Myxobolus cerebralis*. Trans. Am. Fish. Soc. 129:859–865.

Schmid, B., C. Helfrich-Förster, and T. Yoshii.
2011. A new imageJ plugin "ActogramJ" for chronobiological analyses. J. Biol. Rhythms 26:464–467.

Schulz, R., and J. M. Dabrowski.
2001. Combined effects of predatory fish and sublethal pesticide contamination on the behavior and mortality of mayfly nymphs. Environ. Toxicol. Chem. 20:2537–2543.

Söderhäll, K., and L. Cerenius.
1998. Role of the prophenoloxidase-activating system in invertebrate immunity. Curr. Opin. Immunol. 10:23–28.

Thompson, M.
1998. Assessments of the population biology and critical habitat for the horseshoe crab, *Limulus polyphemus*, in the South Atlantic Bight. M.S. thesis. Univ. Charleston, Charleston, SC.

Walls, E. A., and J. M. Berkson.
2000. Effects of blood extraction on the mortality of the horseshoe crab, *Limulus polyphemus*. Va. J. Sci. 51:195–198.
2003. Effects of blood extraction on horseshoe crabs (*Limulus polyphemus*). Fish. Bull. 101:457–459.

Watson, W. H., III.
1980. Long-term patterns of gill cleaning, ventilation and swimming in *Limulus*. J. Comp. Physiol. 141:77–85.

Watson, W. H., III, and G. A. Wyse.
1978. Coordination of the heart and gill rhythms in *Limulus*. J. Comp. Physiol. 124:267–275.

Watson, W. H., III, S. K. Johnson, C. D. Whitworth, and C. C. Chabot.
2016. Rhythms of locomotion and seasonal changes in activity expressed by horseshoe crabs in their natural habitat. Mar. Ecol. Prog. Ser. 542:109–121.

National Marine
Fisheries Service
NOAA

Fishery Bulletin
established in 1881

Spencer F. Baird
First U.S. Commissioner
of Fisheries and founder
of *Fishery Bulletin*

Abstract—The whale shark (*Rhincodon typus*) and the giant manta (*Mobula birostris*) are migratory species that occasionally occur in the same foraging habitat. Both planktotrophic elasmobranch species can be found seasonally in aggregations from 2 individuals to hundreds of animals in the northern Caribbean Sea off the Yucatan Peninsula of Mexico because of the abundance of food in this area. The aim of this study was to assess the distribution and abundance of the whale shark and giant manta by conducting aerial surveys from May through September during 2016–2018. A total of 953 whale sharks and 466 giant mantas were sighted during 17 aerial surveys. The largest groups of whale sharks and giant mantas were recorded in July 2017 and September 2016, respectively. Aerial survey data were used to estimate the mean density of each species in this aggregation area: 14 whale sharks/100 km^2 and 8 giant mantas/100 km^2. These values were used to estimate the spatiotemporal variability of the number of whale sharks and giant mantas feeding at the surface. The results of this study indicate that both species were not distributed homogeneously in the assessed area, a situation that often interferes with the implementation of suitable strategies for managing tourist activities.

Manuscript submitted 21 December 2019.
Manuscript accepted 28 July 2020.
Fish. Bull. 118:240–249 (2020).
Online publication date: 18 August 2020.
doi: 10.7755/FB.118.3.3

The views and opinions expressed or implied in this article are those of the author (or authors) and do not necessarily reflect the position of the National Marine Fisheries Service, NOAA.

Use of aerial surveys for assessing abundance of the whale shark (*Rhincodon typus*) and the giant manta (*Mobula birostris*) in the northern Caribbean Sea off Mexico

Jorge A. Trujillo-Córdova[1]
Emanuel Mimila-Herrera[1]
Natalí Cárdenas-Palomo (contact author)[1]
Jorge A. Herrera-Silveira[2]

Email address for contact author: natalicardenaspalomo@gmail.com

[1] Pronatura Península de Yucatán A.C.
Calle 32 No. 269
Pinzon II
97205 Merida, Yucatan, Mexico

[2] Laboratorio de Producción Primaria
Departamento de Recursos del Mar
Centro de Investigación y Estudios Avanzados
Instituto Politécnico Nacional
Carretera Antigua a Progreso km 6
97310 Merida, Yucatan, Mexico

In the northern Caribbean Sea off the Yucatan Peninsula in southeastern Mexico (Fig. 1), whale sharks (*Rhincodon typus*) form seasonal aggregations from May through September. The number of individuals and distribution of whale sharks near the sea surface is highly dynamic, varying among seasons, days, and hours (de la Parra Venegas et al., 2011; Cárdenas-Palomo et al., 2015). The waters of the Caribbean Sea off the northeastern coast of the Yucatan Peninsula is one of the most important aggregation sites for whale sharks, with the largest number of individuals identified to species by using photographs; between 1999 and 2015, 1115 whale sharks were recorded in the Wildbook Whale Shark photo-identification database (available from website) (McKinney et al., 2017; Norman et al., 2017). In addition, in the northern Caribbean Sea off Mexico there are aggregations of giant mantas (*Mobula birostris*), whose population size, movement patterns, and ecology are poorly known (Graham et al., 2012). The productivity in this region is high because of the upwelling on the Yucatan Shelf that fertilizes the ecosystem with nutrients rising from deep waters, enriching marine habitats, and providing food for many species (Merino, 1997; Reyes-Mendoza et al., 2016).

Since 2004, tourism related to whale sharks has increased exponentially, and it is currently a significant source of income for communities near the feeding sites of this species on the northeastern coast of the Yucatan Peninsula (Mimila-Herrera et al., 2016); these communities also use giant mantas as tourist attractions and their meat as bait (Hinojosa-Álvarez, 2009; Graham et al., 2012). Therefore, information about ecological characteristics of these species is needed for their management in this region. To that end, we conducted aerial surveys between 2016 and 2018 to

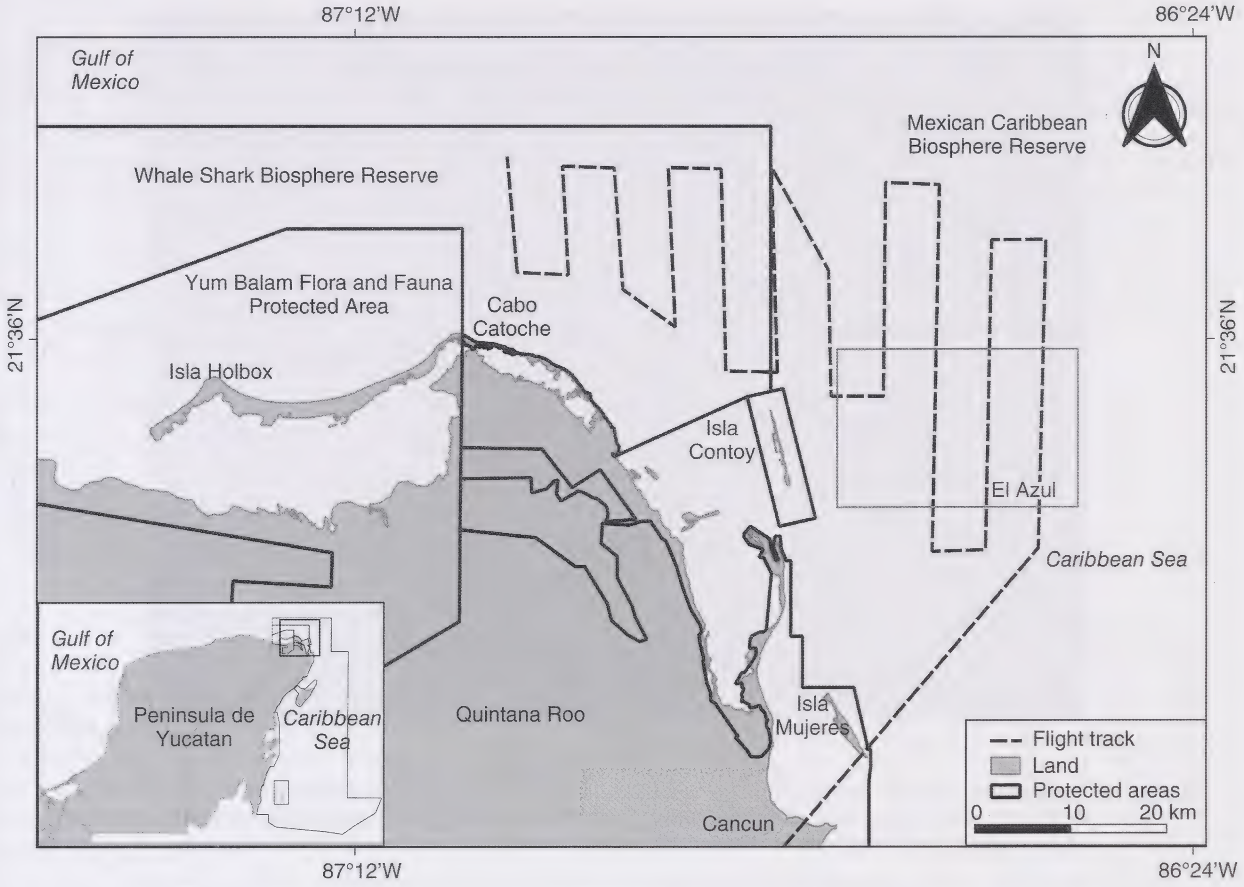

Figure 1

A map of the study area where aerial surveys of whale sharks (*Rhincodon typus*) and giant mantas (*Mobula birostris*) were conducted in the Caribbean Sea off the northeastern coast of the Yucatan Peninsula of Mexico between May and September during 2016–2018. The flight track (dashed line) was designed to cover the major area of aggregations of whale sharks and giant mantas in the region, which includes zones of high abundance of these species in the Whale Shark Biosphere Reserve (outlined with black lines along with other protected areas) and in the Azul area (box outlined in gray), located in the Mexican Caribbean Biosphere Reserve. Surveys were conducted at an average altitude of 380 m above sea level and at a mean speed of 175 km/h. The survey transect had a length of 300 km.

assess the distribution and abundance of whale sharks and giant mantas and to estimate the spatiotemporal variability of the density of these species in the northern Caribbean Sea off Mexico.

Materials and methods

The study area is located in the Caribbean Sea off the northeastern coast of the Yucatan Peninsula, a location where previous research has identified 2 major areas with high abundance of whale sharks (Cárdenas-Palomo et al., 2015): the Whale Shark Biosphere Reserve (WSBR), a protected area decreed on 2009 (DOF, 2009), and a zone called the Azul, which is inside of the Mexican Caribbean Biosphere Reserve (MCBR), decreed in 2016 (DOF, 2016) (Fig. 1). The WSBR has high concentrations of chlorophyll-*a* (>1 mg/m^3), due to the influence of nutrient-rich waters from the Yucatan upwelling system, and a zooplankton biomass of approximately 103.5 mg/m^3 composed mainly of copepods, appendicularians, and chaetognaths (Merino, 1997; Cárdenas-Palomo et al., 2015; Reyes-Mendoza et al., 2016). The WSBR has an average depth of 12 m and an average sea-surface temperature during the rainy season of 26.2°C (Cárdenas-Palomo et al., 2015; Hacohen-Domené et al., 2017). The Azul area is characterized by oligotrophic conditions, such as waters with low levels of nutrients and low concentrations of chlorophyll-*a* (<1 mg/m^3) (Cárdenas-Palomo et al., 2015). In this area, the average depth is approximately 30 m, the sea-surface temperature in the raining season is 27.8°C, and zooplankton have a biomass >3356.1 mg/m^3 and consist mainly of fish eggs (Cárdenas-Palomo et al., 2015). The most numerous aggregation of whale sharks

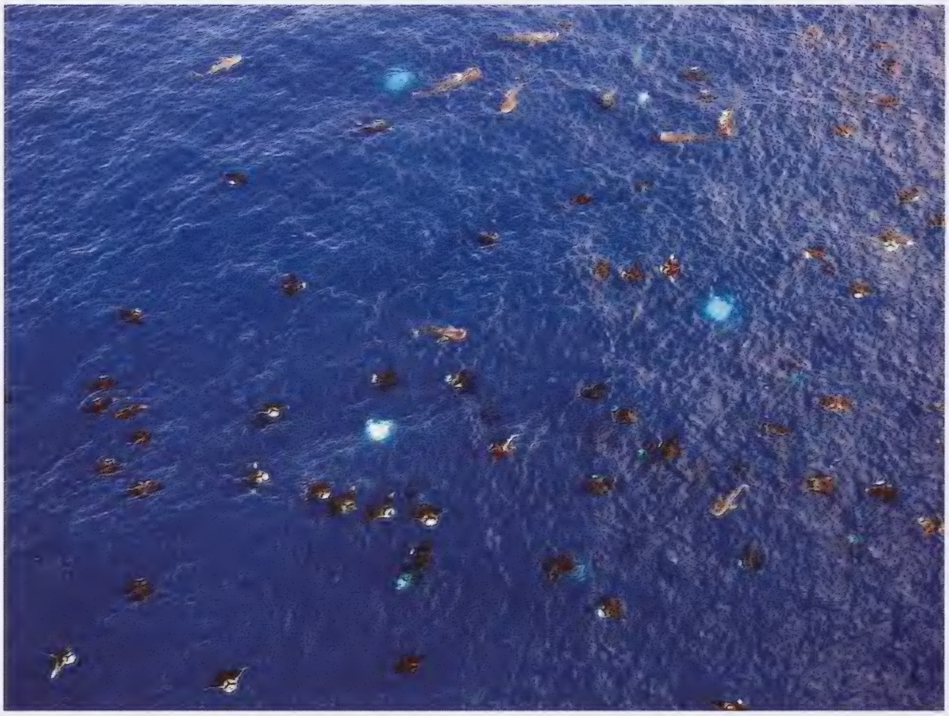

Figure 2

Photograph of whale sharks (*Rhincodon typus*) and giant mantas (*Mobula birostris*) taken in September 2016 during an aerial survey along a transect in the Azul area, a zone of high abundance of these species in the Mexican Caribbean Biosphere Reserve. Photograph by E. Mimila-Herrera.

ever recorded was observed in the Azul area (420 individuals; de la Parra Venegas et al., 2011), and this area is also considered a core foraging location for giant mantas (Graham et al., 2012).

Aerial surveys

From 2016 through 2018, aerial surveys were conducted between May and September with a Cessna 206[1] high-wing aircraft (Textron Aviation, Wichita, KS). Each flight followed the survey transect shown in Figure 1 and was conducted at an average altitude of 380 m above sea level and at a mean speed of 175 km/h. In the northern Caribbean Sea off Mexico under appropriate climatic conditions, whale sharks and giant mantas can be clearly identified from as high as 579 m above sea level (Rowat et al., 2009).

The survey transect was designed to cover the major area of aggregations of whale sharks and giant mantas in the Caribbean Sea off the northeastern coast of the Yucatan Peninsula, and the transect had a mean length of 269 km. The mean duration of surveys was 165 min, and surveys were conducted from 0730 to 1130 or from 1500 to 1800. Because flight times varied, we standardized the results by reporting relative abundance and density, as well as the number of individuals sighted.

For the aerial surveys, an observer was positioned on each side of the airplane. The observers recorded the number of whale sharks and giant mantas observed and their geographical location with GPS. To reduce observer bias, the same 2 people conducted all aerial surveys, and each spotter sat in the same place of the plane. The observers were experienced in identifying marine megafauna from aerial flights by previously examining photographs taken during flights. Additionally, selecting appropriate survey days, based on sea state and weather conditions, made it easier for observers to locate and identify animals (Fig. 2).

For this study, no tests were conducted to estimate the range of lateral vision from the aircraft. Instead, we assumed a 750-m field of vision from either side of the aircraft, resulting in a total width of the survey of 1.5 km, on the basis of Rowat et al. (2009). Furthermore, constant altitude and speed were maintained during the aerial surveys to avoid additional biases. A perception correction factor was not applied because all whale sharks should be observable below the altitude of 800 m (Rowat et al., 2009).

---

[1] Mention of trade names or commercial companies is for identification purposes only and does not imply endorsement by the National Marine Fisheries Service, NOAA.

Data analysis

The area surveyed was calculated as the length of the transect multiplied by the defined width of the survey (1.5 km). To standardize abundance data, density of animals by species was calculated for each flight and by month and year, by using the method described by Rowat et al. (2009), with the following formula:

$$A = C / SI,$$

where A = density;
C = counts of whale sharks or giant mantas; and
SI = survey intensity (in square kilometers).

Densities of whale sharks and giant mantas were compared between areas (the WSBR and Azul area), among years, and among months by using a nonparametric Kruskal–Wallis test ($P<0.05$). Finally, maps of distribution and abundance were generated for each species by using QGIS software, vers. 2.18.26 (QGIS Development Team, 2018).

Results

From 2016 through 2018, 17 aerial surveys were conducted in the WSBR and Azul area. During 28 h of flight, 4571 km were covered along the transect, resulting in a surveyed area of 6857 km^2. A total of 953 whale sharks and 466 giant mantas were seen (Table 1). Occasionally, both species were observed interacting in the same area.

Occurrence of whale sharks

The average number of whale sharks observed per flight was 56 (standard deviation [SD] 59). In July 2017, the largest number of whale sharks counted was 170; these sharks were aggregated in a 3.8-km^2 area. The next 2 largest groups were recorded in August 2016. During the first and second flights in August 2016, 151 and 121 whale sharks were counted, respectively. Overall, the largest aggregations were observed in the Azul area. However, it is most likely that the whale sharks recorded in one month were the same individuals observed in the following month. The largest annual number of sightings of whale sharks was recorded in 2017, with a total of 410 individuals counted, in comparison with 274 and 269 individuals counted in 2018 and 2016, respectively (Fig. 3).

The average density was 14 individuals/100 km^2 (SD 14) during 2016–2018. Although densities of whale sharks recorded in the Azul area were higher than densities in the WSBR, the differences were not statistically significant (Kruskal–Wallis test: P=0.46). Survey results indicate that there were no differences in density of whale sharks among years (Kruskal–Wallis test: P=0.69) (Fig. 4) but that there were significant differences among months (Kruskal–Wallis test: P=0.04). Results from surveys conducted in September indicate a significant decrease in recorded density from levels observed in July and August.

Table 1

Number of whale sharks (*Rhincodon typus*) and giant mantas (*Mobula birostris*) observed during aerial surveys conducted between May and September during 2016–2018 in the northern Caribbean Sea off Mexico. Most surveys were conducted from 0730 to 1130. An asterisk (*) indicates that surveys were conducted in the afternoon from 1500 to 1800.

Date of survey	Surveyed area (km^2)	Number of whale sharks observed	Number of giant mantas observed
26-July-2016	469.5	0	0
27-July-2016	388.5	120	87
25-Aug-2016	486.0	151	0
26-Aug-2016	481.5	121	13
21-Sept-2016	493.5	1	0
22-Sept-2016	415.5	17	125
18-July-2017*	247.5	10	4
20-July-2017	448.5	170	1
12-Aug-2017*	243.0	14	110
13-Aug2017	234.0	56	21
19-Sept-2017	528.0	10	3
20-Sept-2017	384.0	9	3
23-May-2018	363.0	3	36
13-July-2018	472.5	92	31
29-July-2018	367.5	109	7
23-Aug-2018	475.5	68	25
19-Sept-2018	358.5	2	0
Total	6857	953	466

Occurrence of giant mantas

The average number of giant mantas observed per flight was 27 (SD 40). The single largest number of individuals observed during one flight was 125. The largest group was recorded in September 2016, with 120 giant mantas distributed in an area of 1.2 km^2. The second-largest aggregation observed was recorded in August 2017, with 100 giant mantas located north of the Azul area but still in the MCBR. A third group of 80 individuals moving linearly in the Azul area was recorded in July 2016 (Fig. 5).

The largest annual number of giant mantas was recorded in 2016, with a total of 225 individuals counted, a year before the largest annual number of whale sharks was observed. Sightings of 142 and 99 giant mantas were recorded in 2017 and 2018, respectively (Fig. 6). From 2016 through 2018, the average density of giant mantas was 8 individuals/100 km^2 (SD 13). Survey results indicate that there were no differences in density of giant mantas among months (Kruskal–Wallis test: P=0.81), among years (Kruskal–Wallis test: P=0.62), or between areas (Kruskal–Wallis test: P=0.67).

Discussion

The site of aggregation of whale sharks and giant mantas in the northern Caribbean Sea off Mexico covers an area of

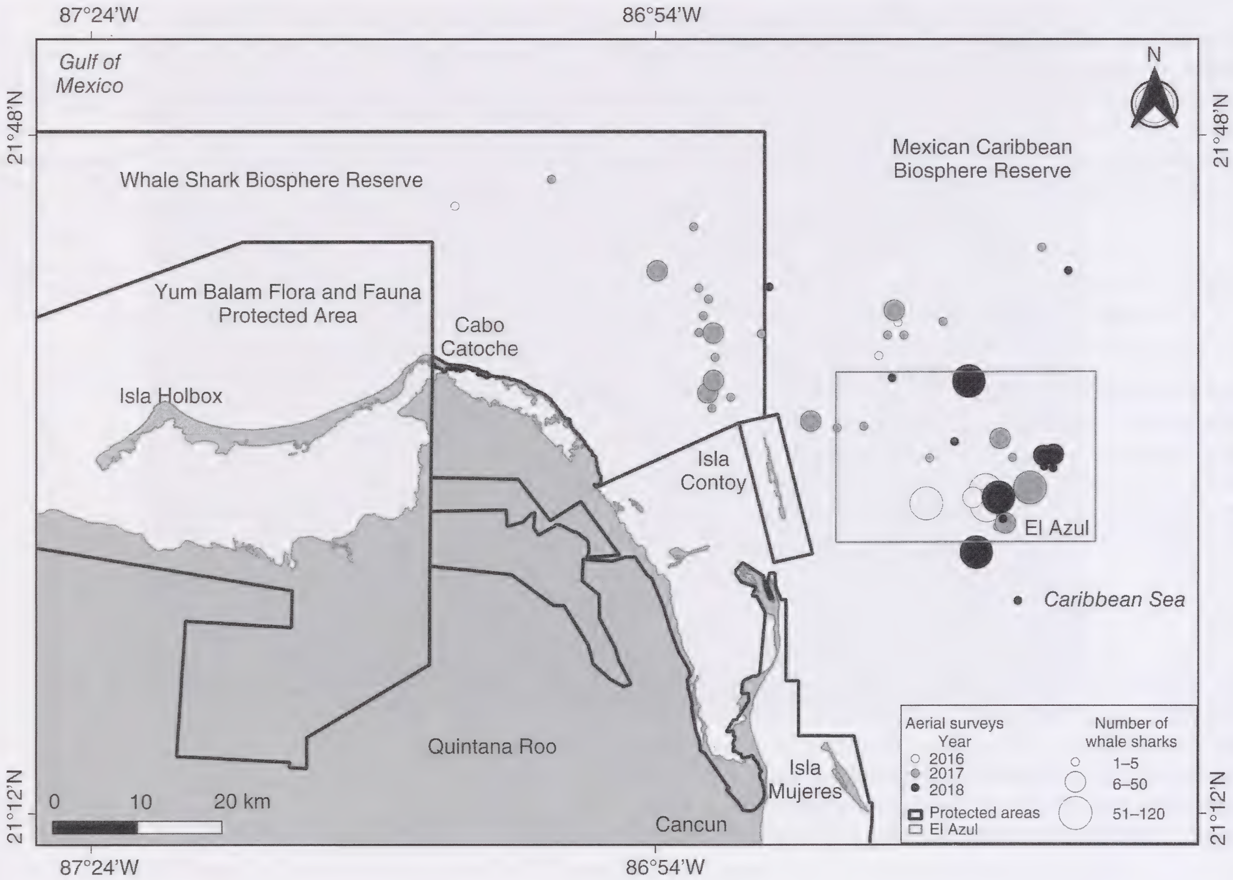

Figure 3

Map showing the distribution and abundance of whale sharks (*Rhincodon typus*) in the northern Caribbean Sea off Mexico based on data obtained from aerial surveys conducted between May and September during 2016–2018. Circle size is proportionate to the number of whale sharks observed, and circle shade corresponds to the year in which the sighting was made. The black and gray lines indicate the boundaries of protected areas and of the Azul area, respectively.

approximately 6334 km^2 (DOF, 2018a). In such large marine areas, aerial surveys facilitate surveys of the abundance of whale sharks and giant mantas by reducing the time spent on monitoring activities. In this study, we spent an average of 165 min on flight time per transect. A survey of the same transect by boat could take an estimated time of 9 h.

Prior to our study, aerial surveys have been used successfully to describe distribution and abundance of marine megafauna, such as marine mammals, manta rays, and whale sharks (Gifford et al., 2007; Rowat et al., 2009; Salberg et al., 2009; Laidre and Heide-Jørgensen, 2011). During most of the aerial surveys conducted (94%), whale sharks and giant mantas were sighted. However, a limitation of aerial surveys in monitoring of marine megafauna is not being able to detect animals at depths >3 m. Nevertheless, aerial surveys are useful for assessing the distribution and abundance of whale sharks and giant mantas because of the time that these animals spend near the sea surface. Also, aerial surveys could help with estimation of the size of aggregations and even with collection of information about tourist activities (e.g., number of boats present).

Another restriction of aerial surveys in monitoring marine megafauna is the limited time available to observe the same point on a transect. Previous studies have determined that whale sharks move between the WSBR and Azul area (Hueter et al., 2013). The use of aerial surveys is a more appropriate technique for assessing abundance of whale sharks because it is easier to observe different groups throughout a survey area and reduce the error of counting the same individual more than once.

Occurrence of whale sharks

Most sightings of whale sharks were recorded in the Azul area, which since 2009 has been reported to have the highest abundance of this species (Cárdenas-Palomo et al.,

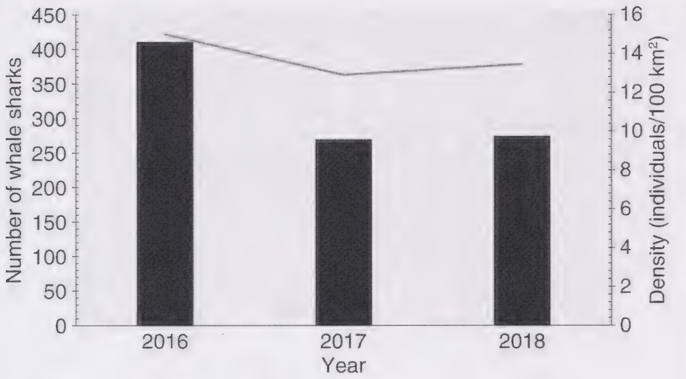

Figure 4

Number of whale sharks (*Rhincodon typus*) recorded during aerial surveys conducted in the northern Caribbean Sea off Mexico between May and September in 2016–2018. The gray line indicates estimates of density of whale sharks based on data from these surveys.

2015; Cárdenas-Palomo et al.[2]). During this study, only 7 groups of more than 70 whale sharks each were observed, all in the Azul area. Despite the importance of this area for whale sharks, it did not become a protected area until 2016, when the MCBR was established.

The Azul area is extensive, with an area of approximately 400 km^2, and it is commonly difficult to move through it by boat at a speed greater than 40 km/h because of sea conditions. As a result, aerial surveys are more efficient than boat censuses because locations of whale sharks can be identified in less time and counts of individuals are more accurate.

In the Caribbean Sea off Mexico, as in many other sites of aggregation of whale sharks around the world, the relationship between abundance and food availability has been identified (Sequeira et al., 2012; Cárdenas-Palomo et al., 2015; Pierce and Norman, 2016). The average zooplankton biomass in the Azul area during the spawning period of the little tunny (*Euthynnus alletteratus*) has been recorded at values >4000 mg/m^3, much higher than the maximum value recorded in the WSBR (approximately 600 mg/m^3). This difference in zooplankton biomass is perhaps the reason that whale sharks prefer to aggregate in the Azul area when fish are spawning (de la Parra Venegas et al., 2011; Cárdenas-Palomo et al.[2]). In our study, whale sharks inside the WSBR were observed only in July 2017. Possibly, at that time, the amount of food available in surface layers in the WSBR had increased as a result of upwelling pulses that raised productivity.

In a previous study conducted in the Azul area during 2005–2009, the reported average number of sightings of whale sharks was 67.5 individuals/flight (de la Parra Venegas et al., 2011). The kind of aircraft used and months in which the monitoring was carried out in that study were the same as those in ours. In our study, an average of 56 individuals/flight were recorded, which is 17% lower than the number of individuals observed during 2005–2009 in the previous study. A declining trend in abundance of whale sharks has already been reported for the Caribbean Sea off Mexico (Cárdenas-Palomo et al.[2]) and for other aggregation sites around the world (Rowat and Brooks, 2012; Rohner et al., 2013; Norman et al., 2017). According to Rohner et al. (2013), it is possible that broad-scale oceanographic variables could be driving the decrease in sightings of whale sharks or that the apparent decrease could be attributed to a genuine population decline. To address these unknowns for the aggregation of whale sharks in the Caribbean Sea off the Yucatan Peninsula, additional research of other ecosystem components, such as direction and intensity of ocean currents, is needed, as is information related to the population ecology and biology of this species.

From 1999 through 2015, 1115 individuals have been identified by using photographs taken in and above the Caribbean Sea off Mexico. Considering that the estimated population size for whale sharks in the western Atlantic Ocean is 2167 individuals (McKinney et al., 2017), the aggregation site in the Caribbean Sea off Mexico is a hotspot for this species (Hueter et al., 2013; Norman et al., 2017). Our knowledge about whale sharks has increased in recent years. However, it is also important to understand threats to habitat that could influence changes in distribution or abundance of this species (e.g., changes in fish spawning, global warming, and possible effects of tourist activities).

Occurrence of giant mantas

Except in 2018, most of the sightings of giant mantas were recorded north of and inside of the Azul area. These results are not consistent with those of previous studies carried out in the region during 2007–2011 (Hinojosa-Álvarez, 2009; Martínez Urrea, 2015). During these studies, areas within the WSBR, one located north of Cabo Catoche, the northernmost point of the Yucatan Peninsula, and another located northwest of Isla Contoy, were identified as the most important sites for this species. The shifts between feeding zones through time could be determined by zooplankton abundance, composition, or spatial availability. Large elasmobranch species seem to prefer sites where zooplankton are abundant,

---

[2] Cárdenas-Palomo, N., J. Trujillo-Córdova, E. Mimila-Herrera, J. Herrera-Silveira, J. I. Velazquez-Abunader, I. Osorio, and O. Reyes-Mendoza. 2020. El hábitat del tiburón ballena. *In* Tiburón ballena en el Caribe Mexicano: acciones para su conocimiento y conservación, p. 31–48. Technical report Project "Manejo sustentable del tiburón ballena en el Caribe Mexicano" conducted by Pronatura Península de Yucatán A.C., CINVESTAV-IPN Unidad Mérida, with the support of World Wildlife Fund and Carlos Slim Foundation. [Available from Pronatura Península de Yucatán A.C., Calle 32 No. 269, Pinzon II, 97205 Merida, Yucatan, Mexico.]

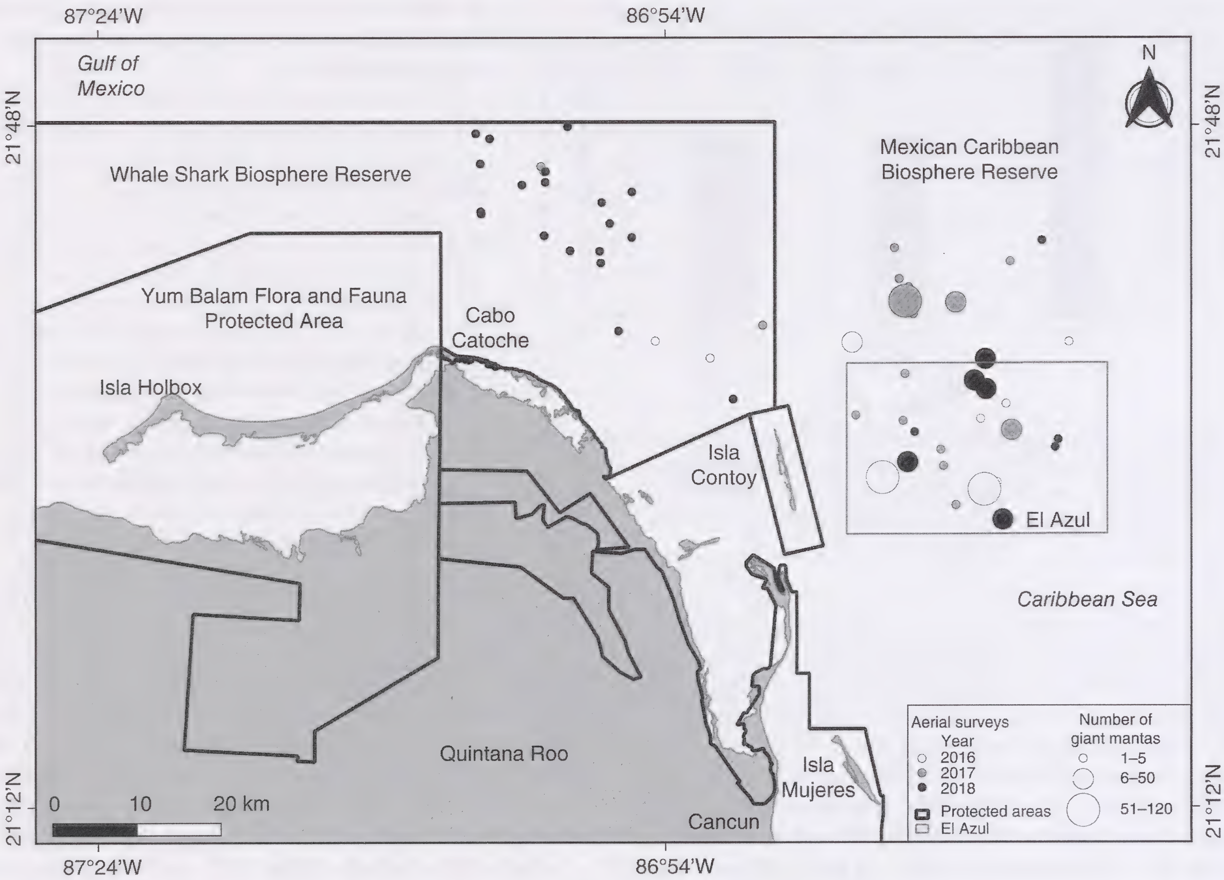

Figure 5

Map showing the distribution and abundance of giant mantas (*Mobula birostris*) in the northern Caribbean Sea off Mexico based on data obtained from aerial surveys conducted between May and September during 2016–2018. Circle size is proportionate to the number of giant mantas observed, and circle shade corresponds to the year in which the observation was made. The black and gray lines indicate the boundaries of protected areas and of the Azul area, respectively.

a preference that may be related to the amount of energy spent to locate, capture, and consume those prey (Nelson and Eckert, 2007).

It should be noted that the zone where giant mantas aggregate in the Caribbean Sea off Mexico has already been identified as a feeding site (Graham et al., 2012; Hacohen-Domené et al., 2017). By tracking movements of animals with satellite tags inside of the Azul area, Graham et al. (2012) described feeding areas of giant mantas in the locations where the largest aggregations were recorded in this study.

Reef manta rays (*Mobula alfredi*) form large aggregations (>30 individuals); in comparison, giant mantas are seldom encountered in such numbers. The overall global population sizes of both species are unknown, but subpopulations appear, in most cases, to be less than 1000 individuals (Marshall et al., 2018). During the 3 years of this study, 3 large groups of giant mantas (>80 individuals) were recorded; the largest group, of at least 120 individuals, was observed in 2016. Hinojosa-Alvarez (unpubl. data, 2010; as cited by Marshall et al., 2018) estimated the size of the subpopulation of giant mantas in the Caribbean Sea near Holbox Island, off the northeastern coast of the Yucatan Peninsula, at around 100 individuals. Our results indicate that this number is underestimated and may not represent the real size of the subpopulation in this area.

Martínez Urrea (2015) reported approximately 300 giant mantas in the Azul area during 2009. However, because the author did not provide a relative abundance index, we cannot determine whether there was an increase or decrease in sightings of giant mantas between 2009 and the years of our study. Nevertheless, it has been estimated that there has been at least a 30% decrease in the worldwide population of giant mantas over the last 75 years or so (Marshall et al., 2018). Efficient conservation strategies,

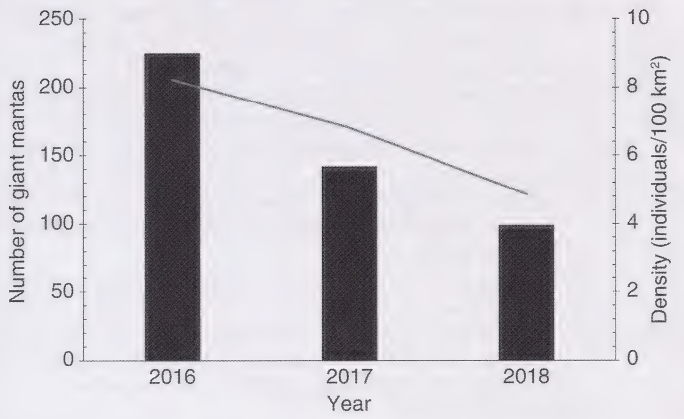

Figure 6

Number of giant mantas (*Mobula birostris*) recorded during aerial surveys conducted in the northern Caribbean Sea off Mexico between May and September in 2016–2018. The gray line indicates estimates of density of giant mantas based on data from these surveys.

therefore, are required to protect areas, such as the northern Caribbean Sea off Mexico, that have a high density of giant mantas.

Shared aggregation areas

Frequently, we observed aggregations of whale sharks and giant mantas sharing the same area, indicating that both species share resources in the Caribbean Sea off the northeastern coast of the Yucatan Peninsula. Although foraging strategy theory includes the notion that species partition resources to avoid competition (Hinojosa-Álvarez, 2009; Motta et al., 2010), recent data indicate that a dietary overlap exists between both of these planktotrophic elasmobranch species. Results from a trophic ecology study, based on an analysis of skin samples obtained from whale sharks and giant mantas from the northern Caribbean Sea off Mexico in 2010–2012, provide evidence of an alternative hypothesis of dietary overlap between these elasmobranch species (Hacohen-Domené et al.[3]). Additionally, Couturier et al. (2013) reported similar dietary preferences between whale sharks and reef manta rays in Mozambique, on the basis of comparisons of fatty acid profiles of skin samples.

Understanding the factors that affect and allow the coexistence of both planktotrophic elasmobranch species is important. Inside the WSBR, the abundance of zooplankton is a consequence of the Yucatan upwelling system. As a highly productive ecosystem, food resources might not be limited in this zone from May through September. However, the Azul area is the most important aggregation area for whale sharks and giant mantas because the quantity of available food there is much higher than in the WSBR, and it is concentrated in small patches, resulting in lower energy costs for species during foraging (Nelson and Eckert, 2007; Motta et al., 2010). In another area north of the Azul area, giant mantas were observed almost exclusively, and a high abundance of this species was observed. This area could be critical habitat for giant mantas, a place where they can forage and avoid competition. To our knowledge, there is no published information about zooplankton in this area.

Diverse economic activities, both extractive and non-extractive, are conducted in the Azul area. These activities produce a high frequency of marine traffic, such as that of cargo ships, tourist cruises, and fishing vessels, as well as that of tour boats that provide viewing of and diving near whale sharks (Graham et al., 2012; DOF, 2018b). Although these activities provide economic benefits to nearby communities, they represent a threat to whale sharks and giant mantas. This harm is evident in the high frequency of injuries by propeller impacts (especially for whale sharks; Pierce and Norman, 2016; Marshall et al., 2018). Other threats to giant mantas are from directed take and bycatch (Graham et al., 2012). Therefore, in the short term, delimiting important sites where these species may be vulnerable can help prioritize protection efforts.

The results of our study contribute to the knowledge of the distribution and abundance of whale sharks and giant mantas. The utility and effectiveness of aerial surveys in monitoring the presence and movements of these species in areas far from a coast have been proven. The distribution and abundance of whale sharks and giant mantas in the northern Caribbean Sea off Mexico indicate spatiotemporal variability, a situation that many times has obstructed the implementation of suitable management strategies for their conservation. Long-term data sets are key for assessing abundance trends of these endangered and mobile species. Because it is one of the few areas where whale sharks and giant mantas coincide in time and space, the northern Caribbean Sea off Mexico is an important location for future research.

Acknowledgments

This research was done under the project titled "Sustainable management of whale shark in the Mexican Caribbean," with the support of the World Wildlife Fund for Nature in alliance with Carlos Slim Foundation. We are grateful to the National Commission of Natural Protected Areas for the support of aerial surveys in 2016. We thank the Jet Planes Agency for the aerial service and the work of their pilots during the aerial surveys.

---

[3] Hacohen-Domené, A., N. Cárdenas-Palomo, S. Kim, G. López-Ibarra, F. Galván-Magaña, and J. Herrera-Silveira. 2019. Unpubl. data. Biol. Dep., Univ. Valle Guatemala, 18 Ave. 11-95 Zone 15, 01015 Guatemala City, Guatemala.

Literature cited

Cárdenas-Palomo, N., J. Herrera-Silveira, I. Velázquez-Abunader, O. Reyes, and U. Ordoñez.
2015. Distribution and feeding habitat characterization of whale sharks *Rhincodon typus* in a protected area in the north Caribbean Sea. J. Fish Biol. 86:668–686.

Couturier, L. I. E., C. A. Rohner, A. J. Richardson, S. J. Pierce, A. D. Marshall, F. R. A. Jaine, K. A. Townsend, M. B. Bennett, S. J. Weeks, and P. D. Nichols.
2013. Unusually high levels of n-6 polyunsaturated fatty acids in whale sharks and reef manta rays. Lipids 48:1029–1034.

de la Parra Venegas, R., R. Hueter, J. G. Cano, J. Tyminski, J. G. Remolina, M. Maslanka, A. Ormos, L. Weigt, B. Carlson, and A. Dove.
2011. An unprecedented aggregation of whale sharks, *Rhincodon typus*, in Mexican coastal waters of the Caribbean Sea. PLoS ONE 6(4):e18994.

DOF (Diario Oficial de la Federación).
2009. Decreto por el que se declara área natural protegida, con la categoría de reserva de la biosfera el área marina conocida como tiburón ballena, localizada frente a las costas del norte del Estado de Quintana Roo. Diario Oficial Fed. 669(5):84–89 (Primera Sección). [In Spanish.] [Available from website.]
2016. Decreto por el que se declara área natural protegida, con el carácter de reserva de la biosfera, la región conocida como Caribe Mexicano. Diario Oficial Fed. 759(5): 1–51 (Segunda Sección). [In Spanish.] [Available from website.]
2018a. Acuerdo por el que se establece como área de refugio para la protección de la especie tiburón ballena (*Rhincodon typus*), en su área de concentración que corresponde a la zona marina que se encuentra entre Isla Mujeres, Puerto Juárez, Chiquilá e Isla Holbox, frente a los municipios de Lázaro Cárdenas, Benito Juárez e Isla Mujeres del Estado de Quintana Roo. Diario Oficial Fed. 776(17):28–31 (Primera Sección). [In Spanish.] [Available from website.]
2018b. Acuerdo por el que se da a conocer la actualización de la Carta Nacional Pesquera. Diario Oficial Fed. 777(10):1–112 (Segunda Sección). [In Spanish.] [Available from website.]

Gifford, A., L. J. V. Compagno, and M. Levine.
2007. Aerial surveys of whale sharks (*Rhincodon typus*) off the east coast of southern Africa. *In* The first international whale shark conference: promoting international collaboration in whale shark conservation, science and management. Conference overview, abstracts and supplementary proceedings; Perth, Australia, 9–12 May 2005 (T. R. Irvine and J. K. Keesing, eds.), p. 53–57. CSIRO Marine and Atmospheric Research, Wembley, Australia. [Available from website.]

Graham, R. T., M. J. Witt, D. W. Castellanos, F. Remolina, S. Maxwell, B. J. Godley, and L. A. Hawkes.
2012. Satellite tracking of manta rays highlights challenges to their conservation. PLoS ONE 7(5):e36834.

Hacohen-Domené, A., R. O. Martínez-Rincón, F. Galván-Magaña, N. Cárdenas-Palomo, and J. Herrera-Silveira.
2017. Environmental factors influencing aggregation of manta rays (*Manta birostris*) off the northeastern coast of the Yucatan Peninsula. Mar. Ecol. 38(3):e12432.

Hinojosa-Álvarez, S.
2009. Ecología trófica de la manta gigante (*Manta birostris*, Dondorff 1798) mediante el análisis de isótopos estables de δ15N y δ13C en las áreas naturales protegidas de Yum Balam e Isla Contoy, Quintana Roo. M.S. thesis, 63 p. Univ. Autón. Méx., Mexico City, Mexico. [In Spanish.] [Available from website.]

Hueter, R. E., J. P. Tyminski, and R. de la Parra.
2013. Horizontal movements, migration patterns, and population structure of whale sharks in the Gulf of Mexico and northwestern Caribbean Sea. PLoS ONE 8(8):e71883.

Laidre, K. L., and M. P. Heide-Jørgensen.
2011. Life in the lead: extreme densities of narwhals *Monodon monoceros* in the offshore pack ice. Mar. Ecol. Prog. Ser. 423:269–278.

Marshall, A., M. B. Bennett, G. Kodja, S. Hinojosa-Álvarez, F. Galván-Magaña, M. Harding, G. Stevens, and T. Kashiwagi.
2018. *Mobula bisrostris* (amended version of 2011 assessment). The IUCN Red List of Threatened Species 2018: e.T198921A126669349. [Available from website.]

Martínez Urrea, D. A.
2015. Influencia de factores ambientales sobre la distribución de la manta gigante (*Manta birostris*) en Holbox, Quintana Roo. M.S. thesis, 75 p. Inst. Politéc. Nac., La Paz, Mexico. [Available from website.]

McKinney, J. A., E. R. Hoffmayer, J. Holmberg, R. T. Graham, W. B. Driggers III, R. de la Parra-Venegas, B. E. Galván-Pastoriza, S. Fox, S. J. Pierce, and A. D. M. Dove.
2017. Long-term assessment of whale shark population demography and connectivity using photo-identification in the Western Atlantic Ocean. PLoS ONE 12(8):e0180495.

Merino, M.
1997. Upwelling on the Yucatan Shelf: hydrographic evidence. J. Mar. Syst. 13:101–121.

Mimila-Herrera, E., J. A. Trujillo-Córdova, N. Cárdenas-Palomo, and O.F. Reyes-Mendoza.
2016. Tourist satisfaction with whale shark watching and swimming tours in the Mexican Caribbean. QScience Proc. (the 4th international whale shark conference) 2016:iwsc4.36.

Motta, P. J., M. Maslanka, R. E. Hueter, R. L. Davis, R. de la Parra, S. L. Mulvany, M. L. Habegger, J. A. Strother, K. R. Mara, J. M. Gardiner, et al.
2010. Feeding anatomy, filter-feeding rate, and diet of whale sharks *Rhincodon typus* during surface ram filter feeding off the Yucatan Peninsula, Mexico. Zoology 113:199–212.

Nelson, J. D., and S. A. Eckert.
2007. Foraging ecology of whale sharks (*Rhincodon typus*) within Bahía de Los Angeles, Baja California Norte, México. Fish. Res. 84:47–64.

Norman, B. M., J. A. Holmberg, Z. Arzoumanian, S. D. Reynolds, R. P. Wilson, D. Rob, S. J. Pierce, A. C. Gleiss, R. de la Parra, B. Galvan, et al.
2017. Undersea constellations: the global biology of an endangered marine megavertebrate further informed through citizen science. BioScience 67:1029–1043.

Pierce, S. J., and B. Norman.
2016. *Rhincodon typus*. The IUCN Red List of Threatened Species 2016:e.T19488A2365291. [Available from website.]

QGIS Development Team.
2018. QGIS Geographic Information System. Open Source Geospatial Foundation Project. [Available from website, accessed December 2018.]

Reyes-Mendoza, O., I. Mariño-Tapia, J. Herrera-Silveira, G. Ruiz-Martínez, C. Enriquez, and J. L. Largier.
2016. The effects of wind on upwelling off Cabo Catoche. J. Coast. Res. 32:638–650.

Rohner, C. A., S. J. Pierce, A. D. Marshall, S. J. Weeks, M. B. Bennett, and A. J. Richardson.

2013. Trends in sightings and environmental influences on a coastal aggregation of manta rays and whale sharks. Mar. Ecol. Prog. Ser. 482:153–168.

Rowat, D., and K. S. Brooks.
2012. A review of the biology, fisheries and conservation of the whale shark *Rhincodon typus*. J. Fish Biol. 80:1019–1056.

Rowat, D., M. Gore, M. G. Meekan, I. R. Lawler, and C. J. A. Bradshaw.
2009. Aerial survey as a tool to estimate whale shark abundance trends. J. Exp. Mar. Biol. Ecol. 368:1–8.

Salberg, A.-B., T. A. Øigård, G. B. Stenson, T. Haug, and K. T. Nilssen.
2009. Estimation of seal pup production from aerial surveys using generalized additive models. Can. J. Fish. Aquat. Sci. 66:847–858.

Sequeira, A., C. Mellin, D. Rowat, M. G. Meekan, and C. J. A. Bradshaw.
2012. Ocean-scale prediction of whale shark distribution. Diversity Distrib. 18:504–518.

National Marine
Fisheries Service
NOAA

Fishery Bulletin
established in 1881

Spencer F. Baird
First U.S. Commissioner
of Fisheries and founder
of *Fishery Bulletin*

Intra- and interannual variation in fecundity and egg size of lumpfish (*Cyclopterus lumpus*) in Iceland

James Kennedy (contact author)[1,2]
Halldór G. Ólafsson[2]

Email address for contact author: james.kennedy@hafogvatn.is

[1] Marine and Freshwater Research Institute
Fornubúðum 5
220 Hafnarfjörður, Iceland

[2] Biopol ehf.
Einbúastíg 2
545 Skagaströnd, Iceland

Abstract—Intra- and interannual variability of fecundity and egg size of lumpfish (*Cyclopterus lumpus*) were assessed for 2009 and for 2014–2019 and compared with fecundity estimates from 1967 and 1969. Downregulation of fecundity was apparent throughout ovary development, but the intensity was reduced close to spawning. The fecundity of fish spawning later in the year was higher than that of fish that spawned earlier. Carcass weight was a better predictor of fecundity than length. The model was improved through the addition of liver weight, but this led to an increase of <1.0% in the explained variance in fecundity. Variation in fecundity between the periods studied (2009 and 2014–2019) was low; however, fecundity in these study periods was higher than in 1967 and lower than in 1969. Whether these differences were due to differences in methods could not be ruled out. Average egg diameter was positively correlated with fish size and decreased from the first to the second batch, and only limited variation between years was observed in this characteristic.

Manuscript submitted 24 October 2019.
Manuscript accepted 10 August 2020.
Fish. Bull. 118:250–267 (2020).
Online publication date: 27 August 2020.
doi: 10.7755/FB.118.3.4

The views and opinions expressed or implied in this article are those of the author (or authors) and do not necessarily reflect the position of the National Marine Fisheries Service, NOAA.

The number of eggs produced by an individual fish influences the reproductive potential of the population (Trippel, 1999); however, information on fecundity and the temporal and spatial variability in this trait is lacking for many fish species. Collection of information on fecundity is not routine for most fish stocks, and spawning stock biomass is generally used as a proxy for total egg production and reproductive potential, despite indications that total egg production and reproductive potential may not be proportional to spawning stock biomass (Marshall et al., 1998). Because fecundity is not routinely estimated, fecundity estimates from a single year, or a small number of years, may be used to estimate annual changes in total egg production (Gundersen et al., 2000; Blanchard et al., 2003; Mehault et al., 2010). This use of temporally limited fecundity data may be problematic because of potential variability in fecundity between years (Rideout and Morgan, 2007).

The lumpfish (*Cyclopterus lumpus*) (Fig. 1) is a semi-pelagic species that inhabits temperate and Arctic regions of the North Atlantic Ocean. In the eastern Atlantic Ocean, it ranges from 80°N, around Svalbard, Norway (Eriksen et al., 2014), to 50°N in the English Channel (Ellis, 2015). In the western Atlantic Ocean, this species ranges from 56°N on the western coast of Greenland to around Newfoundland, Canada, and as far south as New England at about 42°N (Gregory and Daborn, 1982; Rackovan and Howell, 2017). Outside of the spawning period, juveniles and adults are distributed over open water, generally in the upper 50 m of the water column (Holst, 1993; Rosen and Holst, 2013) with adults migrating to coastal areas to spawn as the spawning period approaches.

Male lumpfish migrate to the coast before females, presumably to seek out and establish territory and spawning sites in preparation for the arrival of females. In Iceland, males arrive in January–February, and most females appear in March. Lumpfish spawn around Iceland from January through August; however, an individual fish will spawn only 2 batches of eggs with approximately 10–14 d between spawning events (Fulton, 1907; Bolton-Warberg[1]; Kennedy, 2018). Although

---

[1] Bolton-Warberg, M. 2018. Personal commun. Ryan Inst., Natl. Univ. Ireland, University Rd., Galway H91 TK33, Ireland.

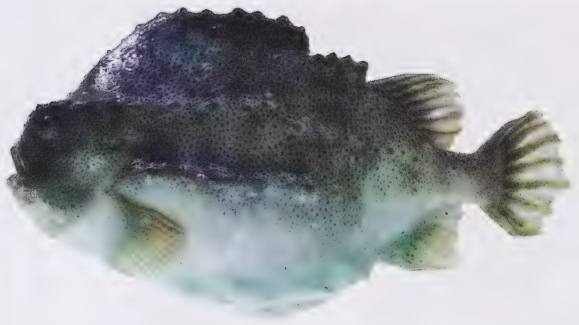

Figure 1

Photograph of a female lumpfish (*Cyclopterus lumpus*) collected at Skagaströnd, Iceland, in 2014 from the landings of the female lumpfish fishery that operates in Húnaflói Bay.

females approach the coast of Iceland in spring, they remain in deeper water (~50–300 m) until they are very close to spawning (Kennedy and Jónsson, 2017). Lumpfish spawn as deep as ~40 m to as shallow as a few meters below the low tide mark (Fulton, 1907; Todd et al., 2018). When ready to spawn, a female seeks out a male and lays her eggs in its nesting site. A male will then care for and defend the eggs until they hatch (Fulton, 1907). It is during this time, when they are in coastal areas, that females are targeted by a commercial fishery for their roe.

The precise timing of when ovary development begins in lumpfish is not known. However, vitellogenesis in preparation for spawning the following year is already underway in July (Kennedy, 2018). Therefore, ovary development takes at least 8 months to complete. During early vitellogenesis, there is a single mode of oocytes within the ovary. When the oocyte diameter of the leading cohort (LC) reaches approximately 2.0 mm, a hiatus forms in the oocyte distribution creating 2 groups of oocytes. One group consists of small oocytes (diameters <1800 µm) that are not spawned and presumably become atretic and are reabsorbed; this group is referred to as the *non-spawning group* (Kennedy, 2018). The other group comprises large oocytes (diameters >1800 µm) and is considered the *spawning group* because its oocytes will be spawned during the current spawning season. A second hiatus forms within the spawning group, creating 2 batches of oocytes that are spawned separately. Because no oocytes are recruited into the vitellogenic pool after spawning has begun, the lumpfish is considered a determinate spawner (i.e., the maximum potential fecundity is set before spawning has begun). Therefore, it is possible to determine potential fecundity of lumpfish by estimating the number of oocytes within the spawning group. However, this maximum potential fecundity may not represent realized fecundity (the actual number of eggs spawned) because fecundity may be reduced as a result of downregulation, the process whereby the number of developing oocytes is reduced as ovary development progresses.

The aim of this study was to assess the potential fecundity of lumpfish in Iceland and how it varies with ovary development, within the spawning season and between years. The fecundity estimates from this study were compared with historical estimates made in 1967 and 1969. Because lumpfish spawn only 2 batches of oocytes and the batches are easily distinguished and do not hydrate their eggs, we took the opportunity to assess variation in egg size between individuals, batches, and years.

Materials and methods

Collection of samples

Lumpfish were sampled during scientific surveys and from landings of the commercial fishery for female lumpfish during 2009 and 2013–2019 (Table 1, Fig. 2). The Icelandic groundfish surveys took place annually during autumn (September–October) and spring (February–March). The samples collected from the commercial fishery were landed in 3 harbors: Skagaströnd, Stykkishólmur, and Þórshöfn. The fish landed at these harbors are caught in Húnaflói Bay, in Breiðafjörður, and on the northern coast of Langanes, respectively (Fig. 2). Fish landed in Skagaströnd accounted for 96% of the fish sampled from the commercial fishery. Lumpfish are known to move between these areas during the spawning season; therefore, taking fish from different areas likely did not affect results of this study (Kennedy et al., 2015).

During surveys, ovaries were sampled from fish within 1 h of capture. Fish collected from the fishery were covered in crushed ice upon landing, and ovaries were sampled within 24 h. For each fish, total length (to the nearest centimeter) and total body, carcass, liver, and gonad mass (with a precision of 2 g) were measured. For fish caught in the fishery, mass of the stomach contents and mass of the stomach and intestines were measured. A macroscopically assessed ovary developmental stage (Kennedy, 2018) (Table 2) and a *spawning year*, the calendar year in which it was next expected to spawn, was assigned to each fish.

Ovary sampling

All tissue and oocyte samples were placed in 45-mL tubes containing 10% buffered formalin, but the sampling varied depending on the developmental stage assigned because of differences in the organization of the ovary. Ovaries at the *developing* stage are homogeneous, and ovaries at the stage called *spawning 1* are not. At the developmental stage spawning 1, ovulation of the first batch of eggs has occurred; therefore, both developing oocytes and ripe eggs are present within the ovary (Kennedy, 2018). The developing oocytes are located in the dorsal area of the ovary, while the eggs are located in the ventral area. For fish classified as in the developing stage, 4–6 g of ovarian tissue was taken from the caudad area of the ovary. For fish at the stage spawning 1,

Table 1

Summary of information for female lumpfish (*Cylopterus lumpus*) collected around Iceland from groundfish surveys conducted in spring (February–March) and autumn (September–October) and from landings of the commercial fishery in 2009 and 2013–2019 and for lumpfish examined during previous studies in 1967 and 1969 (Schopka, 1970; Myrseth, 1971). Information includes year, source of fish sampled or of data, start and end dates of sampling, mean size and size range of fish sampled in total length (TL), number of lumpfish sampled (*n*), and the number of lumpfish with ovaries assigned to each stage of oocyte size frequency distribution (OSFD). The sum of the number of lumpfish with ovaries at each OSFD stage is not always equal to the total number of sampled fish because some fish had ovaries for which the OSFD stage was ambiguous and, therefore, were excluded from all analyses. No lumpfish had ovaries at OSFD stage 1.

							OSFD stage				
Year	Sample or data source	Start date	End date	Mean size (cm TL)	Size range (cm TL)	*n*	2	3	4	5	6
1967	Schopka	7 April	28 April	42	37–51	48		48			
1969	Myrseth	1 May	1 May	42	35–48	50		50			
2013	Autumn	2 Oct.	9 Oct.	39	32–45	16	12				
2014	Autumn	5 Oct.	18 Oct.	39	32–47	30	29				
2015	Autumn	09 Oct.	1 Nov.	39	31–51	54	50				
2014	Spring	1 Mar.	16 Mar.	40	34–49	50	29	19			
2015	Spring	4 Mar.	15 Mar.	40	34–48	65	37	28			
2016	Spring	26 Feb.	18 Mar.	40	34–49	92	63	29			
2017	Spring	27 Feb.	13 Mar	41	34–53	198	99	94		3	
2018	Spring	10 Mar.	21 Mar	40	33–47	84	44	38		2	
2009	Fishery	5 May	3 June	38	31–48	172		172			
2014	Fishery	10 April	3 July	40	30–47	71	3	32	20	8	7
2015	Fishery	24 Mar.	22 May	41	34–48	120	5	77	26	5	7
2016	Fishery	21 Mar.	30 May	40	34–48	221	8	118	70	9	14
2017	Fishery	31 Mar.	7 June	41	34–50	200	1	76	88	15	17
2018	Fishery	3 April	16 May	39	35–46	159		93	47	13	6
2019	Fishery	4 April	21 May	41	35–51	242		154	60	11	12

a sample of ovarian tissue containing developing oocytes and a sample of eggs were taken and stored in separate tubes. A sample of eggs and a section of ovarian tissue were taken from fish at developmental stage *spawning 2* and were stored in the same tube. At the stage spawning 2, the second batch of eggs has been ovulated, and the ovary is again homogenous.

For fish sampled in 2009, fecundity was estimated by using the gravimetric method, and ovaries were not preserved in formalin. A single sample of ~5 g was weighed with a precision of 0.0001 g, and the number of oocytes within the sample was counted. These measurements were used to calculate the oocyte density, which was then used with the fresh ovary weight to calculate fecundity.

Calibration of an auto-diametric method

For fish sampled in 2013–2019, fecundity was estimated by using a combination of gravimetric and auto-diametric methods (Thorsen and Kjesbu, 2001). Calibration between the gravimetric and auto-diametric methods was done with samples collected during the autumn groundfish survey conducted in 2014 (number of fish sampled [*n*]=30) and the spring survey conducted in 2015 (*n*=65), along with samples collected from the fishery in 2015 (*n*=61). Because of the timing of sampling, few fish had oocytes with diameters of 0.8–1.2 mm; therefore, fish from the autumn groundfish survey conducted in 2015 with a gonadosomatic index >5 (*n*=12) were also included in the calibration.

The samples analyzed gravimetrically were collected in pre-weighed tubes, and as a result, the initial weight of the ovarian tissue was known. The ovarian tissue was blot-dried and weighed, and the decrease in weight due to preservation was calculated. Three subsamples were then taken and weighed, either at a precision of 0.0001 g for the samples taken from the autumn survey or to the nearest 0.001 g for samples taken from the spring survey and the fishery. The oocytes in each subsample were separated from the connective tissue by using fine paintbrushes and were photographed under a dissecting microscope; a magnification of 12.5× was used for the autumn survey samples, and a 7× magnification was used for samples from the spring survey and fishery. The images were then analyzed with ImageJ software (vers. 1.49b; Rasband, 2014) and the ObjectJ plug-in (vers. 1.03s, University of Amsterdam, available from website), which were used to measure the diameter of all oocytes present in each image. Light level was standardized by using distilled water and a gray level set at 207 (±2). Ovaries were

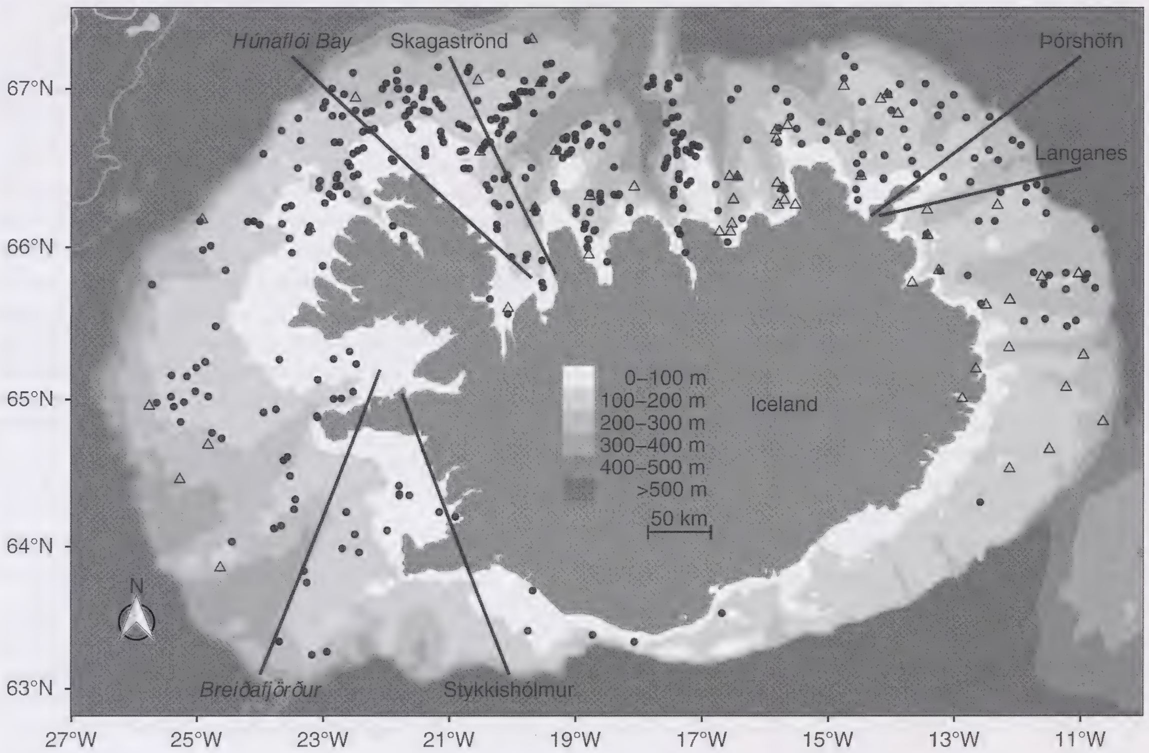

Figure 2

A map of locations where lumpfish (*Cyclopterus lumpus*) were sampled during groundfish surveys conducted around Iceland in the spring (circles) and autumn (triangles) in 2013–2018. Fish also were sampled in 2009 and 2014–2019 from landings of the commercial fishery at 3 harbors: Skagaströnd, Stykkishólmur, and Þórshöfn. Other locations mentioned in the main text are marked. The shades of gray indicate depth contours in 100-m intervals around the island nation.

assigned a stage of oocyte size frequency distribution (OSFD) (Kennedy, 2018) (Table 2). An OSFD stage could not be assigned to a small number of ovaries because the OSFD was ambiguous; these fish were excluded from all analyses. By using the data from the image analysis, several characteristics were calculated for each subsample and ovary, including average oocyte diameter, LC oocyte diameter, and oocyte density.

Average oocyte diameter For ovaries assigned to OSFD stage 2, the average diameter was calculated from all oocytes ≥400 µm. For ovaries assigned to OSFD stages 3, 4, and 5, average diameter was calculated for all the oocytes in the spawning group. Average oocyte diameter was not calculated for oocytes at OSFD stage 6. No lumpfish had ovaries at OSFD stage 1.

Leading cohort oocyte diameter For ovaries assigned to OSFD stage 2, the LC oocyte diameter was calculated from the largest 10% of oocytes ≥400 µm. For ovaries assigned to OSFD stages 3 and 5, LC oocyte diameter was calculated from the largest 10% of oocytes in the spawning group. Leading cohort oocyte diameter was used as an indicator of the progression of ovary development (Kjesbu, 1994). Leading cohort oocyte diameter was not calculated for ovaries at OSFD stages 4 or 6.

Oocyte density of subsamples For ovaries assigned to OSFD stage 2, the oocyte density of the subsamples was from the number of oocytes ≥400 µm in the subsample divided by the weight of the subsample. For ovaries assigned to OSFD stages 3, 4, and 5, the oocyte density of the subsamples was calculated from the number of oocytes in the spawning group divided by the weight of the subsample. Oocyte density of each ovary was estimated by taking the average oocyte density of the 3 subsamples. Oocyte density of the developing oocytes of ovaries at OSFD stage 4 (in which the ovary contains developing oocytes and ripe eggs) was estimated to investigate whether the number of batches present within the spawning group affected the relationship between oocyte diameter and oocyte density. Oocyte density was not calculated for ovaries at OSFD stage 6.

Some ovaries from the autumn survey contained a small number of residual eggs that were not spawned; these samples were excluded from the calibration between

Table 2

Descriptions of the macroscopically determined stages of ovary development, or maturity, and the stages of oocyte size frequency distribution (OSFD) used to assess lumpfish (*Cyclopterus lumpus*) collected around Iceland from groundfish surveys and from landings of the commercial lumpfish fishery during 2009 and 2013–2019. This table essentially is reproduced from Kennedy (2018).

Macroscopic stage	Description	OSFD stage	Description
Immature	Ovary is small, and no developing oocytes are visible.	1	Ovary contains only previtellogenic oocytes.
Developing	Ovary has increased in size and is easy to distinguish in the body cavity. Oocytes within the ovary are clearly visible. Ovary can be orange, purple, or green. A small amount of fluid may be close to the oviduct on the ventral area of the ovary; this fluid should not be confused with the large amount of viscous ovarian fluid and eggs seen in the spawning stage.	2	The oocyte size frequency distribution indicates a single group of oocytes within the ovary with diameters of almost all oocytes <1800 µm. Distribution is unimodal and, as ovary development progresses, becomes negatively skewed.
		3	A hiatus has formed in distribution at diameters around 1400–1600 µm, separating oocytes into 2 distinct groups. The group of large oocytes (with diameters typically >1800 µm) has a bimodal distribution, and the distribution of the group with small oocytes (≤1800 µm) is variable. In a small number of cases, the small oocytes may not be present.
Spawning 1	Separation in the ovary is clear. There are developing oocytes in the dorsal area of the ovary and ripe eggs in the ventral area of the ovary. The developing oocytes are connected to ovarian tissue. The eggs look “wet,” are not connected to the ovarian tissue, flow freely within the ovary, and are bathed within a viscous ovarian fluid.	4	Ovary contains developing oocytes and ripe eggs. The eggs are larger than the developing oocytes. Both the eggs and developing oocytes have a unimodal size distribution. There may also be a group of small oocytes (diameters <1800 µm) with a variable size frequency distribution.
Partially spent	Ovary is similar in appearance to, and difficult to discern from, an ovary in the developing stage.	5	There may be 1 or 2 groups of oocytes present within the ovary. A group of large oocytes (with diameters typically >1800 µm) has a unimodal distribution, and the size frequency distribution of the group with small oocytes (≤1800 µm) is variable. In a small number of cases, the small oocytes may not be present.
Spawning 2	Ovary is flaccid and contains mostly ripe eggs, which flow freely within the ovary. The eggs are not connected to ovarian tissue and are bathed within a viscous ovarian fluid. The dorsal area of the ovary wall has a “banded” appearance.	6	Ovary contains a single group of ripe eggs that have a unimodal distribution. There may also be a group of small oocytes (diameters <1800 µm), with a variable size frequency distribution.
Spent	Ovary is flaccid, and a small number of residual eggs may be visible.	7	Ovary may contain a small number of residual eggs or oocytes with a size distribution similar to that of oocytes at stage 2, 3, or 6.

gravimetric and average oocyte diameter, as well as from all fecundity analyses, because of concerns about nonhomogeneity of the ovary.

Measurements of oocyte size and oocyte density were $\log_{10}$-transformed, and general linear models were fitted by using R (vers. 3.6.1; R Core Team, 2019). These models were used to estimate oocyte density from measurements of oocyte size.

Estimation of fecundity with the auto-diametric method

Fecundity was estimated by using the auto-diametric method for fish with ovaries at OSFD stages 2, 3, and 5. For each fish, a small piece of preserved ovary was blotted to remove excess formalin; then the oocytes were separated and photographed. Images were analyzed and average oocyte diameter was calculated in a manner similar to that described previously. For each fish, a minimum of 150 oocytes ≥400 µm were measured. Oocyte density was estimated from average oocyte diameter by using the relationships described previously (see the "Results" section). Fecundity could then be estimated by multiplying oocyte density by weight of preserved ovary (see the "Results" section). Fecundity was estimated only for fish with an average oocyte diameter >550 µm, the minimum average oocyte size used in the oocyte diameter–oocyte density calibration. Leading cohort oocyte diameter was calculated for each fish in a similar manner to that previously mentioned.

Because oocytes were not measured for samples collected in 2009, the LC oocyte diameter for these samples was calculated on the basis of a linear relationship between $\log_{10}$-transformed oocyte density (calculated as fecundity divided by ovary weight) and $\log_{10}$-transformed LC oocyte diameter. From this relationship, LC oocyte density was calculated with this equation:

$$\log_{10}(\textit{LC oocyte diameter}) = 3.94 + \log_{10}(\textit{oocyte density}) \times -0.27. \qquad (1)$$

Eighty eggs were measured from ovaries at the developmental stages spawning 1 or spawning 2. Preservation in formalin does not affect diameter of oocytes because lumpfish lay demersal eggs that are not hydrated (senior author, unpubl. data).

Effects of preservation

Because the auto-diametric method was calibrated by using ovaries preserved in 10% formalin, the effect of preservation on fresh ovary weight was examined by using the same ovaries used in the auto-diametric calibration. On the basis of these results, preserved ovary weight was estimated by using a combination of average oocyte diameter and fresh ovary weight (see the "Results" section).

Historical estimates

Data on fecundity for 1967 and 1969 were extracted by using digitized images of plots of fecundity versus length from Schopka (1970) and Myrseth (1971). A sampling date was assigned to the data from each study. Schopka (1970) sampled fish during 7–28 April 1967; because it was not possible to assess a specific sampling date to each fish, they were all assigned a day midway through the sampling period: 16 April. Myrseth (1971) collected samples on 1 May 1969.

Statistical analysis

General linear models were fitted to the data, and the best models were chosen on the basis of the coefficient of determination (r^2) and the Akaike information criterion (AIC). Variables included in the models were length, carcass weight, liver weight, date of capture (expressed as day of year), and spawning year. Carcass weight was included in the models, as opposed to whole body weight, because part of whole body weight was composed of ovary weight, which was used to estimate fecundity. In addition, large amounts of water and food (up to 800 g or 23% of total body mass) were present in many stomachs from the fish caught during the spring and autumn surveys but not in those from fish sampled from the commercial fishery. Date of capture was converted to a numerical number (1–365), with 1 September rather than 1 January as day 1 because fish in the same ovary development cycle were captured before and after 1 January.

Expected fecundity before spawning of the first batch was calculated for fish with ovaries at OSFD stage 5 by using the general linear model of *fecundity=length+date of capture*, fitted to data from fish with ovaries at OSFD stage 3. The date of capture of the fish with ovaries at OSFD stage 5 was set as 14 d prior to their date of capture on the basis of the assumption of 14 d between the spawning of the first and second batches of eggs (Fulton, 1907). The result of actual fecundity divided by expected fecundity for fish with ovaries at OSFD stage 5 gives an indication of the proportion of eggs spawned in the first batch of eggs (e.g., a value of 0.50 would indicate that approximately half of the eggs were spawned in the first batch and the remaining half would have been spawned in the second batch). The resultant values of proportion of eggs spawned were tested, with a 1-sample Student's *t*-test, to determine whether the mean proportion of eggs spawned for all ovaries assigned to OSFD stage 5 was significantly different from 0.50. Carcass weight was not used to predict fecundity for fish with ovaries assigned to OSFD stage 5 because carcass weight at length was lower for fish at this stage than for fish with ovaries at OSFD stage 3, indicating carcass weight decreased during the time between these stages. Length was not expected to change between stages.

Ovaries containing eggs

Because of the heterogeneous nature of the ovary, fecundity could not be estimated for ovaries that contained ripe eggs (i.e., ovaries at stages spawning 1 and spawning 2). Average diameter of the developing oocytes and eggs was measured in a manner similar to that described previously. The effect of carcass weight and batch number was investigated by using general linear models, with oocyte diameter and carcass weight $\log_{10}$ transformed. Possible effects of spawning year were investigated by using a Tukey's honestly significant different (HSD) test.

Results

Calibration of the auto-diametric method

For ovaries at OSFD stage 2 (on the basis of $\log_{10}$-transformed data), there was a significant negative linear correlation between average oocyte diameter and oocyte density (linear regression: n=88, r^2=0.99, P<0.001) (Fig. 3).

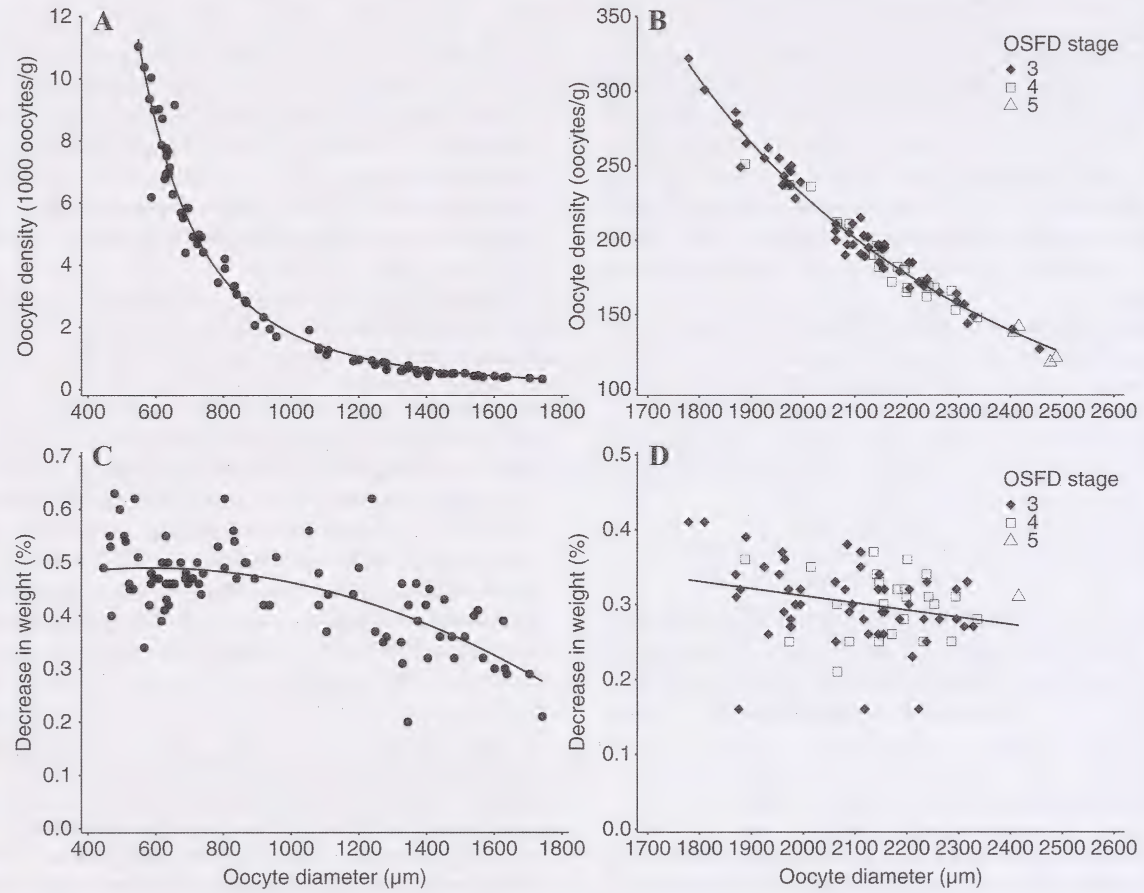

Figure 3

Relationships between oocyte diameter and oocyte density of lumpfish (*Cyclopterus lumpus*) with ovaries at oocyte size frequency distribution (OSFD) (**A**) stage 2 and (**B**) stages 3 (diamonds), 4 (squares), and 5 (triangles) and relationships between oocyte diameter and the decrease in weight of ovaries due to preservation in 10% formalin for lumpfish with ovaries at (**C**) stage 2 and (**D**) stages 3, 4, and 5. Lines indicate the power regression in panels A and B, polynomial regression in panel C, and linear regression in panel D. Ovaries classified as at OSFD stage 2 contain a single group of oocytes between 400 and 1800 µm with a unimodal size frequency distribution. In ovaries classified as at OSFD stage 3, a break in size frequency distribution separates oocytes into a group of large oocytes (diameters >1800 µm) that have a bimodal distribution and a group of small oocytes (diameters ≤1800 µm) that have a variable distribution; the oocyte diameter and oocyte density refer to the group of large oocytes. At OSFD stage 4, ripe eggs and developing oocytes have a unimodal distribution; the oocyte diameter and oocyte density refer to the developing oocytes. At OSFD stage 5, a group of large oocytes has a unimodal distribution and, if present, a group of small oocytes has a variable distribution. Lumpfish were sampled around Iceland in 2009 and 2013–2019 during groundfish surveys and from commercial fishery landings.

By using these data and the following equation, oocyte density was estimated for ovaries at this stage:

$$\textit{Oocyte density} = 10^{-3.15 \log_{10}(\textit{oocyte diameter})+12.68}. \qquad (2)$$

There was no significant difference in the relationship between average oocyte diameter and oocyte density for fish with 2 batches of oocytes in the spawning group (ovaries assigned to OSFD stage 3) and fish with 1 batch of oocytes in the spawning group (ovaries assigned to OSFD stage 4 or 5) (general linear model: $P>0.05$); therefore, the data from these 3 stages were combined. The $\log_{10}$-transformed data indicate that there was a significant negative linear correlation between average oocyte diameter and oocyte density (linear regression: $n=85$, $r^2=0.97$, $P<0.001$) (Fig. 3). By using these data and the following equation, oocyte density was estimated for ovaries at the OSFD stages 3–5:

$$\textit{Oocyte density} = 10^{-2.79 \log_{10}(\textit{oocyte diameter})+11.57}. \qquad (3)$$

Effects of preservation

The decrease in weight of ovarian tissue after fixation in formalin for ovaries in OSFD stage 2 was correlated with average oocyte diameter, and on the basis of AIC values, a second order polynomial regression gave the best fit to the data (polynomial regression: n=86, r^2=0.46) (Fig. 3). The weight of ovaries, adjusted for the effect of preservation, was calculated by using this equation:

$$\textit{Preserved weight} = \textit{fresh weight}\ (1 - [(1.87 \times 10^{-4}\ \textit{oocyte diameter}) + (-1.6 \times 10^{-7}\ \textit{oocyte diameter}^2) + 0.44]). \quad (4)$$

The decrease in weight of ovarian tissue after fixation in formalin for ovaries in OSFD stages 3 and 5 was negatively and linearly correlated with average oocyte diameter (linear regression: n=78, r^2=0.06) (Fig. 3). The weight of ovaries, adjusted for the effect of preservation, was calculated by using this equation:

$$\textit{Preserved weight} = \textit{fresh weight} \times (1 - [-9.6 \times 10^{-5}\ \textit{oocyte diameter} + 0.5]). \quad (5)$$

Fecundity and ovary development

It is common to $\log_{10}$ transform fecundity and body size data for fish in order to satisfy the assumptions of linear regression. However, general linear models of untransformed data gave a better fit than $\log_{10}$-transformed data, with coefficients of multiple determination (R^2) of 0.42 and 0.38 for the general linear model of fecundity and carcass weight with untransformed and transformed data, respectively. All assumptions of linear regression were met when untransformed data were used; therefore, untransformed data were used throughout the data analysis.

For fish with ovaries at OSFD stage 2, the best model for the prediction of fecundity included carcass weight, LC oocyte diameter, and spawning year (Table 3, Suppl. Table 1 [online only]) with fecundity being positively correlated with carcass weight and negatively correlated with LC oocyte diameter (Fig. 4). Fecundity was significantly lower in 2014 than in all other years, and in 2015 it was significantly higher than in all other years, as indicated by results from the Tukey's HSD test. Carcass weight was a better predictor of fecundity than length.

For fish with ovaries at OSFD stage 3, carcass weight was a better predictor of fecundity than length. The best model for the prediction of fecundity included carcass weight, liver weight, date of capture, and LC oocyte diameter (Table 4, Suppl. Table 2 [online only]). In this model, fecundity was positively correlated with carcass weight, liver weight, and date of capture and negatively correlated with LC oocyte diameter (Fig. 5). The addition of liver weight and LC oocyte diameter to the model, although both statistically significant, increased the explanatory power of the model by <1.0% each (Suppl. Table 2) (online only). There was no significant difference in fecundity between years in the study period 2014–2019 (Fig. 6). Mean relative fecundity was 34,700 oocytes/kg body weight (standard deviation [SD] 5900).

Potential fecundity of fish with ovaries at OSFD stage 5 was, on average, 0.54 (SD 0.19) of the fecundity expected of fish with ovaries classified as in OSFD stage 3 on the basis of length (Fig. 7). These values were not significantly different from the expected value of 0.50 (Kennedy, 2018) (Student's t-test: t=1.7, df=63, P=0.09). On removal of 4 outliers (Fig. 7), the average potential fecundity decreased to 0.50 (SD 0.12) of the fecundity expected of fish with ovaries classified as at OSFD stage 3 on the basis of length.

When data from 2009 were included in the general linear model of *fecundity=carcass weight+liver weight+date*

Table 3

Estimates of fecundity from the best general linear model for lumpfish (*Cylopterus lumpus*) with ovaries at oocyte size frequency distribution (OSFD) stage 2. This model included carcass weight, leading cohort (LC) oocyte diameter, and spawning year. Ovaries classified as at OSFD stage 2 contain a single group of oocytes between 400 and 1800 µm with a unimodal size frequency distribution. Fecundity estimates, obtained by using gravimetric and auto-diametric methods, are given in number of oocytes. The model was fit to data from fish sampled around Iceland during 2013–2019. SD=standard deviation.

Term	Estimate	SD	t	P
(Intercept)	51,5269.9	38589.3	3.4	<0.0001
Carcass weight	123.2	11.7	0.5	<0.0001
Spawning year: 2015	−17,0746.5	25,611.0	6.7	<0.0001
Spawning year: 2016	−84,873.4	21,797.4	3.9	<0.001
Spawning year: 2017	−81,345.8	22,167.5	−3.7	<0.001
Spawning year: 2018	−51,092.5	25,423.5	2.0	<0.05
LC oocyte diameter	−244.8	15.0	−16.3	<0.0001

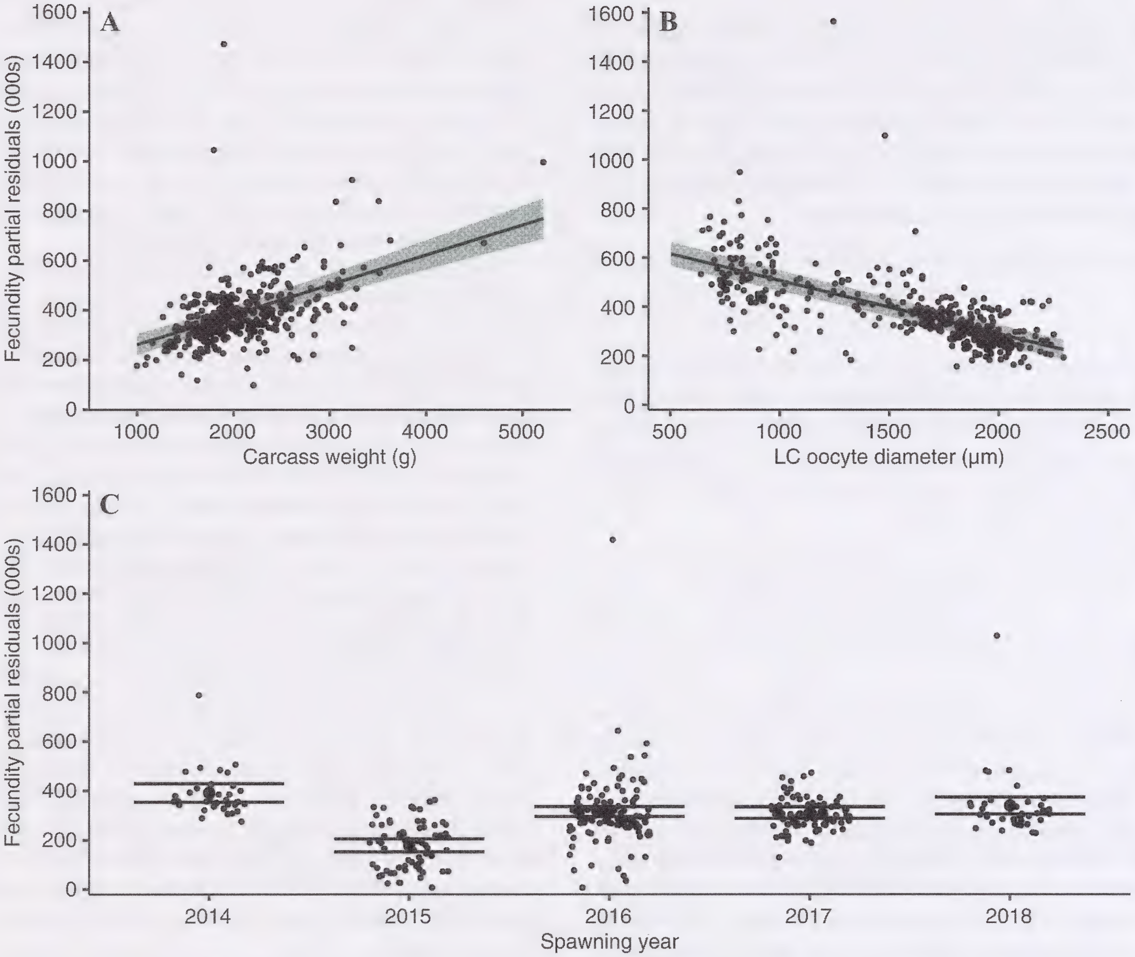

Figure 4

Plots of partial residuals for (**A**) carcass weight, (**B**) leading cohort (LC) oocyte diameter, and (**C**) spawning year, from the model that best explains the variability of fecundity in lumpfish (*Cyclopterus lumpus*) with ovaries at oocyte size frequency distribution (OSFD) stage 2. Ovaries classified as at OSFD stage 2 contain a single group of oocytes between 400 and 1800 µm with a unimodal size frequency distribution. In panels A and B, the linear regression line is shown, and the gray shaded area indicates 95% confidence intervals. In panel C, the horizontal lines indicate 95% confidence intervals. Fecundity estimates, obtained by using gravimetric and auto-diametric methods, are given in number of oocytes. The model was fit to data from fish sampled around Iceland during 2009 and 2013–2019.

of capture+year, spawning year was a significant factor in the model with fecundity significantly lower in 2009 than in 2015 ($P<0.01$), 2016 ($P<0.05$), 2017 ($P<0.01$), and 2019 ($P<0.05$) (Fig. 8). The result was similar when the data for back-calculated LC oocyte diameter was included in this general linear model. The biggest difference was between 2009 and 2017, with fecundity being ~8.7% lower in 2009 than in 2017 for a fish with an average carcass weight (1860 g), average liver weight (111 g), average date of capture (day 106), and average LC oocyte diameter (2306 µm).

Fecundity estimates from 1967 and 1969 were significantly lower and significantly higher, respectively, than in all the years in our study when we used the model of *fecundity=length+date of capture+year* ($P<0.001$) (Figs. 8 and 9). It should be noted that the use of length rather than carcass weight in the model gave a slightly different result in regard to differences in fecundity between 2009 and 2014–2019, with this difference no longer apparent when length was used as the covariate (Fig. 9).

Egg size

The general linear model revealed that $\log_{10}$-transformed average egg diameter was significantly correlated with $\log_{10}$-transformed carcass weight ($P<0.001$). In addition,

Table 4

Estimates of fecundity from the best general linear model for lumpfish (*Cyclopterus lumpus*) with ovaries at oocyte size frequency distribution (OSFD) stage 3. This model included carcass weight, liver weight, day of year captured, and leading cohort (LC) oocyte diameter. In ovaries classified as at OSFD stage 3, a break in size frequency distribution separates oocytes into a group of large oocytes (diameters >1800 µm) that have a bimodal distribution and a group of small oocytes (diameters ≤1800 µm) that have a variable distribution. Fecundity estimates, obtained by using gravimetric and auto-diametric methods, are given in number of oocytes. The model was fit to data from fish sampled around Iceland during 2009 and 2014–2019. SD=standard deviations.

Term	Estimate	SD	*t*	*P*
(Intercept)	–3497.5	13,717.1	0.3	0.80
Carcass weight	37.4	2.4	5.7	<0.0001
Liver weight	76.6	30.8	2.5	<0.05
Day of year 2	301.7	28.8	0.5	<0.0001
LC oocyte diameter	–14.1	6.2	2.3	<0.05

average egg diameter was significantly lower (approximately 1.6%) for fish with ovaries at developmental stage spawning 2 than for fish with ovaries at the stage spawning 1 ($P<0.01$). Average egg diameter was significantly different between years ($P<0.001$) (Fig. 10); however, results of the Tukey's HSD test indicate that the only significant difference was between 2014 and 2016 ($P<0.05$).

Discussion

Lumpfish add to a growing list of diverse fish species for which downregulation of fecundity, the process whereby the number of developing oocytes are reduced as ovary development progresses, has been documented (Vladykov, 1956; Kurita et al., 2003; Saborido-Rey et al., 2015; Flores et al., 2017). In many determinate spawners, there are several months between the commencement of ovary development, with the recruitment of previtellogenic oocytes to the developing pool of vitellogenic oocytes, and the spawning of these oocytes (Rijnsdorp, 1989; van Damme et al., 2009; Skjæraasen et al., 2017). Because the actual energy available for reproduction is difficult to forecast at this early stage of ovary development, more oocytes are recruited to the developing pool than could be taken to full development. As ovary development proceeds, the number of oocytes can be reduced, meaning they can be fine-tuned to the actual energy available through reabsorption of a portion of oocytes through atresia (Kraus et al., 2008; van Damme et al., 2009; Nissling et al., 2016). The energy that was invested into those oocytes can then presumably be made available for other purposes. This process, therefore, maximizes the number of eggs spawned given the amount of energy available.

This downregulation has an implication for the method used when investigating fecundity in fish. If a fish is sampled before downregulation is complete, then realized fecundity (number of eggs actually spawned) will be overestimated. Downregulation in lumpfish takes place mostly during OSFD stage 2. Fecundity decreases at OSFD stage 3, and this decrease is relatively small. Therefore, fecundity of lumpfish can be reliably estimated when ovaries are in OSFD stage 3.

Carcass weight was the best predictor of fecundity and notably outperformed length. This result is consistent with findings from other studies of fish fecundity that indicate that body weight is generally a better predictor of fecundity than length (Koops et al., 2004; Rideout and Morgan, 2010; Tanaka et al., 2017). The addition of liver weight explained only a small percentage of the variation in fecundity. This finding corresponds with those of previous studies in which characteristics intended to measure "condition," or energy reserves, added little in comparison to the factors reflecting body size (Alonso-Fernández et al., 2009; Rideout and Morgan, 2010; Rogers et al., 2019). The reason that such indices of energy reserves have a minor effect on explained variance is likely that, when sampling fish close to spawning, the energy to be used for ovary development has already been transferred from storage to the gonads. Therefore, the remaining energy at the time of sampling consists mainly of the energy required to complete and survive spawning and would not be expected to correlate with fecundity.

It is interesting to note that fish spawning later in the year had a higher fecundity than fish spawning earlier. Intra-annual variation in batch fecundity of indeterminate spawners is well documented (Alheit, 1993), but such variation has rarely been documented in determinate spawners. One of the few examples was reported by

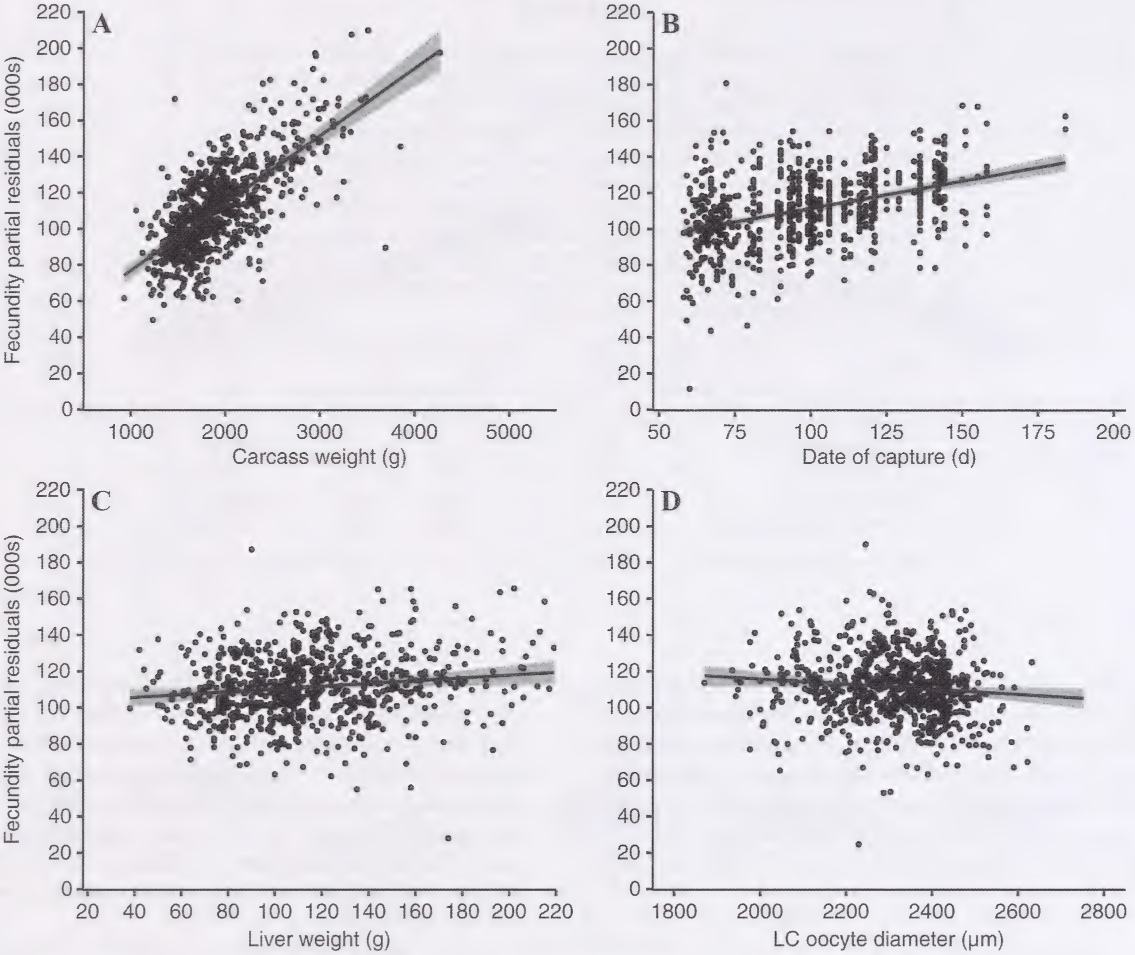

Figure 5

Plots of partial residuals for (**A**) carcass weight, (**B**) date of capture, (**C**) liver weight, and (**D**) leading cohort (LC) oocyte diameter, from the model that best explains variability in fecundity of lumpfish (*Cyclopterus lumpus*) with ovaries at oocyte size frequency distribution (OSFD) stage 3. In ovaries classified as at OSFD stage 3, a break in size frequency distribution separates oocytes into a group of large oocytes (diameters >1800 µm) that have a bimodal distribution and a group of small oocytes (diameters ≤1800 µm). In each panel, the linear regression line is shown, and the gray shaded area indicates 95% confidence intervals. For date of capture, 1 January was set as day 1 to aid interpretation. Fecundity estimates, obtained by using gravimetric and auto-diametric methods, are given in number of oocytes. The model was fit to data from fish sampled around Iceland during 2009 and 2013–2019.

Kjesbu et al. (1998), who found that fecundity was higher for Atlantic cod (*Gadus morhua*) that had already begun spawning than for fish that had not (i.e., early spawners had a higher fecundity than late spawners). The reason for this pattern in Atlantic cod was not clear, but Kjesbu et al. (1998) speculated that it was due to differences in sea temperatures between the timing of vitellogenesis of early and late spawners or was a result of the 2 groups belonging to different subpopulations. The results of our study and the fact that this aspect is rarely addressed in fecundity studies of determinate spawners highlight that a lack of variation in fecundity through the spawning season should not be assumed. Failure to investigate whether this variation indeed occurs in other species and populations could lead to bias when estimating the total egg production of a population or when using the annual egg production method for estimating spawning stock biomass.

What are the potential causes of this intra-annual variation in fecundity of lumpfish? Although the extent of the feeding area of lumpfish from Iceland is not fully known, there are indications that it may cover the Irminger Sea from southeastern Greenland, over the Denmark Strait and into the Norwegian Sea (Nøttestad

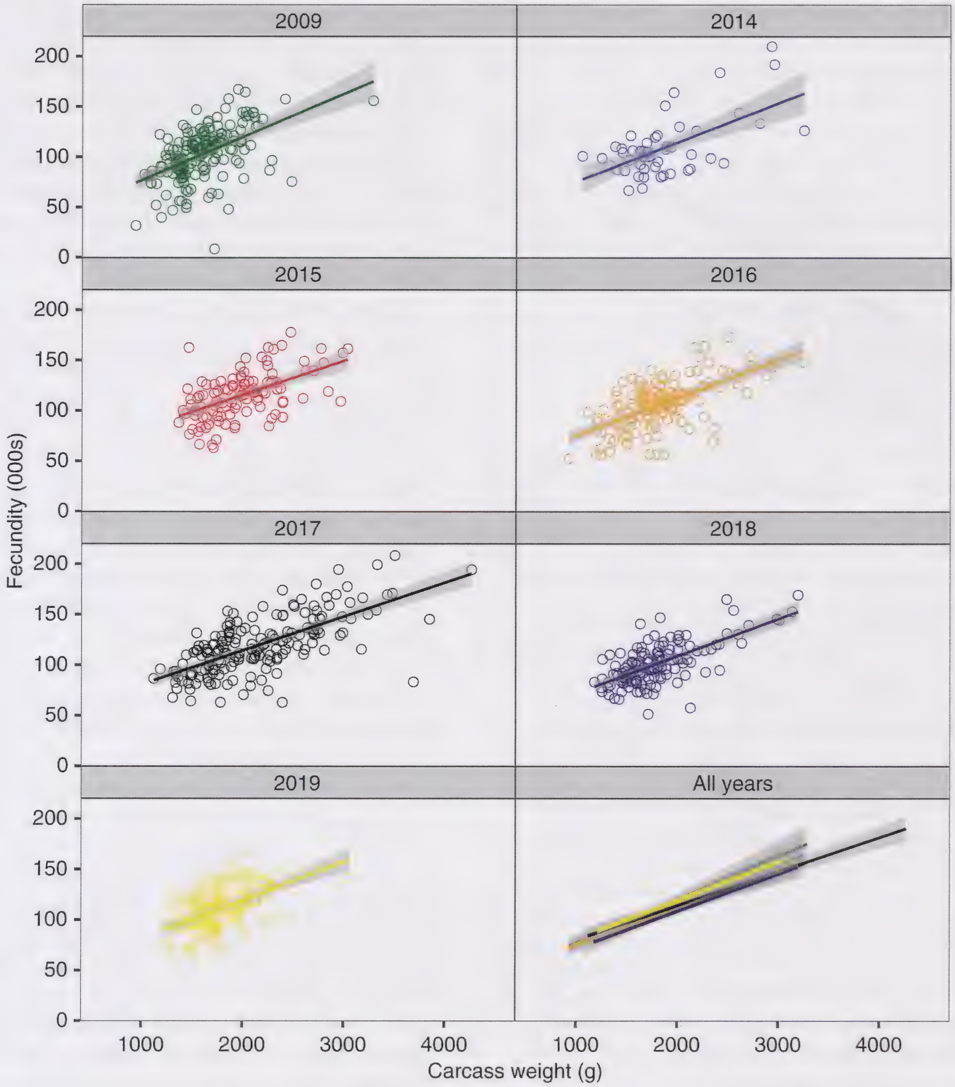

Figure 6

Relationships between carcass weight and fecundity for lumpfish (*Cyclopterus lumpus*) that had ovaries at oocyte size frequency distribution (OSFD) stage 3 and were sampled from the spring groundfish survey and landings of the commercial fishery at harbors around Iceland in 2009, 2014, 2015, 2016, 2017, 2018, and 2019 and in all years. In ovaries classified as at OSFD stage 3, a break in size frequency distribution separates oocytes into a group of large oocytes (diameters >1800 µm) that have a bimodal distribution and a group of small oocytes (diameters ≤1800 µm). In each panel, the linear regression line is shown, and the gray shaded area indicates 95% confidence intervals. Fecundity estimates, obtained by using gravimetric and auto-diametric methods, are given in number of oocytes.

et al.[2]). Over this large area, there will be differences in biotic and abiotic conditions that could drive differences in fecundity and spawning time in different parts of the population. In addition, if early and late spawners begin ovary development at different times of the year, the environmental conditions during vitellogenesis will differ, and that difference could also affect the resultant fecundity (Kjesbu et al., 2010). This aspect of fecundity of lumpfish is interesting in the context of the premise that lumpfish that spawn early or late in a spawning season will spawn early and late in the following season, respectively (Kennedy and Ólafsson, 2019). This intra-annual

---

[2] Nøttestad, L., V. Anthonypillai, S. Vatnehol, A. Salthaug, Å. Høines, A. H. Ólafsdóttir, J. Kennedy, E. Homrum, L. Smith, T. Jansen, et al. 2019. Cruise report from the International Ecosystem Summer Survey in the Nordic Seas (IESSNS) 28th June–5th August 2019. Working document to ICES Working Group on Widely Distributed Stocks (WGWIDE, No. 5), Spanish Institute of Oceanography (IOE), Santa Cruz, Tenerife, Canary Islands, 28 August–3 September 2019, 48 p. [Available from website.]

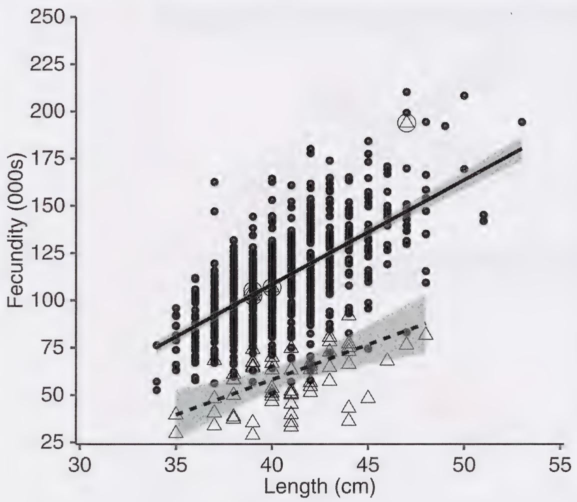

Figure 7

Relationship between total length and fecundity for all lumpfish (*Cyclopterus lumpus*) that had ovaries at oocyte size frequency distribution (OSFD) stages 3 (circles) and 5 (triangles) and were sampled from the spring groundfish survey and landings of the commercial fishery at harbors around Iceland during 2009 and 2014–2019. In ovaries classified as at OSFD stage 3, a break in size frequency distribution separates oocytes into a group of large oocytes (diameters >1800 µm) that have a bimodal distribution and a group of small oocytes (diameters ≤1800 µm). At OSFD stage 5, a break in size frequency distribution separates oocytes into a group of large oocytes (diameters >1800 µm) that have a unimodal distribution and a group of small oocytes (diameters ≤1800 µm). Linear regression lines are shown for OSFD stages 3 (solid) and 5 (dashed), with 95% confidence intervals represented by the gray shaded areas. Outliers are circled. Fecundity estimates, obtained by using gravimetric and auto-diametric methods, are given in number of oocytes.

difference in fecundity means that late-spawning fish, assuming similar spawning mortality, will have greater lifetime fecundity than early-spawning fish. However, greater lifetime fecundity may not translate into greater numbers of surviving offspring because mortality of lumpfish in early life stages may not be equal through the spawning season as a result of differing environmental conditions, prey availability, or predation (Methot, 1983; Narimatsu and Munehara, 1999; Voss et al., 2006).

Although there was interannual variability in the fecundity of lumpfish, the variability during 2009–2019 was low in comparison with the variability observed in other long-term studies of fish fecundity (Kjesbu et al., 1998; Kennedy et al., 2007; Rideout and Morgan, 2007). The extent to which fecundity varies between years in fish species is poorly understood because of a limited number of multiyear studies. Knowledge of what drives variability, or the lack thereof, is also limited, but there is some evidence that levels of specific prey items and abiotic conditions can play a role (Kjesbu et al., 1998). The reasons for the limited variability in fecundity between years observed in our study are unclear. It may be a result of stable environmental conditions and food availability in the years studied, or it may be that lumpfish place a high priority on reproduction and will maintain a similar level of fecundity from year to year at the expense of growth or energy reserves.

There were clear differences in fecundity in our study compared with historical estimates from Schopka (1970) and Myrseth (1971). Both studies used different methods in order to estimate fecundity. Schopka (1970) preserved the gonads in Gilson's fluid and used an automatic egg counter, and Myrseth (1971) froze ovaries and then used the gravimetric method. How the authors of the previous studies accounted for fish that had already spawned one batch differed. Schopka (1970) did not take it into account, and Myrseth (1971) included only fish in which the ovary filled the body cavity down to the abdomen in order to exclude any fish that had spawned one batch. Bear in mind that the number of fish that were caught in the commercial fishery and had ovaries at OSFD stage 5 in our study was low, approximately 7%.

Inclusion of fish with ovaries assigned to OSFD stage 5 in fecundity estimates will lower the estimated population fecundity; however, exclusion of fish with small gonads has the potential to exclude fish with low fecundity and, therefore, lead to an overestimation of population fecundity. The fecundity estimates of 1969 are almost all within the upper range of expected values based on estimates from 2009 and 2014–2019. In contrast, the variability was lower in 1969, and there is a notable lack of fecundity values within the lower range of values seen in 2009 and in 2014–2019. This lower variability and lack of fish within the lower range of fecundity values in 1969 indicates that the difference in fecundity between 1969 and the fecundity estimated in our study is largely driven by the bias in sampling in Myrseth (1971); therefore, the difference between the fecundity in 1969 and in 2009–2019 is likely a result of a difference in method.

In our study, no fish at OSFD stage 3, and approximately one third of fish at OSFD stage 5, had a fecundity <50,000 oocytes. Only one fish from Schopka (1970) had a fecundity <50,000 oocytes, indicating that the occurrence of OSFD stage 5 was lower in the study of Schopka (1970) than in our study. This low occurrence of fish at OSFD stage 5 in Schopka (1970) indicates that not accounting for fish at this stage had no significant influence on the estimation of fecundity in 1967 and does not explain the low fecundity observed by Schopka (1970). However, because methods differed between studies (automatic egg counter, Parrish et al., 1960, versus auto-diametric method), it is not possible to state with certainty that there is a real difference in fecundity between

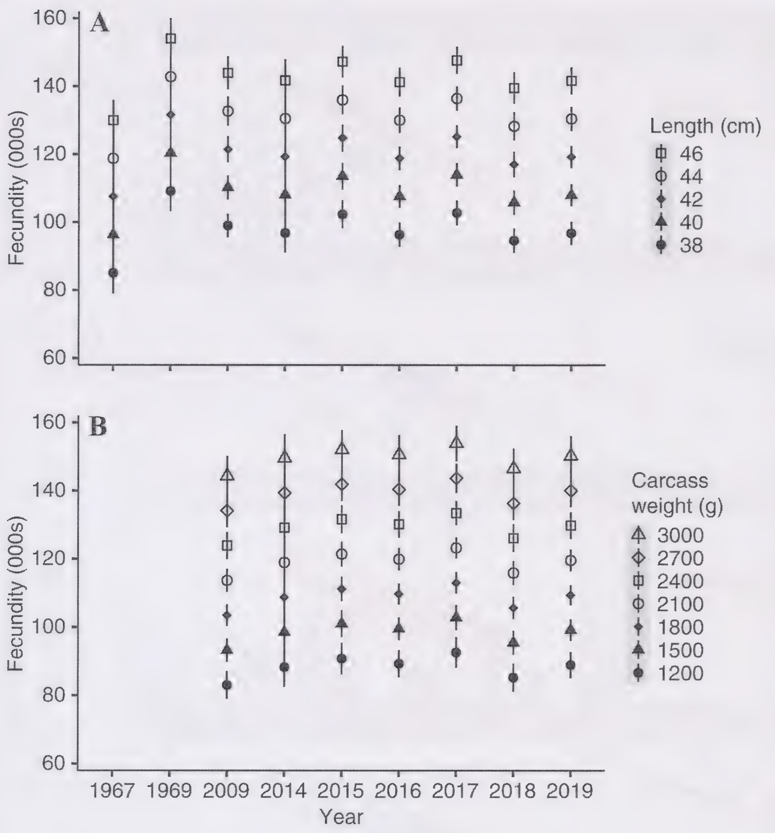

Figure 8

Values of fecundity predicted with a general linear model for lumpfish (*Cyclopterus lumpus*) at different (**A**) total lengths and (**B**) carcass weights. For each year, the average date of capture was set at 20 April in the model. For only analysis by carcass weight, the average liver weight used in the model was 111 g. Data used in the model are from fish sampled for this study around Iceland during 2009 and 2014–2019; data for 1967 and 1969 are from previous studies (Schopka, 1970; Myrseth, 1971).

1967 and 2009–2019. It must also be noted that, even if the difference is real, the historical estimate covers only a single year and it is not possible to know if this was typical of the population around that time. Therefore, we cannot conclude, on the basis of data from this study, that there have been any significant changes in the reproductive capacity of the population of lumpfish over the past 50 years.

There are a small number of studies on fecundity of lumpfish in other areas; however, differences in fecundity between areas needs to be carefully considered. Fecundity in fish is highly variable both within and between years, and it can also vary spatially within a population (Morgan and Rideout, 2008). In a study of lumpfish in Greenland in 2012 and 2014 (Hedeholm et al., 2017), a lumpfish with a carcass weight of 2 kg had a fecundity of 100,000–120,000 oocytes, a value that is broadly similar to fecundity observed in our study. Still, it is difficult to draw conclusions about whether fecundity of lumpfish in Greenland is lower, higher, or similar to that of lumpfish in Iceland. Hedeholm et al. (2017) did not consider temporal variations but did find spatial variation. In contrast, we did not investigate spatial variation but did find temporal variation. Therefore, differing conclusions could be drawn depending on how the comparison is carried out.

Fecundity has been estimated for lumpfish in Canada (Gauthier et al., 2017); unfortunately, the only information presented is fecundity versus ovary weight, making comparisons of the fecundity–size relationship difficult between fish from Iceland and those from Canada. The majority of the data from Gauthier et al. (2017) indicates that fecundity of lumpfish in Canada was 50,000–200,000 oocytes, similar to the range observed in our study; given the nature of the data presented, further comparisons between studies are not possible. Gauthier et al. (2017) also presented information on *hydrated* egg size, which probably refers simply to egg size because lumpfish do not hydrate their eggs. These egg size values ranged from ~1.0 to ~2.0 mm with a median around 1.7 mm. These sizes are considerably smaller than those of eggs sampled from fish captured in Iceland. Gauthier et al. (2017) measured eggs from histological sections, an approach that generally underestimates diameter in comparison with the methods employed during our study. Caution should be applied, therefore, when comparing the results of the 2 studies.

The estimated relative fecundity from our study (34,700 oocytes/kg body weight) was slightly lower than the estimate from Pountney et al. (2020) (40,400 oocytes/kg body weight). The reasons for this difference may be that Pountney et al. (2020) counted all the oocytes >370 µm, a threshold lower than that used in our study (~1600–1800 µm, depending on the oocyte distribution). Therefore, Pountney et al. (2020) likely included oocytes from the non-spawning group, meaning the group of oocytes between 400 and 1800 µm in ovaries classified as at OSFD stage 3 that would have become atretic and not spawned (Kennedy, 2018). In addition, the fish examined by Pountney et al. (2020) were captive bred and would have experienced conditions different than those experienced by the wild fish collected in our study.

Fish with ovaries at OSFD stage 5 had a fecundity roughly half that of fish with ovaries at OSFD stage 3

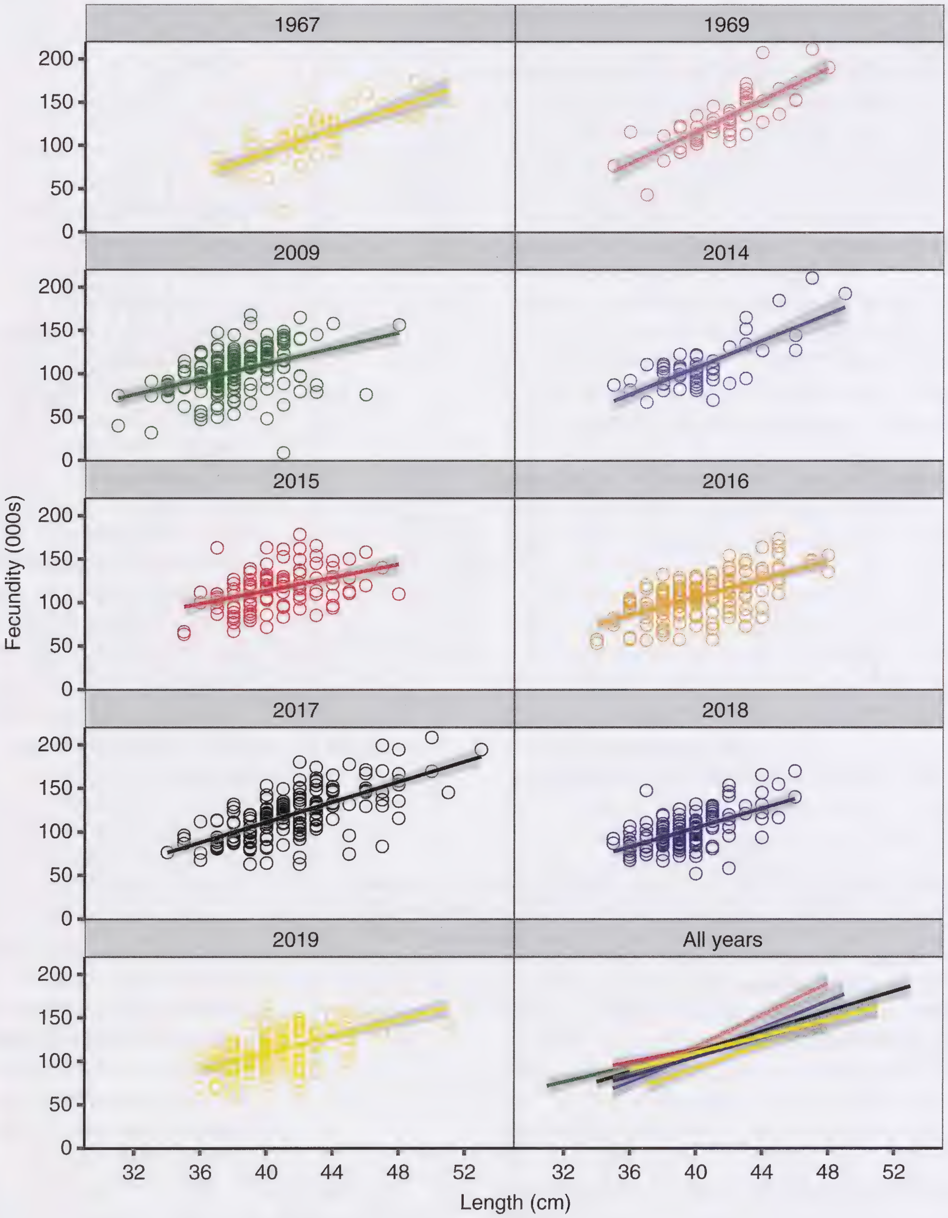

Figure 9

Relationships between total length and fecundity for lumpfish (*Cyclopterus lumpus*) that had ovaries at oocyte size frequency distribution (OSFD) stage 3 and were sampled around Iceland in 1967, 1969, 2009, 2014, 2015, 2016, 2017, 2018, and 2019 and in all years. In ovaries classified as at OSFD stage 3, a break in size frequency distribution separates oocytes into a group of large oocytes (diameters >1800 µm) that have a bimodal distribution and a group of small oocytes (diameters ≤1800 µm). In each panel, the linear regression line is shown, and the gray shaded area indicates 95% confidence intervals. Fecundity estimates, obtained by using gravimetric and auto-diametric methods, are given in number of oocytes. Data for 1967 and 1969 are from Schopka (1970) and Myrseth (1971).

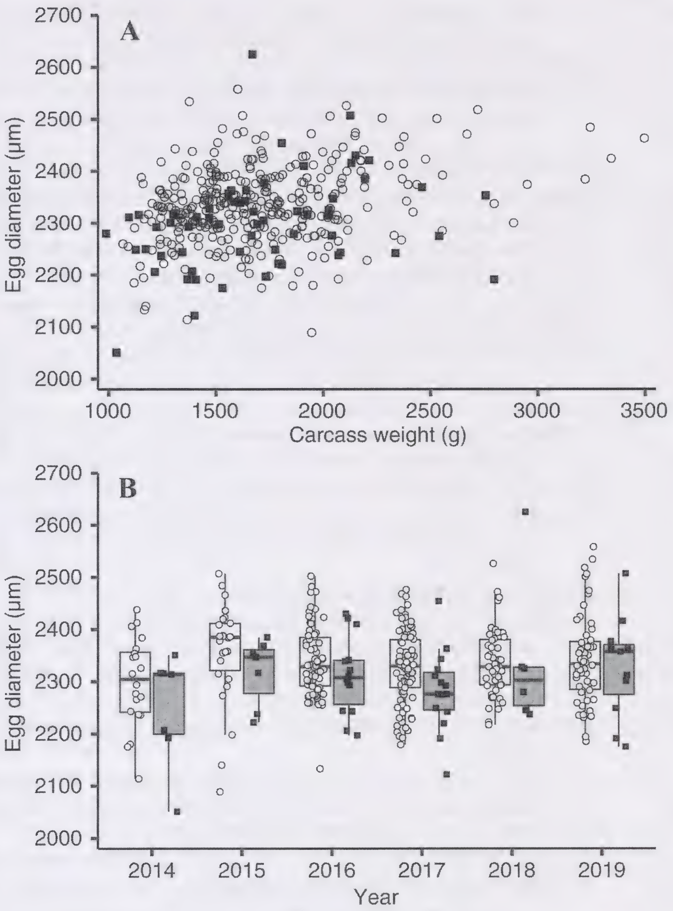

Figure 10

Average egg diameter as a function of (**A**) carcass weight and (**B**) year of capture for lumpfish (*Cyclopterus lumpus*) that were sampled around Iceland in 2014–2019 and had ovaries at the developmental stages spawning 1 (open circles) and spawning 2 (squares). At stage spawning 1, the first batch of eggs have been ovulated and the ovary also contains developing oocytes that will become the second batch. At stage spawning 2, the second batch of eggs have been ovulated. In panel B, the line within the box represents the median value. The bottom and top parts of the box represent the first and third quartiles (25th and 75th percentiles) of average egg diameter. Whiskers above and below the box correspond to 1.5 times the interquartile range.

irrespective of whether outliers were or were not excluded in the estimation of the average proportion of eggs spawned. This finding supports the conclusion of a previous study (Kennedy, 2018), based on oocyte size distributions, that lumpfish spawned 2 batches of eggs with a roughly equal number of eggs. However, in our study, there were 4 notable outliers with ovaries at OSFD stage 5 that had fecundity similar to fish with ovaries classified as at OSFD stage 3. The existence of these outliers indicates that there may be a small number of individuals (~0.5% in this study) that, without reduction in the total number of eggs spawned, will spawn only one batch of eggs. This phenomenon has been reported in lumpfish in an aquaculture scenario in which the incidence of single-batch production was higher than in our study, with estimates of 50% for fish kept at 6°C and 9°C and of up to 78% for individuals held at 14°C (Pountney et al., 2020). The mechanisms behind this single-batch spawning remain unknown.

Egg size increased with carcass weight but decreased from the first batch to the second. This decrease from the first to second batch was investigated by Kennedy (2018), and with an additional 3 years of data from our study, this observation still holds. We also found low variation in egg size between years. Variability in egg size is a rarely investigated component of reproductive biology because of the number of confounding factors, such as fish size, progression through spawning for batch spawners, and the hydration of eggs for species with pelagic eggs. Although a few studies have investigated annual variation in egg size (Almatar and Bailey, 1989; DeMartini, 1990; Hinckley, 1990), a comprehensive investigation into annual variation across species is lacking. The information provided by this study should aid such a study in the future.

Acknowledgments

We would like to thank all the crew and scientific personnel who collected ovarian samples during the scientific surveys. We also are grateful to the fishermen who supplied us with fish. Appreciation goes to L. Kristjánsdóttir and H. Steinsdóttir, who assisted with the laboratory work, to A. Thorsen, who assisted with setting up the image analysis software, and to the 3 anonymous reviewers for their helpful comments on our manuscript. This work was funded by the Marine and Freshwater Research Institute and by Biopol ehf.

Literature cited

Alheit, J.
1993. Use of the daily egg production method for estimating biomass of clupeoid fishes: a review and evaluation. Bull. Mar. Sci. 53:750–767.

Almatar, S. M., and R. S. Bailey.
1989. Variation in the fecundity and egg weight of herring (*Clupea Harengus* L.). Part 1. Studies in the Firth of Clyde and northern North Sea. ICES J. Mar. Sci. 45:113–124.

Alonso-Fernández, A., A. C. Vallejo, F. Saborido-Rey, H. Murua, and E. A. Trippel.
2009. Fecundity estimation of Atlantic cod (*Gadus morhua*) and haddock (*Melanogrammus aeglefinus*) of Georges Bank: application of the autodiametric method. Fish. Res. 99:47–54.

Blanchard, J. L., K. T. Frank, and J. E. Simon.
2003. Effects of condition on fecundity and total egg production of eastern Scotian Shelf haddock (*Melanogrammus aeglefinus*). Can. J. Fish. Aquat. Sci. 60:321–332.

DeMartini, E. E.
1990. Annual variations in fecundity, egg size and condition of the plainfin midshipman (*Porichthys notatus*). Copeia 1990:850–855.

Ellis, J.
2015. Lumpfish (*Cyclopteridae*). *In* Fish atlas of the Celtic Sea, North Sea, and Baltic Sea (H. J. L. Heessen, N. Daan, and J. R. Ellis, eds.), p. 317–319. Wageningen Acad. Publ., Wageningen, Netherlands.

Eriksen, E., C. M. F. Durif, and D. Prozorkevich.
2014. Lumpfish (*Cyclopterus lumpus*) in the Barents Sea: development of biomass and abundance indices, and spatial distribution. ICES J. Mar. Sci. 71:2398–2402.

Flores, A., R. Wiff, E. Díaz, and B. Carvajal.
2017. Temporal variations of potential fecundity of southern blue whiting (*Micromesistius australis australis*) in the Southeast Pacific. J. Sea Res. 126:26–36.

Fulton, T. W.
1907. On the spawning of the lumpsucker (*Cyclopterus lumpus*) and the paternal guardianship of the eggs. Annu. Rep. Fish. Board Scotl. 24(part 3):169–178.

Gauthier, J., F. Grégoire, and C. Nozères.
2017. Assessment of lumpfish (*Cyclopterus lumpus*) in the Gulf of St. Lawrence (3Pn, 4RS) in 2015. Dep. Fish. Oceans, Can. Sci. Advis. Secr. Res. Doc. 2017/051, 47 p. [Available from website.]

Gregory, R. S., and G. R. Daborn.
1982. Notes on adult lumpfish *Cyclopterus lumpus* L. from the Bay of Fundy. Proc. N.S. Inst. Sci. 32:321–326.

Gundersen, A. C., K. H. Nedreaas, O. S. Kjesbu, and O. T. Albert.
2000. Fecundity and recruitment variability of Northeast Arctic Greenland halibut during 1980–1998, with emphasis on 1996–1998. J. Sea Res. 44:45–54.

Hedeholm, R. B., S. Post, and P. Grønkjær.
2017. Life history trait variation of Greenland lumpfish (*Cyclopterus lumpus*) along a 1600 km latitudinal gradient. Polar Biol. 40:2489–2498.

Hinckley, S.
1990. Variation of egg size of walleye pollock *Theragra chalcogramma* with a preliminary examination of the effect of egg size on larval size. Fish. Bull. 88:471–483.

Holst, J. C.
1993. Observations on the distribution of lumpsucker (*Cyclopterus lumpus*, L.) in the Norwegian Sea. Fish. Res. 17:369–372.

Kennedy, J.
2018. Oocyte size distribution reveals ovary development strategy, number and relative size of egg batches in lumpfish (*Cyclopterus lumpus*). Polar Biol. 41:1091–1103.

Kennedy, J., and S. Þ. Jónsson.
2017. Do biomass indices from Icelandic groundfish surveys reflect changes in the population of female lumpfish (*Cyclopterus lumpus*)? Fish. Res. 194:22–30.

Kennedy, J., and H. G. Ólafsson.
2019. Conservation of spawning time between years in lumpfish *Cyclopterus lumpus* and potential impacts from the temporal distribution of fishing effort. Fish. Manage. Ecol. 26:389–396.

Kennedy, J., P. R. Witthames, and R. D. M. Nash.
2007. The concept of fecundity regulation in plaice (*Pleuronectes platessa*) tested on three Irish Sea spawning populations. Can. J. Fish. Aquat. Sci. 64:587–601.

Kennedy, J., S. Þ. Jónsson, J. M. Kasper, and H. G. Ólafsson.
2015. Movements of female lumpfish (*Cyclopterus lumpus*) around Iceland. ICES J. Mar. Sci. 72:880–889.

Kjesbu, O. S.
1994. Time of start of spawning in Atlantic cod (*Gadus morhua*) females in relation to vitellogenic oocyte diameter, temperature, fish length and condition. J. Fish Biol. 45:719–735.

Kjesbu, O. S., P. R. Witthames, P. Solemdal, P., and M. G. Walker.
1998. Temporal variations in the fecundity of Arcto-Norwegian cod (*Gadus morhua*) in response to natural changes in food and temperature. J. Sea Res. 40:303–321.

Kjesbu, O. S., D. Righton, M. Krüger-Johnsen, A. Thorsen, K. Michalsen, M. Fonn, and P. R. Witthames.
2010. Thermal dynamics of ovarian maturation in Atlantic cod (*Gadus morhua*). Can. J. Fish. Aquat. Sci. 67:605–625.

Koops, M. A., J. A. Hutchings, and T. M. McIntyre.
2004. Testing hypotheses about fecundity, body size and maternal condition in fishes. Fish Fish. 5:120–130.

Kraus, G., J. Tomkiewicz, R. Diekmann, and F. W. Köster.
2008. Seasonal prevalence and intensity of follicular atresia in Baltic cod *Gadus morhua callarias* L. J. Fish Biol. 72:831–847.

Kurita, Y., S. Meier, and O. S. Kjesbu.
2003. Oocyte growth and fecundity regulation by atresia of Atlantic herring (*Clupea harengus*) in relation to body condition throughout the maturation cycle. J. Sea Res. 49:203–219.

Marshall, C. T., O. S. Kjesbu, N. A. Yaragina, P. Solemdal, and Ø. Ulltang.
1998. Is spawner biomass a sensitive measure of the reproductive and recruitment potential of northeast Arctic cod? Can. J. Fish. Aquat. Sci. 55:1766–1783.

Mehault, S., R. Domínguez-Petit, S. Cerviño, and F. Saborido-Rey.
2010. Variability in total egg production and implications for management of the southern stock of European hake. Fish. Res. 104:111–122.

Methot, R. D.
1983. Seasonal variation in survival of larval northern anchovy, *Engraulis mordax*, estimated from the age distribution of juveniles. Fish. Bull. 81:741–750.

Morgan, M. J., and R. M. Rideout.
2008. The impact of intrapopulation variability in reproductive traits on population reproductive potential of Grand Bank American plaice (*Hippoglossoides platessoides*) and yellowtail flounder (*Limanda ferruginea*). J. Sea Res. 59:186–197.

Myrseth, B.
1971. Fekunditet, vekst, levevis og ernæring hos *Cyclopterus lumpus* L.: hovedoppgave i fiskeribiologi. M.S. thesis, 113 p. Univ. Bergen, Bergen, Norway. [In Norwegian.]

Narimatsu, Y., and H. Munehara.
1999. Spawn date dependent survival and growth in the early life stages of *Hypoptychus dybowskii* (Gasterosteiformes). Can. J. Fish. Aquat. Sci. 56:1849–1855.

Nissling, A., A. Thorsen, and F. F. G. da Silva.
2016. Fecundity regulation by atresia in turbot *Scophthalmus maximus* in the Baltic Sea. J. Fish Biol. 88:1301–1320.

Parrish, B. B., I. G. Baxter, and M. J. D. Mowat.
1960. An automatic fish egg counter. Nature 185:777.

Pountney, S. M., I. Lein, H. Migaud, and A. Davie.
2020. High temperature is detrimental to captive lumpfish (*Cyclopterus lumpus*, L) reproductive performance. Aquaculture 522:735121.

R Core Team.
2019. R: a language and environment for statistical computing. R Foundation for Statistical Computing,

Vienna, Austria. [Available from website, accessed August 2019.]

Rackovan, J. L., and W. H. Howell.
2017. Spatial and temporal distribution of juvenile *Cyclopterus lumpus* (lumpfish) in a New England estuary. Reg. Stud. Mar. Sci. 16:109–115.

Rasband, W. S.
2014. ImageJ. U.S. Natl. Inst. Health, Bethesda, MD [Available from website, accessed June 2014.]

Rideout, R. M., and M. J. Morgan.
2007. Major changes in fecundity and the effect on population egg production for three species of north-west Atlantic flatfishes. J. Fish Biol. 70:1759–1779.
2010. Relationships between maternal body size, condition and potential fecundity of four north-west Atlantic demersal fishes. J. Fish Biol. 76:1379–1395.

Rijnsdorp, A. D.
1989. Maturation of male and female North Sea plaice (*Pleuronectes platessa* L). ICES J. Mar. Sci. 46:35–51.

Rogers, R., S. Rowe, R. M. Rideout, and M. J. Morgan.
2019. Fecundity of haddock (*Melanogrammus aeglefinus*) off southern Newfoundland. Fish. Res. 220:105339.

Rosen, S., and J. C. Holst.
2013. DeepVision in-trawl imaging: sampling the water column in four dimensions. Fish. Res. 148:64–73.

Saborido-Rey, F., R. Domínguez-Petit, D. Garabana, and Þ. Sigurðsson.
2015. Fecundity of *Sebastes mentella* and *Sebastes norvegicus* in the Irminger Sea and Icelandic waters. Cienc. Mar. 41:107–124.

Schopka, S. A.
1970. Vergleichende untersuchungen zur reproduktivität am hering (*Clupea harengus* L.), kabeljau (*Gadus morhua* L.) und seehasen (*Cyclopterus lumpus* L.) in NO-Atlantischen Gewässern. Ph.D. diss., 134 p. Christian-Albrechts-Universität Kiel, Kiel, Germany. [In German.]

Skjæraasen, J. E., J. A. Devine, J. A. Godiksen, M. Fonn, H. OtterÅ, O. S. Kjesbu, B. Norberg, Ø. Langangen, and Ø. Karlsen.
2017. Timecourse of oocyte development in saithe *Pollachius virens*. J. Fish Biol. 90:109–128.

Tanaka, H., T. Hamatsu, and K. Mori.
2017. Comparison of potential fecundity models for walleye pollock *Gadus chalcogrammus* in the Pacific waters off Hokkaido, Japan. J. Fish Biol. 90:236–248.

Thorsen, A., and O. S. Kjesbu.
2001. A rapid method for estimation of oocyte size and potential fecundity in Atlantic cod using a computer-aided particle analysis system. J. Sea Res. 46:295–308.

Todd, V. L. G., E. W. Lavallin, and P. I. Macreadie.
2018. Quantitative analysis of fish and invertebrate assemblage dynamics in association with a North Sea oil and gas installation complex. Mar. Environ. Res. 142:69–79.

Trippel, E. A.
1999. Estimation of stock reproductive potential: history and challenges for Canadian Atlantic gadoid stock assessments. J. Northwest Atl. Fish. Sci. 25:61–81.

van Damme, C. J. G., M. Dickey-Collas, A. D. Rijnsdorp, and O. S. Kjesbu.
2009. Fecundity, atresia, and spawning strategies of Atlantic herring (*Clupea harengus*). Can. J. Fish. Aquat. Sci. 66:2130–2141.

Vladykov, V. D.
1956. Fecundity of wild speckled trout (*Salvelinus fontinalis*) in Quebec lakes. J. Fish. Res. Board Can. 13:799–841.

Voss, R., C. Clemmesen, H. Baumann, and H. H. Hinrichsen.
2006. Baltic sprat larvae: coupling food availability, larval condition and survival. Mar. Ecol. Prog. Ser. 308:243–254.

National Marine
Fisheries Service
NOAA

Fishery Bulletin
established in 1881

Spencer F. Baird
First U.S. Commissioner
of Fisheries and founder
of *Fishery Bulletin*

Effects of freezing on decomposition of sea turtle carcasses used for research studies

Melissa Cook (contact author)[1]
Jaymie L. Reneker[2]
Redwood W. Nero[3]
Brian A. Stacy[4]
David S. Hanisko[1]

Email address for contact author: melissa.cook@noaa.gov

[1] Southeast Fisheries Science Center
National Marine Fisheries Service, NOAA
3209 Frederic Street
Pascagoula, Mississippi 39567

[2] Riverside Technology Inc.
Southeast Fisheries Science Center
3209 Frederic Street
Pascagoula, Mississippi 39567

[3] Southeast Fisheries Science Center
National Marine Fisheries Service, NOAA
Building 1021
Stennis Space Center, Mississippi 39529

[4] Office of Protected Resources
National Marine Fisheries Service, NOAA
University of Florida
2187 Mowry Road, Building 471
Gainesville, Florida 32611

Abstract—Sea turtles are exposed to numerous anthropogenic threats at sea, and exposure to these threats can result in the stranding of dead animals ashore. In addition to environmental conditions, rate of carcass decomposition is an important but little studied factor in determining whether a sea turtle carcass will strand. Most carcasses of sea turtles collected for research are frozen upon retrieval, and the effects of freezing have not been studied. We compared the decomposition rate of unfrozen and previously frozen carcasses of green (*Chelonia mydas*) and Kemp's ridley (*Lepidochelys kempii*) sea turtles recovered from cold-stunning events. Species had the greatest influence on the rate of decomposition, with green sea turtles becoming positively buoyant and decomposing at a faster rate than Kemp's ridley sea turtles. The effects of freezing were negligible, indicating that frozen carcasses may be a suitable replacement for fresh carcasses in research studies, including studies related to decomposition of sea turtles.

Marine animals found washed ashore (i.e., stranded) are often studied to identify and monitor causes of mortality (e.g., vessel strikes, disease, and fisheries interactions). Examinations of stranded animals can yield valuable information about threats affecting marine species like sea turtles. According to the IUCN Red List of Threatened Species (IUCN, 2019), most populations of sea turtles are vulnerable to extinction worldwide because of predominately anthropogenic threats, including the risk of becoming bycatch in fisheries, consumption of sea turtles and their eggs, habitat destruction, and climate change (Mast et al., 2005; Wallace et al., 2011). Results of studies of stranded sea turtles have improved our understanding of these threats and have contributed other valuable information related to life history, health, and disease.

After a sea turtle dies, a number of factors influence whether or not its carcass will strand ashore and become available for discovery by humans. When sea turtles are killed by vessel strikes or drown in fishing gear, they usually sink to the seafloor because gas volume within the lungs is insufficient to maintain positive buoyancy (Epperly et al., 1996). Once submerged, a carcass stays underwater until the bacteria in the gut produce enough gases (methane, hydrogen sulfide, and carbon dioxide) to float it to the surface (Vass, 2001; Mateus and Pinto, 2016). The buildup of gases can take hours, days, or weeks, depending on factors such as body composition, diet, animal size, water depth, and water temperature. A second influential period occurs if the carcass surfaces. Once on the surface, carcasses are subject to wind and currents, consumption by scavengers, and continued decomposition influenced by ambient air and water temperatures. The combination of these factors influences the beaching process and ultimately whether or not a carcass is ever found. The likelihood of shoreline deposition, or stranding probability, provides critical context for interpreting data derived from stranded animals. For example, if

Manuscript submitted 16 January 2020.
Manuscript accepted 26 August 2020.
Fish. Bull. 118:268–274 (2020).
Online publication date: 10 September 2020.
doi: 10.7755/FB.118.3.5

The views and opinions expressed or implied in this article are those of the author (or authors) and do not necessarily reflect the position of the National Marine Fisheries Service, NOAA.

stranding probability is low, the number of strandings will also likely be low even if at-sea mortality is high.

Decomposition rate influences how long carcasses persist in the environment and, therefore, their availability for detection. In addition, decomposition affects the duration of buoyancy and drift, key factors used in determining where stranded sea turtles may have died (Nero et al., 2013). Despite their importance, decomposition rates in sea turtles have been examined in only a few studies. One challenge is the low availability of carcasses of sea turtles in conditions suitable for decomposition studies because of their protected status and various logistical constraints. Use of previously frozen carcasses is often the only feasible option for such research (Reneker et al., 2018; Santos et al., 2018). However, study of the effects of freezing and thawing on decomposition in any taxa has been limited (e.g., rats; Micozzi, 1986), and there has been no such study for sea turtles. In addition, decomposition rates may vary among sea turtle species because of differences in diet and alimentary anatomy that could also affect postmortem processes and extrapolation of results among species.

The objectives of our study were to compare decomposition rates between previously frozen and unfrozen carcasses of sea turtles and between 2 species of sea turtles with anatomical and dietary differences that could affect postmortem processes. We used the Kemp's ridley sea turtle (*Lepidochelys kempii*), a benthic carnivore, and the green sea turtle (*Chelonia mydas*), an herbivore and a hindgut fermenter with an intestine that is proportionally longer than those of carnivorous cheloniid species (Bjorndal, 1979, 1997). The overall goal of this study was to determine if frozen carcasses are a suitable replacement for fresh carcasses in studies that require carcasses of sea turtles, including research of decomposition of sea turtles.

Materials and methods

Ethics statement

This study was authorized under U.S. Fish and Wildlife Service permit number TE 676395-5. No live animals were killed or harmed for this cadaver study.

Carcasses

All carcasses used in this study were sea turtles that died during cold-stunning events in December 2017. Cold-stunning events, which occur when nearshore water temperatures fall below 10°C, provide the most readily available source of undecomposed carcasses. Therefore, we conducted this study during winter months. The green sea turtles originated from Saint Joseph Bay in Florida, where they are known to predominantly forage on turtlegrass (*Thalassia testudinum*) (Foley et al., 2007). The Kemp's ridley sea turtles were from Cape Cod Bay in Massachusetts. Previous studies of cold-stunned sea turtles from this area have reported a diet of various benthic invertebrates (Innis et al., 2009).

We used 7 individuals of each species with a mean size of 26.6 cm straight carapace length (SCL) and a size range of 21.7–28.1 cm SCL. All turtles were determined to be dead on the basis of the absence of detectable cardiac contraction. We included only carcasses that lacked any odor or visual evidence of decomposition (e.g., bloating and scutes peeling). Three carcasses of each species were frozen immediately (0°C) and kept frozen until they were shipped to the Stennis Space Center (SSC) site of the Mississippi Laboratories, NOAA Southeast Fisheries Science Center, 2–6 d later, depending on the stranding date. The remaining 4 individuals of each species were refrigerated at 3–6°C for 18–30 h (Kemp's ridley sea turtles) or for 5 d (green sea turtles). The green sea turtles that were stranded on Friday, 29 December 2017, could not be shipped until the following Tuesday because of the holiday weekend. All individuals were shipped on ice overnight (<24 h) to the SSC facility. The temperature in the ice chest was maintained at 1°C during shipping. The carcasses used in our study beached in near freezing conditions and were then stored frozen, or nearly frozen, before and during shipment. Therefore, we assumed that decomposition was minimal prior to placement of sea turtles into the tank at the beginning of the study and considered the time of this placement the start time for all observations. Frozen carcasses were thawed in a freshwater bath and warmed to ~4°C over a period of 1–2 h prior to the initiation of observations of decomposition.

Decomposition observations

Experiments in which decomposition of carcasses was monitored were conducted simultaneously for all individuals of each species. The observations of Kemp's ridley sea turtles began on 13 December 2017; the observations of green sea turtles began on 3 January 2018. Decomposition was tracked in 2 phases: time until positive buoyancy was attained and time until positive buoyancy was lost. Both phases hinge on key postmortem events related to dispersal and discovery of sea turtle carcasses. For logistical reasons, the first phase was conducted within an indoor laboratory and the second was conducted in an outdoor floating pen.

We measured the time required for carcasses to float in a 1173-L polyethylene water storage tank (0.81 m wide × 2.34 m high). The tank was covered in a 0.10-m layer of fiber insulation to reduce thermal swings from the ambient air conditions, and the depth of water in the tank was 2.31 m. To provide controlled conditions, the tank was filled with fresh tap water obtained from the SSC facility and had a pressure of 101.33 kPa, equivalent to approximately 2.20 m of seawater. Temperatures were maintained near 20°C by using 3 thermostatically controlled 300-W aquarium heaters, and water flow from a circulation pump kept water in the tank well mixed. Temperature was also monitored manually with a YSI-85[1] meter

---

[1] Mention of trade names or commercial companies is for identification purposes only and does not imply endorsement by the National Marine Fisheries Service, NOAA.

(YSI, Yellow Springs, OH) during daily visual inspections. Status of the carcasses was also monitored with a wide-angle Mobius ActionCam HD digital camera (Mobius, New York), which was mounted on the top of the tank looking down and was set to take photographs every minute. When placed into water, most carcasses sank immediately to the bottom of the tank. Five carcasses initially floated and were compressed against the bottom of the water bath to expel excess air in the lungs until negative buoyancy was attained. This treatment was intended to ensure that carcasses were similarly buoyant at the beginning of the study. Carcasses were kept in the tank until they floated to the surface.

Once carcasses became buoyant and floated to the surface, they were released in the Bay-Waveland Yacht Club harbor at 30°19′30″N, 89°19′32″W so that the final stages of decomposition could occur in a natural setting where the products of the process could dissipate and be ameliorated by the environment. This harbor is about 13,000 m^2 in size and is contiguous with Saint Louis Bay, Mississippi, through a 20-m channel. Temperature and weather conditions in the harbor typically follow those of the nearby Mississippi Sound within 1–2°C and were downloaded from the NOAA National Data Buoy Center website for the NOAA meteorological station WYCM6-844737 located about 100 m from the harbor at 30°19′35″N, 89°19′33″W. Carcasses were placed into a hoop net constructed of two 0.9-m diameter metal rings, attached to each other with 0.6-m-long polyethylene netting (Fig. 1A). An outer PVC hoop with floats was attached to the top hoop to ensure the upper edge of the hoop net was ~10 cm above the waterline so that carcasses could not float out of the net (Fig. 1B). The net was tethered to a pier at the Bay-Waveland Yacht Club and left to float in approximately 1.5 m of water. Carcasses were checked daily in the morning and evening.

Water temperature and salinity were recorded by using a YSI-85 instrument, and decomposition was evaluated by visual inspection. Stage of decomposition was characterized by using previously developed coding based on the degree of bloating and percentage of the carcass above the waterline (Reneker et al., 2018) and a carcass condition classification system used by the national Sea Turtle Stranding and Salvage Network. Carcasses were classified into the following decomposition stages (codes): carcass not buoyant (code 1); carcass positively buoyant and floats (code 2.1); carcass buoyant but not fully bloated, with 50–90% of the carapace above the waterline (code 2.2); carcass severely bloated, with 90–100% of the carapace exposed and the head and neck distended (code 3.1); degassing begins, carcass becomes less buoyant, with <90% of the carapace exposed, and the head is limp and beginning to hang (code 3.2); and carcass barely buoyant or negatively buoyant and nearly completely degassed with extensive external decomposition and disarticulation of joints (code 3.3). Daily monitoring was performed until carcasses sank or were no longer individually identified.

Accumulated degree hours and statistical analyses

We measured decomposition rate by using accumulated degree hours (ADH), which is a measurement used in forensic science to study postmortem events and submerged human bodies (Mateus and Pinto, 2016). The unit of ADH measures the accumulation of thermal energy created by the biological and chemical reactions that occur throughout decomposition. The use of ADH allows the standardization of decomposition rate over time and among varying environmental conditions (Simmons et al., 2010). We calculated ADH by summing the hourly mean water temperatures beginning at the time a carcass was placed in the tank through the time it was in the harbor; temperatures were

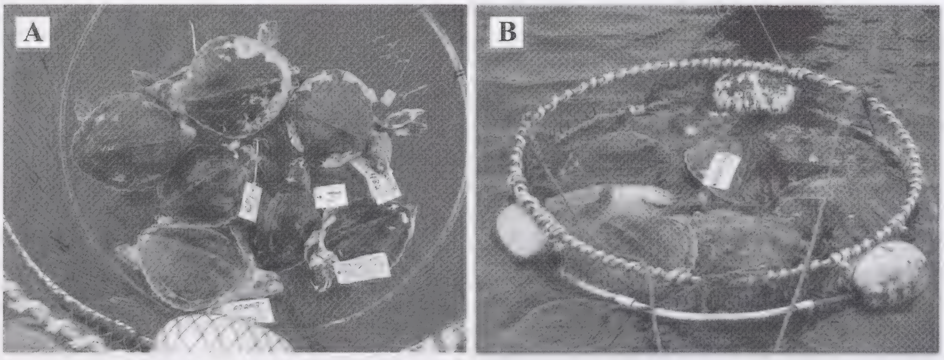

Figure 1

Images of buoyant carcasses of Kemp's ridley (*Lepidocheyls kempii*) and green (*Chelonia mydas*) sea turtles in a (**A**) hoop net tethered to a pier, with (**B**) surface floats attached, in Saint Louis Bay in Mississippi. Carcasses were left in the hoop net so that stages of decomposition could be evaluated in a natural setting. All carcasses used in this study were those of sea turtles that died during cold-stunning events in December 2017.

summed sequentially as a carcass progressed through each stage of decomposition. Although carcasses were exposed to ambient air and water temperatures, only water temperature was considered relevant when calculating ADH. We made this choice because water has a much higher specific heat conductivity than air and is the primary driver of heat loss or gain in carcasses because they are always at least 50% submerged.

A generalized linear mixed model (GLMM) was used to examine the effects of species (Kemp's ridley and green sea turtles) and carcass status (unfrozen and frozen) on the number of ADH at specific decomposition stages. The GLMM included a random factor for each carcass to account for correlated within-subject measurements across the decomposition stages and used a heterogeneous compound symmetry covariance structure to account for nonhomogeneous variance in ADH with advancing decomposition stage. A Type III test of fixed effects (level of significance=0.05) was used to test for significance of species or status effects and for significant interactions between species and decomposition stage or between status and decomposition stage from the GLMM. The analysis was implemented by using the GLIMMIX procedure in the SAS/STAT component of SAS, vers 9.4 (SAS Institute Inc., Cary, NC).

Results

Under controlled conditions, a carcass achieved positive buoyancy in 48.3–154.8 h (mean: 92.5 h). The ADH required for a carcass to float (code 2.1), as well as to reach subsequent decomposition stages for all carcasses, are presented in Table 1 and Figure 2. Tank temperature averaged 20.2°C and 19.2°C for the Kemp's ridley and green sea turtles, respectively, and the temperature required for carcasses to become positively buoyant varied considerably. The first carcass to float was an unfrozen Kemp's ridley sea turtle (791.3 ADH), followed by a frozen green sea turtle (998.6 ADH). The last carcass to become positively buoyant was also an unfrozen Kemp's ridley sea turtle (2529.7 ADH).

Fluctuating weather temperatures greatly extended the length of the field portion of this study. Two exceptionally rare cold weather periods occurred in January. Mean daily water temperature ranged from 2.0°C to 24.1°C (mean: 12.8°C). Air temperature also varied, from −8.7°C to 27.2°C (mean: 12.2°C). The use of ADH provided a standardized way to compare decomposition rates between carcasses under these irregular and variable conditions. Carcasses became negatively buoyant and sunk after an average of 5090.0 ADH (range: 3762.5–6528.8 ADH). The first carcass to sink was a frozen green sea turtle, and the last carcass to

Table 1

Accumulated degree hours (ADH) required for frozen and unfrozen carcasses of Kemp's ridley (*Lepidochelys kempii*) and green (*Chelonia mydas*) sea turtles to reach each stage of decomposition. All carcasses were those of sea turtles that died during cold-stunning events in Cape Cod, Massachusetts (Kemp's ridley sea turtles), and Saint Joseph Bay, Florida (green sea turtles), in December 2017. Straight carapace lengths (SCLs), measured from notch to tip, are provided. Abbreviations in the carcass ID indicate that a sea turtle was an unfrozen Kemp's ridley sea turtle (KU), frozen Kemp's ridley sea turtle (KF), unfrozen green sea turtle (GU), or frozen green sea turtle (GF). For the following decomposition stages (codes), ADH are given: carcass positively buoyant and floats (code 2.1); carcass buoyant but not fully bloated, with 50–90% of the carapace above the waterline (code 2.2); carcass severely bloated, with 90–100% of the carapace exposed (code 3.1); degassing begins, carcass becomes less buoyant, with <90% of the carapace exposed (code 3.2); and carcass barely buoyant or negatively buoyant with extensive external decomposition (code 3.3).

		ADH				
Carcass ID	Length (cm SCL)	Code 2.1	Code 2.2	Code 3.1	Code 3.2	Code 3.3
KU-474	27.4	791.31	2093.67	3745.72	4880.08	5708.79
KU-475	26.8	1321.68	3369.66	4504.81	4973.90	6081.47
KU-482	25.9	1744.84	3051.41	3188.46	4302.07	4688.47
KU-483	25.9	2529.72	3452.13	4952.14	5700.09	6528.81
KF-433	21.7	1385.12	2081.80	4082.81	4938.31	6045.88
KF-435	23.5	1647.20	2757.11	3153.97	5123.08	6230.65
KF-438	21.8	1470.23	2763.72	4274.19	5408.54	6237.26
GU-148	25.6	1681.44	2423.45	3271.93	3610.29	4700.76
GU-149	27.8	1428.75	2318.78	3304.43	3408.55	3763.42
GU-151	25.9	1498.92	3061.84	3302.88	3407.00	3995.62
GU-152	23.2	1533.45	2426.20	3274.68	3613.04	4305.78
GF-144	27.7	998.60	1807.60	2021.79	2250.21	5003.42
GF-145	26.9	1153.48	1863.33	2593.46	3407.67	3762.54
GF-146	28.1	1346.19	2589.21	3299.30	3610.99	4206.61

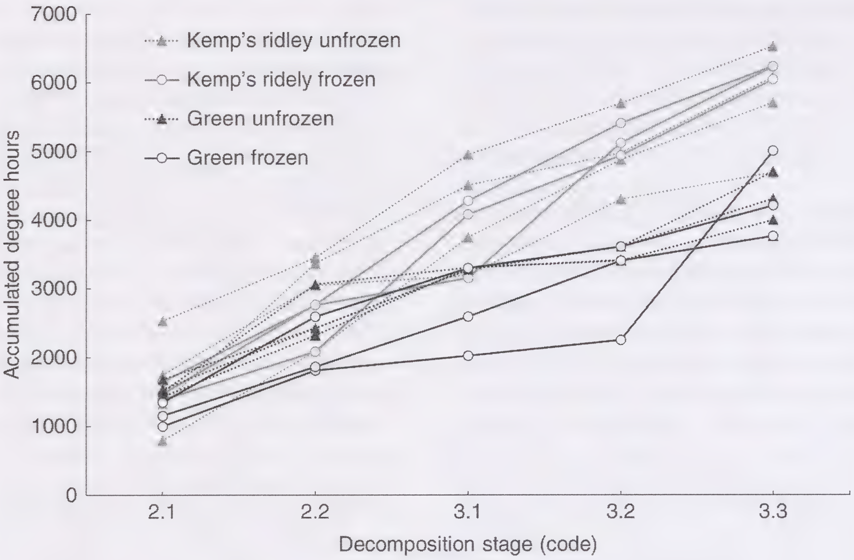

Figure 2

Accumulated degree hours, by stage of decomposition (code), for frozen (circles) and unfrozen (triangles) carcasses of Kemp's ridley (*Lepidocheyls kempii*) and green (*Chelonia mydas*) sea turtles collected in December 2017 from Cape Cod, Massachusetts, and Saint Joseph Bay, Florida, respectively. Carcasses were placed in controlled conditions in a tank with ~20°C freshwater until they floated (code 2.1) and then placed in brackish water in a harbor in Saint Louis Bay, Mississippi, where they were exposed to ambient air and water temperatures. Carcasses were monitored through a sequence of decomposition stages until severe decomposition and loss of buoyancy occurred (code 3.3). The other decomposition stages are carcass buoyant but not fully bloated, with 50–90% of the carapace above the waterline (code 2.2); carcass severely bloated, with 90–100% of the carapace exposed (code 3.1); and degassing begins, carcass becomes less buoyant, with <90% of the carapace exposed (code 3.2).

sink was an unfrozen Kemp's ridley sea turtle, which was also the last Kemp's ridley sea turtle that became positively buoyant.

Results of the Type III test of the GLMM fixed effects indicate a significant species effect (P=0.0004) and a significant interaction of species with decomposition stage (P<0.0001) on ADH. In contrast, analysis with the Type III test of the GLMM fixed effects found that carcass status (frozen or unfrozen) had neither a significant effect (P=0.3367) nor a significant interaction (P=0.1161) with decomposition stage on ADH. The mean ADH for carcasses to float was 1555.7 ADH (standard deviation [SD] 527.3) for Kemp's ridley sea turtles and 1377.3 ADH (SD 234.1) for green sea turtles. An even greater variability occurred between the mean ADH required for each species to sink. Kemp's ridley sea turtles sank at 4688.5–6528.8 ADH, and green sea turtles sank at 3762.5–5003.4 ADH (Table 2).

Discussion

The duration required for carcasses of sea turtles to become positively buoyant and eventually sink was not significantly different between unfrozen and frozen carcasses. The decomposition rates varied within and between species. Significant differences were observed in decomposition rates between green and Kemp's ridley sea turtles. The initial time to float varied among carcasses considerably more and took slightly longer for Kemp's ridley sea turtles than for green sea turtles. Under nearly the same conditions, green sea turtles became buoyant and floated 8.9 h faster than Kemp's ridley sea turtles. Kemp's ridley and green sea turtles also differed in the mean ADH required to reach each decomposition stage; green sea turtles decomposed at a faster rate. These dissimilarities may be due to the diets of the 2 species and to associated differences in gastrointestinal anatomy and physiology. The longer intestine of the herbivorous green sea turtle and partially digested plant matter within the gut may lead to accelerated postmortem gas production and buoyancy in comparison to those of the carnivorous Kemp's ridley sea turtle. Moreover, green sea turtles that experience cold stunning in Florida typically have abundant digesta within their gastrointestinal tracts upon death (Foley et al., 2007); whereas, some cold-stunned Kemp's ridley sea turtles found in Massachusetts are devoid of gut contents (Innis et al., 2009).

Table 2

Summary of accumulated degree hours (ADH) required for carcasses of Kemp's ridley (*Lepidochelys kempii*) and green (*Chelonia mydas*) sea turtles to reach positive buoyancy, float, and become negatively buoyant and sink. All carcasses were kept in a tank and submerged in 2.3 m of water held at 20°C. The carcasses used in this study were those of sea turtles that died during cold-stunning events in Cape Cod, Massachusetts, and Saint Joseph Bay, Florida, in December 2017. SD=standard deviation.

		ADH			
Carcass type	Sample size	Mean	SD	Minimum	Maximum
Unfrozen—float	8	1423.19	292.55	791.31	1744.84
Unfrozen—sink	8	4911.27	918.80	3763.42	6081.47
Frozen—float	6	1524.24	543.04	998.60	2529.72
Frozen—sink	6	5328.22	1174.48	3762.54	6528.81
Kemp's ridley—float	7	1555.73	527.31	791.31	2529.72
Kemp's ridley—sink	7	5931.62	601.40	4688.47	6528.81
Green—float	7	1377.26	324.09	998.60	1681.44
Green—sink	7	4248.31	468.13	3762.54	5003.42

The calculation of ADH allowed standardization of temperature on the rate of decomposition and comparison between carcasses. The results of this study indicate the effectiveness of using ADH to measure and document the progression of sea turtle carcasses through each stage of decomposition. The extremely cold air and water temperatures to which carcasses were exposed during this study resulted in very long periods of positive buoyancy; carcasses floated for up to 65 d. In the northern Gulf of Mexico, sea turtles are found in water temperatures of 14°C or higher. Results of our research indicate that under these conditions, in 2.3 m of water, a carcass would float for approximately 13–22 d before sinking. Ideally, field studies on the decomposition of sea turtles would occur in spring or summer when strandings of sea turtles peak. However, timing of our field experiments were constrained to winter months because of the availability of fresh carcasses salvaged during cold-stunning events. Moreover, our objective was to examine the suitability of frozen carcasses for decomposition research and for studies in which frozen carcasses are used, such as drifting and stranding studies (Reneker et al., 2018; Santos et al., 2018); our goal was not to define precise rates of decomposition under various conditions of interest.

Micozzi (1986) found that previously frozen rats had accelerated disarticulation and decomposed from the "outside-in" but that unfrozen rats decayed from the "inside-out" because of internal anaerobic decomposition and rapid growth of intestinal microorganisms. The skin and external surfaces of previously frozen rats were considerably more susceptible to invasion by insects and microorganisms than unfrozen rats. On the basis of these observations, he recommended that earlier studies should be repeated with cadavers that were not previously frozen (Micozzi, 1986). In contrast, we found no significant differences in factors of interest related to prior freezing of carcasses of sea turtles. The only appreciable difference in our study was that unfrozen carcasses floated slightly longer than frozen carcasses. If the externum had in fact decayed at a more rapid rate, the opposite effect would have occurred because gases would have escaped from disruptions in the skin, causing previously frozen carcasses to lose buoyancy more quickly. There have been too few published studies of the effects of freezing and thawing of animals on which we can base comparison of our observations with those of the Micozzi (1986) rat study. Capacities for thermoregulation and anatomic differences could affect decomposition rates and effects of prior freezing of vertebrate taxa. The internal microbiota of homeotherms may respond differently to freezing than poikilothermic reptiles. In addition, the heavily keratinized integument of reptiles may influence external taphonomic processes.

All carcasses progressed sequentially through the decomposition stages with the amount of time it took to reach a decomposition stage varying among carcasses. For example, most green sea turtles were classified as code 3.3 within 15 d; however, a frozen green sea turtle (GF-144) required 20 d to reach this stage. Species, rather than carcass status (unfrozen or frozen), significantly influenced the rate of decomposition. Results of this study indicate that decomposition rates of frozen sea turtle carcasses are similar to those of fresh carcasses and that frozen carcass may be a viable alternative for studies on decomposition and in certain studies in which fresh carcasses of sea turtles otherwise would be required.

Acknowledgments

We thank the staff and volunteers from the Massachusetts and Florida Sea Turtle Stranding and Salvage Networks for salvaging carcasses, especially R. Prescott and K. Dourdeville from Massachusetts Audubon Wellfleet, and for helping with the fresh and frozen carcass study, K. Sampson and A. Foley for authorizing carcass use, and N. Evou for supplying carcasses. Without their dedication and response effort, this study would not have been possible. We also thank the staff and patrons of the Bay-Waveland Yacht Club for the use of their facility. This research was supported with Sea Turtle Early Restoration Project funds administered by the Regionwide Trustee Implementation Group as part of the Deepwater Horizon Natural Resource Damage Assessment.

Literature cited

Bjorndal, K. A.
1979. Cellulose digestion and volatile fatty acid production in the green turtle, *Chelonia mydas*. Comp. Biochem. Physiol. A 63:127–133.
1997. Foraging ecology and nutrition of sea turtles. *In* The biology of sea turtles (P. L. Lutz and J. A Musick, eds.), p 199–231. CRC Press, Boca Raton, FL.

Epperly, S. P., J. Braun, A. J. Chester, F. A. Cross, J. V. Merriner, P. A. Tester, and J. H. Churchill.
1996. Beach strandings as an indicator of at-sea mortality of sea turtles. Bull. Mar. Sci. 59:289–297.

Foley, A. M., K. E. Singel, P. H. Dutton, T. M. Summers, A. E. Redlow, and J. Lessman.
2007. Characteristics of a green turtle (*Chelonia mydas*) assemblage in northwestern Florida determined during a hypothermic stunning event. Gulf Mex. Sci. 25:131–143.

Innis, C., A. C. Nyaoke, C. R. Williams III, B. Dunnigan, C. Merigo, D. L. Woodward, E. S. Webe, and S. Frasca Jr.
2009. Pathologic and parasitologic findings of cold-stunned Kemp's ridley sea turtles (*Lepidochelys kempii*) stranded on Cape Cod, Massachusetts, 2001–2006. J. Wildl. Dis. 45:594–610.

IUCN (International Union for Conservation of Nature and Natural Resources).
2019. The IUCN Red List of Threatened Species, vers. 2019-2. [Available from website, accessed August 2019.]

Mast, R. B., B. J. Hutchinson, E. Howgate, and N. J. Pilcher.
2005. MTSG update: IUCN/SSC marine turtle specialist group hosts the second burning issues assessment workshop. Mar. Turtle Newsl. 110:13–15.

Mateus, M., and L. Pinto.
2016. Report on the accumulated degree days and post mortem submersion interval for an infant drowning accident. J. Forensic Invest. 4(2):3.

Micozzi, M. S.
1986. Experimental study of postmortem change under field conditions: effects of freezing, thawing and mechanical injury. J. Forensic Sci. 31:953–961.

Nero, R. W., M. Cook, A. T. Coleman, M. Solangi, and R. Hardy.
2013. Using an ocean model to predict likely drift tracks of sea turtle carcasses in the north central Gulf of Mexico. Endang. Species Res. 21:191–203.

Reneker, J. L., M. Cook, and R. W. Nero.
2018. Preparation of fresh dead sea turtle carcasses for at-sea drift experiments. NOAA Tech. Memo. NMFS-SEFSC-731, 14 p.

Santos, B. S., D. M. Kaplan, M. A. M. Friedrichs, S. G. Barco, K. L. Mansfield, and J. P. Manning.
2018. Consequences of drift and carcass decomposition for estimating sea turtle mortality hotspots. Ecol. Indic. 84:319–336.

Simmons, T., R. E. Adlam, and C. Moffatt.
2010. Debugging decomposition data—comparative taphonomic studies and the influence of insects and carcass size on decomposition rate. J. Forensic Sci. 55:8–13.

Vass, A. A.
2001. Beyond the grave—understanding human decomposition. Microbiol. Today, November 2001.

Wallace, B. P., A. D. DiMatteo, A. B. Bolten, M. Y. Chaloupka, B. J. Hutchinson, F. A. Abreu-Grobois, J. A. Mortimer, J. A. Seminoff, D. Amorocho, K. A. Bjorndal, et al.
2011. Global conservation priorities for marine turtles. PLoS ONE 6(9):e24510.

National Marine
Fisheries Service
NOAA

Fishery Bulletin
established in 1881

Spencer F. Baird
First U.S. Commissioner
of Fisheries and founder
of *Fishery Bulletin*

Temperature-related changes in species composition of juvenile finfish on a rock reef in Long Island Sound

Renee Mercaldo-Allen (contact author)[1]
Paul Clark[1]
Dylan Redman[1]
Yuan Liu[1,2]
Shannon Meseck[1]
Lisa Milke[1]
Julie M. Rose[1]
Ronald Goldberg[1]

Email address for contact author: renee.mercaldo-allen@noaa.gov

[1] Milford Laboratory
Northeast Fisheries Science Center
National Marine Fisheries Service, NOAA
212 Rogers Avenue
Milford, Connecticut 06460

[2] Integrated Statistics
16 Sumner Street
Woods Hole, Massachusetts 02543

Abstract—We assessed changes in relative abundance of juvenile fish on a natural cobble and boulder reef near Milford, Connecticut, in summer (June–August) during the years 2004–2008 and in 2016. Fish traps, used to sample structure-oriented fish, were soaked for ~24 h 2–3 times per week. Catch per unit of effort was used as an index of fish abundance and to standardize differences in sampling effort among study years. Juvenile finfish assemblages during 2004 and 2005 differed most in species composition from the assemblage in 2016. Abundance of 2 warm-adapted species, the black sea bass (*Centropristis striata*) and the oyster toadfish (*Opsanus tau*), was observed to increase over the study period, and numbers of cunner (*Tautogolabrus adspersus*) and other cold-adapted species declined. Water temperature was a statistically significant predictor of changes in finfish assemblage over the period of this study, explaining 8.6% of the observed variation in species composition in the data set. A widely documented trend of gradually warming water temperatures from a local, long-term temperature record was consistent with observations from this study of warm-adapted and cold-adapted fish species on a natural rock reef in Long Island Sound.

Recent changes in abundance and distribution of finfish and invertebrate species off the coast of the northeastern United States have corresponded with warming of oceanic (e.g., Nye et al., 2009; Rijnsdorp et al., 2009; Walsh et al., 2015; Hare et al., 2016) and estuarine (e.g., Collie et al., 2008; Howell and Auster, 2012; Crosby et al., 2018) waters. Fish assemblages in estuarine environments, such as Long Island Sound (LIS), experience a broad range of water temperatures and may respond to temperature variations more rapidly than species found in deeper offshore waters (Collie et al., 2008). For this reason, estuaries represent sentinel environments for monitoring changes in composition of faunal communities that result from a changing climate. Importantly, environmental variability in coastal estuaries can influence the structure of fish assemblages on a local scale (Chin et al., 2018), but long-term changes related to rising water temperatures may alter the composition of benthic food webs (Rice et al., 2015). Habitat preferences, physiological tolerances, and life stage of fish species, along with the rate and magnitude of environmental change, may determine the response of individual species to changing temperatures.

Natural rock reefs, composed of patches of cobble and boulder, provide habitat for many ecologically and economically important finfish species (Peters and Cross, 1992; Steimle and Zetlin, 2000). Complex seafloor habitat, with physical relief, seabed roughness, biogenic structure, and large sediment grain size, attracts small and juvenile fish (Diaz et al., 2003). Epifaunal growth on cobble and boulders, such as that of seaweeds, sponges, hydroids, and bryozoans, provides camouflage and cryptic shelter that protect vulnerable fish from predation (Auster et al., 1995; Steimle and Zetlin, 2000) and provide a ready food source (Diaz et al., 2003; Scharf et al., 2006). Rock reef environments may be particularly important in the central basin of LIS, where natural structured habitat is sparse and much of the seafloor consists of featureless sand and shell. Cobble and boulders occur in

Manuscript submitted 22 February 2020.
Manuscript accepted 28 August 2020.
Fish. Bull. 118:275–283 (2020).
Online publication date: 11 September 2020.
doi: 10.7755/FB.118.3.6

The views and opinions expressed or implied in this article are those of the author (or authors) and do not necessarily reflect the position of the National Marine Fisheries Service, NOAA.

discrete patches in this basin and represent a relatively small proportion of the overall seafloor area (Poppe et al., 2000).

High site fidelity on structured seafloor habitat has been reported for shelter-oriented, temperate reef fish species, including the cunner (*Tautogolabrus adspersus*), tautog (*Tautoga onitis*), and black sea bass (*Centropristis striata*) (Olla et al., 1979; Auster[1]; Able et al., 2005; Drohan et al., 2007). Increasing habitat complexity appears to enhance successful settlement and recruitment in young-of-the-year cunner (Tupper and Boutilier, 1997). In addition to seafloor complexity, composition and distribution of juvenile finfish assemblages may be influenced by ecological factors (e.g., inter- and intraspecific competition, recruitment, and predation) and sensitivity or tolerance to variation in environmental characteristics (e.g., temperature and salinity).

Results of analysis of a long-term record of temperatures measured at the Milford Laboratory, NOAA Northeast Fisheries Science Center, in the central basin of LIS indicate a 50-year trend of increasing water temperatures (Rice et al., 2015; COA[2]) that may be influencing the composition of finfish assemblages. To test whether fish populations in LIS are changing in response to rising water temperatures, we conducted a fish trapping study during 6 summers in 2004, 2005, 2006, 2007, 2008, and 2016 to assess species composition of the juvenile finfish assemblage and relative species abundance over a 12-year period on a rock reef in this same region of coastal Connecticut.

Materials and methods

Characteristics of study site

We studied a natural rock reef in a coastal embayment west of Charles Island near Milford, Connecticut, in LIS at approximately 41°11′13.73″N and 73°3′48.65″W (Fig. 1). The horseshoe-shaped reef covers an area of approximately 0.25 km^2, is discontinuous, and varies in rock density and size, with up to 70% cover of cobble and boulders and vertical relief up to 1-m high. Mean low water on the reef was 3–4 m, with a 2-m tidal range.

Methods for describing seafloor habitat and categorizing sediments are detailed in Mercaldo-Allen et al. (2011), but briefly, rock sizes were classified, by using the Udden-Wentworth grain-size scale (Lewis and McConchie, 1994), as pebbles (4–65 mm), cobble (65–250 mm), or boulders (250 mm–1 m). To describe seafloor topography, we collected sediments for grain-size analysis with a Smith–McIntyre benthic grab and used observations made by scuba divers and video and still images taken by a seabed observation and sampling system (USGS[3]). Seafloor sediments around reef structure ranged from all silt clay to a mixture of silt clay and sand and contained discontinuous patches of shell hash or pebbles and a fine silt layer. Communities of seaweeds, sponges, hydroids, and bryozoans heavily colonized cobble and boulder habitat.

Trap deployment

We used traps to sample fish because they are suitable for use on the irregular topography of rock reefs. Trapping provides a means of assessing relative abundance and diversity of species of juvenile fish in complex environments where other sampling options are limited (e.g., Grabowski et al., 2005; Tallman and Forrester, 2007). Fish traps primarily target demersal and epibenthic species, and trap openings and mesh sizes select for specific life stages. For this study, trap openings targeted the juvenile phase. For the deployments in 2004–2006, a commercially available collapsible shrimp and minnow trap (46 × 23 × 23 cm; Memphis Net and Twine[4], Memphis, TN), lined with 2-mm polyethylene mesh, was used, and for deployments in 2007, 2008, and 2016, traps with a similar design and functionality and with similar dimensions were constructed in-house of a sturdier wire frame lined with 3-mm mesh (Fig. 2). Because we targeted juvenile fish at ages of 1 year or older (>9 mm standard length), the nominal 1-mm difference in mesh size between the traps did not affect retention of this size class in traps. Traps had a single, central chamber and double entries. They were fitted with a flexible, 6.4-cm-diameter ring opening at both entrances, limiting the size of fish that gained entry into a trap. A 5-kg steel plate along the base of each trap provided ballast and stability.

We deployed strings of 3–4 traps evenly across 5 areas of the reef that had dense cobble and boulder structure (Fig. 1). Traps in each string were spaced 7.6 m apart. Fishing effort during sampling trips consisted of 15 traps deployed in 2004, 30 traps deployed in 2005–2006, 24 traps deployed in 2007–2008, and 20 traps deployed in 2016. We used catch per unit of effort (CPUE) to standardize for differences in number of traps and sampling trips among study years. We calculated CPUE by summing the number of all fish caught in the months of June, July, and August and dividing by the total annual fishing effort (number of traps multiplied by number of sampling trips). We categorized fish as warm or cold adapted on the basis of temperature adaptation groupings of species from a trawl survey conducted by the Connecticut Department of Energy and

---

[1] Auster, P. J. 1989. Species profiles: life histories and environmental requirements of coastal fishes and invertebrates (North Atlantic and mid-Atlantic)—tautog and cunner. U.S. Fish Wildl. Serv. Biol. Rep. 82(11.105), U.S. Army Corps Eng., TR EL-82-4, 13 p. [Available from website.]

[2] COA (Coastal Ocean Analytics LLC). 2016. Detecting climate change impacts in Long Island Sound, 134 p. Prepared for the U.S. Environmental Protection Agency. Long Island Sound study. EPA grant number LI96144501. NEI job code: 0302-005. Project code: 2013-007. [Available from website.]

[3] USGS (U.S. Geological Survey). 2000. Seabed observation and sampling system. U.S. Geological Survey, USGS Fact Sheet FS-142-00, 2 p. [Available from website.]

[4] Mention of trade names or commercial companies is for identification purposes only and does not imply endorsement by the National Marine Fisheries Service, NOAA.

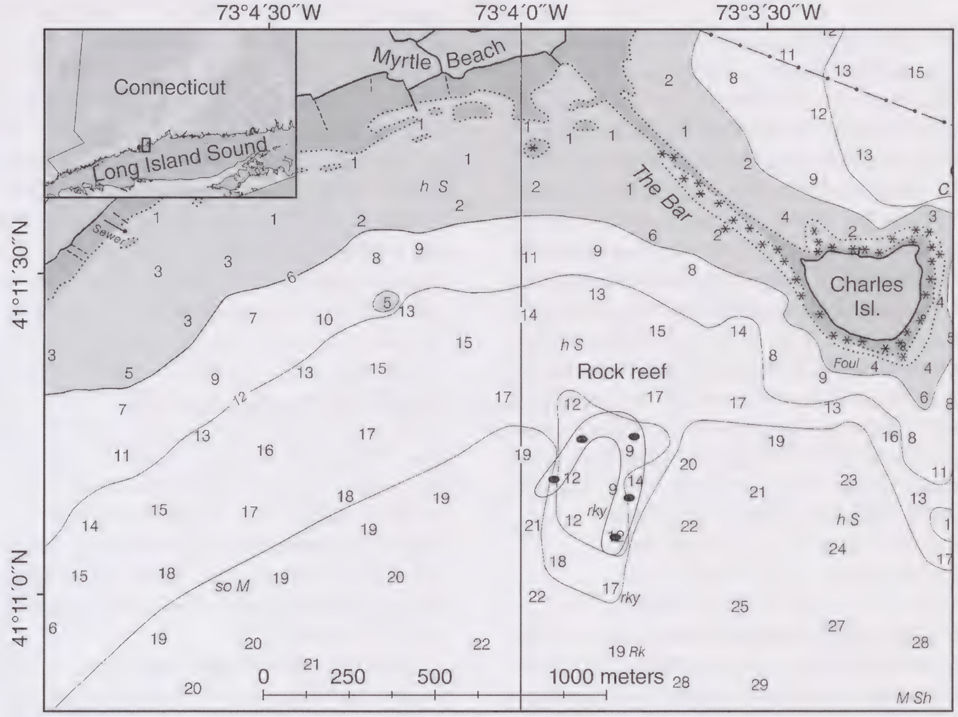

Figure 1

Map of a horseshoe shaped cobble and boulder reef located near Milford, Connecticut, in Long Island Sound, showing areas (black circles) where fish traps were deployed to assess changes in the relative abundance of juvenile finfish during the summer months (June–August) of 2004–2008 and 2016. Small numerals indicate mean lower low water in meters. Light gray shading indicates areas with depths <1.8 m (<6 ft) at low tide. Darker shading indicates areas exposed at low tide. Dotted lines indicate low tide lines. Solid lines indicate depth contours in meters. Asterisks (*) indicate the presence of rocks.

Environment Protection (CT DEEP) in LIS (Howell and Auster, 2012).

Structure-oriented fish have little incentive to leave shelter to enter unbaited traps; therefore, whole fresh northern quahog (*Mercenaria mercenaria*) were placed in perforated plastic cups inside traps as an attractant. Traps were set or retrieved beginning at the same time daily (0800) and processed in the same sequential order to ensure an approximate 24-h soak time and reduce the likelihood of predation in the traps. Data from sampling with traps that soaked for a longer or shorter period were not included. Once each trap was retrieved, we inspected it and identified, enumerated, and released all organisms found inside. We conducted sampling trips to deploy traps 2–3 d/week, from June through August, aboard the Milford Laboratory's 15-m NOAA Ship *Victor Loosanoff* or a smaller 7-m vessel.

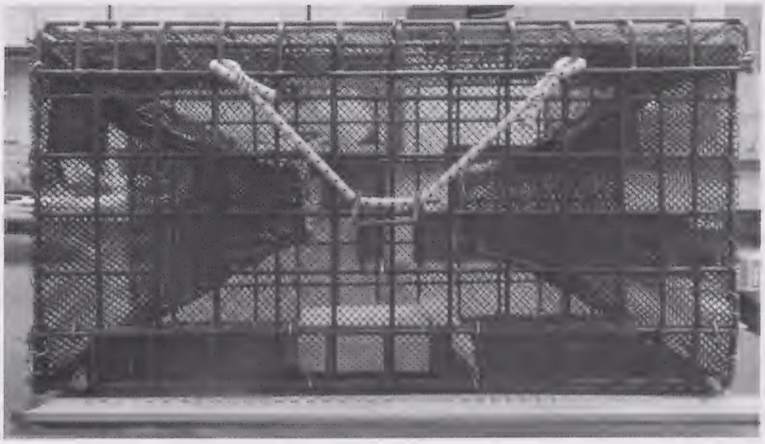

Figure 2

Photograph of the basic style of trap used for sampling of juvenile fish on a cobble and boulder reef in Long Island Sound during the summer months of 2007, 2008, and 2016. Traps were constructed of a wire frame lined with 3-mm mesh. Strings of 3–4 traps were deployed evenly across 5 areas on the reef.

Water temperatures

We assessed trends in local summertime temperatures by using a publicly available, long-term historical database maintained by the Milford Laboratory (available from website). Initially, a Bristol thermograph located on a dock in Milford Harbor recorded water temperatures during 1948–1975. From 1976 to the present, including our study period, daily surface temperatures were measured by using thermometer readings of sand-filtered seawater pumped from Milford Harbor. Studies that have analyzed these data have reported increasing water temperatures in LIS over the last 5 decades (see Rice et al., 2015; COA[2]). Because shifts in species distribution and composition of assemblages may occur when summer temperatures approach or exceed tolerance limits, we examined mean water temperatures during June–August, when fish trapping took place and water temperatures were highest, over the 12-year study period.

Statistical analysis

We analyzed fish assemblage data by using the statistical software program PRIMER, vers. 7 (PRIMER-e Ltd., Auckland, NZ) with the PERMANOVA+ add-on package. The Bray–Curtis coefficient was used to generate a similarity matrix across all pairs of samples. Bray–Curtis is commonly used in multivariate analysis of species assemblage data because it has beneficial properties of coincidence, complementarity, relative invariance, independence of joint absence, localization, and dependence on totals (Clarke et al., 2006). Nonmetric multidimensional scaling was used to visualize similarities in fish assemblage across all samples. The routine in PERMANOVA+ for canonical analysis of principal coordinates was used to identify fish in the benthic assemblage that were associated with each year. We used the Spearman rank correlation to assess the strength of the association between individual species abundance and sampling year. The analysis of similarity (ANOSIM) test in PRIMER was used to test for the significance of differences among fish assemblages for all pairs of years sampled. We used the distance-based linear model routine in PERMANOVA+ to analyze the relationship between the multivariate fish assemblage and local water temperature, by matching daily water temperatures from the Milford Laboratory data set to dates during which fish traps were deployed. We assessed temperature trends by using the robust Theil-Sen regression estimator and a bootstrap method to test significance (Wilcox, 2017). We chose this approach over the classic ordinary least-squares estimator because of its improved performance under conditions of non-normality or heteroscedasticity.

Results

Results of ANOSIM of fish assemblages indicate significant differences ($P<0.003$) between pairs of years of the study period (2004, 2005, 2006, 2007, 2008, and 2016) except between 2004 and 2005 ($P=0.138$, ANOSIM test statistic $R=0.033$) (Table 1). Species composition of fish assemblages was most different between 2004 and 2016 ($R=0.923$) and between 2005 and 2016 ($R=0.967$), and pairs of years that were further apart in time generally had greater R-values (Table 1). The nonmetric multidimensional scaling plot in Figure 3A illustrates differences in assemblages between years. The canonical analysis of principal coordinates also visualizes this overall temporal trend, with greater dissimilarity in fish assemblages between years that were further apart in time (Fig. 3B). Results of Spearman rank correlation analysis (>25%) indicate that the warm-adapted species black sea bass (coefficient of correlation [ρ]=0.770) and oyster toadfish (*Opsanus tau*) ($\rho=0.561$) were more abundant in 2008 and 2016 than in the other study years and that the cold-adapted species cunner ($\rho=-0.493$) and grubby (*Myoxocephalus aenaeus*) ($\rho=-0.391$) were more abundant in 2004–2006. The relationship between the fish assemblages and water temperatures was significant, with variation in temperatures explaining 8.6% of the variation in the fish assemblages ($P=0.0001$, coefficient of determination [r^2]=0.086).

Relative abundance, measured as CPUE, was plotted for the most abundant species, including the cunner, black sea bass, oyster toadfish, grubby, rock gunnel (*Pholis gunnellus*), scup (*Stenotomus chrysops*), and tautog (Fig. 4). To account for numerical dominance of black sea bass and cunner, we used 2 different y-axes, with values on the first y-axis up to 0.60 in the graphs for these 2 dominant species and values on the second y-axis up to 0.06 in

Table 1

Results of analysis of similarity comparing finfish assemblages on a cobble and boulder reef in Long Island Sound between years: 2004, 2005, 2006, 2007, 2008, and 2016. Differences in assemblages were statistically significant ($P<0.05$) in all comparisons, except for the difference between 2004 and 2005. R=test statistic from analysis of similarity.

Comparison	R	P
2004 vs. 2005	0.033	0.1380
2004 vs. 2006	0.376	0.0001
2004 vs. 2007	0.141	0.0030
2004 vs. 2008	0.512	0.0001
2004 vs. 2016	0.923	0.0001
2005 vs. 2006	0.386	0.0001
2005 vs. 2007	0.206	0.0006
2005 vs. 2008	0.560	0.0001
2005 vs. 2016	0.967	0.0001
2006 vs. 2007	0.250	0.0001
2006 vs. 2008	0.529	0.0001
2006 vs. 2016	0.781	0.0001
2007 vs. 2008	0.337	0.0001
2007 vs. 2016	0.758	0.0001
2008 vs. 2016	0.280	0.0002

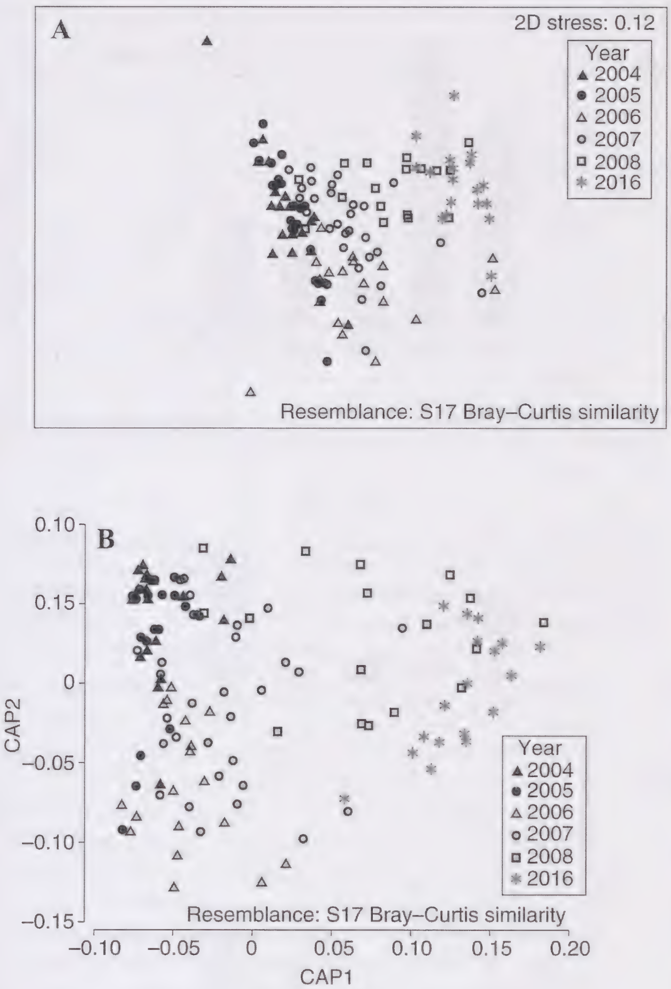

Figure 3

(**A**) Nonmetric multidimensional scaling plot of finfish community composition and (**B**) canonical analysis of principal components (CAP) used to visualize monthly patterns in finfish assemblages on a cobble and boulder reef in Long Island Sound during 2004, 2005, 2006, 2007, 2008, and 2016. Data used in the plot and analysis come from sampling with fish traps.

graphs for the less abundant fish species. Plots were not produced for the following fish species that were observed in low abundance (<4 individuals) during a single year: winter flounder (*Pseudopleuronectes americanus*) in 2004, Atlantic tomcod (*Microgadus tomcod*) in 2005, northern pipefish (*Syngnathus fuscus*) in 2006, feather blenny (*Hypsoblennius hentz*) in 2008, spotted hake (*Urophycis regia*) in 2008, and bluefish (*Pomatomus saltatrix*) in 2016.

Using temperatures from the Milford Laboratory database, we plotted mean summertime water temperatures from 2000 through 2016 in the central basin of LIS (Fig. 5). Results from regression analysis indicate a significant positive trend (slope=0.09, P=0.01) between year and water temperature over time.

Discussion

Changes in abundance of individual fish species over the time series indicate an increase in prevalence of warm-adapted species on the reef from 2004 through 2016. Although juvenile black sea bass were not observed in traps during 2004, their numbers rose steadily over the periods of this study with the highest numbers occurring in 2008 and 2016. This trend was also present in data from the CT DEEP trawl survey, with numbers of juvenile and adult black sea bass collected in 2013 greatly exceeding levels observed between 1984 and 2011 (Gottschall and Pacileo[5]). In addition, data from a long-term trawl survey (1976–present) conducted by the Millstone Power Station in Niantic, Connecticut, indicate historically elevated catches of juvenile and adult black sea bass since 2013 (DENC[6]). Further, a record high number of young-of-the-year black sea bass was documented in beach seine surveys conducted by CT DEEP at 8 inshore locations during 2015 (Molnar and Howell[7]). A similar pattern was observed for juvenile oyster toadfish, although they were not as abundant as black sea bass, with consistently low numbers on the reef during 2004–2007 and higher numbers observed in 2008 and 2016. Overall, numbers of oyster toadfish collected during individual trawl tows are often low because this species prefers rocky substrate where trawling is generally limited (Gottschall and Pacileo[5]; Crosby et al., 2018; DENC[6]); hence, fish trapping may be a better means for estimating abundance of oyster toadfish.

In our study, no consistent trends were observed in overall abundance of juvenile tautog and scup on the reef. There was interannual variation in abundance of juvenile tautog collected in fish traps, variation similar to that observed in the data from the CT DEEP trawl survey (Gottschall and Pacileo[5]) and near Millstone Power Plant in Niantic (DENC[6]). Scup, which did not appear in traps in 2004, increased in abundance during 2005–2008, with lower numbers observed in

---

[5] Gottschall, K., and D. Pacileo. 2016. Job 5: marine finfish survey. Long Island Sound trawl survey, 99 p. *In* A study of marine recreational fisheries in Connecticut. Federal aid in sport fish restoration F15AF00222 (F-54-R-35). Annual performance report, March 1, 2015–February 29, 2016. Conn. Dep. Energy Environ. Prot., Hartford, CT. [Available from website.]

[6] DENC (Dominion Energy Nuclear Connecticut). 2018. Fish ecology studies. *In* Annual report 2017. Monitoring the marine environment of Long Island Sound at Millstone Power Station, p. 145–14217. DENC, Waterford, CT. [Available from Millstone Environmental Lab, 314 Rope Ferry Rd., Waterford, CT 06385.]

[7] Molnar, D., and P. Howell. 2016. Job 8: estuarine seine survey, 22 p. *In* A study of marine recreational fisheries in Connecticut. Federal aid in sport fish restoration F15AF00222 (F-54-R-35). Annual progress report, March 1, 2015–February 29, 2016. Conn. Dep. Energy Environ. Prot., Hartford, CT. [Available from website.]

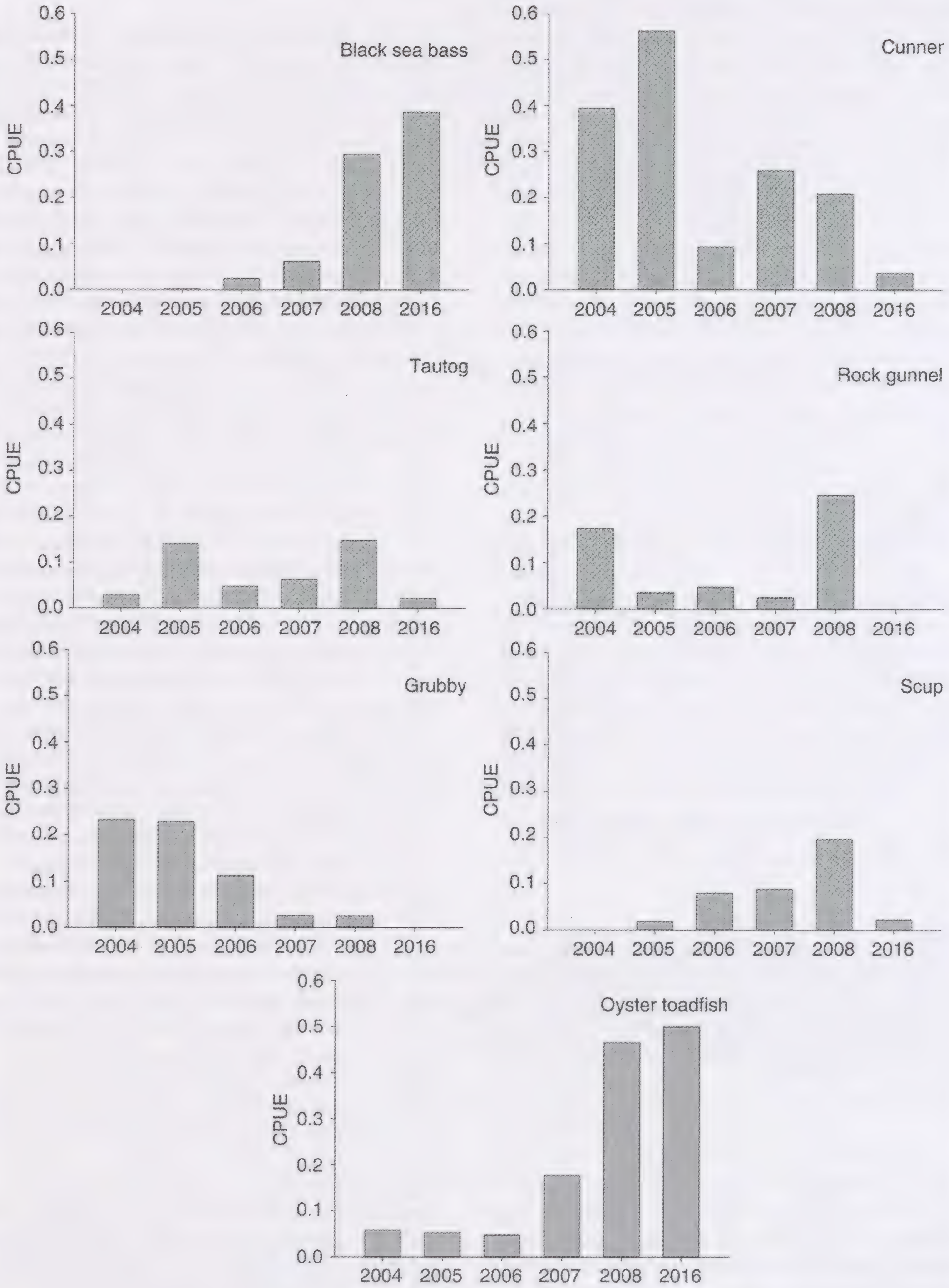

Figure 4

Abundance of juveniles for dominant finfish species caught in traps on a cobble and boulder reef in Long Island Sound during June, July, and August in 2004–2008 and in 2016. Catch per unit of effort (CPUE), used as an index of abundance, was calculated by summing the number of all fish caught and dividing by the total annual fishing effort (number of traps multiplied by number of sampling trips). The dominant species were the black sea bass (*Centropristis striata*), cunner (*Tautoga adspersus*), tautog (*Tautoga onitis*), rock gunnel (*Pholis gunnellus*), grubby (*Myoxocephalus aenaeus*), scup (*Stenotomus chrysops*), and oyster toadfish (*Opsanus tau*). Note that the graphs for black sea bass and cunner have a different range of CPUE values on the y-axis (up to 0.6) than graphs for the other species (values up to 0.06).

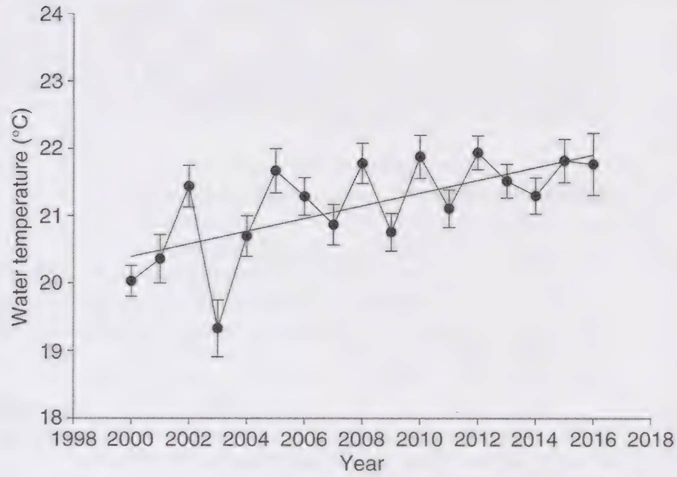

Figure 5

Mean summer (June–August) water temperatures (°C) in the central basin of Long Island Sound at Milford Laboratory, NOAA Northeast Fisheries Science Center, from 2000 through 2016. The regression line illustrates the trend of warming temperatures (slope=0.09, *P*<0.01), and the error bars indicate standard errors of the mean.

sampling with traps in 2016. Data from the CT DEEP trawl survey indicate a notable increase in abundance of young-of-the-year, juvenile, and adult scup after 1999, followed by interannual variability during subsequent years, which overlap with our study period. Long-term trawl surveys (1974–2016) conducted in eastern LIS also found no discernable trend in abundance of scup over the last 2 decades (Snyder et al., 2019). These findings contrast with those of other studies, which report increased abundance of this warm-adapted species. Elevations over time in the number of scup collected during trawl surveys in Niantic Bay have been reported (DENC[6]). Similarly, numbers of scup increased consistently from 1959 to 2005 in a nearby estuary in Rhode Island (Collie et al., 2008).

A progressive decline in abundance of cold-adapted species occurred over the study period. Abundance of cunner, the most numerous species in traps during 2004 and 2005, trended downward, reaching the lowest levels in 2016. Data from both the CT DEEP trawl survey (Gottschall and Pacileo[5]) and from a monitoring program in Norwalk Harbor, Connecticut (Crosby et al., 2018), indicate a long-term decline in abundance of cunner from 1984 to the present. Collie et al. (2008), in a study in Rhode Island, found similar reductions in numbers of cunner over an earlier time frame, from 1959 to 2005, and suggested that declines in estuarine species with discrete populations, like cunner, could signal a response to climate change. Populations of cunner may be shifting northward (Rose, 2005) or may be stressed by low tolerance to rapidly warming thermal conditions (Crosby et al., 2018). Because cunner are relatively unfished, variations in population size or distribution could relate directly to changes in environmental conditions.

Numbers of grubby on the reef declined from 2004 to 2008, and none were collected during 2016. Similarly, Roseman et al. (2005) noted a reduction in numbers of grubby in the Niantic River and Bay in eastern LIS over an earlier 26-year period (1976–2002), a decline that was attributed to a reduction in eelgrass (*Zostera marina*) or increased water temperatures. Fewer grubby were caught over time from 1976 to 2016 during the trawl survey at Millstone Power Station in Niantic (DENC[6]). Because grubby also experience low exploitation, changes in their population dynamics could indicate a response to environmental or habitat variability (Roseman et al., 2005). Rock gunnel, most abundant in fish traps in 2008, were also absent from collections at the reef in 2016. In trawl surveys of Norwalk Harbor, Crosby et al. (2018) collected no rock gunnel in bottom-trawl tows after 2009. Rock gunnel, often found in shallow intertidal waters, have a broad physiological tolerance for variable environmental conditions (Shorty and Gannon, 2013) and are likely to have low sensitivity to warming. These findings indicate that reductions in abundance of rock gunnel may relate to factors other than temperature. Winter flounder, observed in low numbers on the reef in 2004, were not caught in fish traps during 24-h soaks in subsequent years. Observations from long-term studies indicate that abundance of winter flounder in LIS has been on the decline for more than 20 years (e.g., Howell and Auster, 2012; Crosby et al., 2018).

Increases in relative abundance of black sea bass and oyster toadfish on the reef may account for the reductions in the numbers of cunner, grubby, and rock gunnel that we observed. Juvenile black sea bass and oyster toadfish, although opportunistic benthic omnivores, are also voracious predators known to consume young-of-the-year or small-bodied fish (e.g., Sedberry, 1988; Steimle and Zetlin, 2000; Collette and Klein-MacPhee, 2002; Byron and Link, 2010). Young-of-the-year cunner have been found in stomachs of juvenile black sea bass collected in traps (P. Clark, unpubl. data). Highly abundant black sea bass and increasingly numerous oyster toadfish may also be outcompeting these small-bodied species for habitat and resources.

Water temperature was a statistically significant predictor that explained 8.6% of the observed variation in juvenile finfish assemblages in LIS across our time series. Shifts in the composition of finfish assemblages linked to increased water temperature have been widely reported in southern New England. Benthic cold-adapted species, most notably the winter flounder and American lobster (*Homarus americanus*), have declined in abundance in LIS (Howell and Auster, 2012; Gottschall and Pacileo[5]; Snyder et al., 2019). A study in Norwalk Harbor conducted during 1987–2016 found changes in demersal fish assemblages related to increased mean water-column temperature (Crosby et al., 2018). Through analysis of the 25-year CT DEEP data set (1984–2008), Howell and Auster (2012) discerned a shift in seasonal patterns of abundance of finfish species, from high numbers of cold-adapted (northern) species in spring and warm-adapted (southern) species in autumn to dominance of warm-adapted species during both seasons. In another estuary in southern New England, Collie et al. (2008) observed changes in finfish species composition from 1959 through 2005 that were associated with increased sea-surface temperatures in Narragansett Bay and Rhode Island Sound during spring and summer.

Results from synthesis of temperature data collected from a variety of locations along the Connecticut coastline, including those from the Milford Laboratory historical database, substantiate other indications that summer and winter temperatures in LIS have been rising since 1965 (e.g., Rice et al., 2015; COA[2]). Four decades of data on water temperatures in eastern LIS indicate a rise of 0.45°C/decade (Snyder et al., 2019), with an annual mean increase of 0.08°C (standard deviation 0.03) from 1991 to 2013 (Staniec and Vlahos, 2017). Using the temperature record of the Milford Laboratory, Rice et al. (2015) calculated a warming rate of 0.03°C/year for surface waters from 1948 to 2012 in the central basin of LIS. Temperatures in Niantic Bay increased by 0.04°C/year from 1976 to 2015 (DENC[8]). Average summer surface temperatures measured by CT DEEP from 1991 to 2016 increased by 1°C (Gottschall and Pacileo[5]). In studies in Norwalk from 1987 to 2016, a 1.26°C rise in water temperature was observed (Crosby et al., 2018). Subtle increases in water temperature, as slight as 1°C, can alter abundance and distribution of individual fish species and influence composition of finfish assemblages (Howell and Auster, 2012).

Results of our comparison of juvenile finfish assemblages on a rock reef in LIS, through the use of legacy data from 2004 through 2008 and recent data from 2016, indicate variability in species composition that is consistent with observations from previous studies (e.g., Howell and Auster, 2012; Crosby et al., 2018). We observed a decline in abundance of cunner, a cold-adapted species, and numbers of black sea bass and oyster toadfish, both warm-adapted species, increased steadily. On the local scale of our study at a rock reef near Milford, composition of the fish community differed most between the earliest years of 2004 and 2005 and the most recent year 2016. A widely documented trend of gradually increasing water temperatures may have contributed to changes in species composition and abundance on this discrete cobble and boulder reef in LIS.

Acknowledgments

We thank R. Alix, A. Allen, E. Bates, G. Fignar, A. Grusky, E. Estela, C. Kuropat, J. Pereira, G. Phillips, J. Reidy, A. M. Salvato, W. Schreiner, G. Sennefelder, L. Vinokur, and J. Ziskowski for technical assistance. L. Poppe, D. Blackwood, and I. Babb provided video imagery. L. Williams allowed us to place fish traps on his leased shellfish grounds. NOAA dive team members B. Smith, M. Dixon, and D. Veilleux provided underwater photography and habitat assessments.

Literature cited

Able, K. W., L. S. Hales Jr., and S. M. Hagan.
2005. Movement and growth of juvenile (age 0 and 1+) tautog (*Tautoga onitis* [L.]) and cunner (*Tautogolabrus adspersus* [Walbaum]) in a southern New Jersey estuary. J. Exp. Mar. Biol. Ecol. 327:22–35.

Auster, P. J., R. J. Malatesta, and S. C. LaRosa.
1995. Patterns of microhabitat utilization by mobile megafauna on the southern New England (USA) continental shelf and slope. Mar. Ecol. Prog. Ser. 127:77–85.

Byron, C. J., and J. S. Link.
2010. Stability in the feeding ecology of four demersal fish predators in the US Northeast Shelf Large Marine Ecosystem. Mar. Ecol. Prog. Ser. 406:239–250.

Chin, A. T. M., J. Linke, M. Boudreau, M.-H. Thériault, S. C. Courtenay, R. Cormier, and M.-J. Fortin.
2018. Beta diversity changes in estuarine fish communities due to environmental change. Mar. Ecol. Prog. Ser. 603:161–173.

Clarke, K. R., P. J. Somerfield, and M. G. Chapman.
2006. On resemblance measures for ecological studies, including taxonomic dissimilarities and a zero-adjusted Bray–Curtis coefficient for denuded assemblages. J. Exp. Mar. Biol. Ecol. 330:55–80.

Collette, B. B., and G. Klein-MacPhee (eds.).
2002. Bigelow and Schroeder's fishes of the Gulf of Maine, 3rd ed., 748 p. Smithsonian Inst. Press, Washington, DC.

Collie, J. S., A. D. Wood, and H. P. Jeffries.
2008. Long-term shifts in the species composition of a coastal fish community. Can. J. Fish. Aquat. Sci. 65:1352–1365.

Crosby, S. C., N. L. Cantatore, L. M. Smith, J. R. Cooper, P. J. Fraboni, and R. B. Harris.
2018. Three decades of change in demersal fish and water quality in a Long Island Sound embayment. Estuar. Coasts 41:2135–2145.

Diaz, R. J., G. R. Cutter, and K. W. Able.
2003. The importance of physical and biogenic structure to juvenile fishes on the shallow inner continental shelf. Estuaries 26:12–20.

Drohan, A. F., J. P. Manderson, and D. B. Packer.
2007. Essential fish habitat source document: black sea bass, *Centropristis striata*, life history and habitat characteristics, 2nd ed. NOAA Tech. Memo. NMFS-NE-200, 68 p.

Grabowski, J. H., A. R. Hughes, D. L. Kimbro, and M. A. Dolan.
2005. How habitat setting influences restored oyster reef communities. Ecology 86:1926–1935.

Hare, J. A., W. E. Morrison, M. W. Nelson, M. M. Stachura, E. J. Teeters, R. B. Griffis, M. A. Alexander, J. D. Scott, L. Alade, R. J. Bell, et al.
2016. A vulnerability assessment of fish and invertebrates to climate change on the northeast U.S. continental shelf. PLoS ONE 11(2):e0146756.

Howell, P., and P. J. Auster.
2012. Phase shift in an estuarine finfish community associated with warming temperatures. Mar. Coast. Fish. 4:481–495.

---

[8] DENC (Dominion Energy Nuclear Connecticut). 2018. Winter flounder studies. *In* Annual report 2017. Monitoring the marine environment of Long Island Sound at Millstone Power Station, p. 111–143. DENC, Waterford, CT. [Available from Millstone Environmental Lab, 314 Rope Ferry Rd., Waterford, CT 06385.]

Lewis, D. W., and D. McConchie.
1994. Analytical sedimentology, 197 p. Chapman & Hall, New York.

Mercaldo-Allen, R., R. Goldberg, P. E. Clark, and C. A. Kuropat.
2011. Observations of juvenile lobsters, *Homarus americanus*, on a rock-reef in Long Island Sound. Northeast. Nat. 18:45–60.

Nye, J. A., J. S. Link, J. A. Hare, and W. J. Overholtz.
2009. Changing spatial distribution of fish stocks in relation to climate and population size on the northeast United States continental shelf. Mar. Ecol. Prog. Ser. 393:111–129.

Olla, B. L., A. J. Bejda, and A. D. Martin.
1979. Seasonal dispersal and habitat selection of cunner, *Tautogolabrus adspersus*, and young tautog, *Tautoga onitis*, in Fire Island Inlet, Long Island, New York. Fish. Bull. 77:255–261.

Peters, D. S., and F. A. Cross.
1992. What is coastal fish habitat? *In* Stemming the tide of coastal fish habitat loss: proceedings of a symposium on conservation of coastal fish habitat; Baltimore, MD, 7–9 May 1991 (R. H. Stroud, ed.), p. 17–22. Natl. Coalition Mar. Conserv., Savannah, GA.

Poppe, L. J., H. J. Knebel, Z. J. Mlodzinska, M. E. Hastings, and B. A. Seekins.
2000. Distribution of surficial sediment in Long Island Sound and adjacent waters: texture and total organic carbon. J. Coast. Res. 16:567–574.

Rice, E., H. G. Dam, and G. Stewart.
2015. Impact of climate change on estuarine zooplankton: surface water warming in Long Island Sound is associated with changes in copepod size and community structure. Estuar. Coasts 38:13–23.

Rijnsdorp, A. D., M. A. Peck, G. H. Engelhard, C. Möllmann, and J. K. Pinnegar.
2009. Resolving the effect of climate change on fish populations. ICES J. Mar. Sci. 66:1570–1583.

Rose, G. A.
2005. On distributional responses of North Atlantic fish to climate change. ICES J. Mar. Sci. 62:1360–1374.

Roseman, E. F., C. A. Tomichek, T. Maynard, and J. A. Burton.
2005. Relative abundance, age, growth, and fecundity of grubby *Myoxocephalus aenaeus* in Niantic River and Niantic Bay, Long Island Sound. J. Sea Res. 53:309–318.

Scharf, F. S., J. P. Manderson, and M. C. Fabrizio.
2006. The effects of seafloor habitat complexity on survival of juvenile fishes: species-specific interactions with structural refuge. J. Exp. Mar. Biol. Ecol. 335:167–176.

Sedberry, G. R.
1988. Food and feeding of black sea bass, *Centropristis striata*, in live bottom habitats in the South Atlantic Bight. J. Elisha Mitchell Sci. Soc. 104:35–50.

Shorty, J. T., and D. P. Gannon.
2013. Habitat selection by the rock gunnel, *Pholis gunnellus* L. (Pholidea). Northeast. Nat. 20:155–170.

Snyder, J. T., M. M. Whitney, H. G. Dam, M. W. Jacobs, and H. Baumann.
2019. Citizen science observations reveal rapid, multidecadal ecosystem changes in eastern Long Island Sound. Mar. Environ. Res. 146:80–88.

Staniec, A., and P. Vlahos.
2017. Timescales for determining temperature and dissolved oxygen trends in the Long Island Sound (LIS) estuary. Cont. Shelf Res. 151:1–7.

Steimle, F. W., and C. Zetlin.
2000. Reef habitats in the Middle Atlantic Bight: abundance, distribution, associated biological communities, and fishery resource use. Mar. Fish. Rev. 62(2):24–42.

Tallman, J. C., and G. E. Forrester.
2007. Oyster grow-out cages function as artificial reefs for temperate fishes. Trans. Am. Fish. Soc. 136:790–799.

Tupper, M., and R. G. Boutilier.
1997. Effects of habitat on settlement, growth, predation risk and survival of a temperate reef fish. Mar. Ecol. Prog. Ser. 151:225–236.

Walsh, H. J., D. E. Richardson, K. E. Marancik, and J. A. Hare.
2015. Long-term changes in the distributions of larval and adult fish in the northeast U.S. shelf ecosystem. PLoS ONE 10(9):e0137382.

Wilcox, R. R.
2017. Understanding and applying basic statistical methods using R, 504 p. John Wiley & Sons, Hoboken, NJ.

National Marine
Fisheries Service
NOAA

Fishery Bulletin
established in 1881

Spencer F. Baird
First U.S. Commissioner
of Fisheries and founder
of *Fishery Bulletin*

Costs of at-sea monitoring under government and private contracts in the groundfish fishery of the northeastern United States

Greg Ardini (contact author)
Chad Demarest
Katherine McArdle

Email address for contact author: gregory.ardini@noaa.gov

Northeast Fisheries Science Center
National Marine Fisheries Service, NOAA
166 Water Street
Woods Hole, Massachusetts 02543

Abstract—An at-sea monitoring (ASM) program has been a required supplement to the Northeast Fisheries Observer Program, National Marine Fisheries Service (NMFS), for monitoring catch in the groundfish fishery in the northeastern United States since the inception of comprehensive sector-based management in May 2010. For the initial years of this management program, the NMFS contracted with ASM providers and covered all costs for ASM-related services. Since March 2016, vessel owners who target groundfish collectively as groups called *sectors* have been required to cover the cost of the at-sea component of the ASM program through annual contracts with providers. Although subsequent developments have resulted in the NMFS reimbursing sectors for the majority of billed costs, the salient shift has been from government to private negotiation of ASM contracts. We investigated whether private contracting has reduced ASM costs by applying the terms of contracts to trip-level data from the groundfish fishery over the fishing years of 2013–2018. The payment regime of these contracts was compared with average costs per sea day from NMFS-negotiated contracts. We found that private contracts resulted in average cost reductions of 14% for the at-sea component of the ASM program. Cost reductions may, however, result in other complications, such as reduced observer pay and consequent issues of retention or data quality.

Manuscript submitted 16 December 2019.
Manuscript accepted 8 September 2020.
Fish. Bull. 118:284–296 (2020).
Online publication date: 6 October 2020.
doi: 10.7755/FB.118.3.7

The views and opinions expressed or implied in this article are those of the author (or authors) and do not necessarily reflect the position of the National Marine Fisheries Service, NOAA.

Amendment 16 to the fishery management plan (FMP) for the Northeast multispecies fishery, which includes several groundfish species, required implementation of a comprehensive, cooperative catch allocation scheme called *sector management*. This system of management allows vessel owners to pool allocations of harvest rights and fish them collectively within *sectors* (Federal Register, 2010). Sectors can be formed by any group of 3 or more individuals who hold limited-access groundfish permits and do not have ownership interests that overlap (Federal Register, 2010). Although amendment 16 did not mandate joining a sector, the majority of vessels active in the groundfish fishery enrolled in 1 of 17 sectors for fishing year (FY) 2010, rather than operate under the alternative management system based on input controls, called the *common pool* (note that the groundfish fishing year runs from May through April). The sector component of the groundfish fishery has continued to make up the vast majority of effort and catch (Murphy et al.[1]). Amendment 16 stipulated a variety of catch reporting requirements for sectors, including the following: all legal-sized fish must be landed, catch must be accurately reported by statistical area, sector-level catch must be reported weekly to the National Marine Fisheries Service (NMFS), and a list of ports where members land their fish must be specified.

Beginning in FY2012, sector participants were also required to fund an at-sea monitoring (ASM) program, designed to collect catch and discard data for sector-enrolled vessels, with the NMFS agreeing to fund the program in the interim (Federal Register, 2010). The transition to industry-funded monitoring, however, did not occur in FY2012 as originally planned, and the federal government continued to fully subsidize monitoring until March 2016.

To implement industry funding of monitoring, sectors that target groundfish were required to have contracts in place with private ASM service providers. These contracts, which have been renegotiated on an annual basis, specify costs for all components of ASM services, including observer time at sea, observer travel, and observer training. Also specified in the contracts are other miscellaneous costs, such as the cost of observer travel in the event that a vessel fails to take a trip after its captain had notified an intent to fish. Before a sector vessel embarks on a groundfish trip, the captain must declare an intent to fish through the Pre-trip Notification System (PTNS). Any trip during which species managed under the groundfish FMP will be targeted is eligible to be chosen by the PTNS to have the vessel carry an ASM observer. Trips during which fishermen will target species managed under other FMPs, such as those for the spiny dogfish (*Squalus acanthias*) or the goosefish (*Lophius americanus*), may also be eligible, with a few exceptions (Federal Register, 2016; for more information on PTNS trip selection, see Palmer et al.[2]).

---

[1] Murphy, T., G. Ardini, M. Vasta, A. Kitts, C. Demarest, J. Walden, and D. Caless. 2018. 2015 final report on the performance of the Northeast multispecies (groundfish) fishery (May 2007–April 2016). NOAA, Natl. Mar. Fish. Serv., Northeast Fish. Sci. Cent. Ref. Doc. 18-13, 128 p. [Available from website.]

Under contracts negotiated by sectors, the duties of ASM observers are still defined by the NMFS; these duties have remained consistent since the ASM program was first implemented. Each sector has been required to submit their ASM contract to the NMFS to ensure compliance with applicable sector operation regulations. During FY2016–2018, each of the sectors that actively fished (16 sectors in FY2016–2017 and 14 sectors in FY2018) contracted with 1 of 4 NMFS-approved ASM providers. Within each sector's operations plan, which were reviewed and approved by the NMFS, the sector indicated the intent to actively participate, or not, in the groundfish fishery in the fishing year or years specified in the plan. Sectors that indicated intent to actively fish for groundfish were required to contract with a provider of ASM observers. Those sectors that indicated that they would not be actively fishing for groundfish could operate on a lease-only basis for quota and, therefore, not be required to contract with an ASM provider. In order for a sector to have contracted with an ASM provider, the NMFS must have approved the provider's ability to meet the objectives of the ASM program. During FY2016–2018, 5 providers received approval, and one of those providers did not contract with any sector throughout this period. Three of the 4 providers that contracted with sectors during this period had contracted with the NMFS for ASM coverage prior to March 2016.

Although sectors have been the nominal payer since March 2016, a majority of actual ASM costs have been reimbursed by the NMFS. Rates of reimbursement were 85% in FY2016 (starting in July) and 85% in FY2017 (NMFS[3,4]). For FY2018, sectors were fully reimbursed for their ASM costs (NMFS[4]). Regardless of cost reimbursement, the negotiation of private contracts by multiple buyers (sectors) and multiple sellers (providers) indicates the potential for a competitive ASM services market. Furthermore, there are differences, such as those in landing ports and fishing trip durations, within and between groundfish sectors that affect the cost of placing monitors on vessels. In theory, competition between sectors in negotiating contracts would result in lower costs compared with costs of the more homogeneous contracts negotiated by the NMFS.

The transition from government-funded monitoring to industry-funded monitoring is not unique to the Northeast groundfish fishery. When catch shares were implemented in 2011 in the trawl fishery that targets groundfish off the Pacific coast of the United States, most monitoring costs were subsidized. This subsidy decreased over time, and the fishing industry in this region was fully responsible for monitoring costs starting in 2016 (PFMC and NMFS[5]). To our knowledge, however, no previous work has compared government and industry rates for providing observers in fisheries of the United States.

We tested the hypothesis that rates are lower for private contracts than for government contracts by calculating the actual costs incurred for the at-sea component of the ASM program under NMFS contracts (FY2013–2015) and comparing these costs to costs under privately negotiated contract terms during FY2016–2018. Using actual trips with an ASM observer during FY2013–2018, we applied the average costs under NMFS contracts and the private contract terms to directly compare costs under the 2 different contracting schemes. We tracked changes in aggregate at-sea costs, as well as the distribution of these costs across trip type (single day versus multiple days), vessel type (large trawl, small trawl, or gill net), and landing region. We also estimated changes in the total cost of the ASM program under NMFS and sector contracts by including the costs of observer travel and at-sea observer training. Because we were unable to separate these costs to the trip level, we included them only in the aggregate. Finally, we looked at changes in fishing practices, specifically trip duration, used on ASM trips that may have resulted from cost-reduction incentives incorporated in the contracts negotiated by sectors.

Materials and methods

Government-negotiated contracts

The ASM program was fully funded by the NMFS from the start of FY2010 (May 2010) through February 2016. The NMFS contracted with 3 different service providers throughout this time period. At-sea monitoring contracts were renegotiated during FY2012–2013, changing the ASM billing schedule from full to partial sea days and resulting in substantially lower costs. Under the full-sea-day billing schedule of FY2010–2011, the NMFS was charged on the basis of rounding the duration of an observer trip up to the nearest whole sea day (e.g., a 15-h trip would be billed as a 24-h trip). Under a schedule based on partial sea days, the NMFS was charged on the basis of rounding the duration of an observer trip up to the nearest quarter sea day (e.g., a 15-h trip would be billed as an 18-h trip). The net effect of this change was to decrease at-sea costs by 25%.

---

[2] Palmer, M. C., P. Hersey, H. Marotta, G. R. Shield, and S. B. Cierpich. 2013. The design, implementation and performance of an observer Pre-trip Notification System (PTNS) for the Northeast United States groundfish fishery. NOAA, Natl. Mar. Fish. Serv., Northeast Fish. Sci. Cent. Ref. Doc. 13-21, 82 p. [Available from website.]

[3] NMFS (National Marine Fisheries Service). 2017. NOAA Fisheries announces at-sea monitoring coverage levels for groundfish sector fishery. [Available from Sustain. Fish. Div., Gt. Atl. Reg. Fish. Off., Natl. Mar. Fish. Serv., 55 Great Republic Dr., Gloucester, MA 01930.]

[4] NMFS (National Marine Fisheries Service). 2018. NOAA Fisheries announces reimbursement of sector at-sea monitoring costs. [Available from website, accessed September 2018.]

[5] PFMC (Pacific Fishery Management Council) and NMFS (National Marine Fisheries Service). 2017. West Coast groundfish trawl catch share program: five-year review, 487 p. PFMC, Costa Mesa, CA. [Available from website.]

To establish costs under the government contracts, we used billing information for FY2013–2015 from the Fisheries Sampling Branch of the NOAA Northeast Fisheries Science Center, allowing us to assign a cost per observed sea day (hereafter, we refer to observed sea days as *sea days*) for all aspects of the ASM program. A sea day is based on the billing schedule, with trip duration rounded up to quarter days (6 h) under the renegotiated NMFS contracts, such that a trip for which a vessel departed and landed on the same day and was at sea for 20 h would count as a full sea day (1.0 d). In terms of days absent, another margin we consider in our analysis, this same trip would simply be 0.83 d (20 h/24 h) absent. Days absent is calculated as the amount of time between when the vessel leaves the dock and when it lands, as filled out in the vessel trip report by the captain. The trip duration recorded by the captain and observer are not always identical but are generally close.

From September 2013 through December 2015, the average cost per sea day was $685 (in 2017 U.S. dollars). The monthly data indicate limited variability with costs in a range of $653–729 per sea day. The relative consistency in at-sea rates was largely based on the fact that the billing schedule (quarter sea days) did not change over the time period. The average cost for travel and lodging over the time period was $101 per sea day. Training costs, associated with at-sea training, were $70 per sea day. Adding the 3 components together, total ASM costs were $856 per sea day (Table 1).

Privately negotiated contracts

Sectors that target groundfish negotiated contracts with service providers on an annual basis for FY2016–2018. Once a sector and provider reached an agreement, the sector sent the contract to the NOAA Greater Atlantic Regional Fisheries Office for approval. We used the approved contracts for all active groundfish sectors for each of the 3 fishing years. For FY2016–2017, 16 sectors had approved ASM contracts in place, and 14 sectors received approval for FY2018. Sectors contracted with 4 service providers in total in each year. Some sectors negotiated contracts that specified a universal daily rate per 24-h period of service, and other sectors had contracts set up for charging on a prorated basis or for charging partial rates for the first and last days of a fishing trip. For some contracts, daily rates were different between single-day trips and multiday trips. The contracts also included observer travel costs in different ways. Some sectors were billed for travel costs only if the port of departure and return port were not among those listed in the contract or if the departure port and landing port were not the same. Other contracts stipulated that sectors would be charged only if observers had to travel a certain distance to board the departing vessel. Lastly, in contrast to the NMFS contracts, the costs associated with new observer training trips at sea were borne by the providers and incorporated into their charged costs per sea day.

We estimated the variable cost of ASM services for each sector as a function of the relevant component provisions contained within each contract. Broadly, variable costs for ASM services are the sum of the daily rates applied to monitored trips, any compensated travel costs, and, when applicable, lodging costs. Each component of these costs are uniquely specified in the contracts. Arithmetically, a

Table 1

Costs per sea day for at-sea monitoring (ASM) paid by the National Marine Fisheries Service (NMFS) for fishing years (FY) 2013–2015 of the groundfish fishery in the northeastern United States. Costs are given in 2017 U.S. dollars. Note that FY2013 included only the period September 2013–April 2014 and that FY2015 included only the period May 2015–December 2015. Costs for January and February 2016 were not factored into the calculations of costs per sea day for FY2015 because of subcontracting between ASM providers in these months.

Fishing year	No. of ASM sea days	NMFS cost	At-sea cost per sea day	Travel cost per sea day	Training cost per sea day	Total cost per sea day
2013	1557	$1,084,591	$696	$108	$56	$859
2014	3327	$2,271,070	$683	$93	$63	$833
2015	1192	$805,558	$676	$111	$108	$894
Total	6076	$4,161,220	$685	$101	$70	$856

full specification of the cost equation may be represented as follows:

$$ASM_{\text{cost}} = \sum\nolimits_{i=1}^{16}\sum\nolimits_{t=1}^{n}\left[\begin{array}{l}\Big(\left(\alpha_1\beta_1\right)_{\mathrm{i}}\, D_{\text{first}}\Big)\\ +\Big(\left(\alpha_2\beta_2\right)_{\mathrm{i}} \sum D_{\text{whole}}\Big)\\ +\Big(\left(\alpha_3\beta_3\right)_{\mathrm{i}}\, D_{\text{last}}\Big)\\ +\Big(\left(\alpha_4\beta_4\right)_{\mathrm{i}}\, T\Big)+\Big(\left(\alpha_5\beta_5\right)_{\mathrm{i}}\, L\Big)\end{array}\right], \quad (1)$$

where, for i sectors and t trips,

ASM_{cost} = cost of ASM services;
α = a binary variable taking the value of 1 when a cost component applies and 0 when it does not;
β = the applicable marginal rate for each billable service subcomponent;
D = billable days absent (with partial first, last, and any intervening whole days treated uniquely);
T = billable travel miles; and
L = billable lodging days.

Ideally, total ASM costs under contracts negotiated by sectors would be estimated by using equation 1; however, we ran into 2 issues regarding travel and lodging costs. First, some sectors were charged for observer travel and lodging only when the observer traveled considerable distance to reach the vessel's port of departure. The observer travel distance is generally from their assigned home port to their port of departure and landing. Because we did not have access to observer travel distances, we were not able to determine the frequency with which travel and lodging charges were applicable for these sectors. Second, even for those sector trips for which we knew observer travel costs were incurred, on the basis of the ASM contract, we did not feel it was appropriate to estimate observer travel costs, such as lodging, and tolls, because we did not know where observers traveled from. We were, however, able to obtain the percentage of total ASM charges that were accrued to travel and lodging in FY2016 directly from the 4 ASM providers. Because the conditions for being charged for observer travel were generally unchanged between the 3 contract years for all providers, we assumed that travel as a percentage of costs remained the same in the contracts for FY2017 and FY2018. We estimated total ASM costs to the fishery by first calculating at-sea costs ($At\text{-}sea_{\text{cost}}$) by using the following equation, which contains only the at-sea components of equation 1. We then took the at-sea costs and added observer travel costs based on the information obtained from contract providers.

$$At\text{-}sea_{\text{cost}} = \sum\nolimits_{i=1}^{16}\sum\nolimits_{t=1}^{n}\left[\begin{array}{l}\Big(\left(\alpha_1\beta_1\right)_{\mathrm{i}}\, D_{\text{first}}\Big)\\ +\Big(\left(\alpha_2\beta_2\right)_{\mathrm{i}} \sum D_{\text{whole}}\Big)\\ +\Big(\left(\alpha_3\beta_3\right)_{\mathrm{i}}\, D_{\text{last}}\Big)\end{array}\right]. \quad (2)$$

Comparisons of contracts

To facilitate consistent comparison of ASM costs between the sector and NMFS contracts, records for all groundfish sector trips from September 2013 through August 2018 were retrieved from the Data Management and Imputation System maintained by the Greater Atlantic Regional Fisheries Office. Groundfish trip records were merged with a table of ASM trips from the Northeast Fisheries Science Center by using SAS Universal Viewer[6] 1.4 (SAS Institute Inc., Cary, NC), ensuring that only those trips that had an ASM observer on board were included. By linking each vessel with its sector affiliation, the data allowed exact matching of trips and contracted providers. When sectors negotiated ASM contracts for FY2016–2018, the membership of a sector may or may not have been the same as in previous years. A change in membership may have affected the negotiated contract terms. Sector affiliations for active vessels, however, did not change a great deal in our data set. Among the 366 active vessels, 300 (82%) were active in only one sector throughout the 6-year comparison period.

Trip duration was calculated primarily by taking the difference between the observer recorded date and time of disembarking and of boarding the vessel. For a small number of observations, the observer did not record this information; in these cases, we used trip length recorded by the captain on the vessel trip report. Our data set contained 4072 trips with an ASM observer out of 34,956 groundfish trips made by sectors during the study period, yielding a composite ASM observer coverage rate of 11.65%.

We calculated at-sea costs and total ASM costs by sea day and day absent. We then aggregated these costs by fishing year. For perspective on the relative magnitude of total ASM costs, we calculated ASM costs as a percentage of operating profit from sector groundfish trips. We defined operating profit as net revenue minus operating costs and sector fees. Operating costs were estimated by using a linear equation with cost information collected by observers in the ASM program and Northeast Fisheries Observer Program (NEFOP). The equation includes variability for monthly fuel prices, trip duration, number of crew members, vessel size, and gear type. Groundfish sector fees, used to cover administrative costs associated with running a sector, are collected from vessel landings or quota contributions. Sector fees were estimated as a flat fee of \$0.035 per pound of groundfish landed and \$0.0075 per pound of landed fish that were not groundfish on groundfish trips. (For more information on the estimation of operating costs, see Federal Register, 2019). All revenues and costs were adjusted to 2017 U.S. dollars by using the gross domestic product implicit price deflator (USBEA[7]).

---

[6] Mention of trade names or commercial companies is for identification purposes only and does not imply endorsement by the National Marine Fisheries Service, NOAA.

[7] USBEA (U.S. Bureau of Economic Analysis). 2018. Gross domestic product: implicit price deflator [A191RI1Q225SBEA], retrieved from Federal Reserve Economic Data (FRED). Federal Reserve Bank of St. Louis, St. Louis, MO. [Available from website, accessed May 2018.]

Additionally, we analyzed at-sea costs by trip type (single day and multiple days), vessel type (based on gear and length), and region of landing. Vessel types included small trawl vessels, with lengths of 0–18.3 m (0–60 ft); large trawl vessels, with lengths ≥18.3 m, and gill-net vessels of all lengths (average length: 13.0 m for gill-net vessels and 18.8 m for trawl vessels). The regions for which data were analyzed included Massachusetts; Maine and New Hampshire; and Rhode Island, Connecticut, and mid-Atlantic states. Because we were unable to disaggregate observer travel costs, we did not compare total ASM costs at these margins. Furthermore, it is important to note that *total* ASM costs refer to only those costs defined in Table 1. Shoreside infrastructure costs of the ASM program, such as recruiting and training new observers, are covered by the NMFS; these costs were not included in our comparison.

Finally, we analyzed changes in fishing behavior, as measured by trip duration, on trips with an ASM observer between the period when contracts were negotiated by the NMFS (September 2013–February 2016) and the period covered by privately negotiated contracts (March 2016–August 2018). We did not include January and February 2016 when comparing trip duration. These months also were not included in our calculation of rates per sea day under NMFS contracts because subcontracting of providers during these 2 months affected rates. We measured changes in trip duration across vessel categories that were different than those used in our ASM cost comparison analysis. Rather than a combination of gear and vessel size, we chose to analyze changes in trip duration only by vessel size category. The following 4 size categories based on vessel length were used: <13.7 m (<45 ft), 13.7–18.3 m (45–60 ft), 18.3–22.9 m (60–75 ft), and ≥22.9 m (≥75 ft). In our analysis, we specifically measured differences in days absent, the primary driver for the at-sea cost component of the ASM program. In doing so, we also compared trip length to lengths of trips with NEFOP observers. The purpose of this comparison was to determine if any apparent changes in aspects of ASM trips may have been driven by factors affecting all observed groundfish trips rather than by cost reductions from incentives embedded in the privately negotiated contracts.

Results

Comparisons of at-sea and total costs

Results from comparisons of at-sea and total costs by sea day and day absent across the 6-year period of FY2013–2018, for the entire fleet of groundfish vessels that operate in sectors are presented in Table 2. During the 3 years for which we examined data of sector contracts, at-sea costs were similar, ranging from $579 to $602 per observed sea day. At-sea costs per sea day were $83 (12.08%) to $106 (15.41%) lower under privately negotiated contracts than under NMFS contracts. Total costs per sea day were $233 (27.21%) to $257 (30.02%) lower between private and government contracts, with travel costs based on data for FY2016 used for all 3 years. In many contracts, the sector was only responsible for covering travel costs if a vessel landed in a different port than the port at which the observer boarded or if the vessel landed in a port outside of the primary ports listed in the contract. For vessels operating in sectors under these contract specifications during FY2016, 30% of (79 of 260) ASM trips resulted in the sector being charged for observer travel.

The ASM cost relative to total days absent, a measure of cost per total fishery effort from observed and unobserved trips, was ~$80 for private contracts at the aggregate coverage rate of 11.65% for the study period. This relative cost is distinguished from the cost per observed sea day or observed day absent, margins that are clearly less sensitive to overall coverage rates. No trend emerged from data for the 3 years of sector contracts that were analyzed (there was a slight increase in costs in FY2017 and a slight decrease in costs in FY2018); coverage rates were relatively similar during FY2016–2018. Given these findings, we hereafter present results for analysis of private contracts as the average of the 3 years of contract terms.

We next focused on a fishery-wide comparison of both at-sea costs and total costs aggregated over the 6-year period (Table 3). Sector contracts on average resulted in at-sea costs that were $0.83 million (13.63%) lower than costs under NMFS contracts and in total costs that were $2.17 million (28.45%) lower. At-sea cost reductions were consistent, ranging from 12.20% in FY2018 to 14.96% in FY2016. At-sea costs accounted for 80.02% of total costs under NMFS contracts and for 96.60% of total costs under private contracts over the course of the study period. Total costs were estimated to be 2.67% of operating profit generated from sector groundfish trips aggregated over the 6-year period, with a high of 4.57% in FY2014 and a low of 1.07% in FY2018 (Table 4). Year-to-year variation was driven largely by the ASM coverage rate. Total ASM costs were estimated to be 1.91% of operating profit under the averaged sector contracts, with a high of 3.28% in FY2014 and a low of 0.79% in FY2018. Operating profit was 75.47% of gross revenue over the course of the study period, with lower percentages in FY2013–2014.

A declining trend was evident both in ASM costs as a percentage of operating profit and in coverage rates during our 6-year study period (excluding the incomplete FY2013). Because our time series is limited, our analysis of the relationship between these 2 factors is not complete. As one would expect, higher ASM coverage resulted in greater payments to ASM providers under both NMFS and sector contracts. The number of ASM trips was also affected by the implementation of the extra-large-mesh (ELM) exemption that began in FY2016. This rule eliminated ASM coverage requirements for ELM trips fishing in portions of southern New England because of generally low amounts of groundfish caught on such trips (Federal Register, 2016). These exempted fishing trips were not counted as sector groundfish trips (the coverage rate denominator), inducing

Table 2

At-sea and total costs in the Northeast groundfish fishery under contracts negotiated by the National Marine Fisheries Service (NMFS) and under privately negotiated contracts, applied to the period from September 2013 through August 2018. The NMFS negotiated contracts for fishing years (FY) 2013–2015, and fishery management representatives for groups of groundfish vessel owners, known as *sectors*, negotiated contracts for FY2016–2018. The number of observed sea days is based on the billing schedule for sea days paid by the NMFS (rounded up to quarter days). The number of observed days absent was calculated as the sum of trip durations recorded by captains on all observed trips. The number of total days absent was calculated as the sum of trip durations recorded by captains on all observed and unobserved trips. Costs are given in 2017 U.S. dollars. Note that the NMFS-negotiated at-sea cost per sea day ($685) and total cost per sea day ($856) are identical to those in Table 1. *n*=number of days.

Observed or total days	Contract	Average at-sea cost	Average total cost
Cost per observed sea day (*n*=8918)	NMFS contracts	$685	$856
	FY16 contracts	$579	$599
	FY17 contracts	$602	$623
	FY18 contracts	$593	$615
	Average	$592	$612
Cost per observed day absent (*n*=7743)	NMFS contracts	$789	$986
	FY16 contracts	$667	$690
	FY17 contracts	$694	$718
	FY18 contracts	$683	$709
	Average	$681	$705
Cost per day absent (observed and unobserved: *n*=66,626)	NMFS contracts	$92	$115
	FY16 contracts	$78	$80
	FY17 contracts	$81	$83
	FY18 contracts	$79	$82
	Average	$79	$82

a significant decline in the number of sector groundfish trips for FY2016–18 relative to FY2013–2015. Had the ELM exemption been in place during FY2013–2015, many fewer trips would have been observed during that period. Revenue from the exempted trips, however, was included in annual gross revenue totals (Table 4) in order to maintain a consistent approach in the calculation of ASM costs relative to revenue.

Disaggregated at-sea cost comparison

The difference in at-sea costs between NMFS and sector contracts was heavily influenced by trip duration. On single-day trips, for which the sail and land dates are the same, costs associated with private contracts were comparable with those under NMFS contracts (Fig. 1). In fact, average at-sea costs on single-day trips were $26 (6.23%) higher under sector contracts ($451) than under government contracts ($425). The regression line for the cost of private contracts (adjusted coefficient of determination [adj. r^2]=0.634) crosses the line for the cost of NMFS contracts at 3 different junctures, at trip durations of around 7, 15, and 24 h. Costs under sector contracts generally exceeded costs under NMFS contracts for trips <12 h in length. For trips with durations between 12 and 18 h, costs were generally comparable. For trips >18 h in length, costs were lower under contracts negotiated by sectors.

On multiday trips, for which sail and land dates differ, costs associated with sector contracts were lower, somewhat substantially, than costs under contracts negotiated by the NMFS (Fig. 2). The average cost for multiday trips was $613 (18.01%) lower under private contracts ($2789) than under NMFS contracts ($3402). The regression line for sector contracts on multiday trips (adj. r^2=0.976) fits the data well, providing a reliable estimate of the effect that trip duration has on costs. Annual changes in cost by trip type are shown in Figure 3.

Because trips with short and long durations yielded considerably different results, it follows that cost savings from sector contracts also varied when examined across vessel characteristics (Table 5). Operators of large trawlers (≥18.3 m in length), who primarily take multiday trips, achieved an 18.54% reduction in costs under private contracts. In contrast, minimal cost savings were associated with operation of small trawlers (<18.3 m in length) and

Table 3

Estimated at-sea monitoring (ASM) costs (in millions of 2017 U.S. dollars) for all sector-enrolled vessels in the Northeast groundfish fishery for fishing years (FY) 2013–2018 under contracts negotiated by the National Marine Fisheries Service (NMFS) and under contracts negotiated by fishery management representatives for groups of groundfish vessel owners, known as *sectors*. Estimates of costs under sector contracts were calculated by applying the terms of 3 different contract years (FY2016, FY2017, and FY2018) to each ASM trip that occurred during FY2013–2018 and averaging the 3 values. Trips taken by sectors include only trips that were eligible to have an ASM observer. Note that FY2013 included only the period September 2013–April 2014 and that FY2018 included only the period May–August 2018.

				At-sea cost		Total cost	
Fishing year	No. of sector trips	No. of ASM trips	ASM coverage rate	NMFS contracts	Sector contracts (avg. FY16–18)	NMFS contracts	Sector contracts (avg. FY16–18)
2013	5549	580	10.45%	$1.06	$0.90	$1.32	$0.93
2014	8972	1616	18.01%	$2.27	$1.97	$2.83	$2.03
2015	7640	972	12.72%	$1.29	$1.13	$1.61	$1.17
2016	5112	475	9.29%	$0.83	$0.71	$1.04	$0.73
2017	5304	315	5.94%	$0.51	$0.44	$0.64	$0.46
2018	2379	114	4.79%	$0.15	$0.13	$0.19	$0.14
Total	34,956	4072	11.65%	$6.11	$5.28	$7.63	$5.46

Table 4

Total estimated at-sea monitoring (ASM) costs as percentages of operating profits (in millions of 2017 U.S. dollars) for all sector-enrolled vessels in the Northeast groundfish fishery for fishing years (FY) 2013–2018 under contracts negotiated by the National Marine Fisheries Service (NMFS) and under contracts negotiated by groups of groundfish vessel owners, known as *sectors*. Fishery management representatives for sectors negotiated contracts for FY2016–2018. Estimates of costs under sector contracts were calculated by applying the terms of 3 different contract years (FY2016, FY2017, and FY2018) to each ASM trip that occurred during FY2013–2018 and averaging the 3 values. Note that FY2013 included only the period September 2013–April 2014 and that FY2018 included only the period May 2018–August 2018.

			NMFS contracts		Sector contracts		
Fishing year	Gross revenue	Operating profit	Total cost	Cost as percentage of operating profit	Total cost	Cost as percentage of operating profit	ASM coverage rate
2013	$55.92	$37.07	$1.32	3.56%	$0.93	2.51%	10.45%
2014	$85.86	$61.96	$2.83	4.57%	$2.03	3.28%	18.01%
2015	$76.39	$59.37	$1.61	2.71%	$1.17	1.97%	12.72%
2016	$72.11	$57.62	$1.04	1.80%	$0.73	1.27%	9.29%
2017	$65.57	$51.77	$0.64	1.24%	$0.46	0.89%	5.94%
2018	$22.43	$17.68	$0.19	1.07%	$0.14	0.79%	4.79%
Total	$378.29	$285.48	$7.63	2.67%	$5.46	1.91%	11.65%

gillnetters, which are used primarily to take single-day trips. For regional landings, cost savings were more uniformly distributed. For all 3 regions, at-sea cost reductions of at least 10% were achieved with contracts negotiated by sectors. Because of a considerably higher volume of trips landing in Massachusetts than in the other 2 regions, absolute cost reductions for trips in Massachusetts greatly exceeded absolute cost reductions for trips landing in Maine and New Hampshire or in Rhode Island, Connecticut, and mid-Atlantic states.

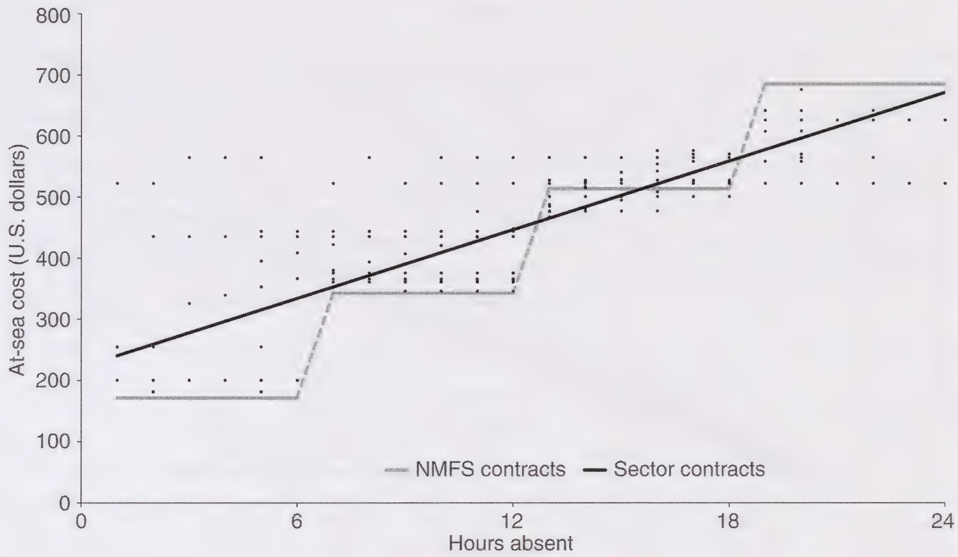

Figure 1

At-sea cost per trip (in 2017 U.S. dollars) as a function of hours absent on single-day trips in the groundfish fishery of the northeastern United States under contracts negotiated by the National Marine Fisheries Service (NMFS; gray line) and under contracts negotiated by fishery management representatives for groups of vessel owners, known as *sectors* (black line), for fishing years (FY) 2013–2018 (number of trips=2601; adjusted coefficient of determination=0.634). Each black dot indicates the estimated cost of a trip under sector contracts. Estimates of costs under sector contracts were calculated by applying the terms of 3 different contract years (FY2016, FY2017, and FY2018) to each ASM trip and averaging the 3 values. Values for costs under NMFS contracts represent actual trip costs (costs increase in 6-h increments, as indicated by the dashed parts of the gray line).

Effects on trip duration

Lastly, because our cost analysis was retrospective, we checked for changes in trip duration resulting from embedded incentives in sector contracts. In doing so, we chose to remove ASM trips made during FY2013–2015 that would have fallen under the ELM exemption had they been taken in FY2016–2018. We felt the removal of these trips was appropriate for making an accurate comparison between the 2 ASM contract periods of FY2013–2015 and FY2016–2018 because of ELM trips being considerably shorter than ASM trips. For example, ELM-exempt trips had average durations of 11 h over FY2016–2018 and ASM trips had average durations of 52 h over this time period. Private contracts do not appear to have had significantly incentivized changes in trip length when an ASM observer was on board (Table 6). Vessels in the smallest 2 categories, <13.7 m and 13.7–18.3 m, generally took single-day trips, and minimal changes in mean and median trip duration were observed for these vessels between the 2 contract periods. Vessels in the largest 2 size categories, 18.3–22.9 m and ≥22.9 m, generally took multiday trips. The mean length of ASM trips taken by vessels in the largest 2 size categories was shorter during the private contract period than during the NMFS contract period. However, this decrease was not as sharp, in absolute or percentage terms, as the reduction in mean trip duration of trips with NEFOP observers between the 2 periods. The ASM trips made by vessels in the size category of 18.3–22.9 m, in fact, experienced an increase in median trip length during the sector contract period compared with those during the NMFS contract period.

Over all vessel size categories, average ASM trip duration increased from 2.14 d under contracts negotiated by the NMFS to 2.28 d under contracts negotiated by sectors. Average length of trips with NEFOP observers decreased from 2.06 d to 1.81 d between contract periods. These results cannot be attributed to differences in coverage distribution for the 2 observer programs across vessel size categories. For both programs, coverage shifted away from the smallest vessels in the groundfish fishery (Table 6). During the NMFS contract period, 40% of (1078 of 2670) ASM trips and 46% of (867 of 1876) NEFOP trips were made on vessels <13.7 m. During the private contract period, these percentages dipped to 28% (289 of 1030 trips) and 35% (414 of 1185 trips), respectively. The share of ASM trips made by the largest vessels (≥22.9 m) increased by 8% (from 14% to 22%) over the sector contract period, but an increase of only 1% (from 12% to 13%) occurred for NEFOP trips over the same period.

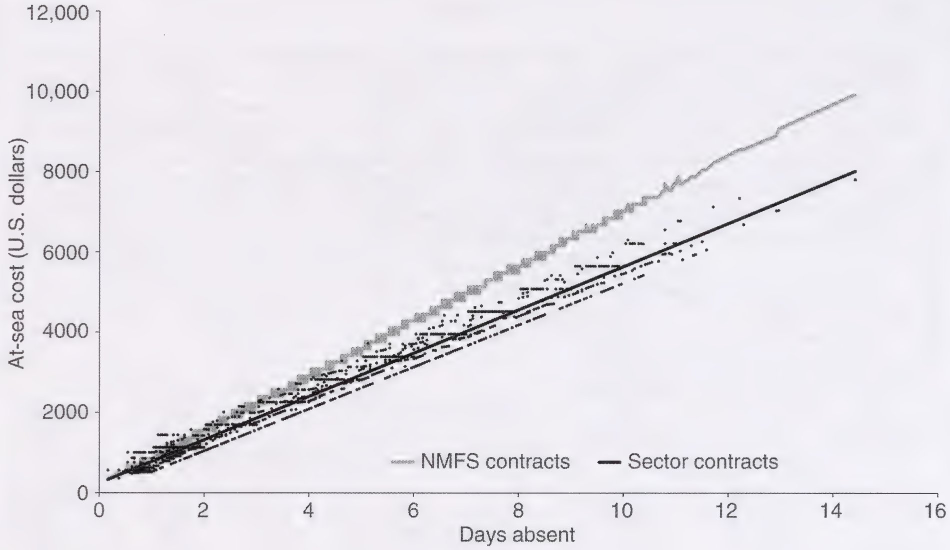

Figure 2

At-sea cost per trip (in 2017 U.S. dollars) as a function of days absent on multiday trips in the groundfish fishery of the northeastern United States under contracts negotiated by the National Marine Fisheries Service (NMFS; gray line) and under contracts negotiated by fishery management representatives for groups of vessel owners, known as *sectors* (black line), for fishing years (FY) 2013–2018 (number of trips=1471; adjusted coefficient of determination=0.976). Each black dot indicates the estimated cost of a trip under sector contracts. Estimates of costs under sector contracts were calculated by applying the terms of 3 different contract years (FY2016, FY2017, and FY2018) to each ASM trip and averaging the 3 values. Values for costs under NMFS contracts represent actual trip costs (costs increase in 6-h increments).

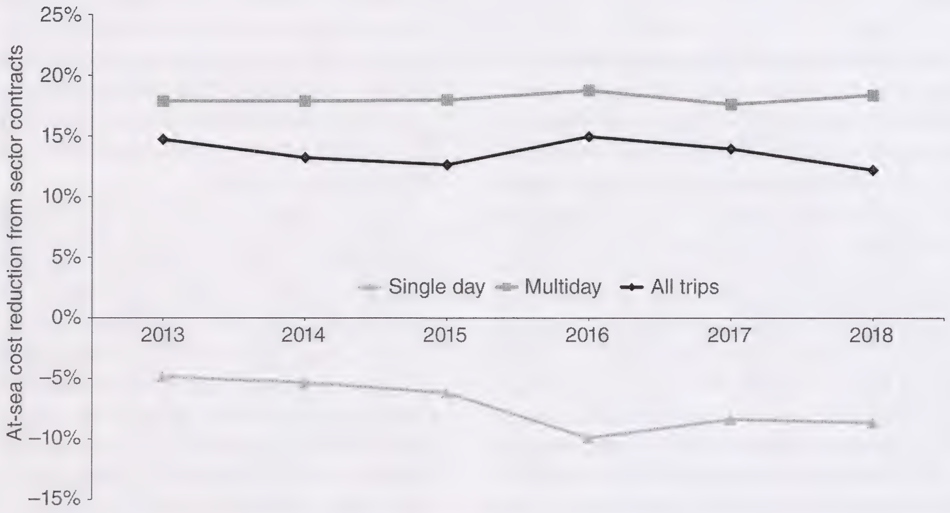

Figure 3

Estimated reductions in at-sea costs in the groundfish fishery of the northeastern United States under contracts negotiated by fishery management representatives for groups of groundfish vessel owners, known as *sectors*, compared with those under contracts negotiated by the National Marine Fisheries Service. Estimates are given for single-day (triangles), multiday (squares), and all (diamonds) trips during fishing years 2013–2018.

Table 5

Trip type and at-sea cost (in millions of 2017 U.S. dollars) by vessel type and landing region for the sector portion of the Northeast groundfish fishery over fishing years (FY) 2013–2018 under contracts negotiated by the National Marine Fisheries Service (NMFS) and under privately negotiated contracts. Fishery management representatives for groups of groundfish vessel owners, known as *sectors*, negotiated the private contracts. Estimates of costs under sector contracts were calculated by applying the terms of 3 different contract years (FY2016, FY2017, and FY2018) to each ASM trip that occurred during FY2013–2018 and averaging the 3 values. Vessel types include large trawlers ≥18.3 m (≥60 ft) in length, small trawlers <18.3 m in length, and gillnetters of all lengths (average length for gillnetters was 13.0 m). The landing regions include Connecticut (CT), Rhode Island (RI), and mid-Atlantic states (mid-Atl.), Massachusetts (MA), and Maine (ME) and New Hampshire (NH).

	No. of trips			At-sea cost		
Category	Single day	Multiday	Percentage of Multiday trips	Sector contracts	NMFS contracts	Cost reduction under sector contracts
Vessel type						
Gillnetter	1453	209	12.58%	$1.09	$1.12	2.79%
Large trawlers	249	1000	80.06%	$3.44	$4.23	18.54%
Small trawlers	945	116	10.93%	$0.65	$0.65	0.97%
Region						
CT/RI/mid-Atl.	507	119	19.01%	$0.43	$0.49	11.74%
MA	1679	998	37.28%	$4.09	$4.78	14.45%
ME/NH	542	227	29.52%	$0.76	$0.84	10.02%

Discussion

The ASM costs in the Northeast groundfish fishery were lower under private contracts than under those negotiated by the NMFS during our comparison period of September 2013–August 2018. We estimated that average at-sea costs were 14% lower over this period when applying contract terms negotiated by sectors (for FY2016–2018) than when applying average costs under NMFS contracts (for September 2013–December 2015). Aggregate reductions in costs for the at-sea component of the ASM program were driven by sectors composed primarily of vessels that took multiday trips, generally large trawlers. We found that at-sea rates for single-day trips were slightly higher under sector contracts than under NMFS contracts. Providers are likely to have lower marginal per-observed-day costs on multiday trips, perhaps because of lower associated administrative and transportation costs. Alternatively, higher costs for single-day trips under sector contracts may reflect a broad shift in fishery effort toward large vessels (≥22.9 m) (Murphy et al.[1]) and optimization of contracts by providers to cover sectors that contain large vessels. In either case, our hypothesis of lower costs under private contracts was realized, although the role of vessel heterogeneity within and between sectors did not appear to be a major factor in these cost reductions. That is, uniformly, sectors were able to negotiate lower rates than those under NMFS contracts for multiday trips but not for single-day trips.

On the demand side, the implementation of the ELM exemption (Federal Register, 2016), which started in FY2016 and continued in FY2017–2018, effectively lengthened ASM trips. Trips under ELM exemption were substantially shorter (36 h) on average than other groundfish trips that were eligible to be selected to carry an ASM observer over the course of FY2016–2018. This exemption alone likely accounted for a shift toward observer coverage on multiday trips during the sector-funded ASM period: 69% of trips covered by an ASM observer during FY2013–2015 were single-day trips. This percentage fell to 62% of trips during FY2016–2018. Other changing conditions in the fishery, such as quota allocations and quota prices, may have also contributed to this shift toward multiday trips. In any case, if sectors were aware that fewer short duration trips would be covered, they may have placed a greater focus on costs for multiday trips in contract negotiations. If the shift to sector negotiation of ASM had occurred in FY2012, as originally stipulated (Federal Register, 2010), the at-sea rates under private contracts may have looked quite different because of a higher proportion of coverage on single-day trips than on multiday trips.

When observer travel and training costs were included, the savings under private contracts were significantly larger (28%). We were unable to analyze effects of distribution for total ASM costs because we had only aggregated provider-level information on observer travel costs. Because observer travel was a small cost component, and observer training was not a separable cost to any sector, total ASM costs would have been only slightly higher than at-sea costs for any particular segment of the sector

Table 6

Duration of trips, in days and by vessel size, in the sector portion of the Northeast groundfish fishery that were observed through the at-sea monitoring (ASM) program and the Northeast Fisheries Observer Program (NEFOP). The ASM program operated under contracts negotiated by the National Marine Fisheries Service (NMFS) from September 2013 through February 2016 and under contracts negotiated by fishery management representatives for groups of groundfish vessel owners, known as *sectors*, from March 2016 through August 2018. Vessel size categories are based on length: <13.7 m (<45 ft), 13.7–18.3 m (45–60 ft), 18.3–22.9 m (60–75 ft), and ≥22.9 m (≥75 ft). The numbers of ASM and NEFOP trips (*n*) are given separately for trips that occurred during the period of NMFS-negotiated ASM contracts and for trips that occurred during the period of sector-negotiated ASM contracts. SD=standard deviation.

	ASM contract period	
Vessel size	NMFS	Sector
Vessels <13.7 m		
ASM trips (NMFS: *n*=1078; sector: *n*=289)		
Mean	0.75	0.69
Median	0.50	0.50
SD	0.96	0.95
NEFOP trips (NMFS: *n*=867; sector: *n*=414)		
Mean	0.80	0.76
Median	0.54	0.50
SD	0.90	1.03
Vessels 13.7–18.3 m		
ASM trips (NMFS: *n*=725; sector: *n*=315)		
Mean	0.93	0.83
Median	0.63	0.54
SD	1.10	1.01
NEFOP trips (NMFS: *n*=482; sector: *n*=395)		
Mean	1.10	0.86
Median	0.60	0.58
SD	1.29	1.03
Vessels 18.3–22.9 m		
ASM trips (NMFS: *n*=481; sector: *n*=196)		
Mean	3.49	3.04
Median	2.42	2.73
SD	3.05	2.51
NEFOP trips (NMFS: *n*=302; sector: *n*=221)		
Mean	4.03	3.07
Median	3.52	1.96
SD	3.13	2.83
Vessels ≥22.9 m		
ASM trips (NMFS: *n*=386; sector: *n*=230)		
Mean	6.65	5.61
Median	6.94	5.46
SD	2.65	2.54
NEFOP trips (NMFS: *n*=225; sector: *n*=155)		
Mean	6.37	5.26
Median	6.58	5.17
SD	2.76	2.53

portion of the groundfish fishery. Under NMFS contracts, observer travel and training imposed much higher costs than under private contracts. Therefore, for owners of small trawl and gill-net vessels, who experienced minimal at-sea cost reductions from sector contracts, reductions in total ASM costs were likely more substantial than at-sea cost reductions.

It is important to note that we assigned at-sea costs on a trip basis in our analysis. In actuality, no regulatory restriction currently exists on how sectors secure payment to ASM providers. Sectors may bill vessels individually for each ASM trip or estimate their aggregate ASM costs and apportion them across their membership in some other envy-free manner. The method of assigning costs is an important consideration. A payment mechanism such as the one we assumed in our study may provide an incentive for vessel operators to cut short trips with an ASM observer, although we did not find evidence of such a behavioral change following the transition to sector negotiation of ASM contracts when we compared ASM trips with NEFOP trips. Importantly, federal reimbursement of sector costs may have muted any such incentive. Intra-sector cost incidence is a critical component of the shift from government to private contracts, and one for which we currently have no data to examine.

Although sector negotiation of contracts appears to have reduced the cost of ASM services, the transition may have induced other effects to the monitoring program, either directly or indirectly, that are beyond the scope of our study. To the extent that ASM is a cost to sectors and their members, the shift to private contracts may create consistent pressure on fishery managers to reduce observer coverage. As evidence of this pressure, changes were made to the calculation of the total (ASM and NEFOP trips combined) target rate of observer coverage for the groundfish fishery in FY2016 (Federal Register, 2016), and the target rate was lowered from a range of 22–26% for FY2012–2015 to 14% for FY2016. The target rates for FY2017 and FY2018 were slightly higher (16% and 15%, respectively; NMFS[8]). Under lower observer coverage, concerns over data reliability may increase. For example, a decrease in precision of discard estimates occurred during FY2016–FY2018 from the level of precision found during FY2013–FY2015 (GARFO[9]). Evidence of changes in fishing behavior when an observer is on board, observer bias, has also been reported (NEFMC, 2019). Additionally, if compensation to the ASM observers themselves was to decline under sector contracts, employee turnover may increase and the quality of recruited monitors may decrease. Higher turnover would not only result in relatively higher observer training costs but also decrease the quality of the data collected by observers. In essence, the shift to privately negotiated contracts for ASM services presents a principal-agent problem, the effects of which are not yet well understood.

The long-term applicability of our findings to other fisheries in the United States is uncertain. In the future, other fisheries may follow the Northeast groundfish fishery in implementing additional monitoring requirements and in transitioning from government to industry payment to cover these additional costs. The trawl fishery that targets groundfish off the Pacific coast of the United States followed this general path upon implementation of individual fishing quotas, although individual vessel owners in this trawl fishery do not have the same ability to negotiate costs per sea day as sectors in the Northeast groundfish fishery (Edick[10]; Westly[11]). Our results may be applicable to the partial-observer-coverage fisheries in Alaska, some of which operate under catch shares (for a complete list of partial-coverage fisheries in Alaska, see AFSC and ARO[12]). These fisheries currently have landings fees in place to pay for observer coverage. The NMFS collects and administers the fees, which are used to pay contracting costs with a third-party provider of observers. A co-op model may potentially decrease observer costs by allowing fishing fleets to contract directly with observer providers, as is currently done in the full-observer-coverage co-op fisheries in Alaska (Figus[13]).

Given the possibility of electronic monitoring having an increasing role in at-sea coverage in U.S. fisheries, including in the Northeast groundfish fishery, it is important to mention that this technology was not part of our cost comparison. Given the large upfront cost associated with electronic monitoring (Cap Log Group[14]), a cost comparison of government and industry payment of electronic monitoring services would look quite different than the comparison we present here.

Acknowledgments

The authors would like to thank M. Grant of the Greater Atlantic Regional Fisheries Office, who was instrumental in providing information necessary for this paper. This work would not have been possible without the collective efforts of the Fisheries Sampling Branch of the Northeast Fisheries Science Center and all the men and women who go to sea as observers and at-sea monitors. We are also very grateful for the providers of at-sea monitoring for answering our inquiries.

---

[8] NMFS (National Marine Fisheries Service). 2017. NOAA Fisheries announces reimbursement rate of 60 percent for at-sea monitors in 2017. [Available from Sustain. Fish. Div., Gt. Atl. Reg. Fish. Off., Natl. Mar. Fish. Serv., 55 Great Republic Dr., Gloucester, MA 01930.]

[9] GARFO (Greater Atlantic Regional Fisheries Office). 2020. Summary of analyses conducted to determine at-sea monitoring requirements for multispecies sectors FY2020, 12 p. GARFO, Gloucester, MA. [Available from website.]

[10] Edick, D. 2019. Personal commun. Alaskan Observers, 130 Nickerson St., Unit 206, Seattle, WA 98109.

[11] Westly, E. 2019. Personal commun. Saltwater Inc., 733 N St., Anchorage, AK 99501.

[12] AFSC (Alaska Fisheries Science Center) and ARO (Alaska Regional Office). 2019. North Pacific Observer Program 2018 annual report. NOAA, Natl. Mar. Fish. Serv., Alaska Fish. Sci. Cent., AFSC Processed Rep. 2019-04, 148 p. [Available from website.]

[13] Figus, E. 2019. Personal commun. North Pacific Fishery Management Council, 1007 W. 3rd Ave., Ste. 400, Anchorage, AK 99501.

[14] Cap Log Group. 2019. Projected cost of providing electronic monitoring to 100 vessels in New England's groundfish fishery, 20 p. Report commissioned by the Nature Conservancy. [Available from website.]

Literature cited

Federal Register.

2010. Magnuson-Stevens Fishery Conservation and Management Act provisions; fisheries of the northeastern United States; Northeast (NE) multispecies fishery; amendment 16. Fed. Regist. 75:18262–18353. [Available from website.]

2016. Magnuson-Stevens Fishery Conservation and Management Act provisions; fisheries of the northeastern United States; Northeast multispecies fishery; framework adjustment 55. Fed. Regist. 81:26412–26452. [Available from website.]

2019. Magnuson-Stevens Fishery Conservation and Management Act provisions; fisheries of the northeastern United States; Northeast multispecies fishery; framework adjustment 58. Fed Regist. 84:34799–34815. [Available from website.]

NEFMC (New England Fishery Management Council).

2019. Scientific and statistical committee sub-panel peer review report for the groundfish plan: development team analyses of groundfish monitoring, 19 p. NEFMC, Newburyport, MA. [Available from website.]

National Marine
Fisheries Service
NOAA

Fishery Bulletin
established in 1881

Spencer F. Baird
First U.S. Commissioner
of Fisheries and founder
of *Fishery Bulletin*

Stress response and postrelease mortality of blacktip sharks (*Carcharhinus limbatus*) captured in shore-based and charter-boat-based recreational fisheries

D. Nick Weber (contact author)[1,2]
Bryan S. Frazier[1]
Nicholas M. Whitney[3]
James Gelsleichter[4]
Gorka Sancho[2]

Email address for contact author: d.nick.weber@gmail.com

[1] Marine Resources Research Institute
South Carolina Department of Natural Resources
217 Fort Johnson Road
Charleston, South Carolina 29412
Present address of contact author:
153 Tidal Hall
Texas A&M University—Corpus Christi
6300 Ocean Drive
Corpus Christi, Texas 78412

[2] Grice Marine Laboratory
Department of Biology
College of Charleston
205 Fort Johnson Road
Charleston, South Carolina 29412

[3] Anderson Cabot Center for Ocean Life
New England Aquarium
1 Central Wharf
Boston, Massachusetts 02110

[4] Department of Biology
University of North Florida
1 UNF Drive
Jacksonville, Florida 32224

Abstract—In the coastal waters of the southeastern United States, the blacktip shark (*Carcharhinus limbatus*) is targeted by recreational anglers and is currently one of the most often captured large coastal shark species. We estimated postrelease mortality (PRM) rates for blacktip sharks captured on rod and reel by shore-based and charter-boat-based fishermen by using acoustic transmitters (number of sharks=81). Additionally, 24 blacktip sharks were tagged with pop-off satellite archival tags (PSATs) to validate the survivorship obtained through analysis of data from the acoustic transmitters. The stress response associated with both recreational capture methods was quantified by using numerous blood chemistry characteristics. Overall, 18.5% of blacktip sharks died postrelease (17.1% and 20.0% of those captured from shore and from charter boats, respectively). The results of survivorship analysis based on data from transmitters are consistent with results inferred from data from PSATs, supporting our use of acoustic transmitters to assess PRM in blacktip sharks. Fight time had a significant effect on blood pH, lactate, hematocrit, potassium, and glucose for sharks caught from shore but only on lactate for sharks caught from charter boats. In general, the blood chemistry characteristics assessed were poor predictors of PRM. Fifty percent of foul-hooked sharks (i.e., sharks hooked anywhere but the jaw) died postrelease, indicating the importance of the effect of hook placement on PRM.

In the late 1900s, shark populations in the western North Atlantic Ocean declined drastically in size (Musick et al., 1993), because of overexploitation and sharks being captured as bycatch in commercial fisheries (Bonfil, 1994; Rose, 1996). In an effort to ensure the sustainability of shark fisheries, a variety of national and international management measures, including mandated release of imperiled species, were introduced (Ellis et al., 2017). These management measures have since been augmented by an increasing emphasis on the catch and release of sharks by recreational anglers (Bartholomew and Bohnsack, 2005; Skomal, 2007), and the release of captured sharks by both commercial and recreational anglers has become a common practice (Press et al., 2016; Ellis et al., 2017). Although catch and release is broadly advocated to minimize effects on fish stocks, postrelease mortality (PRM) may still occur as a result of the physiological stress or physical injury of capture (Bartholomew and Bohnsack, 2005; Cooke and Schramm, 2007). Therefore, there is an increasing interest in understanding the conditions that bring about PRM, as well as in how to minimize PRM rates (Cooke and Cowx, 2004; Gallagher et al., 2014).

Postrelease mortality rates vary widely among shark species (Ellis et al., 2017) and depend on factors such as gear type, duration of capture, respiratory mode (Dapp et al., 2016), and aerobic scope (Priede, 1985; Korsmeyer et al., 1996; Talwar et al., 2017). Traditionally, PRM rates have been assessed by using pop-off satellite archival tags

Manuscript submitted 20 February 2020.
Manuscript accepted 25 September 2020.
Fish. Bull. 118:297–314 (2020).
Online publication date: 9 October 2020.
doi: 10.7755/FB.118.3.8

The views and opinions expressed or implied in this article are those of the author (or authors) and do not necessarily reflect the position of the National Marine Fisheries Service, NOAA.

(PSATs) (e.g., Heberer et al., 2010; French et al., 2015), but the cost of such tags often precludes the use of large sample sizes (Donaldson et al., 2008), making accurate assessments of PRM for a species difficult. To circumvent this issue, the use of acoustic telemetry to assess PRM has been investigated in recent years (Kneebone et al., 2013; Kilfoil et al., 2017). Results of previous research indicate that acoustic transmitters can be used to assess PRM in the presence of acoustic receiver arrays (Kneebone et al., 2013; Kilfoil et al., 2017). Because the number of acoustic receivers deployed along the eastern coast of the United States continues to grow (Kneebone et al., 2013), the applicability and effectiveness of this method will likely increase. The smaller size of acoustic transmitters, compared with the size of the electronic tags traditionally used to assess PRM (e.g., PSATs), could reduce any potential effects of the tag on a shark's behavior postrelease. Additionally, the lower cost of acoustic transmitters could allow the assessment of larger sample sizes across a wider range of conditions, providing more robust estimates of PRM.

Efforts have been made to link PRM with perturbations in blood chemistry caused by the stress of capture (Whitney et al., 2017). The stress experienced by captured sharks has traditionally been quantified by an assessment of the acid-base status of blood (e.g., Mandelman and Skomal, 2009), based on the notion that stress causes a decrease in blood pH, known as acidemia, due to both metabolic and respiratory acidoses (Skomal, 2007). Additionally, stress-related cellular fluid shifts, which can result in haemoconcentration and disruptions to ionic and osmotic homeostasis (Wood, 1991; Skomal and Mandelman, 2012), have been quantified through changes in plasma electrolyte concentrations (e.g., Marshall et al., 2012; French et al., 2015). Because interspecific differences in responses to capture stress may be linked to the metabolism and physiology of the species in question (Skomal and Mandelman, 2012), analyzing a suite of blood chemistry characteristics may allow for a better understanding of the implications of capture on subsequent mortality events (Skomal, 2007; French et al., 2015). Moreover, when blood chemistry measurements are coupled with estimates of PRM, insights into the causes of physiological stress and mortality, as well as into potential mitigation measures, can be gained (Skomal, 2007; Mandelman and Skomal, 2009).

The blacktip shark (*Carcharhinus limbatus*) is a relatively large coastal species with a circumglobal distribution in temperate coastal waters (Compagno, 1984; Castro, 2011). In the western North Atlantic Ocean, blacktip sharks migrate seasonally, inhabiting the nearshore waters of Georgia, South Carolina, and North Carolina during the summer months and moving southward to southeastern Florida during the winter months (Castro, 1996; Kajiura and Tellman, 2016). The coastal distribution of blacktip sharks, combined with the seasonal predictability of their center of abundance (Kajiura and Tellman, 2016), makes them easily accessible for both commercial and recreational fisheries. Consequently, the blacktip shark is currently one of the most often landed large coastal shark species (NMFS, 2019). Compared with other large coastal sharks, blacktip sharks have an intermediate life history, defined by the fact that they have a relatively low age at maturity (4–7 years; Killam and Parsons, 1989), reproduce biennially (Castro, 1996), and have an average of 4–6 pups per reproductive cycle (Bigelow and Schroeder, 1948). Collectively, proximity to the coast, intermediate life history characteristics, and exposure to high commercial and recreational fishing pressure make the blacktip shark particularly sensitive to overfishing.

Few studies have investigated the effects of capture on the blacktip shark, but blood chemistry characteristics measured in blacktip sharks caught on drumlines and longlines indicate that the magnitude of the stress response in this species is greater than that in other carcharhinid species (Mandelman and Skomal, 2009; Marshall et al., 2012; Gallagher et al., 2014). Data on acid-base blood chemistry obtained from blacktip sharks caught on longlines indicate that this species may have a strictly respiratory response to capture because the observed acidosis was driven by increases in pCO_2 (Mandelman and Skomal, 2009). Consequently, it has been suggested that blacktip sharks could lack the mechanisms (e.g., splenic red blood cell ejection and red blood cell swelling through Na^+—H^+ exchangers; Nikinmaa, 1992; Brill et al., 2008) responsible for maintaining or increasing oxygen delivery during strenuous activity (Mandelman and Skomal, 2009). Although the results of this research indicate that blacktip sharks may be particularly sensitive to the stress associated with capture, Whitney et al. (2017) found a relatively low rate of PRM in the recreational fishery for blacktip sharks in the Gulf of Mexico. Additional data are needed on both the physical and physiological effects of recreational rod-and-reel capture on the blacktip shark, and how these effects influence PRM.

Recreational fishing is increasing in popularity worldwide (Arlinghaus and Cooke, 2009; Press et al., 2016). In particular, a specialized method of fishing that targets large coastal sharks from beaches, known as shore-based or land-based shark angling, has been receiving increasing attention in terms of management and conservation in recent years (Ajemian et al., 2016; Shiffman et al., 2017). The Florida Fish and Wildlife Conservation Commission recently formally defined shore-based shark fishing and instituted a mandatory shore-based shark fishing permit in response to perceived issues with handling methods and mortality of captured sharks (Shiffman et al., 2017). Because shore-based anglers typically bring captured sharks onto the beach for hook removal and photographs, sharks caught from the shore may be subject to increased handling stress and increased exposure to air, reducing the shark's ability to breathe (Casselman[1]). However, shore-based anglers often fish at night and on deserted beaches, and there are limited data available on their fishing and handling techniques or on the effects on the survival of released sharks.

---

[1] Casselman, S. J. 2005. Catch-and-release angling: a review with guidelines for proper fish handling practices, 26 p. Fish Wildl. Branch, Ontario Minist. Nat. Resour., Peterborough, Canada. [Available from website.]

Given the attention that recreational shore-based shark fishing has been receiving (Ajemian et al., 2016; Shiffman et al., 2017), and an increased emphasis on catch-and-release angling (Bartholomew and Bohnsack, 2005), the determination of gear- and species-specific PRM rates is critical to the effective management of shark species. Through collaboration with recreational anglers, in this study we assessed PRM rates of blacktip sharks captured and released in both the shore-based and charter-boat-based recreational fisheries and quantified the physiological stress response associated with both recreational capture methods.

Materials and methods

Research was completed under the South Carolina Code of Law Section 50-5-20[2] that authorizes the South Carolina Department of Natural Resources to conduct research in state waters. Research was conducted in accordance with the College of Charleston Institutional Animal Care and Use Committee (IACUC) through protocol no. IACUC-2017-007.

Sampling location and design

Blacktip sharks were caught with rod and reel by recreational anglers from the shore (i.e., beach) and from charter fishing boats. All fishing from charter boats was conducted by the clients who hired the charter boat; therefore, a wide range of angler experience was sampled. Anglers used their personal fishing equipment, which varied in size and strength, and no input was provided by the authors on the fishing equipment (e.g., rod-and-reel type and size or hook type and size) or capture techniques used. Sampling was conducted from May through October 2017 and from February through October 2018, in the coastal waters of South Carolina and Florida, at locations chosen by participating anglers (Fig. 1, A and B). During each angling trip, reel type (i.e., conventional level wind versus spinning), hook type (circle versus J), and sea-surface temperature were recorded.

Once an angler hooked a shark, the *fight time*, defined as the time from the initial strike until the time the shark was landed and secured by anglers, was recorded to the nearest second. Once secured, the shark went through the sampling procedure in the state that the angler handled it (e.g., sharks caught from charter boats were sampled either on board the boat or in the water, depending on whether or not the charter captain decided to bring the shark on board for photographs or hook removal). All sharks caught by shore-based anglers were brought out of the water and onto the beach. Sharks were then sampled while the recreational anglers completed their routine (which often included hook removal, measurement, and photographs), to minimize any increase in handling time due to the sampling procedure. Blood was drawn through caudal venipuncture immediately after the shark was secured, a tag was or tags were applied, fork length was measured (in centimeters), and sex was determined. Phlebotomies were performed through caudal venipuncture to ensure that blood sampling was quick, efficient, and minimally invasive (Lawrence et al., 2020).

Once the sampling procedure was complete, anglers were responsible for releasing the shark. The *handling time*, defined as the time from when the shark was initially secured to the release of the shark, was recorded to the nearest second. Upon release, the condition of the shark was assigned to 1 of 5 categories, ranging from condition 1 (excellent) to condition 5 (moribund), on the basis of the shark's behavior at release (Table 1). If the anglers decided to revive the shark (i.e., hold the shark in the water until they deemed it strong enough for release), the *revival time* was recorded. Hook status was recorded as removed or retained, and hook location was recorded. The authors provided no input to the anglers regarding hook removal, and some anglers chose to leave hooks that could not be easily removed.

Blood chemistry

Blood samples (3 mL) were drawn by using 18-gauge, sterilized needles and heparin-rinsed syringes, and samples were immediately injected into 10-mL vacutainers that contained sodium heparin. To avoid compromising accuracy of blood gas analysis after phlebotomy (Whitney et al., 2017), a subsample of whole blood (90 µL) was immediately (within 30 s) analyzed for pH and lactate by using an i-STAT[3] portable blood analyzer (Zoetis Inc., Parsippany-Troy Hills, NJ) with a CG4+ cartridge (Zoetis Inc.). This analyzer has been used in prior field studies on elasmobranch species (e.g., Mandelman and Skomal, 2009; Brooks et al., 2012; Gallagher et al., 2014), and the relative accuracy of measurements of pH and lactate in ectothermic sharks has been validated (Gallagher et al., 2010; Harter et al., 2015). Measurements of blood pH were temperature corrected to sea-surface temperatures at the locations of capture by using the following equation:

$$pH_{TC} = pH_{M} - 0.011(T - 37),$$

where pH_{TC} = temperature-corrected pH values;
pH_{M} = measured pH values; and
T = sea-surface temperatures

(Mandelman and Skomal, 2009; Gallagher et al., 2010; Brooks et al., 2012; Kneebone et al., 2013; Gallagher et al., 2014; Whitney et al., 2017). All pH values subsequently reported herein were temperature corrected in this manner.

---

[2] Jurisdiction of Department of Natural Resources, S.C. Code § 50-5-20 (2000). [Available from website.]

[3] Mention of trade names or commercial companies is for identification purposes only and does not imply endorsement by the National Marine Fisheries Service, NOAA.

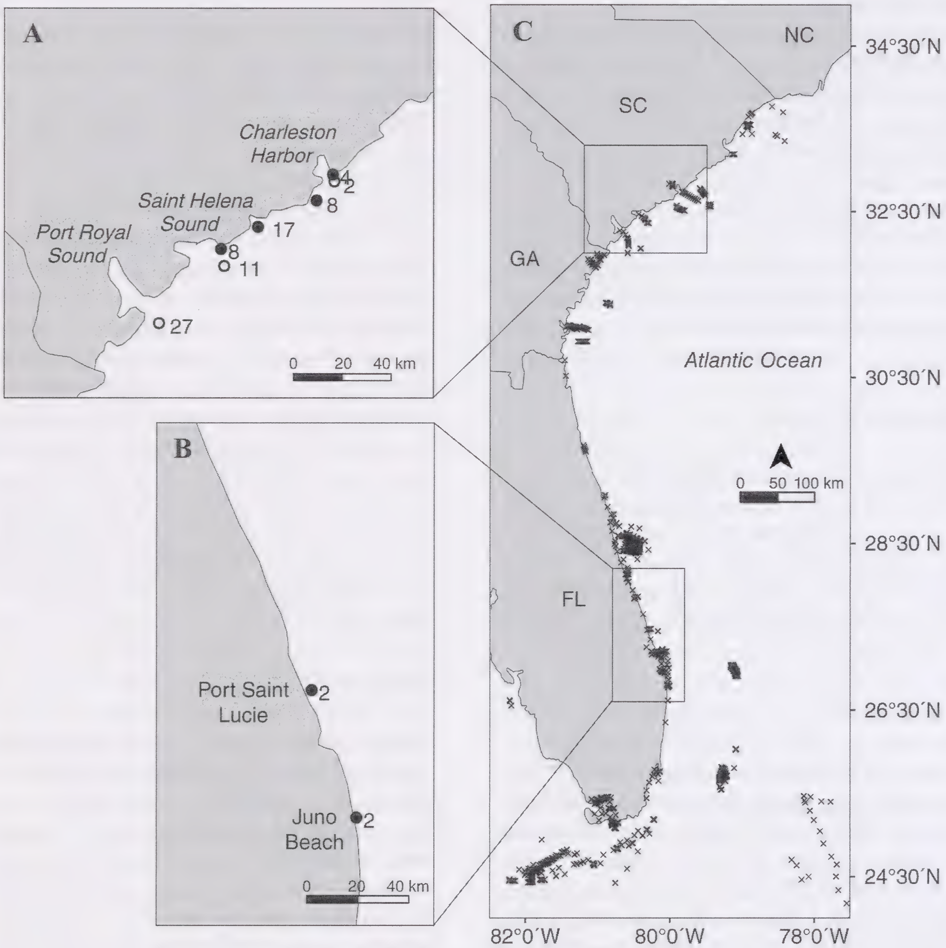

Figure 1

Maps showing the sites where blacktip sharks (*Carcharhinus limbatus*) were caught and tagged off the coasts of (**A**) South Carolina and (**B**) Florida from May through October 2017 and from February through October 2018 and (**C**) locations of acoustic receivers present along the southeastern coast of the United States. Open circles indicate sites where sharks were caught from charter boats, and solid circles indicate sites where sharks were caught from shore. The numerals next to circles indicate the number of blacktip sharks tagged at each sampling site.

A separate subsample of whole blood (0.2 mL) was simultaneously placed on ice (within 30 s) for hematocrit analysis, which was completed within 4 h of capture (Manire et al., 2001). At the time of hematocrit analysis, whole blood samples (3 samples per shark) were transferred into microcapillary tubes and centrifuged (centrifuge, Vernitron Medical Products Inc., South Hackensack, NJ) for 5 min at 10,000 rpm (10,062 × gravity). Hematocrit was determined as the percentage of total blood volume composed of red blood cells, calculated by using an EZ Reader Microhematocrit Card (LW Scientific Inc., Lawrenceville, GA).

The remaining whole blood was centrifuged (E8 Portafuge, LW Scientific Inc.) for 5 min at 3500 rpm (1534 × gravity), to separate the plasma and the red blood cells. Three subsamples of plasma (each 0.5 mL) were frozen immediately in liquid nitrogen and, subsequently, stored at −80°C. At the time of plasma electrolyte analysis, plasma samples were thawed and diluted with deionized water (dH_2O) at a plasma-to-dH_2O ratio of 2:3, and approximately 55 μL of the diluted samples was injected into a Critical Care Xpress benchtop analyzer (CCX, Nova Biomedical, Waltham, MA) to quantify levels of Na^+, Cl^-, K^+, Ca^{2+}, Mg^{2+}, and glucose. All concentrations were within the detection limits of the instrument used to measure them.

Postrelease mortality

Blacktip sharks were tagged with V16-4H acoustic transmitters (Vemco, Bedford, Canada) that measured 18.2 by

Table 1

Number of tagged blacktip sharks (*Carcharhinus limbatus*) assigned to categories of release condition on the basis of behavior at the time of release. Blacktip sharks were caught from shore (number of samples [*n*]=41) and from charter boats (*n*=40), tagged, and then released in coastal waters of South Carolina and Florida between May and October 2017 and between February and October 2018.

Condition category	Issues observed and resulting diagnosis	Capture method	
		Shore	Charter
1	Excellent: rapidly swam with no signs of distress	10	28
2	Good: stressed, swam away but appeared slow or disoriented	14	10
3	Fair: swam laboriously or had signs of physical trauma	10	0
4	Poor: attempted to swim and had potentially lethal physical trauma (e.g., excessive bleeding or deep hooking)	7	2
5	Moribund: made no effort to swim	0	0

88 mm, had a 30-s nominal delay in transmission rate, and were deployed in an external case. The tagging was accomplished by threading monofilament through a hole drilled into the radial musculature at the base of the first dorsal fin and crimping the monofilament together behind the dorsal fin. This technique of using an external attachment allowed handling times to be short and, therefore, minimized any bias introduced by the tagging procedure (Kilfoil et al., 2017). Survivorship was assessed by passively monitoring sharks following release and examining movements of sharks among fixed acoustic receivers deployed along the southeastern coast of the United States as part of the Atlantic Cooperative Telemetry (ACT) and FACT Networks (Fig. 1C).

To identify and remove false detections potentially created by collisions of acoustic transmitters (Heupel et al., 2006), the full detection database was filtered by using the glatos package (vers. 0.4.2; Holbrook et al., 2020), which flags false detections on the basis of the "short-interval" criteria described by Pincock[4], in the statistical program R (vers. 3.5.1; R Core Team, 2018). Specifically, detections isolated on a single receiver for more than 30 times the nominal delay of the transmitter (i.e., 15 min) were considered to be false and were removed. Because most mortalities associated with a capture event occur within 12 h of release (Marshall et al., 2015; Talwar et al., 2017; Whitney et al., 2017), sharks that were detected multiple times by an acoustic receiver more than 10 d postrelease were considered to have survived the capture event. Moreover, because tags that are ingested during predation events are typically regurgitated within approximately 8 d of ingestion (Kerstetter et al., 2004), we assumed survival only for individuals detected more than 10 d postrelease to account for possible capture-related predation events (i.e., acoustic detections recorded <10 d postrelease could represent movements of the transmitter consumer rather than the target individual).

To validate the data obtained from the acoustic transmitters and used for survivorship analysis, a subset of sharks were also tagged with PSATs (PSATLife, Lotek Wireless Inc., Newmarket, Canada). The PSATs (40 × 125 mm) are designed for monitoring postrelease survival and were programmed to record pressure, external temperature, and light intensity every 10 s over a 28-d deployment. If the PSAT was not recovered, summary data were obtained from PSATs through the use of satellite-derived pressure-temperature profiles (means for 5-min periods). Recovery of PSATs allowed more detailed analysis of the entire archived data set, which included pressure, external temperature, and light intensity measured every 10 s. The PSATs were programmed to release prematurely if pressure values remained constant (±50,000 Pa) over a 3-d period, a consistency in pressure values that would be observed in data from a tag on a dead shark on the ocean floor (Heberer et al., 2010). The PSATs were attached in the same way as the acoustic transmitters, by threading monofilament through a hole drilled into the radial musculature at the base of the first dorsal fin. Survival of sharks tagged with PSATs was inferred by assessing the pressure, external temperature, and light intensity profiles, following protocols previously used to infer mortality from PSAT data records (Heberer et al., 2010).

Data analysis

Postrelease mortality rates were calculated as the percentage of the total number of tagged individuals that either died after release (as indicated by PSAT data) or were assumed to have died as a result of capture (because they were not detected by an acoustic receiver more than 10 d after release). For individuals whose PSAT was shed <10 d postrelease, acoustic telemetry data were used to verify survivorship. We used the Clopper–Pearson interval to calculate 95% confidence intervals (CIs) for mortality rates. Linear regressions were used to determine if fight time (i.e., time on the line) had an effect on blood chemistry characteristics. Analyses of covariance (ANCOVA) were used to determine if blood chemistry characteristics differed between the 2 recreational capture methods, capture from shore and capture from charter boats, to account for extraneous variability due to differences in fight time between capture methods.

---

[4] Pincock, D. G. 2012. False detections: what they are and how to remove them from detection data. AMIRIX Document DOC-004691, vers. 03, 10 p. [Available from website.]

To predict PRM by using the measured blood chemistry characteristics, generalized linear models (GLMs) with a binomial probability distribution and a logit link function were fitted to the data for all sharks combined (number of sharks [n]=81) and then separately to data for sharks caught from shore (n=41) and to data for sharks caught from charter boats (n=40) (Schlenker et al., 2016; Talwar et al., 2017). Before constructing the GLMs, principal components analyses were performed to examine potential correlations between explanatory variables and to reduce the number of explanatory variables included in the GLMs (Suppl. Fig. 1) (online only). The full models for all sharks combined and for sharks caught from shore described the relationships between PRM as a binary response variable and 4 potential explanatory variables, including pH, K^+, Na^+, and glucose. The full model for sharks caught from charter boats included pH, K^+, glucose, and hematocrit as variables. Nonsignificant factors were removed in backward stepwise fashion, starting with the least significant factor and evaluating the increases in deviance and in the Akaike information criterion (AIC) (Akaike, 1973) with each removal (Talwar et al., 2017). The model with the fewest number of explanatory variables and lowest AIC was considered the best-fit model.

To predict PRM with the observed capture characteristics, GLMs were used to describe the relationship between PRM as a binary response variable and water temperature, fight time, handling time, hook location (*foul-hooked*, i.e., hooked anywhere but the jaw, versus not foul-hooked), release condition, and capture method (from shore versus from charter boat). Because the majority of sharks caught from shore were caught with spinning reels (76%) and the majority of sharks caught from charter boats were caught with conventional level-wind reels (85%), reel type was omitted from the GLM. As previously described, GLMs were fitted to the data for all sharks combined (n=81) and then separately to data for sharks caught from shore (n=41) and to data for sharks caught from charter boats (n=40). The best-fit model was again selected in a backward stepwise fashion and had the fewest number of explanatory variables and lowest AIC.

Fisher's exact tests were used to test the null hypothesis that the distribution of survivors and mortalities was equal across both hook locations and release conditions. All analyses were conducted by using R, and all graphs were created in RStudio (vers. 1.1.456; RStudio, Boston, MA). The level of significance for all tests was 0.05.

Results

Capture characteristics

A total of 81 blacktip sharks were caught and tagged with acoustic transmitters (from shore: n=41; from charter boats: n=40). A subset of those individuals (shore: n=12; charter boats: n=12) were also tagged with PSATs. There were no significant differences in fork length, fight time, handling time, or water temperature between recreational capture methods (Table 2). Additionally, there was no difference in fight time between reel types. All participating recreational anglers chose to use circle hooks, and hook locations were as follows: jaw, including corner, bottom, and top jaw (n=75); basihyal (n=3); gut (n=1); throat (n=1); and tail (n=1). Any shark not hooked somewhere in the jaw was considered to be foul-hooked in all subsequent analyses. Anglers chose to remove the hook in all but 3 instances (corner jaw: n=1; basihyal: n=1; gut: n=1).

Observed postrelease mortality

Fifteen blacktip sharks (shore: n=7; charter boats: n=8) died within 10 d of being released by recreational anglers, resulting in postrelease mortality rates of 17.1% (95% CI: 7.2–32.1) for sharks caught from shore and 20.0% (95% CI: 9.1–35.6) for sharks caught from charter boats. No immediate mortalities were observed, with all individuals swimming away at the time of release. Only 4 of the 81 tagged sharks were revived by anglers before being released, and revival times ranged from 1 to 4 min. Six of the 15 sharks considered to have died after release were assigned release conditions of 3 (fair: n=2) or 4 (poor: n=4), either because of signs of physical injury or trauma (e.g., excessive bleeding from the hook location) or because of a complete lack of movement during the handling procedure and difficulty swimming postrelease. Additionally, of the sharks considered to have died, one was hooked in the tail and one was hooked in the jaw but with its tail wrapped in the fishing line. Both individuals were reeled in backward, with fight times (6 min 35 s and 8 min 57 s, respectively) exceeding the average fight time observed throughout the study (4 min 55 s [standard deviation (SD) 2 min 27 s]). The 7 remaining sharks that died had no signs of injury or trauma and were assigned release conditions of 1 (excellent: n=6) or 2 (good: n=1).

Five of the 15 sharks that died were tagged with both PSATs and acoustic transmitters (shore: n=3; charter boats: n=2; Table 3); whereas, the mortalities of the other 10 sharks were confirmed with acoustic data only. Data obtained from the PSATs attached to these sharks indicate that 2 PSATs were ingested within 6 h of being deployed. Shark 9 was actively swimming when its PSAT was ingested 6 h postrelease (Fig. 2A). This PSAT recorded fluctuating pressure (0–97,200 Pa) and light intensity (93–384) for the 6 h prior to ingestion, variations that are consistent with vertical movements in the water column during daytime hours. Subsequent to its ingestion, the tag provided data that indicate darkness for 3 d followed by a

Table 2

Capture characteristics, blood chemistry characteristics, and postrelease mortality rates for blacktip sharks (*Carcharhinus limbatus*) caught with rod and reel by recreational anglers from shore and from charter boats in the coastal waters of South Carolina and Florida between May and October 2017 and between February and October 2018. Mean values are provided with standard deviations in parentheses. Once caught, sharks were tagged and measured, and blood samples were taken from them. Upon release, the condition of sharks was assessed (see Table 1). pH_{TC}=temperature-corrected blood pH.

	Capture characteristics							
Capture method	No. tagged	Fight time (min)	Handling time (min)	Water temp. (°C)	Proportion female (%)	Fork length (cm)	Release condition	Postrelease mortality (%)
Charter	40	4.75 (2.02)	3.55 (1.22)	26.9 (2.5)	71	124.2 (19.2)	1.4 (0.7)	20.0
Shore	41	5.09 (2.82)	3.33 (1.16)	27.7 (2.6)	77	124.5 (24.4)	2.4 (1.0)	17.1

	Acid-base status			Plasma electrolytes and metabolites					
Capture method	pH_{TC}	Lactate (mmol/L)	Hematocrit (%)	Na^+ (mmol/L)	Cl^- (mmol/L)	K^+ (mmol/L)	Ca^{2+} (mmol/L)	Mg^{2+} (mmol/L)	Glucose (mg/dL)
Charter	7.34 (0.08)	2.01 (0.87)	25.2 (2.1)	273.1 (9.2)	267.3 (7.3)	5.7 (0.7)	2.8 (0.1)	1.1 (0.2)	56.3 (5.9)
Shore	7.33 (0.10)	1.74 (1.07)	24.1 (3.0)	273.4 (7.4)	266.5 (6.0)	5.3 (0.7)	2.7 (0.2)	1.1 (0.3)	58.3 (4.9)

Table 3

Characteristics of the capture of blacktip sharks (*Carcharhinus limbatus*) tagged with both pop-off satellite archival tags and acoustic transmitters in the coastal waters of South Carolina and Florida between May and October 2017 and between February and October 2018. Upon release, the condition of sharks was assessed (see Table 1). Asterisks (*) indicate sharks that, through the use of data from tags, were determined to have died after release.

Shark ID no.	Capture method	Reel type	Fight time (min)	Handling time (min)	Hook location	Bleeding (yes or no)	Release condition
7	Shore	Spinning	6.83	2.58	Jaw	N	3
9*	Shore	Conventional	4.38	3.75	Jaw	Y	3
14	Charter	Conventional	7.78	4.83	Jaw	N	2
17	Charter	Conventional	4.50	4.10	Jaw	N	1
22	Charter	Spinning	5.12	2.80	Jaw	N	1
27	Shore	Spinning	8.90	6.68	Jaw	N	4
28	Shore	Conventional	9.53	3.78	Jaw	N	3
30*	Shore	Spinning	7.00	3.07	Jaw	N	1
31	Shore	Spinning	5.82	2.72	Jaw	N	2
34	Shore	Spinning	14.07	2.83	Jaw	N	4
40	Charter	Conventional	3.13	2.80	Jaw	N	1
43*	Charter	Conventional	4.02	3.17	Throat	Y	4
44	Charter	Conventional	6.38	3.48	Jaw	N	2
52	Shore	Spinning	5.62	2.78	Jaw	N	2
55	Shore	Spinning	7.92	4.82	Jaw	N	2
58*	Shore	Spinning	6.58	4.30	Tail	N	4
59	Shore	Spinning	3.40	4.05	Jaw	N	2
61	Charter	Conventional	3.92	4.70	Jaw	N	2
63	Shore	Conventional	8.45	3.78	Gut	N	4
64	Charter	Conventional	6.63	3.95	Jaw	N	1
67	Charter	Conventional	6.38	2.73	Jaw	N	1
68	Charter	Conventional	3.37	2.92	Jaw	N	2
75	Charter	Conventional	5.37	5.68	Jaw	N	1
77*	Charter	Conventional	8.95	4.88	Jaw	N	2

return to a cyclical pattern of day and night (Fig. 2A). Brief increases in light intensity during the ingestion period may indicate partial regurgitation of the PSAT. Shark 43, on the other hand, sank to the bottom immediately after release, where it remained for 5 h before the tag was ingested (Fig. 2B). The data from this PSAT indicate little variation in pressure during the 5-h period prior to ingestion (198,400–215,900 Pa) and a complete lack of light intensity (98–109), values consistent with the lack of movement of a dead shark lying on the seafloor. Subsequent to its ingestion, the PSAT attached to shark 43 provided data that indicate darkness for 4.5 d followed by a return to a cyclical pattern of day and night, similar to what was observed for shark 9 (Fig. 2B). Because both predation events occurred within 6 h of capture, they were attributed to capture and included in the estimates of mortality.

Of the 24 PSATs deployed, all but 2 PSATs sent data to the Argos satellite system, and 12 PSATs were physically recovered—including 1 of the 2 PSATs that did not transmit data. Excluding the PSATs deployed on the 5 sharks that died, 12 PSATs detached prematurely and 6 PSATs were retained for the entire 28-d deployment. Tag retention periods ranged from 17 min to 28 d (mean: 11.8 d [SD 10.6]). The PSAT pressure profiles indicate that none of the premature detachments resulted from tags remaining at a constant depth; when a PSAT stays at the same depth, the burning of the release pin is triggered. Therefore, the 2 most plausible explanations for the premature detachments are that the anchors were pulled out of the dorsal musculature (e.g., as a result of tag consumption by a predator) or that the tethers broke. Two of the 12 PSATs that were physically recovered, both of which detached prematurely, had numerous bite marks on them, indicating that the tags were bitten off. Survival for individuals whose PSATs were shed prematurely (i.e., <10 d after release) was confirmed by using acoustic telemetry (Table 4).

The data obtained from the acoustic transmitters associated with the 5 double-tagged sharks that died indicate the same survivorship outcomes as the data from the PSATs (Fig. 3). None of the acoustic transmitters that were attached to sharks determined to be dead by using data from PSATs were detected on an acoustic receiver more than 5 d postrelease (Table 4). Both of the acoustic transmitters associated with the PSATs that were ingested were detected on acoustic receivers during the period that the PSAT was inside of the stomach of the predator or scavenger (the PSAT-ingestion period was determined by a lack of light intensity, relative stability of temperature, and continuation of vertical movements indicated by changes in pressure). However, the acoustic transmitters were not detected following regurgitation of the PSATs (within 5 d of ingestion), and the last acoustic detections for both tags were recorded within 9 km (5 nautical miles)

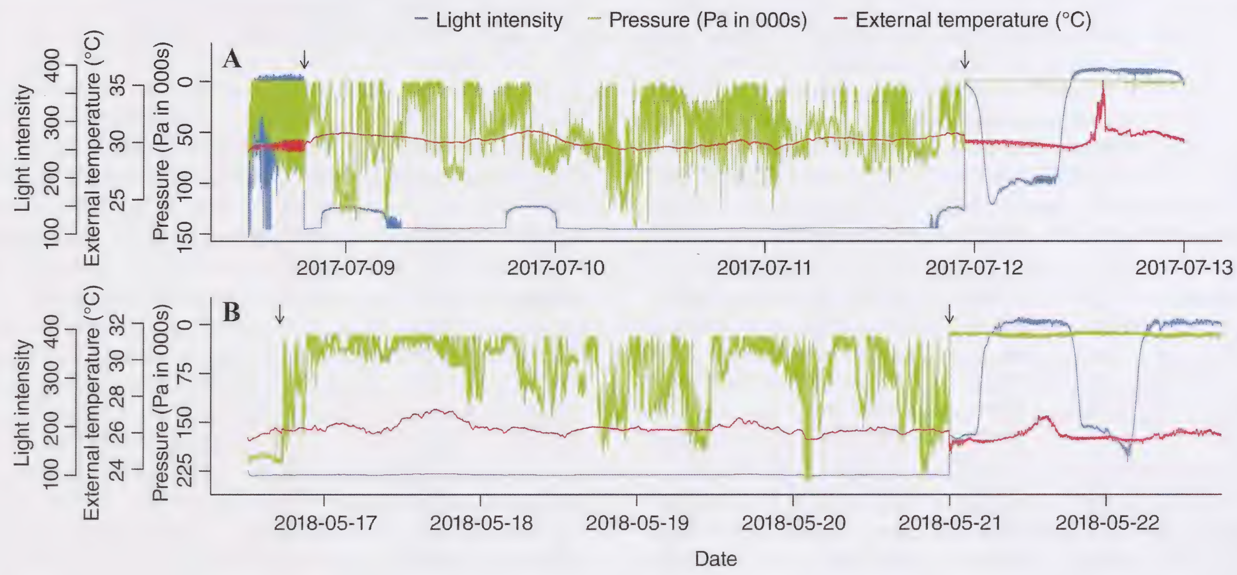

Figure 2

Pressure, external temperature, and light intensity profiles from pop-off satellite archival tags (PSATs) attached to 2 blacktip sharks (*Carcharhinus limbatus*) during (**A**) July 2017 (shark 9) and (**B**) May 2018 (shark 43) in the coastal waters of South Carolina and Florida, both showing a period of ingestion by another shark. Green, red, and blue lines indicate pressure, external temperature, and light intensity, respectively. Shark 9 was actively swimming at the time of ingestion, 6 h after release. Shark 43 sank to the ocean floor immediately following release, and it remained there for 5 h prior to ingestion. Both PSATs were regurgitated within 5 d of ingestion. The first black arrow in each panel denotes the time of assumed predation, and the second black arrow denotes the time of assumed regurgitation.

Table 4

Summary of results from survivorship analysis based on data from pop-off satellite archival tags (PSATs) and acoustic transmitters deployed on blacktip sharks (*Carcharhinus limbatus*) in the coastal waters of South Carolina and Florida between May and October 2017 and between February and October 2018. Asterisks (*) indicate sharks that were determined to have died after release. The dagger (†) indicates an individual whose PSAT never transmitted data to the Argos satellite system and was never recovered; consequently, data were not available (NA) for this individual.

		Acoustic transmitter characteristics		
Shark ID no.	Duration of PSAT deployment (d)	No. of detections while PSAT attached (no. of unique receivers)	No. of detections after PSAT detached (no. of unique receivers)	No. of days between dates of tagging and last detection
7	8.29	0 (0)	1163 (21)	301
9*	3.42	150 (5)	0 (0)	3
14	10.92	44 (4)	3296 (52)	413
17	4.63	5 (1)	1271 (12)	206
22	4.21	21 (5)	3022 (28)	213
27	1.17	21 (1)	309 (15)	219
28†	NA	NA	9368 (104)	637
30*	0.01	0 (0)	0 (0)	0
31	8.25	0 (0)	10,167 (72)	428
34	7.25	0 (0)	289 (12)	103
40	16.13	858 (3)	462 (11)	64
43*	4.46	41 (3)	0 (0)	2
44	5.63	48 (3)	2400 (29)	183
52	27.46	483 (4)	4475 (50)	333
55	27.33	1 (1)	7932 (23)	270
58*	0.04	0 (0)	0 (0)	0
59	5.88	71 (3)	307 (5)	23
61	12.92	1911 (6)	10,889 (53)	321
63	27.33	30 (4)	28 (3)	123
64	27.42	61 (4)	1930 (26)	185
67	9.68	125 (5)	721 (14)	135
68	27.04	1300 (2)	11,748 (63)	305
75	27.29	174 (7)	1609 (17)	68
77*	0.02	91 (2)	40 (3)	3

of the location where the PSATs surfaced—indicating that both the PSATs and acoustic transmitters were ingested and regurgitated at the same time.

Along the southeastern coast of the United States, 286,683 acoustic detections were recorded by acoustic receivers (Suppl. Fig. 2) (online only), and each acoustic transmitter was detected an average of 3542 times (SD 4285). Filtering, based on a 15-min isolation interval, identified 323 false detections (0.11%), which were subsequently removed from the data set. The greatest movement detected by using acoustic telemetry was from waters off the Hudson Shelf in New York to waters near Miami, Florida (straight-line distance of 1734 km). Fifteen of the 19 double-tagged sharks that survived were detected by acoustic receivers while their PSATs were still attached, and all 19 sharks were detected after their PSATs detached. Additionally, for the individual whose PSAT did not transmit data and was not recovered, 9368 acoustic detections were recorded by 104 different acoustic receivers over 637 d, ranging from Back Sound, North Carolina, to Fort Pierce, Florida, and verifying survival of this shark.

Physiological effects of capture

Fight time had a significant effect on blood pH, hematocrit, lactate, potassium, and glucose. Blood pH decreased significantly (P=0.02, coefficient of multiple determination [R^2]=0.11; Fig. 4A), and lactate (P=0.00, R^2=0.40; Fig. 4B), hematocrit (P=0.01, R^2=0.16; Fig. 4C), potassium (P=0.02, R^2=0.10; Fig. 4D), and glucose (P=0.02, R^2=0.11; Fig. 4E) increased significantly with increasing fight times in sharks caught from shore. Lactate (P=0.00, R^2=0.45; Fig. 4B) increased significantly with increasing fight times for sharks caught from charter boats. However, the aforementioned relationships between fight time and blood pH,

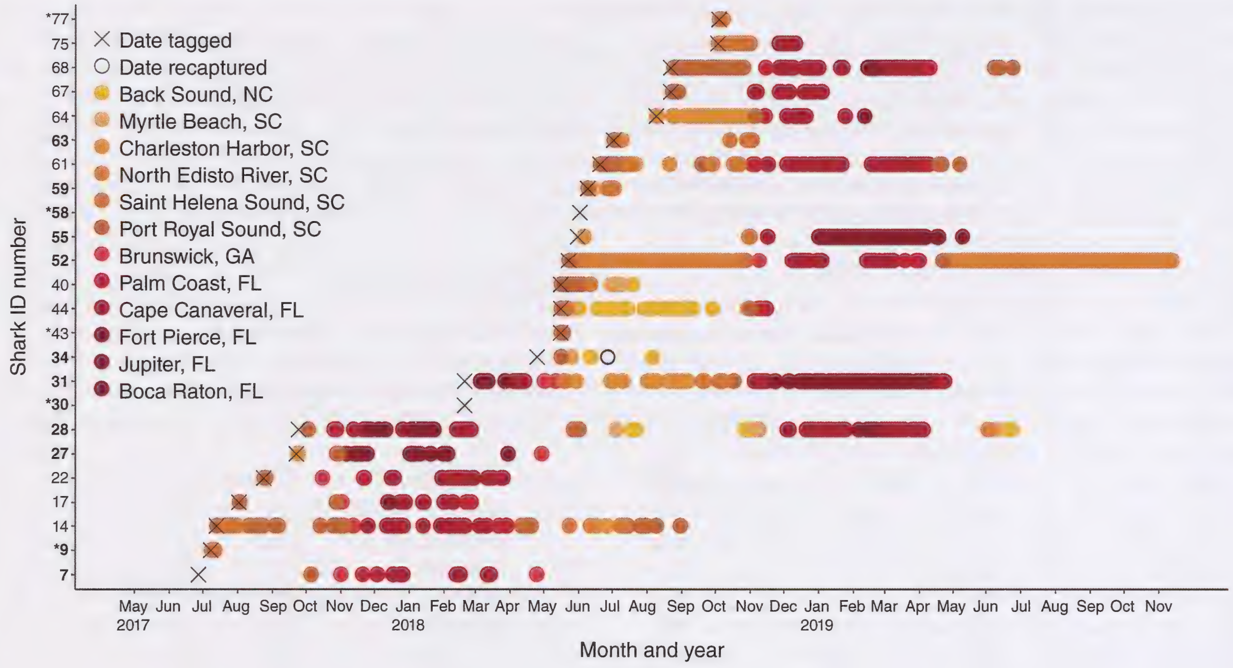

Figure 3

Detections of acoustic transmitters attached to 24 blacktip sharks (*Carcharhinus limbatus*) that were also tagged with pop-off satellite archival tags (PSATs) from June 2017 through December 2019 off the coast of the southeastern United States, by month and location. Each line of circles begins at the date tagged and shows the movement patterns of sharks over time. Asterisks next to shark ID numbers indicate the 5 sharks determined to have died after release by using PSAT data. The ID numbers for sharks caught from shore appear in bold, and the ID numbers for sharks caught from charter boats are not in bold.

hematocrit, potassium, and glucose were relatively weak (as indicated by relatively low R^2 values). There was no change in sodium, chloride, calcium, or magnesium associated with fight time for either capture method ($P>0.05$). The effect of fight time on any of the blood chemistry characteristics did not differ between capture methods (ANCOVA: $P>0.05$; Fig. 4, A–E).

Predicted postrelease mortality

The GLM analysis determined that a model including both pH and glucose provided the best fit to binary PRM data for all sharks combined (n=81; AIC for full model=74.96, AIC for reduced model=71.24) and to data for sharks caught from shore (n=41; full-model AIC=39.65, reduced-model AIC=36.47), and a model including only potassium provided the best fit to data for sharks caught from charter boats (n=40; full-model AIC=43.13, reduced-model AIC=38.40). None of the blood chemistry characteristics were a significant predictor of mortality in any of the 3 best-fit models ($P>0.05$).

With respect to predicting PRM by using the observed capture characteristics, a GLM model including only release condition provided the best fit to binary PRM data for all sharks combined (n=81; full-model AIC=72.52, reduced-model AIC=63.24) and to data for sharks caught from charter boats (n=40; full-model AIC=39.63, reduced-model AIC=33.39). A model including water temperature (P=0.06), fight time (P=0.01), and release condition (P=0.02) provided the best fit to data for sharks caught from shore (n=41; full-model AIC=41.33, reduced-model AIC=34.34).

Hook location did not have a significant effect on the distribution of survivors and mortalities (Fisher's exact test: P=0.07), likely a result of small sample sizes for hook locations other than the jaw. Of the individuals hooked in the jaw (including corner, bottom, or top jaw), 16.0% died; whereas, 33.3% of individuals hooked in the basihyal died and 100% of individuals hooked either in the throat or tail died. The assigned release condition did not have a significant effect on the distribution of survivors and mortalities (Fisher's exact test, P=0.13). Of the individuals assigned a release condition of excellent, 18.4% died; whereas, 8.3%, 20.0%, and 44.4% of individuals assigned a condition of good, fair, and poor died, respectively (Fig. 5).

Discussion

The results of this study provide insights into both the physical and physiological effects of recreational rod-and-reel

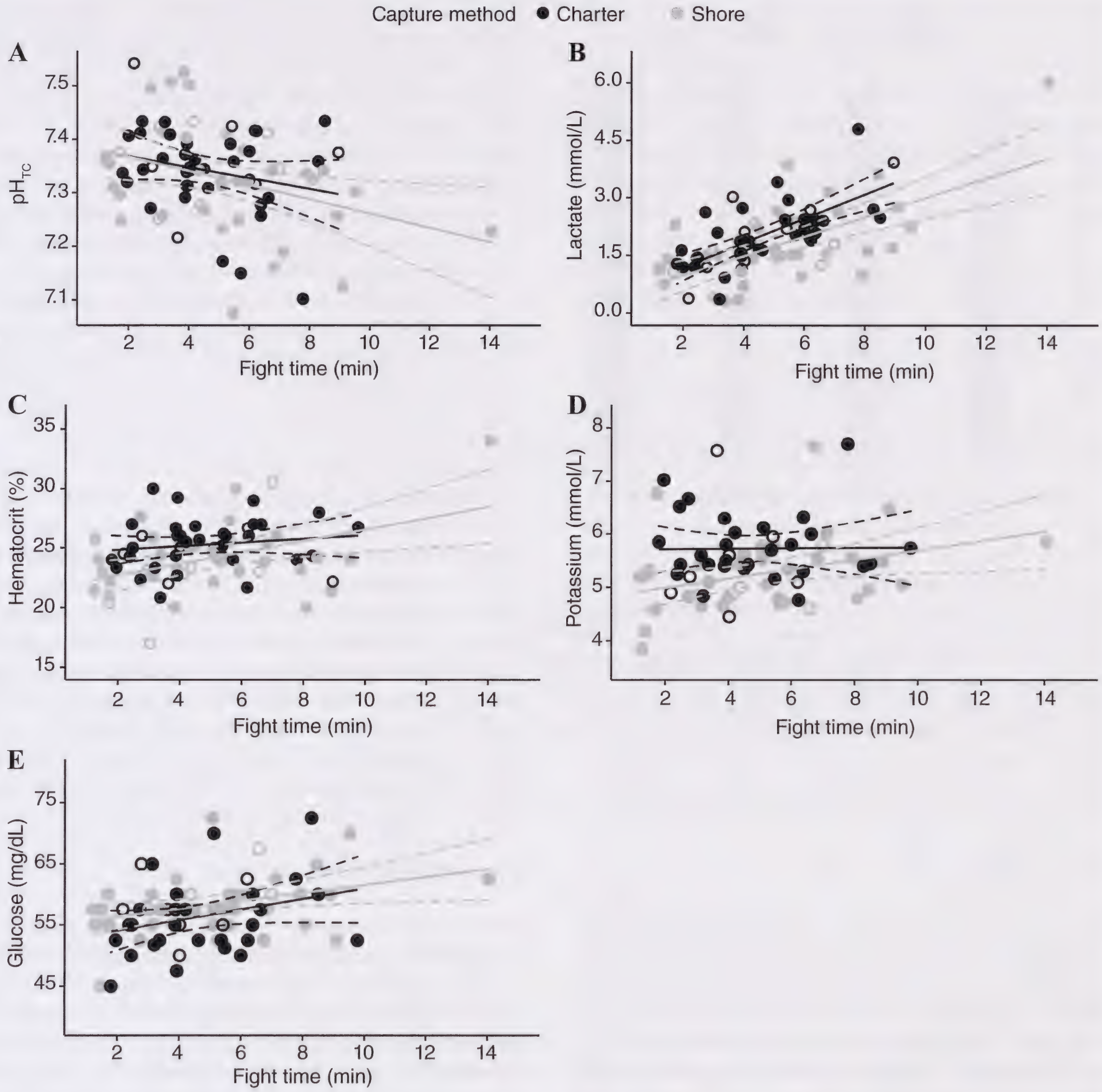

Figure 4

Linear regressions fitted to data of blood chemistry characteristics versus fight time for blacktip sharks (*Carcharhinus limbatus*) caught by recreational anglers in the coastal waters of South Carolina and Florida between May and October 2017 and between February and October 2018. Blood chemistry characteristics are (**A**) temperature-corrected blood pH (pH_{TC}), (**B**) lactate, (**C**) hematocrit, (**D**) potassium, and (**E**) glucose. Fight time refers to the time from the initial strike until the time the shark was secured by anglers. Gray circles represent sharks caught from shore, and black circles represent sharks caught from charter boats. Open circles indicate sharks determined to have died after release. Solid lines indicate regression model predictions, and dashed lines indicate 95% confidence intervals.

capture on the blacktip shark, and how these effects influence PRM rates. Furthermore, this study produced data on the physiological stress and mortality experienced by individuals of this shark species when caught from shore, in a recreational fishery receiving increasing management and conservation attention. Postrelease mortality rates were 17.1% for sharks caught from shore and 20.0% for sharks caught from charter boats, and the results of survivorship analysis based on data from acoustic transmitters were consistent with results inferred from data from PSATs, validating our use of acoustic transmitters to assess PRM. Significant physiological changes were documented in the blood chemistry of sharks, and changes were influenced by fight time.

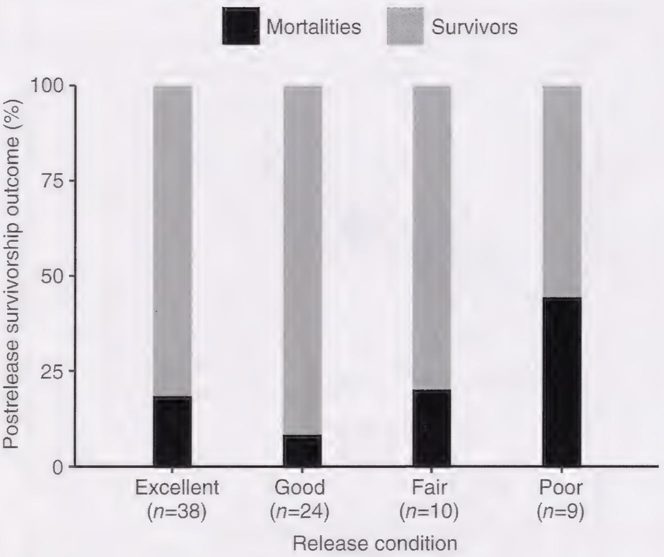

Figure 5

Proportions of blacktip sharks (*Carcharhinus limbatus*) determined to have survived and died after release on the basis of data from tags, by release condition. Blacktip sharks were caught and tagged off the coasts of South Carolina and Florida between May and October 2017 and between February and October 2018. Release conditions are based on behavior at the time of release (see Table 1). *n*=number of sharks.

Postrelease mortality

The PRM rates observed in this study are higher than PRM rates reported for many other shark species caught on rod and reel, such as the rates of 10% for shortfin makos (*Isurus oxyrinchus*) (French et al., 2015), 12.5% for juvenile lemon sharks (*Negaprion brevirostris*) (Danylchuk et al., 2014), and 10% for Atlantic sharpnose sharks (*Rhizoprionodon terraenovae*) (Gurshin and Szedlmayer, 2004). In addition, the observed PRM rates are approximately twice as high as the rate of 9.7% reported by Whitney et al. (2017) for blacktip sharks caught in the charter-boat-based recreational fishery in Florida. This difference in PRM rates may be partially attributable to the higher incidence of physical injury or trauma (*n*=6), foul-hooking (*n*=6), and live predation (*n*=1) observed in our study but not by Whitney et al. (2017).

All sharks captured in our study were caught by recreational anglers using their personal fishing equipment; therefore, a wide range of angler experience and of gear types and strengths were sampled. No at-vessel or at-shore mortalities were observed, and all 5 of the mortality events inferred from PSATs occurred within 6 h of release. This result indicates that mortalities associated with rod-and-reel capture of blacktip sharks do not occur at landing but can occur up to 6 h postrelease and is consistent with results from previous research on blacktip sharks indicating that behavioral recovery from rod-and-reel capture takes an average of 10.5 h (Whitney et al., 2016). This result is also consistent with those of other studies that indicate that most capture-related mortalities of sharks occur 1–4 h after release (Heberer et al., 2010; Marshall et al., 2015; Whitney et al., 2017).

Acoustic receiver coverage along the eastern coast of the United States is not consistent, and many acoustic receivers tend to be closer to shore, given the inherent issues with anchoring receivers in open water. Therefore, it is possible that surviving blacktip sharks, not tagged with a PSAT, avoided acoustic detection (e.g., by staying farther offshore) and as a result were considered to be dead in our study. Additionally, it is possible that consumption of acoustic tags, without predation on blacktip sharks themselves, could explain the lack of acoustic detections for individuals that were tagged only with acoustic transmitters and were considered to have died during our study. Because 10 of the 15 mortalities were confirmed from acoustic data alone, the mortality rates presented herein may be overestimated. However, given the preference of blacktip sharks for nearshore waters and observed high detection rates of blacktip sharks tagged with acoustic transmitters in this study (Table 4) and in other ongoing studies (Bowers[5]), the probability of a tagged blacktip shark escaping detection during migration is likely low.

Predation postrelease

Postrelease mortality rates of blacktip sharks may be influenced by the presence of larger shark species, such as the tiger shark (*Galeocerdo cuvier*), great hammerhead (*Sphyrna mokarran*), and bull shark (*C. leucas*), that are commonly found off the southeastern coast of the United States (Ulrich et al., 2007; Castro, 2011). In our study, data profiles from PSATs deployed on 2 blacktip sharks (sharks 9 and 43) indicate that the tags were ingested within 6 h of release. Shark 9 was actively swimming at the time of PSAT ingestion, but it may have been behaving erratically given that the PSAT was ingested (6 h after release) within the behavioral recovery window for blacktip sharks caught on rod and reel (mean: 10.5 h; Whitney et al., 2016). Shark 43 sank to the ocean floor immediately after release, where it remained for 5 h until the PSAT was scavenged. It was impossible to determine with certainty if only the PSATs were consumed or if the PSATs and the blacktip sharks were consumed. However, the acoustic data obtained from the tags deployed on both of these individuals (sharks 9 and 43) indicate that the acoustic transmitters were ingested and regurgitated at the same time as the PSATs. Therefore, it is unlikely that both the PSATs and acoustic transmitters were ingested without predation upon the blacktip shark itself.

---

[5] Bowers, B. 2019. Personal commun. Charles E. Schmidt Coll. Sci., Fla. Atl. Univ., 777 Glades Rd., Boca Raton, FL 33431.

Although these events could be the first instances of live predation on a blacktip shark recorded by a PSAT, Lear and Whitney (2016) documented postrelease scavenging of a blacktip shark by a larger shark. In addition, live predation events on other species are prevalent in the literature; for example, such events have been reported for the white marlin (*Kajikia albida*) and opah (*Lampris guttatus*) (Kerstetter et al., 2004), the albacore (*Thunnus alalunga*) (Cosgrove et al., 2015), and the tope (*Galeorhinus galeus*) (Rogers et al., 2017; Tolentino et al., 2017). Many shark species have been described to evert their stomachs in response to physical stimuli, such as the ingestion of hard, inedible objects (e.g., the shortfin mako; Brunnschweiler et al., 2011), and the timing between the ingestion and regurgitation events in our study (3.0 and 4.5 d) is similar to that reported in other studies (Kerstetter et al., 2004; Brunnschweiler, 2009; Lear and Whitney, 2016; Rogers et al., 2017). It is possible that the presence of an external PSAT could increase predation risk, because of an increase in visibility to predators (Manabe et al., 2011; Béguer-Pon et al., 2012). However, because both predation events observed in our study occurred in highly turbid waters with low visibility (<0.5 m) off South Carolina, the large sharks that prey on blacktip sharks in such areas likely do not rely heavily on vision to target prey (Gardiner et al., 2014). Given that blacktip sharks are known to form large aggregations (Castro, 2011), it is possible that individuals of conspecifics could have dislodged other PSATs without consuming the blacktip sharks, possibly explaining the premature PSAT detachments observed in our study (Rogers et al., 2017).

Validation of acoustic telemetry for assessment of survival

Some individuals were tagged with both PSATs and acoustic transmitters in our study, and the results indicate that acoustic transmitters can be used effectively to assess PRM in migratory, coastal shark species released in regions with a high prevalence of acoustic receivers. In our study, data obtained from acoustic transmitters indicate the same survivorship outcome as data obtained from the PSATs for all double-tagged individuals. In particular, none of the 5 sharks for which mortalities were confirmed with data from the PSATs were detected on an acoustic receiver more than 10 d postrelease, although all 18 of the individuals that were confirmed to have survived with data from the PSATs, including those with PSATs that were shed prematurely, were detected from 23 to 637 d postrelease (mean: 238.4 d [SD 150.3]) (Table 4).

The electronic tags designed for assessing PRM (e.g., PSATs) can be cost prohibitive (Musyl et al., 2011; Whitney et al., 2016; Rogers et al., 2017), forcing many researchers to use relatively small sample sizes or to deploy tags only on individuals that they believe have a chance at survival (i.e., they do not want to "waste" a tag on an individual that they believe will die), potentially biasing PRM estimates (Rogers et al., 2017). Additionally, the vast majority of PSATs (~80%) are shed before their programmed pop-up date (Arnold and Dewar, 2001; Gunn and Block, 2001), and others often fail to transmit data to the satellite system altogether (Musyl et al., 2011). In our study, 67% of PSATs deployed on surviving sharks were shed prematurely, and 2 PSATs failed to send data to the satellite system (failure rate of 8.3%). Therefore, in addition to the cost of such electronic tags precluding the use of large sample sizes, researchers also face relatively high tag failure rates.

The lower cost of acoustic transmitters could allow for the inclusion of much larger sample sizes and, therefore, more robust assessments of PRM. Additionally, the smaller size of acoustic transmitters, compared with the sizes of other electronic tags (e.g., PSATs), could reduce any potential effects of the tag on a shark's behavior postrelease and, as a result, are likely more appropriate for the assessment of PRM in smaller fish species. Although the effectiveness of using acoustic transmitters to assess PRM depends on the prevalence of acoustic receivers, the number of acoustic receivers deployed along the eastern coast of the United States is increasing (Kneebone et al., 2013), and the rising number of receivers will likely increase the applicability of this method.

Physiological effects of capture

The stress experienced by captured sharks has traditionally been quantified through an assessment of the acid-base status of blood. In this study, pH decreased with increasing fight time for sharks caught from shore, and lactate increased for sharks caught by using both capture methods, indicating that blacktip sharks experienced proton (H^+) loading in blood and tissues due to the dissociation of lactic acid generated by anaerobic glycolysis (Skomal and Mandelman, 2012; Kneebone et al., 2013). These findings indicate that rod-and-reel capture of blacktip sharks results in blood acidosis that is at least partially metabolic in origin, and they are consistent with the results reported by Whitney et al. (2017). Mandelman and Skomal (2009) found that increases in pCO_2 explained all of the variation in pH in blacktip sharks captured with longlines, indicating that acidemia in blacktip sharks caught with longlines is driven strictly by respiratory acidosis. Because measurements of pCO_2 made by the i-STAT system have not been validated, we do not report pCO_2 values from our study; therefore, the potential contribution of CO_2 to the observed acidosis cannot be determined. Regardless, differences in lactate profiles between studies indicate that the origin of the acidosis could be associated with the type of gear used and support the growing awareness that fishery-specific assessments of the stress experienced by captured sharks are necessary (Skomal, 2007; Heberer et al., 2010).

In general, exhaustive exercise leads to elevated concentrations of both glucose (Sherwin et al., 1980; Sheridan and Muir, 1988) and potassium (Medbø and Sejersted, 1990). Catecholamines are responsible for stimulating glucose release from the liver during exercise (i.e., glycogenolysis; Sherwin et al., 1980; Sheridan and Muir, 1988) to meet the energy demands of muscles, and it has been suggested that the mobilization of glucose may be integral to survival (Marshall et al., 2012). Increases in plasma potassium can result from several factors, including a release of potassium from muscle cells due to increased electrical activity (Fenn, 1938; Sejersted and Sjøgaard, 2000) and a decrease in plasma water due to increased intracellular lactate levels that cause a net fluid shift from extracellular to intracellular compartments (van Dijk and Wood, 1988; Wood, 1991). In our study, both glucose and potassium rose with increasing fight times for sharks caught from shore but not for sharks caught from charter boats. Given that fight times did not differ between capture methods, elevated glucose and potassium levels in sharks caught from shore may reflect a higher degree of struggling on the line. Moreover, rhabdomyolysis, a syndrome characterized by muscle necrosis and the release of intracellular electrolytes, often due to muscle trauma associated with intense exercise, can also lead to elevated potassium concentrations (Keltz et al., 2013). The origin of the high glucose and potassium concentrations in sharks caught from shore could simply be a normal response to exercise, but conditions such as rhabdomyolysis cannot be excluded.

The effect of fight time on numerous blood chemistry characteristics for sharks caught from shore (pH, lactate, hematocrit, potassium, and glucose), but not for sharks caught from charter boats (only lactate), could be a result of the tackle (i.e., fishing gear) used by the participating recreational anglers. In particular, the majority of sharks caught from shore were caught with spinning reels (76%), and the majority of sharks caught from charter boats were caught with conventional level-wind reels (85%). Because conventional reels typically have a higher drag capacity than spinning reels, making it more difficult for hooked fish to "run," conventional reels may restrict the movement of captured sharks and, as a result, lessen the degree of muscular exertion and metabolic stress. Additionally, many shore-based fishermen put out far more fishing line initially (e.g., a couple hundred yards, in order to reach deeper water) than anglers who fish from charter boats, and the additional line may give the shark more room to run, both vertically and horizontally, in the water column. Although traditional sportfishing ethics has encouraged the use of light tackle to give the fish a "fighting chance," research results indicate that slowly and carefully angling a fish can potentially exacerbate the stress response (Malchoff and MacNeill[6]).

The results of our study support the notion that use of heavy fishing tackle minimizes the fight time and therefore likely reduces the physiological stress experienced by captured sharks. Future research employing the use of serial blood sampling (e.g., sampling before and after handling by anglers) could improve our understanding of the effects of capture on shark species and of how those effects are influenced by both gear type and handling technique.

Overall, blacktip sharks caught on rod and reel (this study; Whitney et al., 2017) have relatively less drastic physiological disruptions than individuals caught on longlines (Mandelman and Skomal, 2009; Marshall et al., 2012) and drumlines (Gallagher et al., 2014; Jerome et al., 2018). Mean blood lactate values for blacktip sharks caught on longlines (14.82 mmol/L, Mandelman and Skomal, 2009; 36.8 mmol/L, Marshall et al., 2012) and drumlines (8 mmol/L, Gallagher et al., 2014; 6.3 mmol/L, Jerome et al., 2018) are much higher than the mean lactate value reported in our study (2.48 mmol/L). The concentrations of plasma electrolytes in blacktip sharks caught on longlines (potassium: 10.2 mmol/L; sodium: 298 mmol/L; Marshall et al., 2012) are also higher than the values reported in our study (potassium: 5.5 mmol/L; sodium: 273.3 mmol/L). Collectively, the more drastic physiological changes observed in blacktip sharks captured on longlines or drumlines are likely due to the duration of the struggle on the line (e.g., up to 3 h, Mandelman and Skomal, 2009; 2–12 h, Marshall et al., 2012; mean of 46.5 min, Jerome et al., 2018).

Prediction of postrelease mortality

Estimates of mortality for released fish are critical components for estimation of total mortality and are therefore of critical importance to fisheries managers. Because the direct estimation of PRM across species and gear types is likely unrealistic, previous studies have aimed to predict PRM through the use of blood chemistry characteristics (Moyes et al., 2006; Heberer et al., 2010; Schlenker et al., 2016; Talwar et al., 2017) and various capture characteristics (Manire et al., 2001; Hueter et al., 2006; Musyl and Gilman, 2018). In our study, none of the blood chemistry characteristics could be used to predict mortality with any degree of significance. Because all blood samples were screened for pH, lactate, hematocrit, sodium, chloride, potassium, calcium, magnesium, and glucose, the lack of ability to use any of the blood characteristics to predict mortality indicates that many of the observed mortalities were not a result of the potentially exhaustive exercise associated with struggling on a fishing line.

In general, the assigned release condition was the best predictor of PRM, indicating that many of the sharks that died had observable signs of injury or trauma. Noticeable injuries were often related to the location of the hook and typically involved significant bleeding. However, 18.4% of individuals assigned a release condition of excellent died postrelease, indicating that many succumbing individuals have no sign of physical injury or trauma and that assignment of release condition can be somewhat subjective.

In our study, 6 of the 81 tagged blacktip sharks were considered to be foul-hooked, with hook locations of the basihyal, throat, gut, and tail. Three of the 6 foul-hooked sharks died within 10 d of release, for a PRM rate of 50% for foul-hooked sharks. Hook location has been shown to influence survival in many species (Muoneke and Childress, 1994), and mortality is often associated with damage to gills or visceral tissue caused by deeply embedded hooks (Heberer et al., 2010). All recreational anglers in our study chose to use circle hooks—again, no input was provided by the authors on the type or size of hook that should be used. Therefore, it is possible that instances of foul-hooking would have been higher if J hooks were used (Prince et al., 2002; Promjinda et al.[7]; Pacheco et al., 2011), although Whitney et al. (2017) found no difference in the incidence of foul-hooking or PRM between the use of J hooks and the use of circle hooks.

---

[6] Malchoff, M. H., and D. B. MacNeill. 1995. Guidelines to increase survival of released sport fish. Released fish survival. Sport fish fact sheet, 6 p. Cornell Coop. Ext., Sea Grant, Cornell Univ., Ithaca, NY. [Available from website.]

The hook location not only can influence PRM through physical trauma (e.g., damage to gills or visceral tissue) but also can impair locomotion and a shark's ability to ventilate properly (Heberer et al., 2010). The blacktip shark is a ram-ventilating species that must move forward to subject its gills to ventilation because the orientation and morphology of elasmobranch gill slits preclude water flow over gills when individuals are pulled backward (Heberer et al., 2010; Wegner et al., 2010). Therefore, sharks hooked in the tail (i.e., caudal fin) or tail-wrapped in the fishing line and reeled in backward experience reduced water flow over the gills and can ventilate only during brief periods of forward swimming. Indeed, in our study, the only shark hooked in the tail died postrelease. Additionally, the shark that was hooked in the jaw but tail-wrapped in the line and dragged backward also died postrelease. The survival implications for sharks hooked in the tail are well-documented; for example, in another study, 78% of common thresher sharks (*Alopias vulpinus*) hooked in the tail died postrelease (Sepulveda et al., 2015).

Overall, PRM rates in our study are similar for blacktip sharks captured in recreational fisheries from shore (17.1%) and from charter boats (20.0%) and are higher than PRM rates that have been reported for many other shark species caught on rod and reel. The agreement between the results we obtained from analyzing data from the acoustic transmitters and from the PSATs verify that acoustic transmitters can be used to effectively assess PRM in migratory, coastal shark species released in regions with a high prevalence of acoustic receivers (e.g., the eastern coast of the United States). Significant physiological disruptions in the blood chemistry of sharks were identified, and fight time had a significant effect on pH, lactate, hematocrit, potassium, and glucose. Fifty percent of foul-hooked sharks died postrelease, with important implications for the use of gear and methods that reduce foul-hooking.

Acknowledgments

We thank all participating recreational fishermen and all acoustic telemetry data contributors, including staff of the FACT and ACT Networks. We are grateful to A. Galloway, A. Bland, C. Morgan, D. Edmunds, C. Innis, and R. Knotek. Additionally, we thank M. Janech, L. Burnett, and both the anonymous reviewers for their comments on previous versions of this manuscript. This work was supported by the NOAA Cooperative Research Program (grant no. NA16NMF4540081), the American Elasmobranch Society, and the Slocum-Lunz Foundation. This paper is contribution 829 of the South Carolina Marine Resources Center.

Literature cited

Ajemian, M. J., P. D. Jose, J. T. Froeschke, M. L. Wildhaber, and G. W. Stunz.
2016. Was everything bigger in Texas? Characterization and trends of a land-based recreational shark fishery. Mar. Coast. Fish. 8:553–566.

Akaike, H.
1973. Information theory and an extension of the maximum likelihood principle. *In* 2nd international symposium on information theory (B. N. Petrov and F. Csáki, eds.), p. 267–281. Akad. Kiadó, Budapest.

Arlinghaus, R., and S. J. Cooke.
2009. Recreational fisheries: socioeconomic importance, conservation issues and management challenges. *In* Recreational hunting, conservation and rural livelihoods: science and practice (B. Dickson, J. Hutton, and W. M. Adams, eds.), p. 39–58. Blackwell Publ., Oxford, UK.

Arnold, G., and H. Dewar.
2001. Electronic tags in marine fisheries research: a 30-year perspective. *In* Electronic tagging and tracking in marine fisheries reviews: methods and technologies in fish biology and fisheries (J. R. Sibert and J. L. Nielsen, eds.), p. 7–64. Kluwer Acad. Press, Dordrecht, Netherlands.

Bartholomew, A., and J. A. Bohnsack.
2005. A review of catch-and-release angling mortality with implications for no-take reserves. Rev. Fish Biol. Fish. 15:129–154.

Béguer-Pon, M., J. Benchetrit, M. Castonguay, K. Aarestrup, S. E. Campana, M. J. W. Stokesbury, and J. J. Dodson.
2012. Shark predation on migrating adult American eels (*Anguilla rostrata*) in the Gulf of St. Lawrence. PLoS ONE 7(10):e46830.

Bigelow, H. B., and W. C. Schroeder.
1948. Fishes of the western North Atlantic. Part 1: lancelets, cyclostomes, and sharks, 576 p. Mem. Sears Found. Mar. Res., Yale Univ. Press, New Haven, CT.

Bonfil, R.
1994. Overview of world elasmobranch fisheries. FAO Fish. Tech. Pap. 341, 119 p. FAO, Rome.

Brill, R., P. Bushnell, S. Schroff, R. Seifert, and M. Galvin.
2008. Effects of anaerobic exercise accompanying catch-and-release fishing on blood-oxygen affinity of the sandbar shark (*Carcharhinus plumbeus*, Nardo). J. Exp. Mar. Biol. Ecol. 354:132–143.

Brooks, E. J., J. W. Mandelman, K. A. Sloman, S. Liss, A. J. Danylchuk, S. J. Cooke, G. B. Skomal, D. P. Philipp, D. W. Sims, and C. D. Suski.
2012. The physiological response of the Caribbean reef shark (*Carcharhinus perezi*) to longline capture. Comp. Biochem. Physiol. A. 162:94–100.

Brunnschweiler, J. M.
2009. Tracking free-ranging sharks with hand-fed intragastric acoustic transmitters. Mar. Freshw. Behav. Physiol. 42:201–209.

---

[7] Promjinda, S., S. Siriraksophon, N. Darumas, and P. Chaidee. 2008. Efficiency of the circle hook in comparison with J-hook in longline fishery. *In* The ecosystem-based fishery management in the Bay of Bengal, p. 167–180. Dep. Fish., Minist. Agric. Coop., Bangkok, Thailand. [Available from website.]

Brunnschweiler, J. M., F. Nielsen, and P. Motta.
2011. In situ observation of stomach eversion in a line-caught shortfin mako (*Isurus oxyrinchus*). Fish. Res. 109:212–216.

Castro, J. I.
1996. Biology of the blacktip shark (*Carcharhinus limbatus*) off the southeastern United States. Bull. Mar. Sci. 59:508–522.
2011. Blacktop shark, *Carcharhinus limbatus. In* The sharks of North America, p. 432–437. Oxford Univ. Press, New York.

Compagno, L. J. V.
1984. FAO species catalog. Vol. 4. Sharks of the world. An annotated and illustrated catalogue of shark species known to date. Part 2. Carcharhiniformes. FAO Fish. Synop. 125, p. 251–655. FAO, Rome.

Cooke, S. J., and I. G. Cowx.
2004. The role of recreational fishing in global fish crises. BioScience 54:857–859.

Cooke, S. J., and H. L. Schramm.
2007. Catch-and-release science and its application to conservation and management of recreational fisheries. Fish. Manage. Ecol. 14:73–79.

Cosgrove, R., I. Arregui, H. Arrizabalaga, N. Goni, and J. D. Nielson.
2015. Predation of pop-up satellite archival tagged albacore (*Thunnus alalunga*). Fish. Res. 162:48–52.

Danylchuk, A. J., C. D. Suski, J. W. Mandelman, K. J. Murchie, C. R. Haak, A. M. L. Brooks, and S. J. Cooke.
2014. Hooking injury, physiological status and short-term mortality of juvenile lemon sharks (*Negaprion bevirostris*) following catch-and-release recreational angling. Conserv. Physiol. 2:cot036.

Dapp, D. R., T. I. Walker, C. Huveneers, and R. D. Reina.
2016. Respiratory mode and gear type are important determinants of elasmobranch immediate and post-release mortality. Fish Fish. 17:507–524.

Donaldson, M. R., R. Arlinghaus, K. C. Hanson, and S. J. Cooke.
2008. Enhancing catch-and-release science with biotelemetry. Fish Fish. 9:79–105.

Ellis, J. R., S. R. M. Phillips, and F. Poisson.
2017. A review of capture and post-release mortality of elasmobranchs. J. Fish Biol. 90:653–722.

Fenn, W. O.
1938. Factors affecting the loss of potassium from stimulated muscles. Am. J. Physiol. 124:213–229.

French, R. P., J. Lyle, S. Tracey, S. Currie, and J. M. Semmens.
2015. High survivorship after catch-and-release fishing suggests physiological resilience in the endothermic shortfin mako shark (*Isurus oxyrinchus*). Conserv. Physiol. 3:cov044.

Gallagher, A. J., L. H. Frick, P. G. Bushnell, R. W. Brill, and J. W. Mandelman.
2010. Blood gas, oxygen saturation, pH, and lactate values in elasmobranch blood measured with a commercially available portable clinical analyzer and standard laboratory instruments. J. Aquat. Anim. Health 22:229–234.

Gallagher, A. J., J. E. Serafy, S. J. Cooke, and N. Hammerschlag.
2014. Physiological stress response, reflex impairment, and survival of five sympatric shark species following experimental capture and release. Mar. Ecol. Prog. Ser. 496:207–218.

Gardiner, J. M., J. Atema, R. E. Hueter, and P. J. Motta.
2014. Multisensory integration and behavioral plasticity in sharks from different ecological niches. PLoS ONE 9(4):e93036.

Gunn, J., and B. Block.
2001. Advances in acoustic, archival, and satellite tagging of tunas. Fish Physiol. 19:167–224.

Gurshin, C. W. D., and S. T. Szedlmayer.
2004. Short-term survival and movements of Atlantic sharpnose sharks captured by hook-and-line in the north-east Gulf of Mexico. J. Fish Biol. 65:973–986.

Harter, T. S., P. R. Morrison, J. W. Mandelman, J. L. Rummer, A. P. Farrell, R. W. Brill, and C. J. Brauner.
2015. Validation of the i-STAT system for the analysis of blood gases and acid–base status in juvenile sandbar shark (*Carcharhinus plumbeus*). Conserv. Physiol. 3:cov002.

Heberer, C., S. A. Aalbers, D. Bernal, S. Kohin, B. DiFiore, and C. A. Sepulveda.
2010. Insights into catch-and-release survivorship and stress-induced blood biochemistry of common thresher sharks (*Alopias vulpinus*) captured in the southern California recreational fishery. Fish. Res. 106:495–500.

Heupel, M. R., J. M. Semmens, and A. J. Hobday.
2006. Automated acoustic tracking of aquatic animals: scales, design and deployment of listening station arrays. Mar. Freshw. Res. 57:1–13.

Holbrook, C., T. Hayden, T. Binder, and J. Pye.
2020. glatos: a package for the Great Lakes Acoustic Telemetry Observation System. R package, vers. 0.4.2. [Available from website, accessed April 2020.]

Hueter, R. E., C. A. Manire, J. P. Tyminski, J. M. Hoenig, and D. A. Hepworth.
2006. Assessing mortality of released or discarded fish using a logistic model of relative survival derived from tagging data. Trans. Am. Fish. Soc. 135:500–508.

Jerome, J. M., A. J. Gallagher, S. J. Cooke, and N. Hammerschlag.
2018. Integrating reflexes with physiological measures to evaluate coastal shark stress response to capture. ICES J. Mar. Sci. 75:796–804.

Kajiura, S. M., and S. L. Tellman.
2016. Quantification of massive seasonal aggregations of blacktip sharks (*Carcharhinus limbatus*) in southeast Florida. PLoS ONE 11(3):e0150911.

Keltz, E., F. Y. Khan, and G. Mann.
2013. Rhabdomyolysis. The role of diagnostic and prognostic factors. Muscles Ligaments Tendons J. 3:303–312.

Kerstetter, D. W., J. J. Polovina, and J. E. Graves.
2004. Evidence of shark predation and scavenging on fishes equipped with pop-up satellite archival tags. Fish. Bull. 102:750–756.

Kilfoil, J. P., B. M. Wetherbee, J. K. Carlson, and D. A. Fox.
2017. Targeted catch-and-release of prohibited sharks: sand tigers in coastal Delaware waters. Fisheries 42:281–287.

Killam, K. A., and G. R. Parsons.
1989. Age and growth of the blacktip shark, *Carcharhinus limbatus*, near Tampa Bay, Florida. Fish. Bull. 87:845–857.

Kneebone, J., J. Chisholm, D. Bernal, and G. Skomal.
2013. The physiological effects of capture stress, recovery, and post-release survivorship of juvenile sand tigers (*Carcharhias taurus*) caught on rod and reel. Fish. Res. 147:103–114.

Korsmeyer, K. E., H. Dewar, N. C. Lai, and J. B. Graham.
1996. The aerobic capacity of tunas: adaptation for multiple metabolic demands. Comp. Biochem. Physiol. A 113:17–24.

Lawrence, M. J., G. D. Raby, A. K. Teffer, K. M. Jeffries, A. J. Danylchuk, E. J. Eliason, C. T. Hasler, T. D. Clark, and S. J. Cooke.
2020. Best practices for non-lethal blood sampling of fish via the caudal vasculature. J. Fish Biol. 97:4–15.

Lear, K. O., and N. M. Whitney.
2016. Bringing data to the surface: utilizing data loggers for large sample sizes from marine vertebrates. Anim. Biotelem. 4:12.

Manabe, R., J. Aoyama, K. Watanabe, M. Kawai, M. J. Miller, and K. Tsukamoto.
2011. First observations of the oceanic migration of Japanese eel, from pop-up archival transmitting tags. Mar. Ecol. Prog. Ser. 437:229–240.

Mandelman, J. W., and G. B. Skomal.
2009. Differential sensitivity to capture stress assessed by blood acid–base status in five carcharhinid sharks. J. Comp. Physiol. B 179:267.

Manire, C., R. Hueter, E. Hull, and R. Spieler.
2001. Serological changes associated with gill-net capture and restraint in three species of sharks. Trans. Am. Fish. Soc. 130:1038–1048.

Marshall, H., L. Field, A. Afiadata, C. Sepulveda, G. Skomal, and D. Bernal.
2012. Hematological indicators of stress in longline-captured sharks. Comp. Biochem. Physiol. A 162:121–129.

Marshall, H., G. Skomal, P. G. Ross, and D. Bernal.
2015. At-vessel and post-release mortality of the dusky (*Carcharhinus obscurus*) and sandbar (*C. plumbeus*) sharks after longline capture. Fish. Res. 172:373–384.

Medbø, J. I., and O. M. Sejersted.
1990. Plasma potassium changes with high intensity exercise. J. Physiol. 421:105–122.

Moyes, C. D., N. Fragoso, M. K. Musyl, and R. W. Brill.
2006. Predicting postrelease survival in large pelagic fish. Trans. Am. Fish. Soc. 135:1389–1397.

Muoneke, M. I., and W. M. Childress.
1994. Hooking mortality: a review for recreational fisheries. Rev. Fish. Sci. 2:123–156.

Musick, J. A., S. Branstetter, and J. A. Colvocoresses.
1993. Trends in shark abundance from 1974 to 1991 for the Chesapeake Bight region of the U.S. Mid-Atlantic coast. *In* Conservation biology of elasmobranchs (S. Branstetter, ed.), 1–19 p. NOAA Tech. Rep. NMFS 115.

Musyl, M. K., and E. L. Gilman.
2018. Post-release fishing mortality of blue (*Prionace glauca*) and silky shark (*Carcharhinus falciformes*) from a Palauan-based commercial longline fishery. Rev. Fish Biol. Fish. 28:567–586.

Musyl, M. K., M. L. Domeier, N. Nasby-Lucas, R. W. Brill, L. M. McNaughton, J. Y. Swimmer, M. S. Lutcavage, S. G. Wilson, B. Galuardi, and J. B. Liddle.
2011. Performance of pop-up satellite archival tags. Mar. Ecol. Prog. Ser. 433:1–28.

Nikinmaa, M.
1992. Membrane transport and control of hemoglobin-oxygen affinity in nucleated erythrocytes. Physiol. Rev. 72:301–321.

NMFS (National Marine Fisheries Service).
2019. 2018 stock assessment and fishery evaluation (SAFE) report for Atlantic highly migratory species, 234 p. Highly Migratory Species Manage. Div., Off. Sustainable Fish., Natl. Mar. Fish. Serv., NOAA, Silver Spring, MD. [Available from website.]

Pacheco, J. C., D. W. Kerstetter, F. H. Hazin, H. Hazin, R. S. S. L. Segundo, J. E. Graves, F. Carvalho, and P. E. Travassos.
2011. A comparison of circle hook and J hook performance in a western equatorial Atlantic Ocean pelagic longline fishery. Fish. Res. 107:39–45.

Press, K. M., J. Mandelman, E. Burgess, S. J. Cooke, V. M. Nguyen, and A. J. Danylchuk.
2016. Catching sharks: recreational saltwater angler behaviours and attitudes regarding shark encounters and conservation. Aquat. Conserv.: Mar. Freshw. Ecosyst. 26:689–702.

Priede, I. G.
1985. Metabolic scope in fishes. *In* Fish energetics: new perspectives (P. Tytler and P. Calow, eds.), p. 33–66. Croom Helm, London.

Prince, E. D., M. Ortiz, and A. Venizelos.
2002. A comparison of circle hook and "J" hook performance in recreational catch-and-release fisheries for billfish. Am. Fish. Soc. Symp. 30:66–79.

R Core Team.
2018. R: a language and environment for statistical computing. R Foundation for Statistical Computing, Vienna, Austria. [Available from website, accessed August 2018.]

Rogers, P. J., I. Knuckey, R. J. Hudson, A. D. Lowther, and L. Guida.
2017. Post-release survival, movement, and habitat use of school shark *Galeorhinus galeus* in the Great Australian Bight, southern Australia. Fish. Res. 187:188–198.

Rose, D. A.
1996. An overview of world trade in sharks and other cartilaginous fishes, 106 p. TRAFFIC Int., Cambridge, UK.

Schlenker, L. S., R. J. Latour, R. W. Brill, and J. E. Graves.
2016. Physiological stress and post-release mortality of white marlin (*Kajikia albida*) caught in the United States recreational fishery. Conserv. Physiol. 4:cov066.

Sejersted, O. M., and G. Sjøgaard.
2000. Dynamics and consequences of potassium shifts in skeletal muscle and heart during exercise. Physiol. Rev. 80:1411–1481.

Sepulveda, C. A., C. Heberer, S. A. Aalbers, N. Spear, M. Kinney, D. Bernal, and S. Kohin.
2015. Post-release survivorship studies on common thresher sharks (*Alopias vulpinus*) captured in the southern California recreational fishery. Fish. Res. 161:102–108.

Sheridan, M. A., and N. A. Muir.
1988. Effects of epinephrine and norepinephrine on glucose release from Chinook salmon (*Oncorhynchus tshawytscha*) liver incubated in vitro. J. Exp. Zool. 248:155–159.

Sherwin, R. S., H. Shamoon, R. Hendler, L. Saccà, N. Eigler, and M. Walesky.
1980. Epinephrine and the regulation of glucose metabolism: effect of diabetes and hormonal interactions. Metabolism 29:1146–1154.

Shiffman, D. S., C. Macdonald, H. Y. Ganz, and N. Hammerschlag.
2017. Fishing practices and representations of shark conservation issues among users of a land-based shark angling online forum. Fish. Res. 196:13–26.

Skomal, G. B.
2007. Evaluating the physiological and physical consequences of capture on post-release survivorship in large pelagic fishes. Fish. Manage. Ecol. 14:81–89.

Skomal, G. B., and J. W. Mandelman.
2012. The physiological response to anthropogenic stressors in marine elasmobranch fishes: a review with a focus on the secondary response. Comp. Biochem. Physiol. A 162:146–155.

Talwar, B., E. J. Brooks, J. W. Mandelman, and R. D. Grubbs.
2017. Stress, post-release mortality, and recovery of commonly discarded deep-sea sharks caught on longlines. Mar. Ecol. Prog. Ser. 582:147–161.

Tolentino, E. R., R. P. Howey, L. A. Howey, L. K. B. Jordan, R. D. Grubbs, A. Brooks, S. Williams, E. J. Brooks, and O. N. Shipley.

2017. Was my science project eaten? A novel approach to validate consumption of marine biologging instruments. Anim. Biotelem. 5:3.

Ulrich, G. F., C. M. Jones, W. B. Driggers III, J. M. Drymon, D. Oakley, and C. Riley.
2007. Habitat utilization, relative abundance, and seasonality of sharks in the estuarine and nearshore waters of South Carolina. Am. Fish. Soc. Symp. 50:125–139.

van Dijk, P. L. M., and C. M. Wood.
1988. The effect of β-adrenergic blockade on the recovery process after strenuous exercise in the rainbow trout, *Salmo gairdneri* Richardson. J. Fish Biol. 32:557–570.

Wegner, N. C., C. A. Sepulveda, K. B. Bull, and J. B. Graham.
2010. Gill morphometrics in relation to gas transfer and ram ventilation in high-energy demand teleosts: scombrids and billfishes. J. Morphol. 271:36–49.

Whitney, N. M., C. F. White, A. C. Gleiss, G. D. Schwieterman, P. Anderson, R. E. Hueter, and G. B. Skomal.
2016. A novel method for determining post-release mortality, behavior, and recovery period using accelerometer data loggers. Fish. Res. 183:210–221.

Whitney, N. M., C. F. White, P. A. Anderson, R. E. Hueter, and G. B. Skomal.
2017. The physiological stress response, post-release behavior, and mortality of blacktip sharks (*Carcharhinus limbatus*) caught on circle and J-hooks in the Florida recreational fishery. Fish. Bull. 115:532–543.

Wood, C. M.
1991. Acid–base and ion balance, metabolism, and their interactions, after exhaustive exercise in fish. J. Exp. Biol. 160:285–308.

Fishery Bulletin

Guidelines for authors

Contributions published in *Fishery Bulletin* describe original research in marine fishery science, fishery engineering and economics, and marine environmental and ecological sciences (including modeling). Preference will be given to manuscripts that examine processes and underlying patterns. Descriptive reports, surveys, and observational papers may occasionally be published but should appeal to an audience outside the locale in which the study was conducted.

Although all contributions are subject to peer review, responsibility for the contents of papers rests upon the authors and not on the editor or publisher. *Submission of an article implies that the article is original and is not being considered for publication elsewhere.*

All submissions are subject to a double-blind review to remove the identity of author and reviewer during the review process.

Plagiarism and double publication are considered serious breaches of publication ethics. To verify the originality of the research in papers and to identify possible previous publication, manuscripts may be screened with plagiarism-detection software.

Manuscripts must be written in English; authors whose native language is not English are strongly advised to have their manuscripts checked by English-speaking colleagues before submission.

Once a paper has been accepted for publication, online publication takes approximately 2 weeks.

There is no cost for publication in *Fishery Bulletin*.

Types of manuscripts accepted by the journal

Articles generally range from 20 to 30 double-spaced typed pages (12-point font) and describe an original contribution to fisheries science, engineering, or economics. Tables and figures are not included in this page count, but the number of figures should not exceed 1 figure for every 4 pages of text. Articles contain the following divisions: abstract, introduction, methods, results, discussion, and conclusions.

Notes are generally less than 10 double-spaced typed pages (12-point font), including the Literature cited section. Like articles, notes describe an original contribution to fisheries science. They follow a format similar to that for articles: abstract, introduction, methods, results, and discussion, but the results and discussion sections may be combined and a conclusions section should not be included. They should include no more than 2 figures or tables (2 of each would be too many). They are distinguished from full articles in that they report a noteworthy new observation or discovery—such as the first report of a new species, a unique finding, condition, or event that expands our knowledge of fisheries science, engineering, or economics—and do not require a lengthy discussion. Manuscripts on range extensions will not be considered.

Companion articles should be submitted together and are published together as a scientific contribution. Both articles should address a closely related topic and may be articles that result from a workshop or conference.

Review articles of exceptional quality may be considered occasionally for publication on a case-by-case basis. They address a timely topic that is relevant to aspects of fisheries science. They should include an abstract, but the format of the article, per se, will be up to the author. Please contact the Scientific Editor to discuss your ideas regarding a potential review article before embarking on such a project.

Preparation of manuscript

Title page should include authors' full names, mailing addresses, and the senior author's email address.

Abstract should be limited to 200 words (one-half typed page), state the main scope of the research, and emphasize the authors' conclusions and relevant findings. Do not review the methods of the study or list the contents of the paper. Because abstracts are circulated by abstracting agencies, it is important that they represent the research clearly and concisely.

General text must be typed in 12-point Times New Roman font throughout. A brief introduction should convey the broad significance of the paper; the remainder of the paper should be divided into the following sections: Materials and methods, Results, Discussion, and Acknowledgments. Headings within each section must be short, reflect a logical sequence, and follow the rules of subdivision (i.e., there can be no subdivision without at least 2 subheadings). The entire text should be intelligible to interdisciplinary readers; therefore, all acronyms, abbreviations, and technical terms should be written out in full and defined the first time they are mentioned. Abbreviations should be used sparingly because they are not carried over to indexing databases and slow readability for those readers outside a discipline. They should never be used for the main subject (species, method) of a paper.

For general style, follow the U.S. Government Publishing Office *Style Manual* (2016, available at website) and *Scientific Style and Format: the CSE Manual for Authors, Editors, and Publishers* (2014, 8th ed.) published by the Council of Science Editors. For scientific nomenclature, use the current edition of the American Fisheries Society's *Common and Scientific Names of Fishes from the United States, Canada, and Mexico* and its companion volumes

(*Crustaceans, Mollusks, Cnidaria and Ctenophora*, and *World Fishes Important to North Americans*). For species not found in the above mentioned AFS publications and for more recent changes in nomenclature, use the Integrated Taxonomic Information System (ITIS, available at website), or, secondarily, the California Academy of Sciences *Catalog of Fishes* (available at website) for species names not included in ITIS. Common (vernacular) names of species should be lowercase. Citations must be given for the identification of specimens. For example, "Fish species were identified according to Collette and Klein-MacPhee (2002); sponges were identified according to Stone et al. (2011)."

Dates should be written as follows: 11 November 2018. Measurements should be expressed in metric units, for example, "58 metric tons (t);" if other units of measurement are used, please make this fact explicit to the reader. Use numerals, not words, to express whole and decimal numbers in the general text, tables, and figure captions (except at the beginning of a sentence). For example, "We considered 3 hypotheses. We collected 7 samples in this location." Use American spelling. Refrain from using the shorthand slash (/), an ambiguous symbol, in the general text.

Cite all software, special equipment, and chemical solutions used in the study within parentheses in the general text, for example, "SAS, vers. 6.03 (SAS Institute Inc., Cary, NC)."

Word usage and grammar that may be useful are the following:

- *Aging*
  For our journal, the word *aging* is used to mean both age determination and the aging process (senescence). Authors should make clear which meaning is intended where ambiguity may arise.

- *Fish and fishes*
  The plural of the word fish (a collective noun that implies individuals without regard to species) is *fish*.
  Example: The *fish* were collected by trawl net.
  Example: The numbers of *fish* collected that season were less than the numbers from previous years.

  The plural for *fish species* is *fishes* (a contrived plural used by taxonomists to mean several or more *fish species*) or one can use *fish species* (which is preferred in this journal for clarity across disciplines).
  Example: The *fishes* of Puget Sound [biodiversity is implied] or
  Example: The *fish species* of Puget Sound [preferred plural for clarity across disciplines].

- *Crab and crabs, squid and squids, etc.*
  The plural of the word *crab* (i.e., many individuals without regard to species) is *crab*.
  Example: The crab were sorted by weight.
  Example: Many red king *crab* were dying [Many individuals of one species of crab.]

  The plural of *crab species* is *crabs* (a word used by taxonomists) or *crab species* (the latter is preferred in this journal for clarity).
  Example: These *crabs* were selected for treatment. [Different crab species are implied.]
  Example: These *crab species* were selected for treatment. [Preferred word choice for clarity of meaning.]
  Example: Snow *crabs* are found throughout the North Pacific Ocean and Bering Sea. [There are 2 species of snow crab and therefore the word *crabs* can be used here.]
  Example: *Two species* of snow *crab* are found throughout the North Pacific Ocean and Bering Sea. [Preferred usage for clarity.]
  Example: Three crabs were selected for treatment. [3 species of crab are implied.]
  Example: Three crab species were selected for treatment. [Preferred word choice for clarity.]

- *Fisherman and fisher*
  We use *fisherman* and *fishermen* in this journal not *fisher* and *fishers*. One can always use crew member, vessel operator, and angler (the latter for recreational fishing.

- *The definite article with common names of species*
  When the singular common name of a species represents the entire class or group to which it belongs, use the definite article.
  Example: Only one species of the genus *Salmo* is found in the Atlantic Ocean—*the* Atlantic salmon (*Salmo salar*).
  Example: The sonic emissions of *the* bottlenose dolphin are complex.

  For plural common names, this rule does not apply.
  Example: Chinook salmon are found throughout the Pacific Ocean.
  Example: Bottlenose dolphins are found in temperate and tropical waters.

- *Sex*
  For the meaning of male and female, use the word *sex*, not *gender*. Do not write "fish were sexed." Write, "sex was determined."

- *Participles*
  As adjectives, participles must modify a specific noun or pronoun.
  Example: Using mark-recapture methods, these scientists determined the size of the population. [Correct. The participle *using* modifies the word *scientists*.]
  Example: These scientists, based on the collected data, concluded that the mortality rate of these fish had increased. [Incorrect. The scientists were not based on the collected data.]
  Example: These scientists concluded, on the basis of collected data, that the mortality rate of these fish had increased. [Correct. The offending participle has been eliminated and an adverbial phrase modifies the verb *concluded*.]

Equations and mathematical symbols should be set from a standard mathematical program (MathType or Equation Editor). Equations formatted in LaTex are not acceptable. For mathematical symbols in the general text (α, χ^2, π, ±, etc.), use the symbols provided by the MS Word program and italicize all variables, except those variables represented by Greek letters and the superscript and subscript parts of variables and expressions. Do not use photo mode when creating these symbols in the general text, and do not cut and paste equations, letters, or symbols from a different software program.

Number equations (if there are more than one) for future reference by scientists; place the number within parentheses at the end of the first line of the equation.

Literature cited section comprises published works and those accepted for publication (in press) in peer-reviewed journals. Follow the name and year system for citation format in this section (i.e., citations should be listed alphabetically by the authors' last names, and then by year if there is more than one citation by the same author. A list of abbreviations for citing journal titles can be found on our website.

Authors are responsible for the accuracy and completeness of all citations. Avoid the use of multiple citations when a single citation sufficiently supports a statement; cite the work that first reported the information that supports a statement, not all of the subsequent works. Literature citation format: Authors (last name, followed by initials for first name and, if given, middle name of first author; then list names of additional authors with initials before last names). Year. Title of article. Abbreviated title of the journal in which it was published. Always include either the range of page numbers (for a journal article) or a total number of pages (for a book or other type of publication). List a sequence of citations in the general text chronologically, for example, "(Smith, 1932: Green. 1947; Smith and Jones, 1985)."

Acknowledgments should be no more than 6 lines of text. Only those who have contributed in an outstanding way should be acknowledged by name. For recognition of other persons or groups, use a general term, such as *crew*, *observers*, or *research coordinators*, and do not include names with these terms.

Digital object identifier (doi) code ensures that a publication has a permanent location online. A doi link (which may include a doi code) should be included at the end of citations of published literature. Authors are responsible for submitting accurate doi links. Faulty links will be deleted at the page-proof stage.

Footnotes are used for all documents that have not been formally peer reviewed and for observations and personal communications, but these types of references should be cited sparingly in manuscripts submitted to the journal.

All reference documents, administrative reports, internal reports, progress reports, project reports, contract reports, personal observations, personal communications, unpublished data, manuscripts in review, and council meeting notes are footnoted in 10-point font and placed at the bottom of the page on which they are first cited. Footnote format is the same as that for formal literature citations. A link to the online source (e.g., [Available from http://www..., accessed July 2017.]), or the mailing address of the agency or department holding the document, should be provided so that readers may obtain a copy of the document.

Tables are often overused in scientific papers; it is seldom necessary to present all the data associated with a study. Tables should not be excessive in size and must be cited in numerical order in the text. Headings should be short but ample enough to allow the table to be intelligible on its own.

All abbreviations and unusual symbols must be explained in the table legend. Other incidental comments may be footnoted with numeral footnote markers. Use asterisks only to indicate significance in statistical data. Do not put a table legend on a page separate from the table; place the legend above the table. *Do not submit tables in photo mode.*

- Note probability with a capital, italic P.
- Provide a zero before all decimal points for values less than one (e.g., 0.07).
- Round all values to 2 decimal points.
- Use a comma in numbers of 5 digits or more (e.g., 13,000 but 3000).

Figures must be cited in numerical order in the text. Graphics should aid in the comprehension of the text, but they should be limited to presenting patterns rather than raw data. The number of figures should not exceed 1 figure for every 4 pages of text.

Figure legends should explain all symbols and abbreviations seen in the figure and should be double spaced on a separate page at the end of the manuscript.

Line art and halftone figures should be saved at resolutions >600 dots per inch (dpi) and >300 dpi, respectively. Color is allowed in figures to show morphological differences among species (for species identification), to show stain reactions, to show gradations (such as those of temperature and salinity within maps), and to distinguish between numerous lines and symbols in graphs. Figures approved for color should be saved in CMYK format.

All figures must be submitted as PDF, TIFF, or EPS files.

- Capitalize only the first letter of the first word and proper nouns in all labels within figures.
- Do not use overly large font sizes for labels in maps and for axis labels in graphs.

- Use the same point size for all labels, except for panel labels (e.g., **A**), which should be slightly larger than other labels (e.g., 11 point versus 8 point).
- Use a sans serif font for all labels. Panel labels (e.g., **A**), however, should be in Times New Roman font.
- Do not use bold fonts or bold lines in figures. Do not use italic fonts. Exceptions include use of italic fonts for labels of bodies of water in maps and a bold font for panel labels (e.g., **A**).
- Do not place outline rules around graphs.
- Do not include vertical and horizontal lines in the background of graphs. Ticks for values on the x-axis and y-axis will suffice.
- Place a north arrow and label degrees latitude and longitude (e.g., 170°E) in all maps. If scale of map requires more than degrees, use degrees minutes, not decimal degrees.
- Place panel labels (e.g., **A**, **B**, **C**) within the upper-left area of each graph or photo in a multi-panel figure, from left to right, then top to bottom. If the letter is not visible against a dark background, put a white box behind it. Do not use white labels.
- Avoid placing labels vertically or diagonally. Y-axis labels can be vertical. Words in horizontal labels can be stacked vertically to fit.
- Use symbols, shadings, or patterns (not clip art) in maps and graphs.
- For scale bars in maps, use kilometers. Use the label *km* or *kilometers* (lowercased).

Supplementary materials that are considered essential, but are too large or impractical for inclusion in a paper (e.g., metadata, figures, tables, videos, and websites), may be provided at the end of an article. These materials are subject to the editorial standards of the journal. A URL to the supplementary material and a brief explanation for including such material should be sent at the time of initial submission of the paper to the journal.

- **Metadata, figures, and tables** should be submitted in standard digital format (MS Word or PDF file) and should be cited in the general text, for example, as "... was determined (Suppl. Table 3, Suppl. Fig. 1)."
- **Websites** should be cited with a URL in the general text.
- **Videos** must not be larger than 30 MB to allow a swift technical response for viewing the video. Authors should consider whether a short video uniquely captures what text alone cannot capture for the understanding of a process or behavior under examination in the article. Supply an online link to the location of the video.

Copyright law does not apply to *Fishery Bulletin*, which falls within the public domain. However, if an author reproduces any part of an article from *Fishery Bulletin*, reference to source is considered correct form (e.g., Source: Fish. Bull. 97:105).

Failure to follow these guidelines and failure to correspond with editors in a timely manner will delay publication of a manuscript.

Submission of manuscript

Submit a manuscript online at the ScholarOne Manuscripts website for *Fishery Bulletin*. Commerce Department authors must provide proof of internal clearance of their manuscripts with either a completed and signed NOAA Form 25-700 or a copy of the clearance email from the Research Publication Tracking System. For further details on electronic submission, please contact the associate editor, Cara Mayo, at

cara.mayo@noaa.gov.

When requested, the text and tables should be submitted in MS Word format. Each figure should be sent as a separate PDF, TIFF, or EPS file. Send a copy of a figure in the original software if conversion to any of these formats yields a degraded version of the figure.

Questions? If you have questions regarding these guidelines, please contact the managing editor, Kathryn Dennis, at

kathryn.dennis@noaa.gov.

Questions regarding manuscripts under review should be addressed to Associate Editor Cara Mayo.

Fishery Bulletin

Subscription form

Superintendent of Documents **Publications** Order Form

*5178

☐ YES, please send me the following publications:

____ Subscriptions to *Fishery Bulletin*
for $32.00 per year ($44.80 foreign)

The total cost of my order is $ _______ . Prices include regular domestic postage and handling and are subject to change.

(Company or Personal Name) (Please type or print)

(Additional address/attention line)

(Street address)

(City, State, ZIP Code)

(Daytime phone including area code)

(Purchase Order No.)

Charge your order. IT'S EASY!

VISA

MasterCard

Please Choose Method of Payment:

☐ Check payable to the Superintendent of Documents

☐ GPO Deposit Account ☐☐☐☐☐☐☐–☐

☐ VISA or MasterCard Account

☐☐☐☐☐☐☐☐☐☐☐☐☐☐☐☐☐☐☐☐

☐☐☐☐ (Credit card expiration date)

To fax your orders (202) 512-2104

(Authorizing Signature)

Mail to: Superintendent of Documents
P.O. Box 979050, St. Louis, Missouri 63197
Tel. no. (U.S. callers): 866-512-1800
Tel. no. (International callers): 1-202-512-1800

Thank you for your order!

Also available online at
https://bookstore.gpo.gov/products/fishery-bulletin
email: ContactCenter@gpo.gov

SMITHSONIAN LIBRARIES
3 9088 02042 4396